CRANFIELD INSTITUTE OF TECHNOLOGY

School of
Mechanical Engineering

PhD THESIS

Academic Year 1981 - 82

JUAN OLIVERAS M.

"ACOUSTIC EMISSION PULSE ANALYSIS: an integrated system for transducer calibration and signal processing"

Supervisor: R.H.BANNISTER

OCTOBER 1982

ABSTRACT

The present thesis covers the pioneering effort of establishing an infrastructure for conducting research into the analysis of Acoustic Emission signatures, with emphasis being placed upon the recovery of the true surface waveform for a given transient input.

The topics covered in this work are:

- The provision of the necessary computer software for the handling and processing of the data. Here, a method is included for the correction of phase errors introduced by the sampling/multiplexing of the signals, which provides the basis for the implementation of data convolution techniques in the frequency domain.
- The development of an experimental rig and source of excitation, later applied to the design of transducers.
- The development of a new transducer configuration, capable of producing a relatively flat frequency response (±7dB) over the frequency range 300 KHz - 2 MHz.
- The development of a procedure for the calibration of transducers, based upon a modified reciprocity method. The technique produces the calibration of transducers in relative terms, requiring a complementary method to provide the reference level for the calibration.

As a means of assessing the proposed techniques, the transducer calibration was applied to the de-convolution of pulses generated with a step forcing function, and the results compared with an equivalent theoretical model previously published.

ACKNOWLEDGEMENTS

In first place, acknowledgement must go to Dr. R.H.Bannister, in his role of supervisor of the present work, for his support and encouragement; the Venezuelan Council for Scientific and Technological Research (CONICIT), for their full sponsorship during the four and a half years duration of the project; and the British Science and Research Council (SRC), for their financial support in the purchase of part of the instrumentation facilities required for the project.

The author feels specially grateful to Mr. B.Moffitt, head of the Instrumentation Section of the School of Mechanical Engineering, for his valuable advice and support beyond departmental duties, without whose assistance this project would have not been accomplished.

Special thanks are also due to Dr. R.A.Cookson, head of the Applied Mechanics Group, for his most effective help in overcoming the breakdown of some instrumentation; and last, but by no means least, to Mrs. A.Allen-Rowlandson for kindly accepting the task of typing this thesis.

CONTENTS

INTRODUCTION

Engineers working within modern technological fields are aware of the ever growing importance of Non Destructive Testing (NDT) techniques as paramount quality control and surveillance methods for ensuring product reliability and safety. Among these techniques, Acoustic Emission (AE), one of the youngest NDT disciplines, has awakened an extensive interest in every imaginable technical field; from process and production plant engineering, through scientific research in materials, structures, electrical and mechanical engineering, to the most advanced nuclear and aerospace industries.

For the benefit of those not yet familiar with the term Acoustic Emission, it can be formally defined as a transient phenomenon of vibratory character, generated within a solid by the sudden release of stored elastic energy. However, the name Acoustic Emission has later become widely associated with the actual NDT methods which use the described transient phenomena as the basic source of information.

Although the terminology "Acoustic" is somewhat inaccurate for, in general, the observed transient phenomena are not audible, its adoption is due to the historical fact of this discipline starting with the observation and subsequent study of "clicking sounds" produced by some materials when subjected to deformation, reported as early as 1923 (1), 1928 (2), 1929 (3), and more formally by J.Kaiser (4) in 1950.

In spite of the technique normally being associated with modern technology, some basic, even crude applications of AE can be traced back to the very origins of man. For this it is only necessary to imagine the reaction of a primitive "Homo Sapiens" when hearing the creaking of the tree branch supporting his weight. If his experience had not yet taught him the adequate course of action to be taken, he must have learnt soon enough afterwards!

The same line of thought can also be applied to the primitive cave dweller when hearing the rumbling sound of the earth above him before his home roof collapsed; or to the primitive tribes migrating over frozen lakes and rivers, while keeping alert with regard to the sound of cracking ice beneath their feet.

These illustrations of primitive and unconcious use of Acoustic Emission should help the reader to feel familiar with the subject of the present work, and it is with this spirit that they are included.

1.1 AE TECHNIQUES

A detailed account of the historical development of AE studies is beyond the scope and objectives of the present work, and excellent reviews of this kind can be found in previously published reports. An outstanding example, recommendable to any reader interested in such type of reviews, is found in the MSc thesis by M.N.Bentley (5). Consequently, this discussion will concentrate upon the later developments leading to the present "state of the art".

From its formal discovery, AE has evolved at an incredible pace basically due to the worldwide inspired interest, while the major factor limiting further or faster advance has been imposed by the necessary instrumental hardware.

Since the frequency range of AE events is so wide, compared with the audible range traditionally covered in most engineering instrumentation applications, this fact coupled with the rather high requirements of gain and electrical input noise for the amplifiers and high sensitivity for the transducers, implied the development of a whole new generation of instruments. The progressive appearance of more adequate transducers and amplifiers marked the evolution of AE data processing and analysis, from the simple observation of the pulses and their comparison against some basic specimen parameters such as type of failure, grain size, section size, material phase transformations, temperature, strain level and rate, etc.; through the application of

envelope detection techniques to narrow frequency bands within the transducer's output, using these narrow bands as carriers of the information (6); to the present methods of statistical or signature analysis.

As clear evidence of the economic advantages of AE over other industrial plant surveillance methods, an important report was published in 1977 by H.P.Bloch (7), on the evaluation of an Incipient Failure Detection System based upon the "envelope detection" technique (6), and developed "on site" at the Exxon chemical plant at Baytown, Texas, USA. The conclusions, although somehow critical of the reliability of some system links (mostly electronic), emphasize the economic success from implementing the system in greatly reducing maintenance repair work and consequent loss of production, and also in reducing the fire hazard risks.

Perhaps the main feature of AE as an NDT or monitoring technique against alternative methods is its active character, that is, the detected activity is generated while the specimen is undergoing the failure process, while actually supporting the working load. If there is no fault developing within the surveyed structure, there will be no AE activity; regardless of the level of vibration, temperature, fatigue life, etc.

Within present day AE techniques, three main streams can be identified with regard to hardware development and data analysis methods, each of them concentrating on rather specific objectives:

- Location of the AE source
- Assessment and pattern recognition of source activity through statistical methods of analysis
- Assessment and identification of the source event through signature analysis

1.1.1 Source Location

The location of AE sources is of special interest and importance in those applications where large size structures have to be subjected to surveillance during their function or during testing before

certification and approval. In general, AE results are here complemented by other NDT methods like Ultrasonics or X-Ray inspection once the location of the fault has been established within reasonable limits, and its greatest contribution results from the reduction in time, personnel and related costs in comparison with alternative methods.

The usual hardware comprises an array of transducers distributed over the surface of the specimen under surveillance, whose number will depend upon geometrical considerations, and a multi-line monitoring system capable of registering the order and in-between delays of arrival of signals from all transducers. This instrumentation is likely to be interfaced to a minicomputer which will resolve the source position by triangulation techniques assembled within the data processing programs.

Since the most important factor from the processed signals is the leading edge of the corresponding pulse, and the time instant at which the threshold level of each channel is crossed, the transducers here utilized will, in general, be of the resonant type (to achieve maximum sensitivity), and with characteristics of sensitivity and resonant frequency as similar as possible.

1.1.2 Statistical Methods of Analysis

These methods have established themselves as one of the main NDT techniques for the certification of mechanical components and structures, and although they have not yet been accepted as official standards, the process of acceptance is well under way (8).

The first method of analysis developed within this current discipline consisted of the cumulative counting of pulses surpassing a given threshold level per unit of time, while the specimen under study was subjected to loading (9). Subsequently, other parameters like counts rate, ring down counting, and multiple ways of data presentation as histograms or distributions in function of different variables like amplitude, energy (RMS), pulse length, load level or number of cycles have been devised and successfully tried on specific applications.

A great deal of research work has been conducted in materials studies using these methods of data analysis, and although they fall outside the field of interest for the present work, a few articles are briefly reviewed as examples of the wide application of these techniques. No particular reason is behind the selection of these particular articles but the fact that most of them were studied during the preliminary literature survey at the beginning of the present project, and the presentation order is purely chronological.

A general account of factors affecting the AE activity detected from some materials was published by H.L.Dunegan and A.T.Green (10), in which cumulative events counts and counts rates are presented in function of load parameters for several materials, including cast and wrought uranium, and several steel alloys. Although the study is by no means conclusive, it lists a series of factors having been found to influence the AE response of the specimens.

A detailed description of a test facility for conducting this sort of study was presented by D.R.James and S.H.Carpenter (11) shortly after, with a rather comprehensive account of practical problems encountered when attempting the AE measurements (mainly due to interference from background noise and vibration), together with precautionary measures to avoid them.

A novel and ingenious method for the presentation of data for fatigue analysis was published in 1976 by J.M.Carlyle and W.R.Scott (12), in which the actual AE pulses are used, after shaping, to drive the intensity of the beam of an oscilloscope, while the horizontal channel was driven by a signal proportional to the total number of fatigue cycles, and the vertical channel was driven by the specimens load. This method proved capable of producing new interesting results besides being able to detect types of events which could not be detected by previous methods, like the effects from the closure of cracks for decreasing load.

The application of AE to the aeronautics industry, especially in the early detection of fatigue, has been a well explored field of

study not only at British or North-American aerospace establishments. A report from Aérospatiale at Suresnes, France, was published in 1977 (13) on the AE behaviour of light alloys when subjected to fatigue, including the influence of anodic oxidation and the beginning of crack formation. Although the data processing and presentation is conventional, the paper confirms the popularity of AE as an NDT technique.

A good example of fatigue studies using AE methods can also be found in an article by T.C.Lindley et al (14) on the monitoring of fatigue crack growth, developed at the Materials Division of the CEGB Research Laboratories, in which the data is shown to have good correlation with accepted mathematical models for fatigue crack growth in terms of life for high cycle fatigue tests. The work includes a study of the effects of single overloads to the AE generated within the specimens, which were made of different steel, aluminium and Ducol alloys.

Typical instrumentation arrays include one or several piezoelectric transducers mounted on the specimen under observation, connected via their corresponding preamplifiers to a central data processing station. This is usually provided with some sort of signal conditioning facilities, counting/storing circuits to produce the data distributions, data output components in the form of pen recorders, X-Y plotters or paper tape punch stations, and even interfacing facilities for computer control or data transfer and storage in retrieval systems.

In order to evaluate the potential of statistical methods of AE data analysis in machine condition monitoring applications, a short experimental study was conducted, during which a faulty roller element bearing was mounted on an electrical motor, and readings of both vibration and AE activity were made in parallel, to be later analysed on a comparative basis.

A conventional vibration analysis within the audible frequency range did not give clear evidence beyond the indication that the bearing was at fault. Figures 1.1 and 1.2 show the best representation possible of the vibration data, consisting of the frequency spectra of the accelerometer output, with the significant amplitude peaks identified

in terms of speed related roller bearing frequencies and their harmonics. However, an amplitude distribution analysis of the AE detected signals showed the presence of two peaks (clearly noticeable in Figs. 1.3 and 1.4), suggesting the presence of two different source mechanisms which remarkably correlated with the condition of the bearing having a cracked inner race and a pitted outer race.

1.1.3 Single Pulse Analysis

Although statistical methods of AE data analysis constitute a viable and powerful tool for machine condition monitoring and structural integrity surveillance, a major disadvantage is presented by the need of a typical case history for the type of system under observation in order to interpret the obtained results. This not only implies the requirement of a good level of familiarity with both monitored and monitoring systems, but in general, results obtained by different teams of engineers or with different instrumentation sets cannot be directly compared. In view of these difficulties and in the hope that even more information is contained within each AE pulse, the idea of analysing single transient signals developed into a third method of AE analysis.

Once more, this stream of AE technology has evolved in very close relation to the available instrumentation, from the simple pulse shape observation on the screen of an oscilloscope and its recording by photographic means, through different ways of analogue recording and filter-based analysis of the signals, to the present day methods of signal storage and processing by means of digital instruments.

Not surprisingly, the first method of analysis to be applied to AE signature studies was based upon the Fourier transform of the pulses, and it is generally credited to L.J.Graham and G.A.Alers (15) to be the first research team to implement it. Later techniques include the application of shock spectrum analyses, Fourier and shock spectra ratio, pulse rise time and deconvolution analyses, the last two performed in the time domain.

A major part of the effort into these particular methods of AE analysis and related topics such as transducer calibration, has been contributed by research teams within four major world research centres: Rockwell Science Center, National Bureau of Standards and Cornell University in the USA, and the Harwell Research Establishment in the UK. From these four centres, groups of experts (and students in the case of Cornell University) have been concentrating on the difficulties of AE pulse processing with the aim of characterising the activity sources since the early seventies, and not surprisingly most of the articles presently accepted as classics within the discipline have in fact emerged from them. A detailed review of these articles is included later in sections of this work directly related to the treated topics, as this is the most adequate way found to organise such a volume and variety of information in order to present it in a coherent form.

The main difficulty against the development of analysis techniques here related has always been the assessment of how much of the captured signals characteristics corresponds to the transducer and signal conditioning instrumentation, and how much is really representative of the true AE generated wave. To this respect, two basic alternatives have been proposed as solution:

- The provision of "flat frequency response" transducers
- The provision of a calibration method to characterise the transducer's (and instrumentation) effects upon the detected waveforms.

Considering that AE signals have been reported to present frequency components reaching 10 MHz (16), it is very difficult to take the first alternative as being of practical value. In fact, the only known transducers capable of producing a resonance-free response over the above frequency range are air-dielectric capacitive devices, which can be made to have their first resonance at frequencies of the order of 40 MHz, but unfortunately their utilization poses very stringent constraints of construction and installation which make them completely impractical for use outside the laboratory environment.

Their geometry also presents problems. Those capacitive devices designed as line type transducers are manufactured with cylindrical shape, thus their configuration makes them extremely directional and therefore not suitable for general use. Those provided with a flat circular sensing plate in order to achieve omni-directional sensitivity patterns, suffer from a lack of resolution due to their averaging effect across the sensing face over Rayleigh and Lamb type waves, and are only suitable for measuring disturbances normal to the specimen surface at epicentral locations. Additionally, these transducers present such sensitivity to airborne electromagnetic interference that a Faraday cage for the transducer/specimen assembly is an unavoidable necessity.

The AE research group at John Hopkins, Baltimore, USA, have been experimenting with laser based optical AE detection and measurement, where the instrumentation system is based upon a modified Michelson interferometer. As with the case of capacitive transducers, physical contact between probe and specimen is avoided thus providing a potentially very wide resonance free response bandwidth.

Information about the application of optical probes to AE measurements was first obtained at a rather late stage of the project; and the fact that some tests performed with the equipment facilities in this Department showed poor resolution of the frequency-displacement product, conditioned the project to be continued in the persuit of other types of transducers.

Even for the more widely studied frequency range of 0-3 MHz, it is physically impossible to construct a transducer capable of being used in an industrial environment with a characteristic resembling a "flat frequency response", the main reason being that an adequate sensitivity level will impose constraints upon the minimum dimensions of the active sensing element, which in turn conditions the inherent resonances for the device.

Typical instrumental arrays include one or two transducers whose type will depend on the task being performed. In a calibration

by comparison against a standard, for example, the reference transducer will in general be either an optical probe or a capacitive transducer, and the sensor under calibration will most probably be a commercial model for industrial use. The array will also include a signal conditioning line for each transducer; a recording device with sufficient bandwidth which can be of analogue type, as in the case of adapted video recorders, or digital as in the case of transient recorders and digital oscilloscopes; and finally a computerised data processing station which can be directly interfaced with the recording instrument in order to store and process the experimental data, usually complemented by mass storage facilities.

1.2 PROJECT BACKGROUND

Following the preliminary literature survey, it was decided to direct the project towards the study of single pulse analysis for the reasons explained in subsection 1.1.3.

Since this was the first AE research program to be conducted within the Department, there were no instrumentation facilities or background for acquiring these, directly available. Thus, a thorough study of commercial alternatives was carried out in order to begin assembling the instrumentation system which would support the project development. The fact that a minicomputer was available within the departmental group greatly conditioned the decission to use it as the data processing station, constituting the heart of the instrumentation system, and the items to be purchased later would complement it.

In relation to software, the minicomputer was provided with a package of vibration analysis programs, designed to work with the computer's own Analogue to Digital Converter (ADC), and based upon Fast Fourier Transform routines. However, two reasons made this software unsuited for AE analysis: although the programs used frequency spectra as the basic tool for calculations, the function options offered were specifically designed for vibration analysis (i.e. Power Spectral Density, Correlation and Coherence functions), while the project would

need an emphasis to be made upon convolution and averaging methods; and secondly, the ADC unit was far too slow, requiring a speed down factor of 1200 to 1 from an intermediate signal storing device, in order to reach the required sampling rates to store two channels with a 2 MHz bandwidth.

Consequently, the decision to develop a new package of programs was made, and the project started simultaneously in several areas: selection, purchase and assembly of instrumentation into a measuring system, its interface to the computer, provision of necessary software to support the experimental work, design and construction of the physical model of experimentation, design and construction of transducers, and development of a calibration method.

Progress was made in parallel on most of the above areas until a particularly difficult problem would be encountered, in which case all efforts would be concentrated upon its solution. However, due to the variety and extension of the studied subjects, these are presented organised into separate chapters and not in chronological order. But before starting the detailed relation of all the phases that constitute the present work, there are some views which should be emphasised since they justify and support the direction in which the research was conducted.

After deciding from the preliminary literature survey to devote the present project to the study of AE single pulse analysis, all efforts were concentrated upon the development of a calibration method to characterise transducers and signal conditioning equipment; the idea being that once a recorded signal is processed to arrive to the true surface waveform, it should then be possible to apply any analysis method without fears of the "measuring system" overshadowing the true character of the AE pulse. In fact, the actual choice of a particular method of analysis seems of secondary importance when compared with the process of actually "de-colouring" the signal from extraneous distortions.

After reaching the above conclusions, and having decided in which direction to conduct the research program, it was realized that

a great deal of the planning had been inspired by a report published by J.R.Houghton and P.F.Packman at NASA, USA, in 1977 (17), due to the clarity on stating the basic frame of ideas along which the work could develop.

The methodology employed throughout the project was borrowed from linear systems theory, where each link in the instrumentation chain is considered to be a fundamental block, with its characteristics represented by a Transfer Function in terms of the Fourier Transform of the input and output signals.

Finally, due to limitations imposed by time, the actual analysis of the de-coloured AE signals had to be left at a discussion level, and therefore the present work cannot so much be seen as conclusive, but as a pioneering effort to start the AE discipline within the School of Mechanical Engineering here at Cranfield.

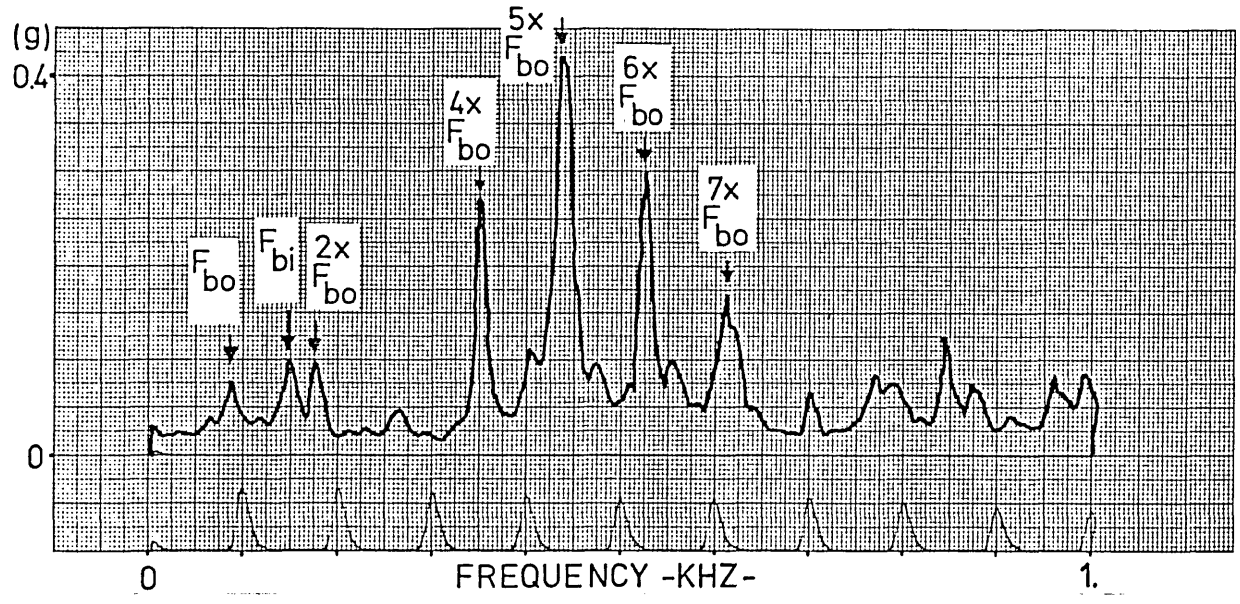

Fig 1.1- Vibration spectrum at 2000 RPM

NOTATION

F_i : Fundamental frequency of rotor

F_{bo} : Ball passing frequency respect to outer race

F_{bi} : Ball passing frequency respect to inner race

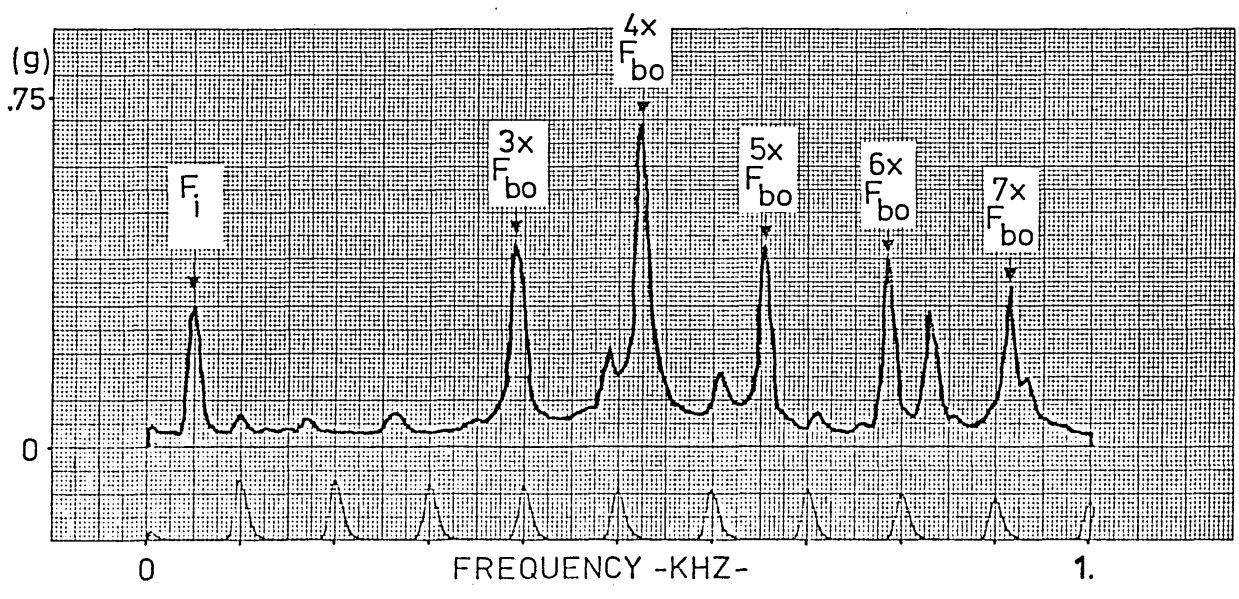

Fig 1.2- Vibration spectrum at 3000 RPM

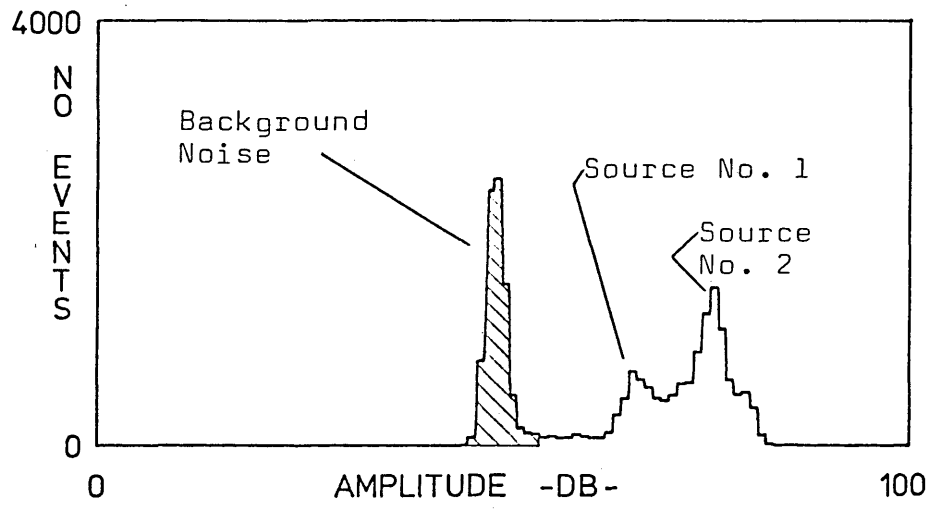

Fig 1.3- AE amplitude distribution at 2000 RPM
(Threshold level: 50 dB)

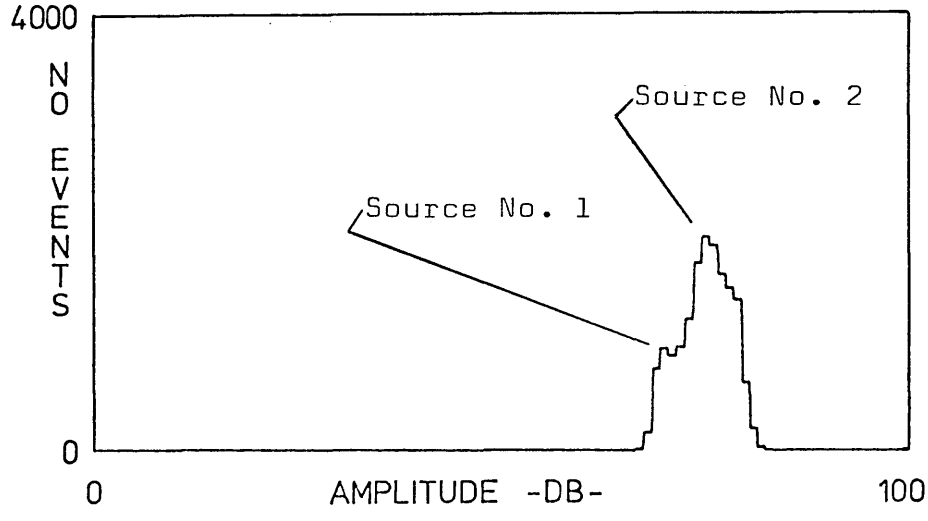

Fig 1.4- AE amplitude distribution at 3000 RPM
The transducer had to be replaced by a less sensitive model due to saturation problems, and the background noise was filtered by increasing the threshold level.
(Threshold level: 70 dB)

SIGNAL PROCESSING HARDWARE

2.1 LITERATURE SURVEY

Among the publications consulted at the beginning of the project (1978), some were found of considerable guidance with respect to instrumental alternatives for AE signature analysis. In one of these papers, K.Ono (18) presents a rather exhaustive review of the methods and instrumentation used to obtain spectral analyses from AE signals, at the same time underlining the limitations in their use. The first method under discussion uses a conventional sweep-type spectrum analyser in conjunction with a wide-band analogue recorder. The method had first been implemented by J.L.Graham and G.A.Alers, who are credited as being the pioneers in AE spectral analysis, in 1971-72 (19), by using a modified video recorder to store the AE transient signals.

The main reasons for using a video recorder are its bandwidth of approx. 3 MHz, resulting from the high relative speed between the recording/playback head and magnetic tape, and the freeze-action capability, which allows sections of the recorded signal 17 msec long to be played in a repetitive mode, thus making the use of a sweep analyser possible. The method, although original and novel, presents several limitations: there is a lack of resolution (in the order of 30-50 KHz) as a consequence of the required sweep speed in the analyser, thus the resulting spectra can be significantly distorted; there is a drop of sensitivity for increasing frequency which results from the convolution of the signal and gate function spectra; and finally, the system is only suitable for recording one channel.

An alternative is provided by the use of a dedicated instrument to obtain the autocorrelation function of the AE pulse, which can subsequently be Fourier transformed into a power density distribution spectrum. This was the approach employed at UCLA, Los Angeles, Cal., USA, which avoids the problems of sampling random data.

However, since the processes involved in the calibration of transducers require the simultaneous time records of two signals, or their corresponding Fourier transforms, the autocorrelogram based method was not suitable for the present project.

A third method of spectral analysis reviewed by Ono was based upon the direct Fourier transform of the signals, obtained by digital means. For this, he suggests the use of a real-time frequency analyser in combination with a transient recorder, but he also mentions that Brown and Tatro, also working within the University of California at the Lawrence Livermore Laboratory, were at the time implementing a digital sampling and direct transform system capable of working at rates up to 6 MHz, which is seen as a promising method to become widespread.

The report goes on to discuss the AE generated during plastic deformation and fracture processes, making a comparison of results obtained by different researchers in the field. From these, Ono concludes that "Frequency Spectrum Analysis is one of the most difficult tasks in AE instrumentation" since the results from these analyses had been far from spectacular. He goes on to point out that all indications suggest AE signals as having "flat frequency spectra", currently associated with "white noise", in contradiction to the conclusion of Graham and Alers (20) already published in previous reports; and he justifies the discrepancies as a product of the frequency domain convolution methods used.

It will be shown later, during the discussion of the above work by Graham and Alers, that the confusion about interpretations of measured spectra, is basically due to the calibration methods employed and the study of frequency spectra in terms of amplitude only.

Ono concludes the report with some rather indefinite concluding remarks, which were found to be of no particular interest to the progress of the present work.

Another important article in reference to the instrumentation used for AE frequency analysis, was published in 1974 by G.Curtis (21), from the materials physics division, AERE, Harwell, Didcot, Berks, UK. The report is basically an account of the experimental work developed at Harwell, with the application of a polymeric film capacitive transducer to wide band AE capture and analysis, and contains a good indication of the state of development of related instrumentation at the time, especially with regard to the capacitive transducer, the first of its kind.

Reference is made to preamplifiers and amplifiers developed at Harwell, having an overall flat frequency response up to 10 MHz, and to the fact that the fastest ADC available at that time limited the highest frequency of analysis at 2 MHz. However, no experimental spectra are presented for frequencies beyond 500 KHz.

Another important piece of research, which has become a fundamental classic among calibration and source recognition studies, was published in 1975 by F.R.Breckenridge et al (22), from the National Bureau of Standards, Washington, DC, USA. In this article data was collected and displayed by use of a high speed storage oscilloscope. Although the technique suits the aims of the particular study in terms of comparing the response of a standard transducer against theoretical calculations of its response, based upon a semi-infinite body model, a different instrumental set-up is reported to have been used for transducer calibration, based around a conventional spectrum analyser, by processing the output of the transducer under calibration to repetitive pulse excitations produced at a rate of 10 to 20 pulses per sec.

The calibration was achieved by comparing the transducer under test with a "standard" which was justified to have a "flat frequency response" for frequencies up to about 40 MHz.

From the study of the related literature available, from which the above are the most significant examples, the decision was made to

implement a digital analysis system based around the minicomputer already available in the Department, employing digital means of storing the raw signals.

2.2 INSTRUMENTATION LAY-OUT

A market research for commercial preamplifiers indicated model 1801 from DUNEGAN/ENDEVCO as the most appropriate choice for its facilities of interchangeable filters, apart from the slightly better specifications of input noise level than competitor brands.

Since no commercial AE preamplifiers were found with bandwidths greater than 2 MHz, and there seemed to be no specific evidence from the available literature to suggest that such a range would not be adequate for the project, 20 KHz to 2 MHz was accepted as the frequency range of interest for this study. Consideration must also be made of the fact that at the time there were no commercial transducers with specified response beyond 1 MHz.

Indeed, no commercial power supply/main amplifier to be in line with the preamplifiers was found to be available at a reasonable cost, and therefore a prototype was developed within the Instrumentation Section of the Department. The amplifier section of the instrument was designed around an integrated circuit op-amp, which was able to provide appropriate bandwidth and noise level figures but not an adequate output voltage capacity, and since the gain had been set at 40 dB, it resulted in an instrument most prone to saturation. However, it was found that the 40 dB amplification provided by the preamplifiers was enough for the laboratory AE measurements, thus the device was used as a power supply only.

For the storage of signals prior to their transfer to the mini-computer for analysis, several options employing either analogue or digital tape recorders, or digital transient recorders were contemplated, but the transient recorder option seemed to offer the best combination of dynamic range, bandwidth and cost. The instrument finally purchased was a two channel recorder model DL 922, from DATALAB,

with a memory extension option to provide record lengths of 2K points per channel, or 4K when recording a single channel. The recorder has a maximum sampling rate of 20 MHz, resulting in a top sampling rate of 10 MHz when digitising two channels, while the inner circuitry was specified to have a 6 MHz bandwidth.

Interfacing cards for the recorder and the minicomputer had also to be purchased.

The minicomputer used for the signal processing is a 16 bit INTERDATA processor, model 8/16, with 64K or RAM, fixed point arithmetic, a 2.5 Mbyte disc drive unit with single removable platter, and controlled from a conventional Teletype terminal.

The data was monitored during processing via a storage oscilloscope connected to the Digital to Analogue Convertor (DAC) output from the computer, while results were normally produced in graphic form via an X-Y plotter, also connected to the same outputs.

Figure 2.1 shows the initial lay-out of the system at the start of the project, and prior to some additions and modifications to be made during the course of the work.

It is perhaps worthwhile to explain that such a system is capable of two channel frequency analysis of signals up to frequencies of 4 to 5 MHz, and it has only recently been superseded by the appearance of faster sampling and storing devices, like the GOULD BIOMATION digital oscilloscope.

2.3 PRACTICAL DIFFICULTIES

Several problems arose from the instrumentation set-up during the development of the project, mainly due to the lack of experience with digital signal processing systems.

The first problem to be encountered was the interfacing of the transient recorder to the minicomputer. After some consultations with members of staff from the Computing Centre, Cranfield, it was decided

that a serial type ASCII coded interface system would be the best option due to its level of standardization for similar equipment within the Institute. However, since the actual interface cards for the recorder and the computer were supplied by the corresponding manufacturers, the cables and connectors provided did not match, neither did the conventions used in the respective installation manuals for the labeling of some of the interfacing functions (signals). This meant that reference had to be made to the appropriate international standards manuals, and extra interconnection cables had to be provided.

Additionally, the interface for the computer is a standard RS-232 card, and it had to be wire-link programmed for the appropriate functions and baud rate. This task was partially performed by the computer maintenance engineer, but some adjustments and modifications had to be made while developing the interface driving software.

This software consists of an Assembler routine which can be called from any user program, and it is designed to transfer any pre-specified number of integer numbers from the transient recorder into an array within the computer's hard core memory. The task of providing the routine was contracted to the Signal Processing and Analysis Group at Cranfield, and the system was finally in running order three months after receiving the parts.

Software had then to be provided for the handling of the data, and this is the subject of the next chapter.

In the early stages of the project, discrepancies between the expected and real performance of the equipment began to emerge. The first discrepancy to be observed was in connection with the dynamic range of the transient recorder. For a digital recorder this figure is directly related to the signal-to-noise ratio, which for an 8-bit word instrument should be 58.96 dB.

This figure is obtained by assuming that all of the 256 levels of the range will be covered by the stored signal, and considering that the error in any quantisation step will be $\pm g/2$ or less (where "g" is

the interval between two consecutive levels).

The quantisation error produces a standard deviation of $g/\sqrt{12}$, which represents a measure of the random noise introduced to the signal, and since the total range for the signal was said to be 256g:

$$\text{S/N ratio} = \frac{256g}{g/\sqrt{12}} = 886.81$$

$$\text{S/N ratio} = 58.96 \text{ dB} \simeq 60 \text{ dB}$$

However, readings from stored records showed samples differing in up to four levels from their true value. This problem, attributed to quantisation errors, combined with the impossibility of covering the total of 256 levels in order to prevent overshooting, resulted in a noise ground floor 38 to 40 dB below the maximum peak values.

Naturally, this situation was improved after applying a triangular (Hanning) smoothing function to the spectra and by averaging in the frequency domain. However, the input signal-to-noise ratio implied that, in order to register a wide frequency range from the transducers, the maximum allowable difference between peaks and troughs for the transducer response, should be of the order of 30 dB over the frequency range of interest.

The next discrepancy between expected and obtained performance was encountered when trying to relate phase measurements from two simultaneous channel recordings.

Initially, when outputting the digital data from the recorder into the computer, points corresponding to each channel were transmitted in alternate form. But the phase relation between seemingly highly repetitive experimental signals varied at random in magnitude and sign from record to record. Since there was no direct control or specification over the order in which the channels would be outputted, it was decided to modify the software in order to transfer the two channels in a sequential mode by forcing the recorder to output one channel at a time, from the controls on the front panel.

This overcame the uncertainty over which channel was being transmitted as first or second, but phase still seemed to behave in a random fashion.

Theoretically, for an accurate multiplexing system sampling two channels simultaneously, a constant delay equal to half the sampling interval should separate corresponding points from each channel. Furthermore, the first point to be sampled and stored should correspond to the channel whose signal is used to trigger the whole process. However, the results seemed to indicate that the recording process could start by sampling the first point from either channel (hence the change of phase sign), regardless of trigger settings, and also the multiplexing delay seemed to vary from record to record (hence the change in magnitude). This prevented the characterisation of the recorder in order to apply a constant phase correction function for all records.

A close scrutiny of the transient recorder technical manual led to the discovery of the specification of the time base jitter, which is quoted to be 50 ηsec. Although such a figure may seem at first too small to be of major concern, the source of error can easily be realized when considering the ideal multiplexing delay magnitude while sampling two channels at 10 MHz, which corresponds to the same value as the time jitter error.

Since the accurate measurement of phase was of vital importance to the project, a considerable effort was concentrated upon solving this problem. Further reviews of published articles related either to AE or digital sampling and storing devices were fruitless; thus is was decided to tackle the problem by introducing some modifications to the instrument itself.

Contacts were made with the technical department at the recorder manufacturer's offices, who confirmed the observed phenomena as being inherent to the instrument's design, but they could not offer any help in suggesting a possible way of overcoming the difficulties. Consultations were also made with the design staff at the Computing Centre, Cranfield, but no specific advice could be obtained.

It was at this stage that the idea emerged of using a sinusoidal signal, injected simultaneously with the inputs to both channels, as a reference or marker to determine the real phase error introduced by the multiplexing process. The implementation of this idea and its application to the automated phase correction of recordings through signal processing software is the subject of an article submitted for publication (23) to the Institute of Physics, Bristol.

The minor modification to the input preamplifier circuit board of the transient recorder was conducted under the direct advice and supervision of Mr. B.Moffitt, head of the Instrumentation Section of the Department, and figure 2.2 shows a diagram of such modification.

A consequence of injecting the same signal to both channels is the danger of introducing cross talk, but the values of the resistors used for the modification were chosen to ensure a maximum cross talk figure of 1:100 (-40 dB), a value in line with the signal-to-noise ratio for the instrument. In other words, the modification was carefully planned to ensure that the transient recorder performance would not be impaired.

The description of the actual manner in which the reference signal is used to correct the phase errors is included in section 3.2.4, within the discussion of software development.

A further practical problem encountered was an accentuated distortion of the phase spectra from recorded signals which was attributed to aliasing. Although this is a problem common to all digital sampling and storing devices, it had been expected that the drop in gain from the amplifiers beyond 2 MHz, combined with the electric impedance loading imposed by the cables and the lower sensitivity of the transducers for high frequencies, would have reduced aliasing to a neglectable level, and experimental evidence in terms of amplitude spectra supported these expectations. However, when taking phase into consideration it was found that considerable distortion made interpretation of the data difficult.

In order to correct the situation, two low-pass filters were designed and constructed. These consisted of seven poles, six zeroes elliptic filter R-C circuits, with a specified band rejection of 70 dB (achieved over one octave), and maximum ripple of ±1 dB over the whole low-pass frequency range.

The design method was found in a technical article published in Electronic Design News, March 1982. Although the article is actually dedicated to the design and construction of active filters, some considerations on the difficulties of obtaining integrated op-amps capable of working within the frequency range of 2 MHz, and the insertion losses to be expected from passive versions of the networks being outweighed by their simplicity of construction, led to the decission in favour of the passive filters. Figure 2.3 shows the circuit diagram for the filters together with a table of component values, corresponding to a cut-off frequency of 2 MHz, and an electric impedance of 500 Ω which was chosen as a good compromise for obtaining sensible inductor values without overloading the preamplifiers.

The inductors were built with high performance ferrite cores, hand wound to the calculated inductance values, and individually calibrated with both an impedance bridge and a Q-meter. After assembly, the filters were tested to obtain their frequency response, and it was found that tolerances in the components combined with value adjustments forced by the use of standard commercial capacitors produced corner frequencies greater than 2.5 MHz.

Subsequently, the filters were adjusted to obtain cut-off frequencies of ∿ 2.3 MHz, and matched phase characteristics. Figures 2.4 and 2.5 show the calibration curves for both filters in terms of amplitude in linear and log scales, and phase in degrees.

Other pieces of circuitry also developed through the project included impedance matching amplifiers to drive capacitive type transducers, and a short-pulse generator to be used as excitation source during the calibration of transducers, but these are reviewed in those sections directly related to their function.

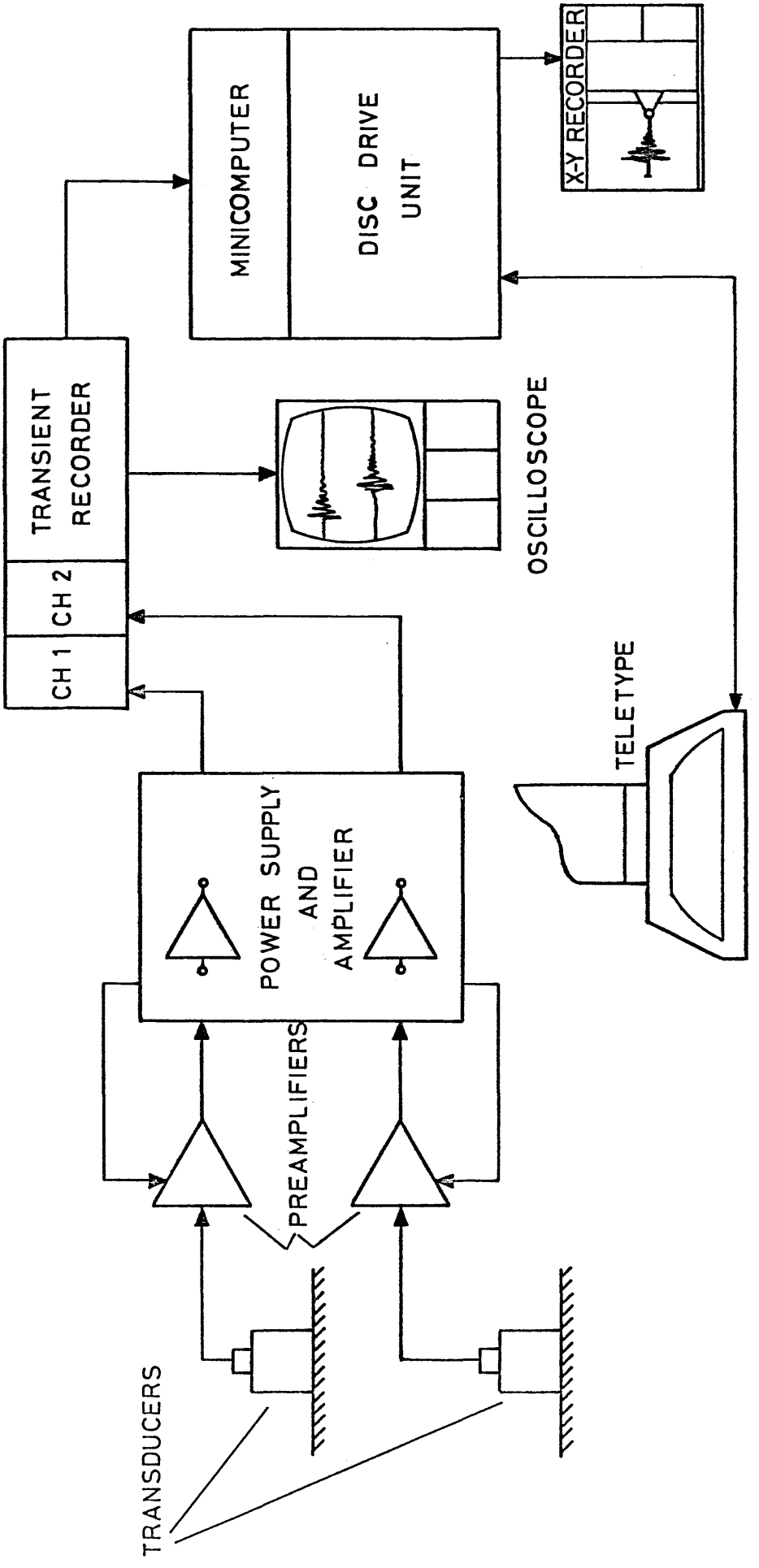

Fig 2.1- Instrumentation block diagram.

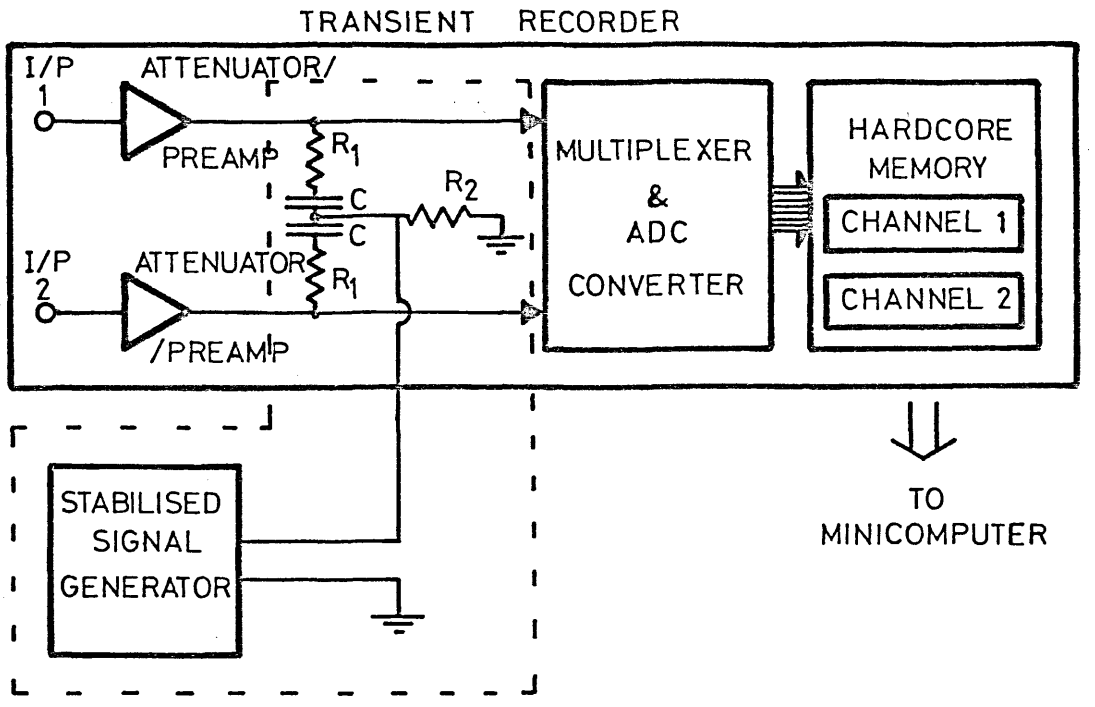

Fig 2.2- Block diagram showing the modification introduced to the recorder. The actual component values used for the present case were R_1 = 4700 Ω, R_2 = 47 Ω and C = 0.015 μF.

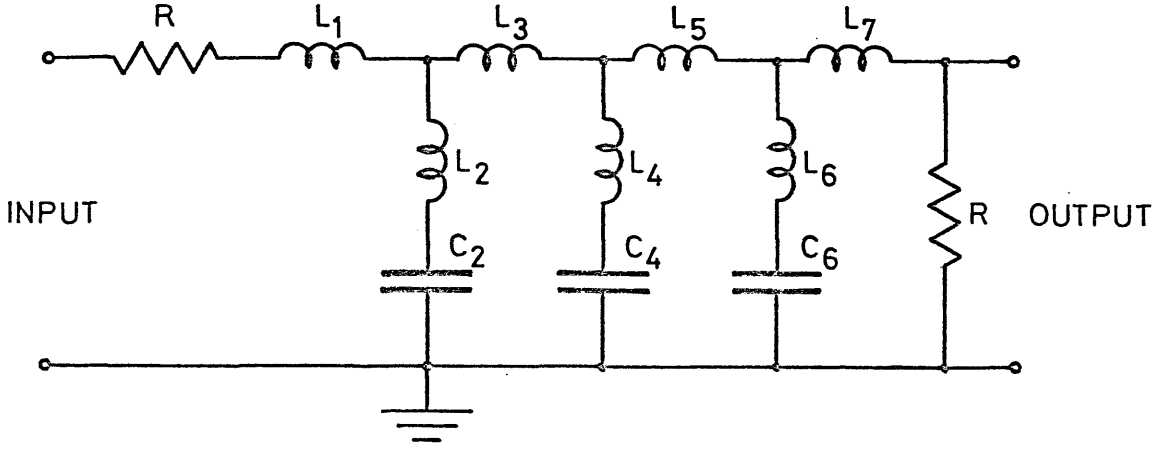

Fig 2.3- Anti-aliasing filter diagram.

Component values:	R = 500 Ω	L_1 = 37.2 μH
C_2 = 129 pF	L_2 = 5.64 μH	L_3 = 43.06 μH
C_4 = 121 pF	L_4 = 12.39 μH	L_5 = 42.36 μH
C_6 = 120 pF	L_6 = 10.22 μH	L_7 = 36.28 μH

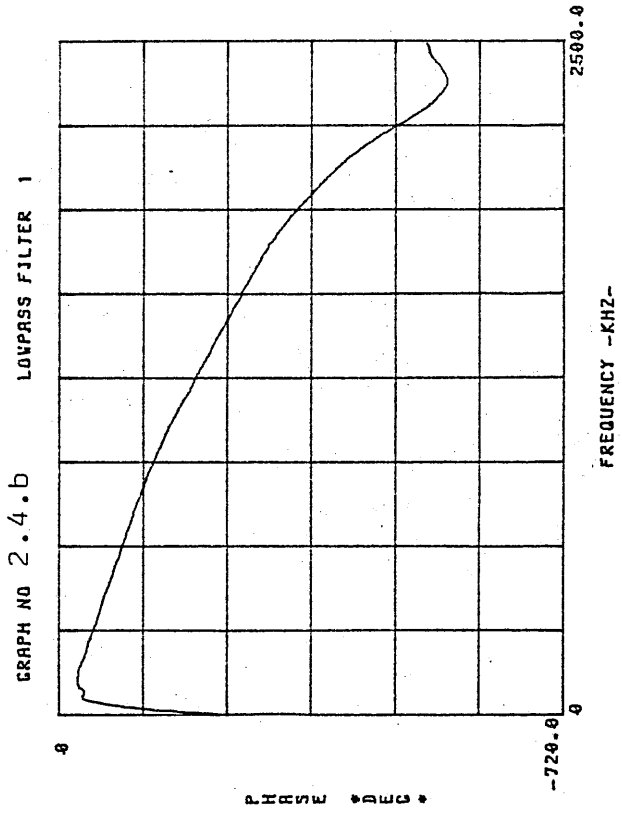

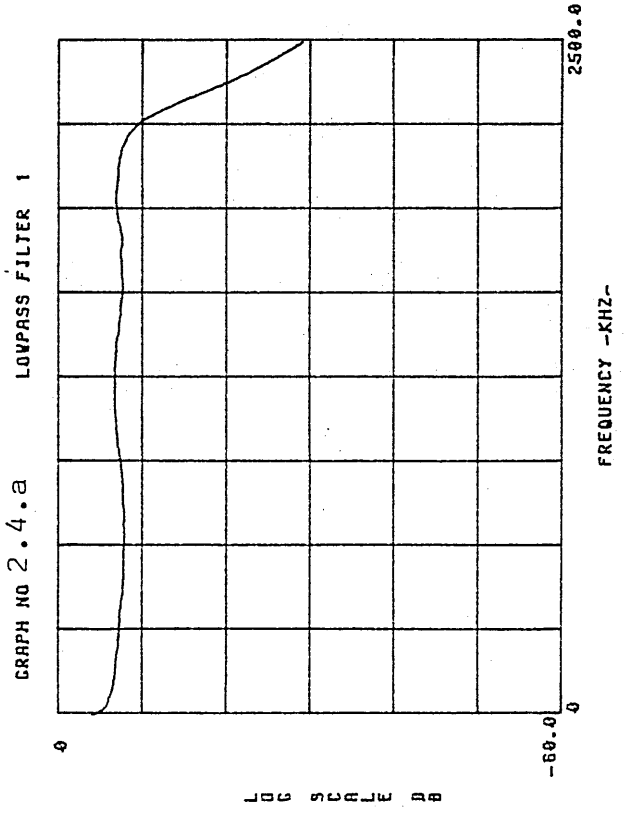

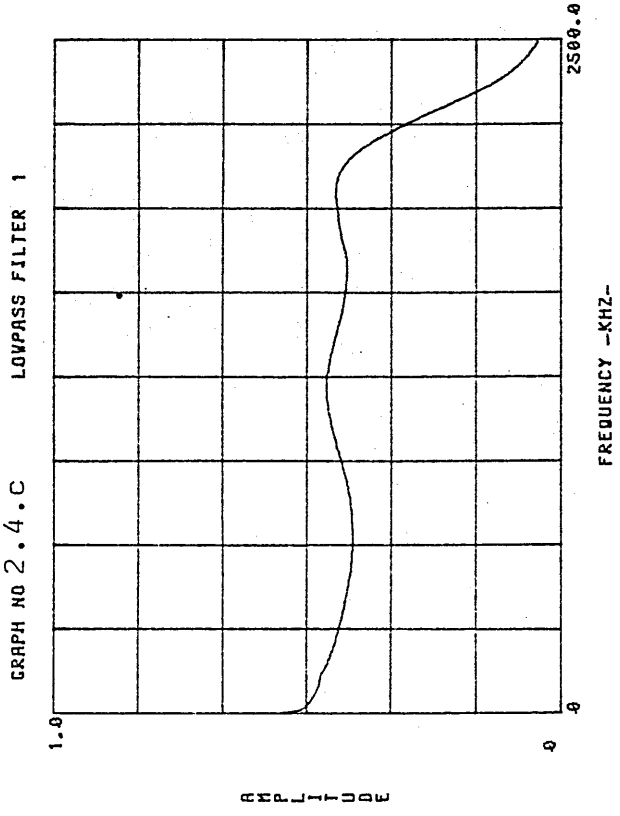

Fig 2.4- Anti-aliasing filter calibration.

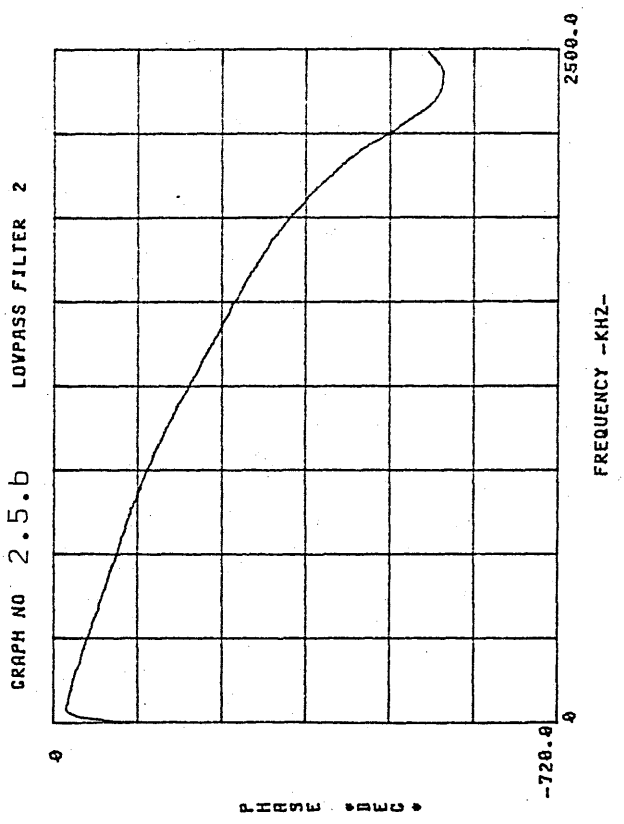

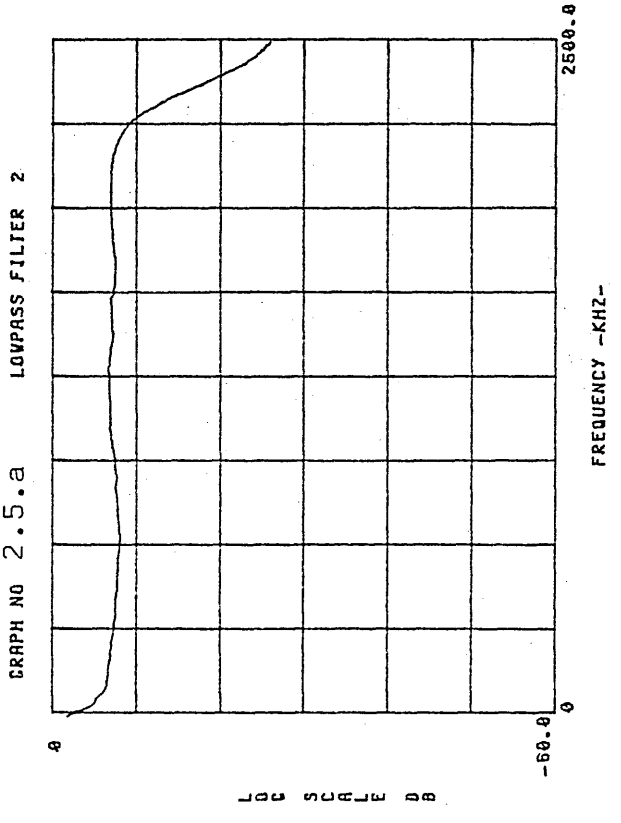

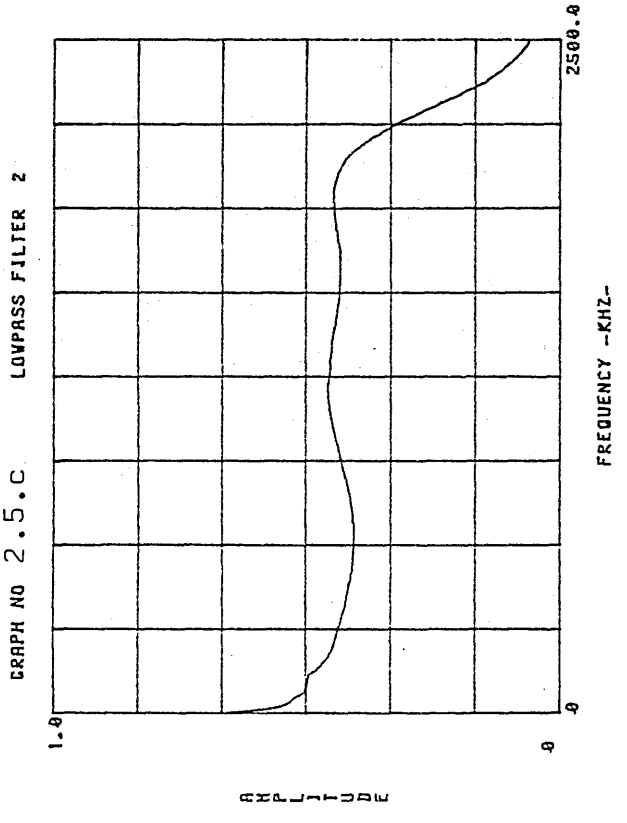

Fig 2.5- Anti-aliasing filter calibration.

DATA PROCESSING SOFTWARE

Due to the experimental character of this project and the methods employed for data acquisition, the amount of calculations involved in the gathering and processing of information is immense. For example, consider the record length of a single signal stored with the transient recorder, it is clear that any calculation performed with such information will involve a minimum of 2048 operations. This fact coupled with the repetitive nature of the calculations make the processes involved an ideal subject for automation through the use of a computer, and the display and analysis of information suited for graphic methods.

Software specially designed for the analysis of mechanical vibrations was made available at the beginning of the project, however the main emphasis was made upon the calculation of power spectral densities, coherence, and correlation functions which are not suited to the processing of AE data. Close examination of the options offered by the package of programs available showed that the only useful function would be the Fourier transform of raw data. Consequently, it was decided to prepare a complete new set of programs, self standing and specially designed for processing and analysing AE data, using the utility subroutine package acquired with the computer.

The literature studied for this section of the work included two books by K.G.Beauchamp (25) (26) on digital signal processing and the applications of the Walsh transform, and a compilation of papers on digital signal processing (27), published in 1972.

Since the memory requirements for the complete processing of the experimental data in a single program would have by far exceeded the capacity of the minicomputer, the software was therefore structured, each program being a self standing unit, capable of handling all required data to and from the magnetic disc cartridge. The programs were designed to be run in sequence and under an interactive mode of operation, under the control of the user via the teletype terminal.

This structure and mode of operation combination provides maximum flexibility, although requiring constant attention of the operator to reply to the requests appearing on the terminal.

All data processing programs contain plotting facilities basically intended for the monitoring on a storage oscilloscope of all processing steps, and a separate plotting program was provided with a very wide choice of options to allow easy handling for the display of results.

The techniques constituting the basis of the software are by now quite standard, and it is therefore considered that a detailed discussion of the theoretical background to the algorithms used would be redundant. However, a detailed account of this mathematical background was presented as an internal progress report (28),which contains all aspects regarding digital conversion, Fourier and Walsh analysis relevant to the software.

A functional description of programs and subroutines is nevertheless included to illustrate the facilities available, and to clarify some of the calculation methods employed which would otherwise stand undefined.

3.1 SUBROUTINES

These cover some calculations or data processes which are run several times within the same program, or are common to several programs, thus lending themselves to be organised as subroutines.

Although the most efficient use of computer time and space is achieved with ASSEMBLER language, the routines were programmed in FORTRAN because of the possessed level of experience with this typical engineering language.

3.1.1 SCALE

As its name suggests, this subroutine scales the vertical

axis of coordinates of plot grids based upon the maximum and minimum values of the data to be plotted. The data limits are rounded to the second most significant digit, thus ensuring that at least 80% of the range is used by the plot. A scaling factor is also calculated as a power ot ten so that the largest of the two limits can be adjusted to range between 10 and 99, scaling the smaller limit accordingly.

3.1.2 SMOOTH

This routine performs the smoothing of data through the application of a triangular or Hanning smoothing function, whose width can be specified to be 3, 5, 7, or 9 points.

The smoothing function can be described as a weighed average carried over the points surrounding the one being smoothed, and mathematically defined as

$$x_k^s = \frac{4}{(n+1)^2} \sum_{j=k-\frac{n-1}{2}}^{k+\frac{n-1}{2}} \left(\frac{n+1}{2} - [j-k] \right) x_j$$

for k = 1,2,3,....,N

where n is the odd integer defining the smoothing window width.

For the extremes of the data block, the weight of the non-existing points is added to that of the central point in the window.

3.1.3 SMTH

This routine also performs the smoothing of data, by applying a rectangular smoothing window, and it is basically intended for use on spectra with gentle slopes, such as those obtained in the calibration of amplifiers.

The window width can be selected to be any odd number of points, and can be sectionally changed over the same data block.

3.1.4 WALSH

As its name suggests, this routine calculates the raw Walsh transform from any input data series. It consists of basically the FORTRAN version of a BASIC subroutine given in reference (26).

The algorithm requires (N+N/2) memory locations to perform all the calculations over N data points, given in normal order, and the transform coefficients are also produced in normal order.

No scaling factor is included within the routine because this allows it to be used for calculating both direct and inverse transforms, leaving the scaling factor to be included in the master program.

3.2 PROGRAMS

As already explained, these were designed for sequential use, depending upon the functions desired. The options covered include the transfer of data from the transient recorder and its permanent storage on magnetic disc; the FFT of data both in terms of amplitude and phase or raw Fourier coefficients; the calculation of transfer functions; the ensemble-average of data spectra, either in terms of amplitude and phase or in terms of Fourier coefficients; the calculation of inverse FFT; the convolution, de-convolution, integration and differentiation with respect to time, log and anti-log scaling, and calculation of square root of spectra; the calculation of direct Walsh transform; Walsh power spectrum; and a general plotting program.

This software was initially developed over a period of about six months at the beginning of the project, but corrections, modifications, improvements and additions were necessary right up to the end of the experimental work. Because of this, although the development process is explained in some cases, the following descriptions correspond to the latest versions of the programs, and they are headed by the call name for each program.

3.2.1 DTRDTP

This program transfers data stored in the transient recorder as blocks of 2048 or 4096 integer values, converts them to floating point positive and negative numbers around the original mean value, thus removing the DC component, scaling the data in terms of the input settings for the transient recorder, and stores the resulting values in consecutive blocks of 1024 floating point numbers on a removable magnetic disc cartridge. The blocks of data are arranged in sequential order, two blocks per channel, with channel 1 stored first, and including a heading block containing the information of a label, number of channels, record length, sampling rate, input sensitivity for each input of the recorder, additional scaling factors and the corresponding physical units, and the total number of records. The header block is copied on to the output file of every program, thus preserving the information contained throughout the whole processing of the data, changing only parameters like the total number of records and header label.

3.2.2 FSPEC

This program transforms the data from the time domain to the frequency domain through a FFT algorithm included within the utility subroutine package supplied with the minicomputer.

Prior to the transformation, a selection of tapering windows can be applied to reduce leakage in the amplitude spectra by shaping the input blocks of data. The available window options include a cosine taper function, usually applied to random type data, defined as

$$W_k = \left[1 - \cos\left(\frac{5k\pi}{N}\right) \right]^2 \qquad \text{for } k = 1,2,3,\ldots,\frac{N}{10}$$

and applied through the direct product

$$x_j^W = \begin{cases} 1.07\, x_j\, W_k & \text{for} \begin{cases} j = k \\ j = N-k \\ k = 1,2,3,\ldots,\frac{N}{10} \end{cases} \\ 1.07\, x_j & \text{for } \frac{N}{10} + 1 \leq j \leq \frac{9N}{10} - 1 \end{cases}$$

where the factor 1.07 is included to compensate for the reduction of the standard deviation of a rectangular window by the taper shaping.

A Hann window is also included, which is usually applied to highly periodical data, defined as

$$W_j = \tfrac{1}{2}\left[1 - \cos\left(\frac{2\pi j}{N}\right)\right] \qquad \text{for } j = 1,2,3,\ldots,N$$

and applied through the direct product

$$x_j^W = 1.63\, x_j\, W_j$$

where the factor 1.63 is included to compensate for the reduction of the standard deviation introduced by the shaping window.

A third option included in the program is an exponential taper window, commonly applied to the analysis of transient signals, which concentrate most of the relevant information within the initial 20 to 30% of the pulse record, and either a cosine or a Hann window would cause a considerable loss of information, while an exponential window will leave the beginning of the record practically unaffected. The exponential function included in this program can be defined as

$$W_j = 10^{-\frac{dB\, j}{20N}} \qquad \text{for } j = 1,2,3,\ldots,N$$

where dB is the maximum attenuation at the end of the record, specified in decibels, and the shaping window is applied through the direct product

$$x_j^W = x_j\, W_j$$

After shaping, the data is Fourier transformed into two sets of coefficients

$$x_j \xrightarrow{FFT} \begin{cases} a_k \\ b_k \end{cases} \qquad \text{for} \begin{cases} j = 1,2,3,\ldots,N \\ k = 1,2,3,\ldots,\frac{N}{2} \end{cases}$$

corresponding to the real and imaginary components of the transform vectors

$$\overline{X}_k = (a_k + \overline{i}\, b_k) = X_k\, e^{-\overline{i}\,\phi_k}$$

The real and imaginary coefficients are combined into amplitude and phase spectra

$$X_k = \sqrt{a_k^2 + b_k^2}$$

$$\phi_k = -\tan^{-1} \frac{b_k}{a_k}$$

In order to obtain the phase angle within one single cycle, over the range $\pm 180^o$, the following equation was employed

$$\phi_k = -\frac{180}{\pi} \left[\tan^{-1} \frac{b_k}{a_k} - \frac{\pi}{2} \left(1 - \frac{|a_k|}{a_k}\right) \left(\frac{|b_k|}{b_k}\right) \right]$$

A problem did arise from the possibility of choosing the length of records between 2K or 4K points, since this collided with the aim of establishing a standard format for data processing after conversion to the frequency domain, thus it was decided to reduce all spectra to the same length of 1024 points. The reduction of amplitude spectra is based upon a criterium of energy, by preserving the energy contained within each elementary frequency bandwidth surrounding each amplitude coefficient.

Considering the kinetic energy as proportional to the square of the first time derivative

$$E^k \propto (\dot{X})^2$$

where $\dot{X}$ is the first derivative of $\underline{X}$ with respect to time, and for harmonic functions

$$E^k \propto \omega^2 X^2$$

In the case of discrete amplitude spectra, the energy can be estimated in terms of the frequency narrowband surrounding each frequency component

$$E^k = \sum E_j^k$$

$$E_j^k \propto \omega_j^2 X_j^2 \frac{\Delta\omega}{\omega_N}$$

where $\underline{E_j^k}$ is a fundamental component of the total kinetic energy,

$\Delta\omega$ is the analysis bandwidth of the spectrum, and ω_N is the Nyquist or folding frequency.

The total energy can then be estimated as the summation of all the fundamental components over the spectrum

$$E^k = \sum_{j=1}^{N} E_j^k \propto \frac{\Delta\omega}{\omega_N} \sum_{j=1}^{N} X_j^2 \, \omega_j^2$$

Considering another series X'_i representing the same spectrum but with twice the number of components

$X_j \quad (j = 1,2,3,....,N)$

$X'_i \quad (i = 1,2,3,....,2N)$

the fundamental energy component can now be written as

$$K_j^k \propto \frac{(X'_{i-1}\,\omega'_{i-1})^2 + (X'_i\,\omega'_i)^2}{2} \frac{\Delta\omega'}{\omega'_N} +$$

$$+ \frac{(X'_i\,\omega'_i)^2 + (X'_{i+1}\,\omega'_{i+1})^2}{2} \frac{\Delta\omega'}{\omega'_N}$$

$$E_j^k \propto \frac{\Delta\omega'}{2\omega'_N} \left[(X'_{i-1}\,\omega'_{i-1})^2 + 2(X'_i\,\omega'_i)^2 + (X'_{i+1}\,\omega'_{i+1})^2 \right]$$

where $i = 2j$.

Equating the expressions for the fundamental energy component in function of the two spectra:

$$\frac{\Delta\omega}{\omega_N} (X_j\,\omega_j)^2 = \frac{\Delta\omega'}{2\omega'_N} \left[(X'_{i-1}\,\omega'_{i-1})^2 + 2(X'_i\,\omega'_i)^2 + (X'_{i+1}\,\omega'_{i+1})^2 \right]$$

where
$$\begin{cases} \omega_j = j\dfrac{\omega_N}{N} \\ \omega'_i = i\dfrac{\omega'_N}{2N} \\ i = 2j \\ \omega_N = \omega'_N \\ \Delta\omega = 2\Delta\omega' \end{cases}$$

Rearranging and simplifying

$$X_j = \frac{1}{j}\sqrt{\frac{1}{16}\left[X'_{2j-1}(2j-1)\right]^2+\frac{1}{2}\left[X'_{2j}(j)\right]^2+\frac{1}{16}\left[X'_{2j+1}(2j+1)\right]^2}$$

This last equation allows the calculation of the amplitude spectrum coefficients in function of a spectrum with a double number of coefficients.

In relation to phase, only the even indexed coefficients are used in the reduced spectra

$$\phi_j = \phi'_{2j} \qquad \text{for } j = 1,2,3,\ldots,N$$

3.2.3 TRFUNC

This program calculates transfer functions in terms of amplitude and phase, through a frequency domain de-convolution of input and output signals, by dividing the amplitude spectra and subtracting the phase spectra.

Both input and output signals have to be sampled and stored simultaneously in order to preserve their phase relationship. However, this is not possible with most digital sampling and storing systems, and a relative time delay between the two records is introduced by a multiplexing process over the inputs to the recording device. This relative time delay should ideally be constant and equal to half the sampling interval for each record.

The effect of such a delay is the introduction of a relative phase shift between the two records which is proportional to frequency, being equal to 0^o for zero frequency, and reaching its maximum value for the Nyquist or folding frequency. For an ideal system, this maximum phase shift equals 90^o.

This can be illustrated by inputting the same signal to both channels of the transient recorder, and calculating the phase difference between the two records. Since the records correspond to exactly the same signal, the real phase difference is zero. However, because of the multiplexing between the two inputs a phase shift is always detected. Figure 3.1 represents a typical result.

Initially, a constant phase correction procedure was provided within the present program, but experimental results showed that the phase shift introduced by the transient recorder varied at random both in magnitude and sign. This means that not only did the multiplexing delay change from record to record, but also the recording process could start by sampling the first point from either channel, thus invalidating the provided correction procedure.

The fact that accurate phase measurements are of capital importance for the achievement of the calibration of transducers to be applied to signal de-convolution, imposed the satisfactory solution of this problem as pre-condition to the development of the project. As explained in section 2.3, a solution was achieved by injecting a highly coherent signal to both channels of the recorder, simultaneously with the experimental signals, to serve as a phase reference or marker.

In order to avoid interference between the experimental and reference signals, the latter was chosen to be a pure sine wave, having a frequency well above the anti-aliasing filters cut-off and lower than the Nyquist frequency for the sampling rate used.

The reference signal was initially adjusted to have a frequency of 4MHz while the anti-aliasing filters bandwidth was 0-2.3MHz, and the data was sampled at 10MHz per channel. However, some interference generated distortion was noticed on the experimental signal spectra at 2MHz, corresponding to a $\frac{1}{2}$ frequency sub-harmonic of the reference tone, and after several tests it was found that the interference could be reduced to unnoticeable levels by increasing the reference signal frequency to 4.5MHz.

For the development of the correction procedure, recordings were made of the same signal through both channels of the recorder, together with the reference tone, a typical time history of which is shown in figure 3.2. The records were then frequency analysed and the corresponding amplitude spectrum is shown in figure 3.3, where the reference tone component is clearly identified.

Polar maps of the FFT's for both channels were then produced as shown in figures 3.4.a and b, where the sudden increase in amplitude marked with points 1,2,3,4, corresponded to the vector of the phase reference tone, and the angle between the vectors from the two maps indicated the phase shift introduced at the multiplexing stage of the recording process.

The correction algorithm begins by printing a request on the teletype for the user to input the approximate value of the reference signal frequency. A search for the corresponding amplitude peak is then performed on the amplitude spectrum from one channel, over a frequency range of ± 10% of the given value, and once located, the detected frequency component is verified by searching over the corresponding phase spectrum for a sharp change of approximately 180^{o}, which has to occur within the next component at either side of the detected peak amplitude. This can be observed from the sequence of the points along the polar maps of figures 3.4.a and b.

After verification, the phase difference between the two channels for the reference tone component is taken to define the phase correction ramp which starts at 0^{o} for zero frequency. In the case of the same signal being recorded through both channels, the application of the correction ramp produces, as expected, a constant phase spectrum at 0^{o}. This is illustrated in figure 3.5 which corresponds to the corrected phase spectrum from figure 3.1, where the random mid-section is caused by the absence of signal components past the anti-aliasing filters cut-off.

The correction of the phase spectra in this way increases the range of variation of the data to more than one cycle, thus necessitating the re-cycling of the angle values within the same limits before any ensemble-averaging can be attempted.

After correction and re-cycling, the data records stand ready for averaging or further convolution or de-convolution processes. And finally, the program also includes an option for trend-shifting of the phase data, in case it is desired to obtain a single continuous curve when phase covers more than one cycle.

3.2.4 AVRGE

This program allows the ensemble-average of amplitude and phase spectra once corrected, and its subsequent smoothing by means of a triangular or Hanning window function, provided by the SMOOTH subroutine.

The program worked satisfactorily when averaging amplitude spectra, and smooth phase spectra varying over a small number of cycles. However, phase results seemed to degrade when phase spectra with steep slopes were averaged. This was attributed to the phase being an ill behaved function when at least one of the real or imaginary components is small, making it most sensitive to random noise present in the recordings.

To overcome this problem, it was decided to prepare a new program to perform the averaging process over the real and imaginary Fourier coefficients.

3.2.5 AVCOEF

This program performs the ensemble average of amplitude and phase spectra by transforming these back to real and imaginary Fourier coefficient sets, averaging and smoothing the coefficients, and converting the results back to amplitude and phase spectra. The option of trend-shifting the phase data was also included in the program.

The results obtained this way showed a far greater consistency, although the time involved in the calculations was considerably longer.

3.2.6 PROCES

This program was designed as a general utility aid for the processing of data in the frequency domain, after the phase has been corrected. Since no further corrections should be necessary, the algorithms involved are relatively simple, thus allowing the assembly of a considerable number of functions within the same program.

The available options include frequency domain convolution (or de-convolution) through the direct product (or division) of the amplitude spectra, and the addition (or subtraction) of the phase spectra; the integration or differentiation with respect to time, by dividing or multiplying respectively the amplitude coefficients by their corresponding frequency, and shifting the phase spectra in $+90^{o}$ when integrating or -90^{o} when differentiating; the smoothing of spectra with a rectangular window whose width can be changed for different sections of the data; the calculation of the square root of spectra by reducing the amplitude coefficients to their square root value, and halving the phase angle values; the conversion of amplitude spectra to absolute logarithmic scale and vice-versa; the linear interpolation of amplitude and phase spectra to reduce the frequency range to half the original bandwidth while retaining the same number of components; and a copying routine for duplicating or editing data files, either within the same disc cartridge or for transfering data between two cartridges.

3.2.7 INVFTR

This program calculates the inverse Fourier transform from amplitude and phase spectra, in order to reconstruct the time history of de-convoluted signals for further analysis purposes.

The amplitude spectra can be either in linear or logarithmic scale, and if a reference value has been used to calculate the spectra in relative logarithmic scale, the same value can be re-introduced in order to recover the original signal magnitude.

Another feature included is the possibility of low-pass filtering the spectra prior to their transformation, thus allowing the removal of the phase reference tone from the reconstructed signal.

3.2.8 WTRANS

This program calculates the Walsh transform of data in the time domain, by use of the subroutine WALSH, described in section 3.1.4.

The program presents a limitation in the sense that only two spectra of 1024 points each can be stored as results of the transform, and therefore only 2048 input data points are required for the calculations. When the records from the transient recorder are 4K points long, only the first 2K are used in the calculations, and the second half of the record is therefore lost.

Although the Walsh transform seems to have considerable potential as a signature analysis tool applicable to AE studies, the results of the transform itself are most dependant on the phase from the original signal. The effects of phase upon the resulting transform are so marked that the raw spectra from a single sinewave may look completely different for records having different phase shifts. Also, changes in the magnitude of the signal will result in differences for the transform distributions.

A reduction in the sensitivity of Walsh transforms to changes of magnitude or phase in the input signal is achieved by calculating a power spectrum from the raw Walsh coefficients, and an additional program was prepared to this purpose.

3.2.9 WPSPEC

This program calculates the Walsh power spectrum of data recordings by applying the Walsh transform, and then recombining the raw transform coefficients into power spectrum components.

Effectively, there are three alternative methods for the calculation of Walsh power spectra:

- An indirect method using the "dyadic" (logic time scale) auto-correlation function (equivalent Wiener-Khintchine method)
- A direct evaluation method, via the squared values of Cal and Sal coefficients from the raw Walsh transform (equivalent to the periodogram method for Fourier power spectrum)
- By narrow-band Walsh filtering

Only the dyadic based method is completely time invariant, but being an indirect method, it requires a considerable amount of computer time, while the narrow-band filtering method is hardware orientated.

It was therefore decided to implement the direct calculation method for the power spectrum, as being the most convenient alternative. This is also the method most widely used in engineering applications.

Once obtained, the Walsh transform coefficients are separated into the so-called Cal and Sal coefficients

$$x_j \xrightarrow{\text{WALSH}} X_j \qquad \text{for } j = 1,2,3,\ldots,N$$

$$X_j \longrightarrow \begin{cases} X_1 = Cal_0 \\ X_{2k+1} = Cal_k \\ X_{2k} = Sal_k \end{cases}$$

$$\text{for } k = 1,2,3,\ldots,\frac{N}{2} - 1$$

The Cal and Sal coefficients are then recombined to produce the power spectrum

$$WPS_0 = Cal_0^2$$
$$WPS_k = Sal_k^2 + Cal_k^2$$

One big disadvantage of the power spectrum with respect to the raw transform is the impossibility of recovering the original signal, thus making the process irreversible.

3.2.10 PLOT

This is a general plotting program, capable of producing graphs of data in the time, frequency or sequency domain, and allowing the frequency or sequency axis to be scaled logarithmically, over an integer number of cycles.

The plotting subroutines supplied with the computer, upon which the program is based, cannot include more than 1024 points per graph, and since the time domain records from the recorder are either 2048 or 4096 points long, an editing algorithm was provided, allowing the plotting of any section of the record, which calculates the maximum number of points that can be included for the range specified by the operator, scaling the position of the points accordingly.

The program scales the vertical axis automatically, in accordance with the data to be plotted, but this scaling can be over-ridden by inputing new grid limits from the terminal, and since the program was intended for general use, new captions for the graph, horizontal and vertical axes have to be specified for every plot.

3.3 SOFTWARE TEST

The programs were progressively assembled, de-bugged and corrected by comparing their performance against analogue measurements whenever possible.

A single test which established the performance of most programs within the package consisted of the calibration of some simple R-C networks, and amplifiers from the instrumentation.

In the case of AE preamplifiers, a random noise source was used to produce the basic signal for the calibration process. A linear attenuator was connected in series to the input of the amplifier, and the signal going into the attenuator was recorded simultaneously with the output from the amplifier. The signals were then processed to calculate the transfer function of the amplifier, repeating the process a number of times to ensemble-average the results, with the aim of reducing the random signal effects on the spectra. The results of such a calibration are displayed in figures 3.6.a and b, which were achieved after approximately six hours work.

As a basis for comparison, a manual calibration for the pre-amplifier was performed using a sine wave generator, connected in

series with the preamplifier, while both input and output signals were displayed simultaneously on an oscilloscope, from which measurements of amplitude and relative phase were made. This manual calibration involved measurements for sixty-two different frequencies ranging from 50KHz to 2MHz, taking several days work, and the results are displayed in figure 3.7.

The discrepancy of about 6 dB between the manual and computerized amplitude calibrations is due to the insertion of the linear attenuator, which has an electric impedance of 75Ω instead of 50Ω for the rest of the instrumentation.

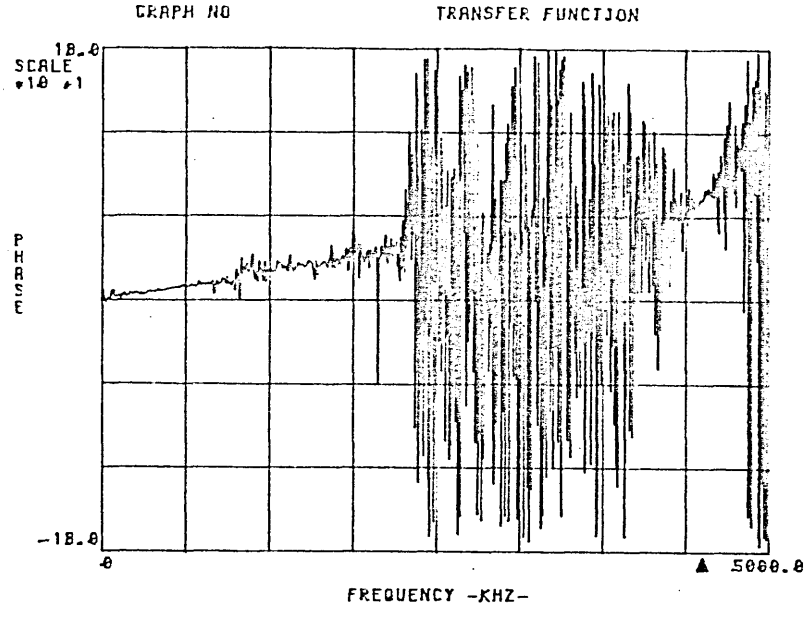

Fig 3.1- Phase difference between the simultaneous recording through channels 1 and 2 of the transient recorder, for the same signal.

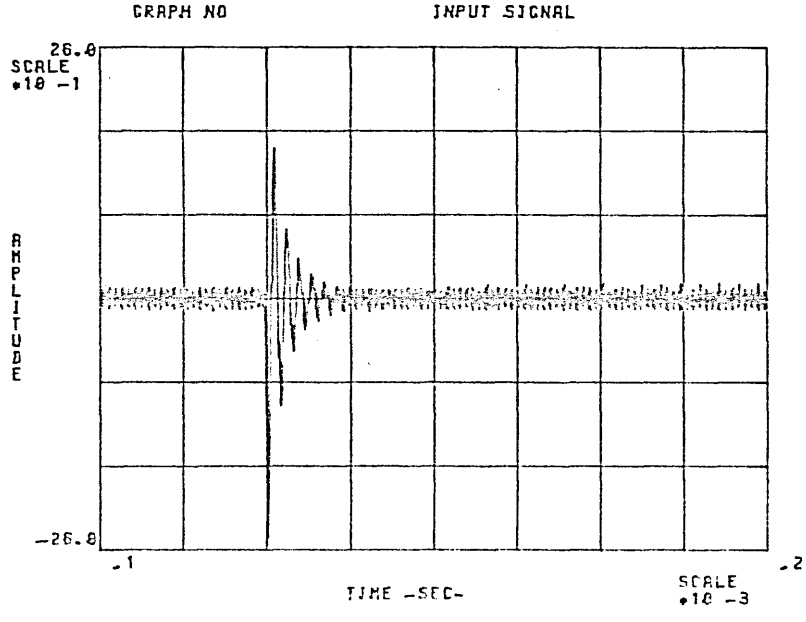

Fig 3.2- Time history of signal fed into both channels of the recorder, showing the phase reference tone.

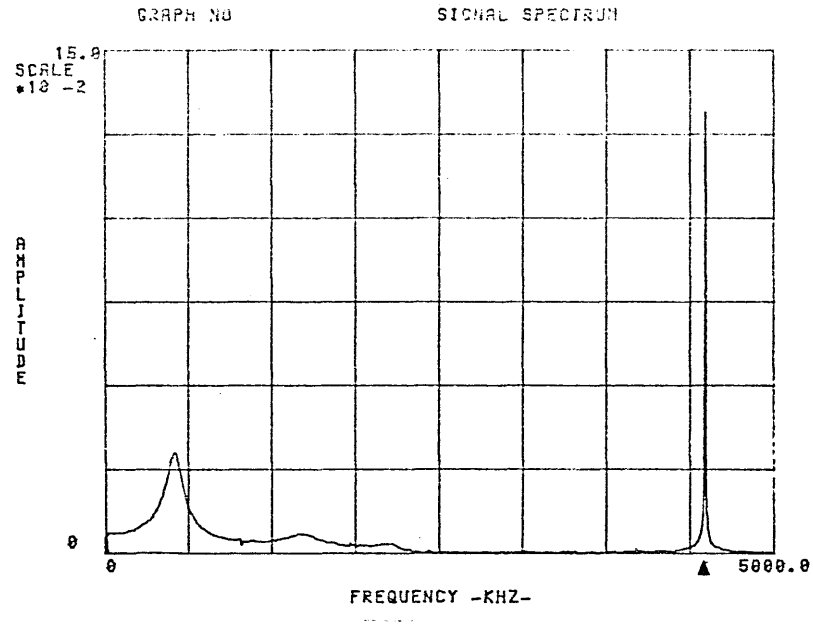

Fig 3.3- Amplitude spectrum from the record shown in Fig 3.2. Note the phase reference tone component.

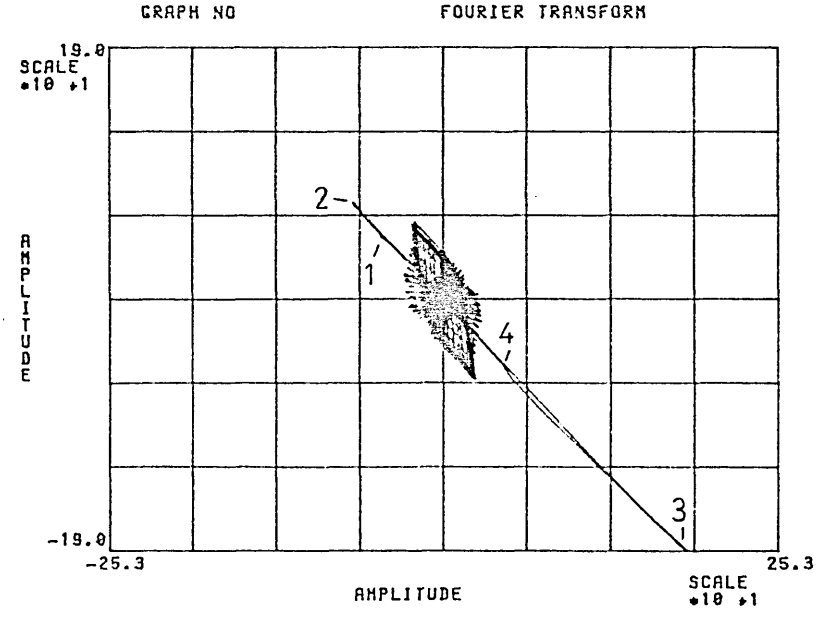

Fig 3.4.a- FFT polar map from the signal shown in Fig 3.2, as recorded through CH 1.

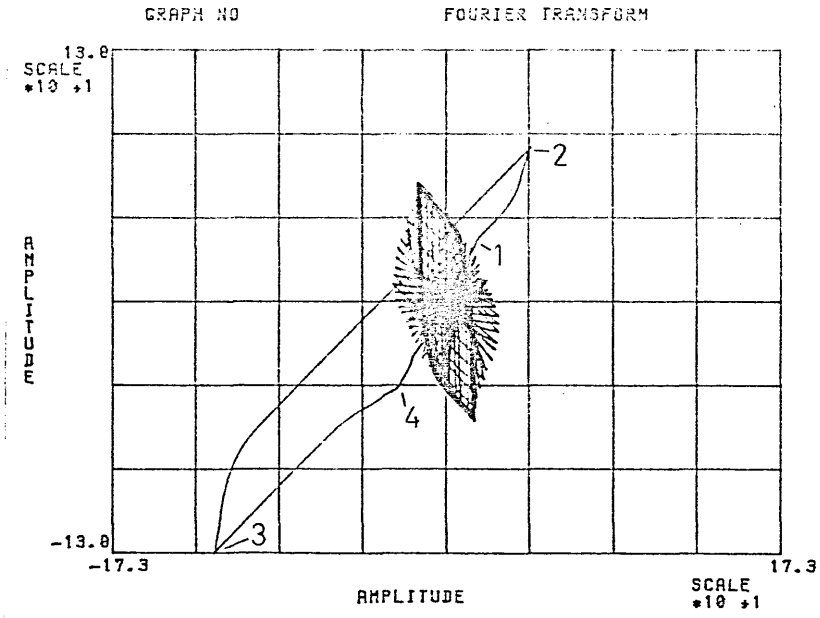

Fig 3.4.b- FFT polar map from the signal shown in Fig 3.2, as recorded through CH 2.

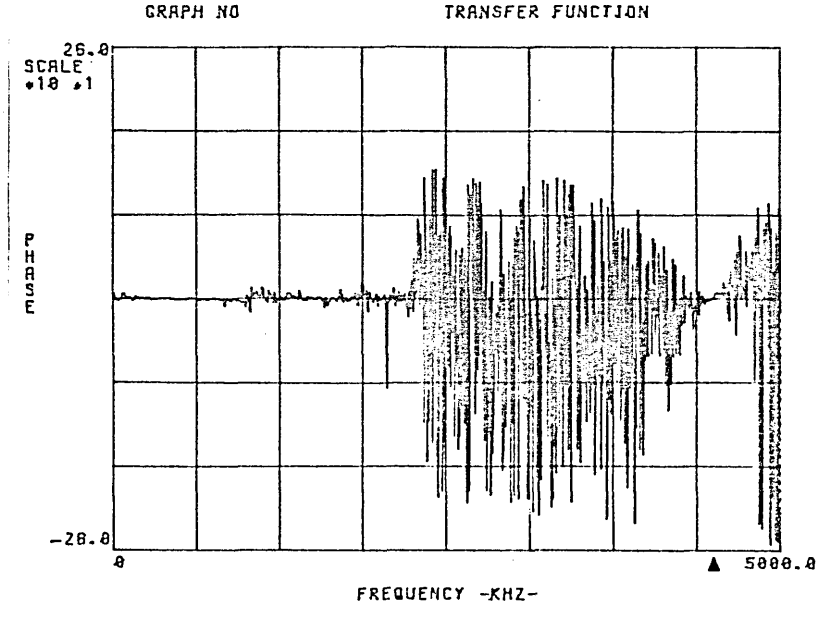

Fig 3.5- Phase difference between the records of CH 1 and CH 2 (shown in Fig 3.1), after applying the correction.

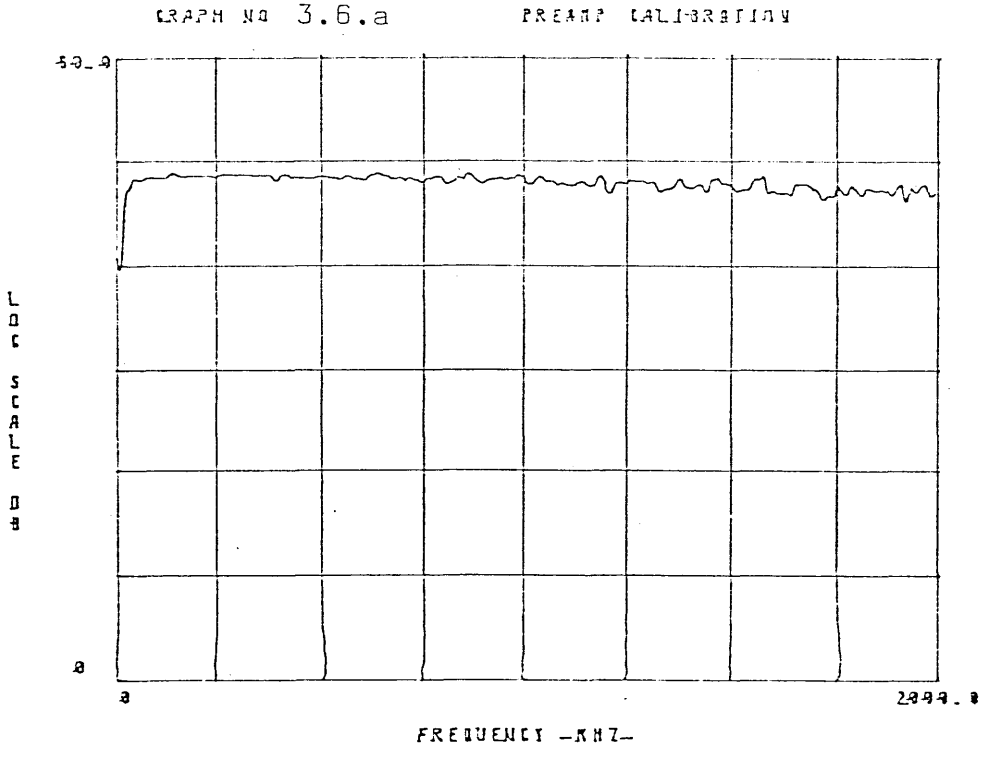

Fig 3.6.a- Amplitude calibration of AE preamplifier.

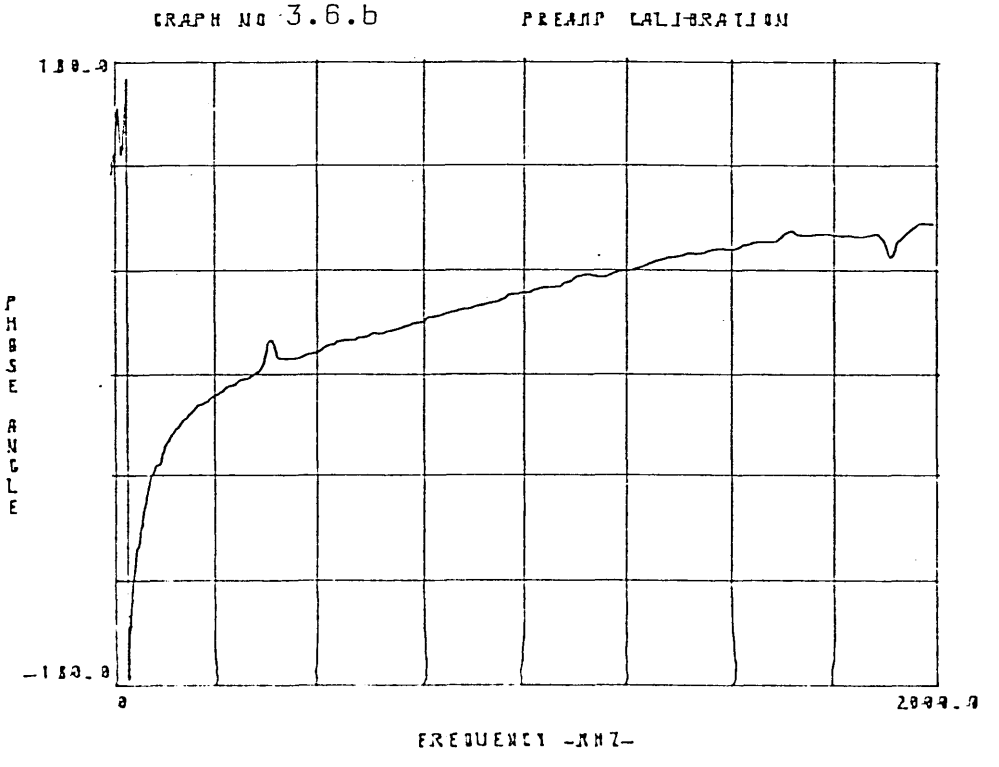

Fig 3.6.b- Phase calibration of AE preamplifier.

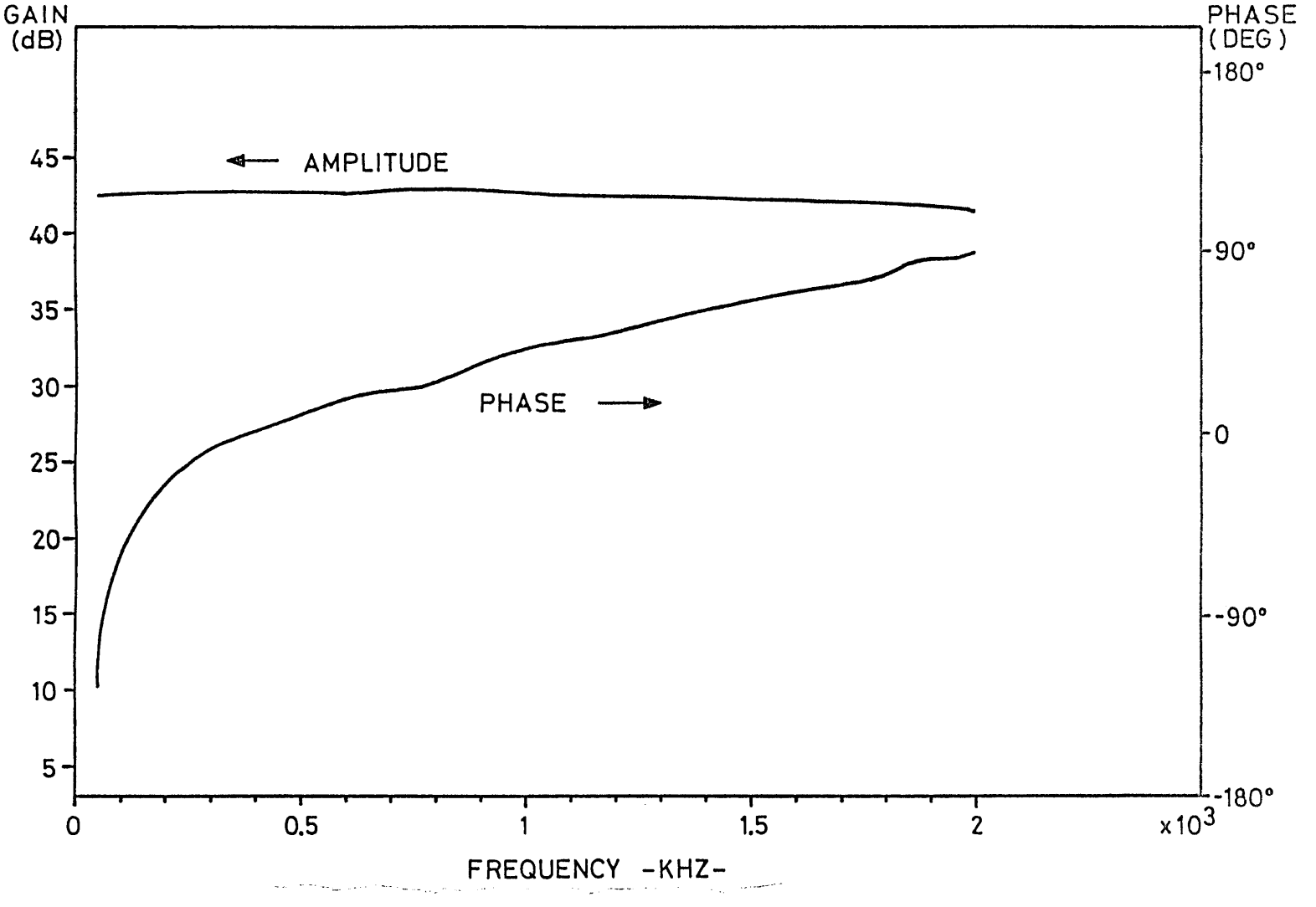

Fig 3.7- Amplitude and phase calibration of AE preamplifier obtained through analogue measurements.

EXPERIMENTAL MODEL

The study of published literature and specifications for commercial transducers during the initial phases of the project, underlined the lack of consensus for a particular method of calibration, and considerable confusion caused by the different standards of specification, adopted by different equipment manufacturers. This background supported the belief that no serious study of AE signature analysis could be undertaken before a number of fundamental questions were answered, regarding the calibration procedures to be used and other factors likely to influence the AE signature, for example transducer/specimen coupling effects, type of excitation to be used during the calibration of the transducers, and type of waves to contribute to the transducer response.

Another aspect which was considered to be of great importance in the practical application of AE to mechanical engineering problems, was the study of the transformation suffered by the surface wave pulses while travelling along a mechanical structure, especially across the interface between components.

However, the calibration of transducers was considered to be of fundamental importance, and therefore it was decided to build the first of a number of experimental rigs with the express purpose of developing and calibrating new transducers.

The provision of such a calibration bench can be divided into two aspects: the construction of a suitable physical model to function as a specimen, onto which the transducers would be mounted, and the development of a suitable source of excitation to simulate AE activity.

The progressive access to published literature dictated the configuration of the model to be constructed, and the modifications and subsequent additions to be made. However, throughout the whole development of experimental models and methods, great importance was given to the consideration that whatever system should emerge from the research program, it should be sufficiently simple to be implemented within an

industrial environment, so that general users could provide themselves with the necessary calibrations performed "in situ".

4.1 LITERATURE SURVEY

Among the literature available since the earliest stages of the project, two papers by L.G.Graham and G.A.Alers (20) (29) were found to describe one of the first methods for the calibration of AE transducers, together with the rig configuration, consisting of a "white noise generator" achieved by grinding fine particles of silicon carbide with a rotating fused silica rod.

The quality of such an excitation source was assessed by using a capacitive microphone, whose response spectrum showed the amplitude to be inversely proportional to the square of frequency. Since the output of a capacitive microphone is linear with displacement, its output analysis indicated the noise source to have a flat acceleration spectrum.

The analysis of the output from piezoelectric transducers showed a trend inversely proportional to frequency, thus, disregarding resonance effects, the piezoelectric transducers output could be considered basically proportional to velocity. This conclusion is of considerable importance in the understanding of the mode of operation of piezoelectric transducers when working at frequencies close to their resonances, and it has been corroborated and applied by most workers in this field.

Another paper also obtained during the early stages of the project was the report by S.L.McBride and T.S.Hutchison (30), in which an alternative means of calibrating transducers is proposed by using a jet of helium gas, sprayed through a capillary tube, to excite an aluminium block and thus generate a prime excitation which is monitored with the transducer under calibration.

The actual calibration was achieved by making a comparison with a standard, which consists of an X-cut quartz crystal disc, with fundamental frequency at 5 MHz, and considered to have a flat frequency

response up to 1 MHz; while the amplitude spectra were obtained by using a sweep frequency analyser.

The output from the standard transducer showed a trend inversely proportional with frequency, from which the gas jet is regarded as a white noise source in terms of acceleration.

Although the method represents an original alternative to previous methods of calibration, the reliance upon a quartz transducer as primary standard, without presenting absolute evidence of its frequency response, was seen as a major weakness. Nevertheless, at the time of this literature survey, the method was considered to have some potential for comparing other calibration methods.

With few exceptions, most of the additional literature consulted indicated a growing concern with regards to the use of continuous means of excitation for the calibration of transducers, since it was felt that such a type of excitation might produce responses with differences from those generated by events of transient character. Indeed, this concern is well founded since it is a well known fact that the resonant response of systems to the excitation of any of their modes will build up progressively, achieving the maximum peak amplitude after a finite time interval. Thus it is most logical to expect a continuous excitation to produce an emphasis of the transducer resonances.

However, transient means of excitation for AE transducer calibration could not be introduced until adequate signal storage and analysis facilities were made available for the frequency range involved, such as the modified video recorder used by Graham and Alers, or the periodic spark excitation system first proposed and used by R.L.Bell (31) from Dunegan/Endevco. At the time of this report being published, Dunegan/Endevco were still supplying their transducers with a calibration curve obtained with a back-to-back calibration method, using an ultrasonics transducer to generate a continuous type of excitation, and the newly proposed method based around the electric spark was the first attempt by commercial transducer manufacturers to depart from calibration

methods using continuous means of excitation, although these methods continued being employed by some manufacturers at least until 1979.

In his report, Bell discusses the existing calibration techniques for piezoelectric transducers, which are of a continous type with the exception of a drop ball calibration bench used for accelerometers. The drop ball method, although of a transient nature, produces excitations with a duration far too long to detect frequencies higher than 10 to 20 KHz.

A method using an electric spark discharge as prime source of excitation is thus proposed, accompanied by the configuration of a suitable calibration bench. The system consisted of a bar which could be made of either aluminium or steel, with a rectangular section of 38.1 x 12.25 mm^2 (1.5 x 0:5 in^2) and a length of 1.47 m (5 foot), which constituted a grounded electrode, while a second electrode was driven by a relaxation oscillator. The air gap between the second electrode and the bar sets the dielectric breakdown voltage for the spark to occur, and the value of the components in the driving circuit control the charging time interval, and thus the frequency of the discharge, and its duration.

The system was reported to possess high repeatability, and a modified version is currently being used for the calibration of commercial transducers. Because of this, and its relative simplicity, the system was adopted as the initial configuration for the experimental rig to be built.

During the construction of the rig, a one day seminar offered by Dunegan/Endevco was attended, during which some interesting discussions with Dr. A.Pollock (a member of the firm's research team) were possible. The seminar covered the development of new calibration techniques being implemented at the time, described in a technical report by C.Feng and R.M.Whittier (32), also from the same firm.

This report was helpful for, besides the contained technical information, it drew attention to a paper published by F.R.Breckenridge et al (22), which is widely accepted as a classic among reports

on AE transducer calibration. Until then, this work by Breckenridge et al had not been noticed mainly due to the title being somewhat misleading, although it had appeared listed within the initial computerized literature search obtained through the Central Library, at Cranfield.

In these last papers (22) (32), a new configuration for calibration benches was proposed, based upon a large block of steel acting as a semi-infinite body model, for which mathematical modelling techniques had been developed by H.Lamb (36), and numerical solutions for surface wave displacements were obtained by C.L.Pekeris (37), in terms of localized step function force excitations. The numerical solutions obtained by Pekeris were presented in a normalized form, so they can be applied to physical models, provided the original hypotheses of homogeneity and isotropy for the model are complied.

A second important aspect found in these papers is the use of capacitive transducers as primary standards. Although the use of capacitive transducers had already been reported by Graham and Alers (15), and G.Curtis (33), the configuration presented by Breckenridge et al, and later adopted by Feng and Whittier, possessed novel characteristics and could be justified to have a flat frequency response with respect to amplitude, over a range far wider than any other transducer tested to the present.

A final aspect from these papers which was considered of value, was the reported use of the fracture of small sections of fine glass capillary as a means of producing a good model for step forcing functions, to provide a basis for the calibration of transducers.

A former paper in which a steel block had been used for the calibration of AE transducers had been published by W.C.Leschek (34), in which the transducers were calibrated by comparison with a standard, whose characteristic response spectrum had been previously obtained using a reciprocity based technique.

The reciprocity principle was also used by H.Hatano and E.Mori (35) for the calibration of AE transducers, while the transmission

pecimen employed in this case was a steel plate. However, the methods of excitation used in these two papers (34) (35)were of the continuous type, which produce less accurate calibrations than those obtained with transient methods of excitation.

4.2 PHYSICAL MODEL

The initial configuration for the calibration bench included a steel bar specimen, similar to that used by Bell (31), with a cross section of 38.1 x 12.25 mm^2 (1.5 x 0.5 in^2) and 1.83 m (6 foot) long, simply supported at points close to the ends, illustrated in figure 4.1.

The bar was cut from a cold drawn mild steel plate, and although it had been specified to be surface ground to a smooth finish, it was delivered with a roughness of over 5 μm rms. Lack of experience and adequate advice led to the purchase of a rather awkward piece of material, inherently unstable, and because of this,no commercial firm would accept it tobe ground to a better surface and flatness condition. It was therefore decided to have it further ground within the Institute, where the largest capacity machine available has a maximum work length of 609 mm (2 foot), and consequently the bar had to be rectified in three stages, producing small steps between the stages.

Subsequently, the bar was hand lapped with diamond compounds of 5, 3 and 1 μm particles, to remove the steps and ensure a flatness of ± 5.1 μm across the width of the bar at three sections, where capacitive transducers would later be mounted.

The rig was then provided with a Perspex cover with sealing ports, in order to enclose the bar in an inert atmosphere and thus prevent surface corrosion. However, discovery was later made of a very effective anti-corrosion protection manufactured by Castrol under the name RUSTILO 30, which produces a very thin (0.6 - 0.7 μm) but enduring coating, capable of preventing any surface corrosion over periods of more than six months without requiring re-application. When measurements had to be made, the protective coating was removed using solvents (usually acetone).

The bar specimen was basically employed for the development of both a suitable excitation source, and new piezoelectric transducers. The project plans were to also develop the calibration method around the bar specimen, but the reflection of surface waves from the sides of the bar made it impossible to obtain coherent phase measurements, and thus a new specimen had to be provided.

The alternatives for a new specimen were a large block as described in references (22) and (32), or an elastic plate, as employed by W.Sachse and A.N.Ceranoglu (38), and J.E.Michaels et al (39). Since a theoretical model for the behaviour of elastic surface waves on plates, under the excitation of localized forcing functions, had been developed by Y-H.Pao et al (40), and A.N.Ceranoglu and Y-H.Pao (41), the option posed by the elastic plate possessed all the background also existing for elastic blocks, with the added advantage of being easier to implement.

Therefore, the new specimen consisted of a mild steel plate section, with nominal thickness of 12.7 mm (0.5 in.), and a surface area of 305 x 305 mm^2 (1 x 1 $foot^2$). Since the surface of the material was considerably marked with scratches and defects, such as inclusions and cracks caused by the rolling of the raw material, the plate had to be ground until a reasonably clean surface was produced. After grinding, the plate was hand lapped to remove the grinder tracks to the limit allowed by the lapping disc, which was made of mild steel and thus it kept sticking and scratching the lapped surface. This was not a particularly grave problem because no capacitive transducers were to be mounted upon the plate, and piezoelectric transducers do not require an extremely smooth surface finish.

The size of this specimen was found to be sufficient to allow the capture of full length surface waves, generated for calibration purposes, before any side reflections distorted the phase information contained in the signals, and the calibration of piezoelectric transducers could be achieved.

4.3 SOURCE OF EXCITATION

Several methods of excitation were tested in the search of an adequate source to be applied to the calibration of transducers. Although preparations were originally made to implement a gas jet excitation source similar to the set-up described in reference (30), the idea was soon dropped in favour of transient type methods.

A system similar to that used by Bell (31) was assembled, consisting of a high voltage generator, a relaxation R-C circuit, and a set of electrodes whose gap could be easily controlled via a micrometer to vary the dielectric breakdown voltage for the spark. Initially, the discharge section had been designed with the bar functioning as the earthed electrode, but this arrangement was reported to generate too much electromagnetic interference (17), thus a second electrode was introduced. Even with this second electrode, the spark generation system radiated a considerable amount of interference, causing the saturation of signal amplifiers and the random behaviour of the transient recorder, which could not be kept functioning in an appropriate manner.

These problems were brought under control by screening all components with aluminium foil, and figure 4.2 illustrates the system as used for the initial phases of transducer development. For this stage of the experimental work, only comparative studies on terms of amplitude spectra were necessary, and in order to assess the amount of energy released in the sparks, a rectifying circuit was connected across a 1 Ω resistor in series with the discharge line, thus providing a means of measuring the current flow for the discharges.

Frequency spectra obtained with this excitation method showed a rather poor energy content for high frequencies, and regardless of all screening precautions, the remaining amount of electromagnetic interference prevented the use of capacitive transducers in combination with spark excitations, which automatically ruled out the use of this set-up for comparison calibrations.

Consequently, experiments were conducted to find alternative means of excitation employing the fracture of glass capillary sections. After repeated contacts with the larger suppliers of laboratory glassware within the UK, it became clear that it would be impossible to obtain capillary tubes of dimensions similar to those quoted in the published literature, and finally, a sample of tubes with 1.5 mm diameter was purchased. The tubes were thinned down by hand, using a Bunsen burner, and the result was as uneven as can be expected, which prevented any control of the magnitude of the excitation generated each time, thus making the capture of adequate signals from the transducers extremely difficult.

After a period of experimentation and trials of approximately two weeks, the method was finally abandoned, having proved too cumbersome due to the lack of the appropriate size capillaries, and an electronic pulse generator was built to drive a piezoelectric exciter. Figure 4.3 shows the circuit diagram of this pulse generator, which was also used to drive a capacitive transducer as exciter.

The combination of a pulse generator and exciter possesses a set of characteristic advantages over any other means of excitation, making it extremely suited for calibration procedures. Some of these advantages can be listed as follows:

- The peak amplitude is easily controllable from the DC voltage source.
- The energy distribution over the excitation frequency spectrum can also be controlled by varying the shape of the pulse, from a step function to impulses of very short duration.
- The pulse signal can be easily monitored as it is inputted to the exciter, thus lending itself to be used in reciprocity calibrations.
- The system can be used to drive piezoelectric or capacitive exciters.

Figure 4.4 shows the pulse generator cirucit and the piezoelectric exciter as used for the development of new transducers.

Some experiments were also performed employing a pulse laser as the source of excitation. The system that was available within the Department was tested using it in its free lasing mode, and the signals generated in this way were of considerable duration, resulting in most of the energy being concentrated over frequencies below 500 KHz, rending it unsuitable for the calibration range intended.

Consequently, the combination of the pulse generator and piezoelectric exciter was found to be the most practical method of excitation, in agreement with the conclusions published by D.M.Egle and A.E.Brown (42).

Finally, the fracture of fine pencil leads was used as a means of producing a well characterised source of excitation, with the aim of establishing a basis for comparison of results with those already published. This method of producing short duration transient surface waves has been well documented and widely used for having similar characteristics to the fracture of glass capillary sections, with the great advantage of being much more controllable and uniform.

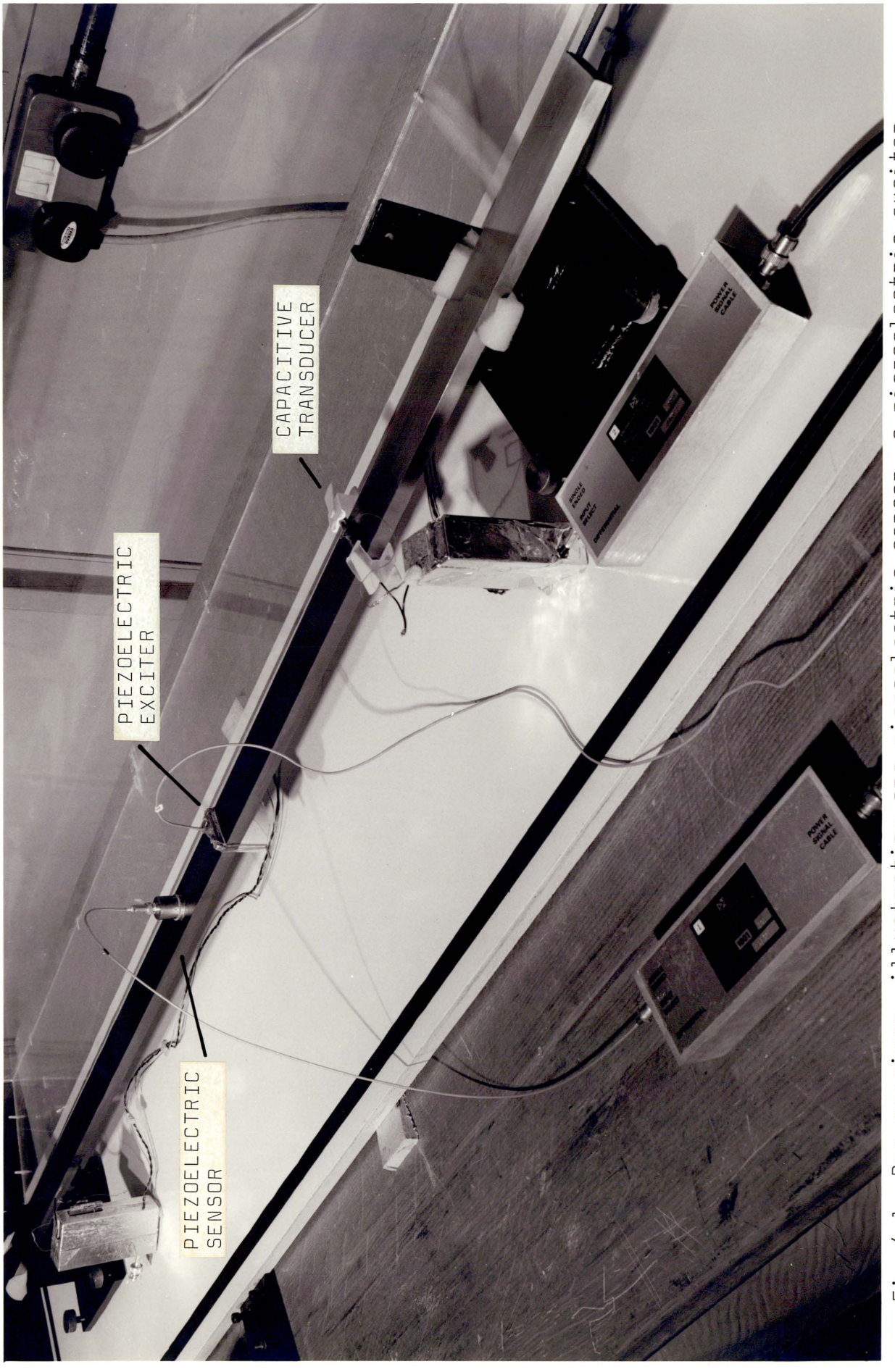

Fig 4.1- Bar specimen, illustrating one piezoelectric sensor, a piezoelectric exciter, and a capacitive transducer.

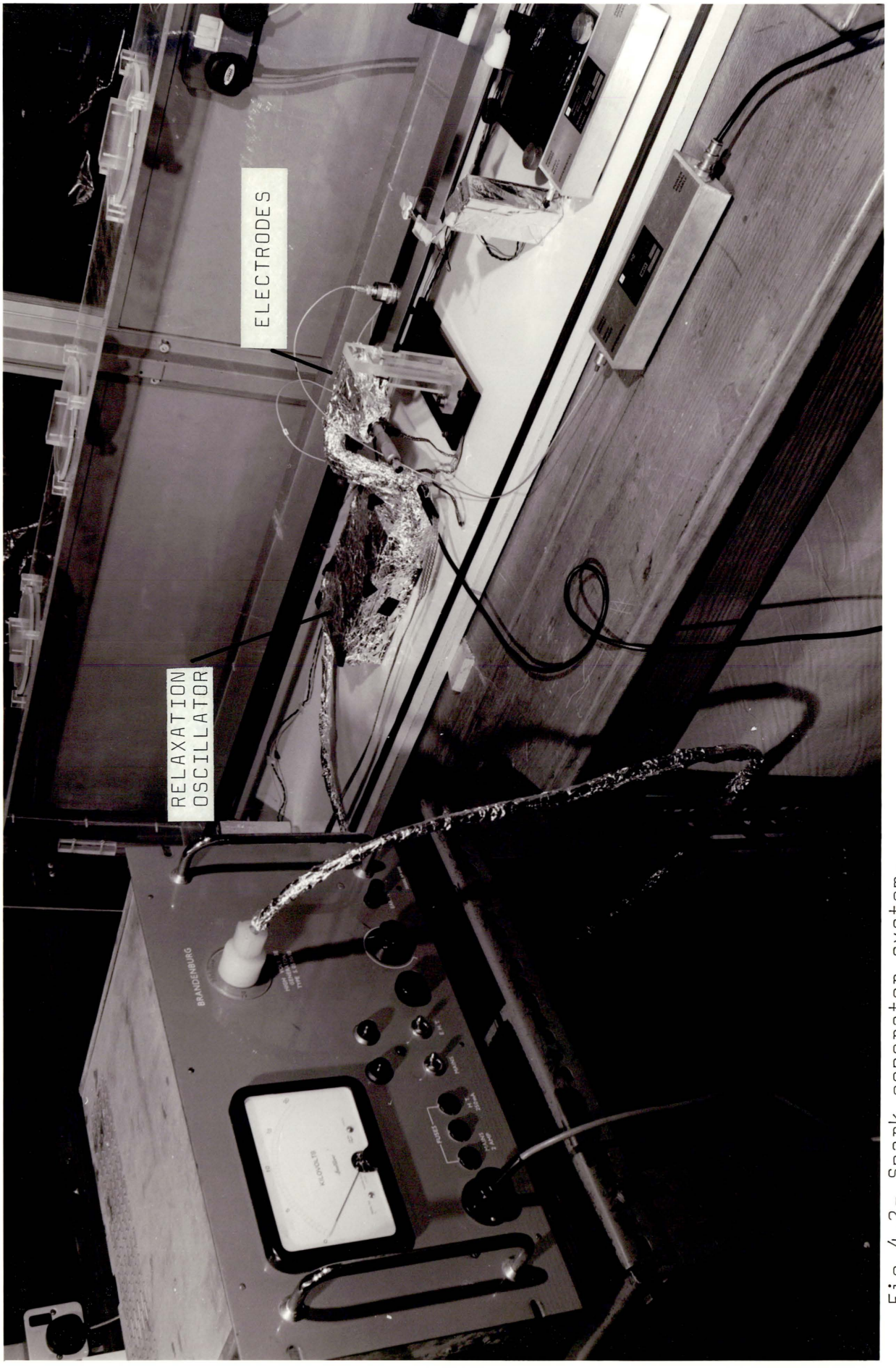

Fig 4.2- Spark generator system.

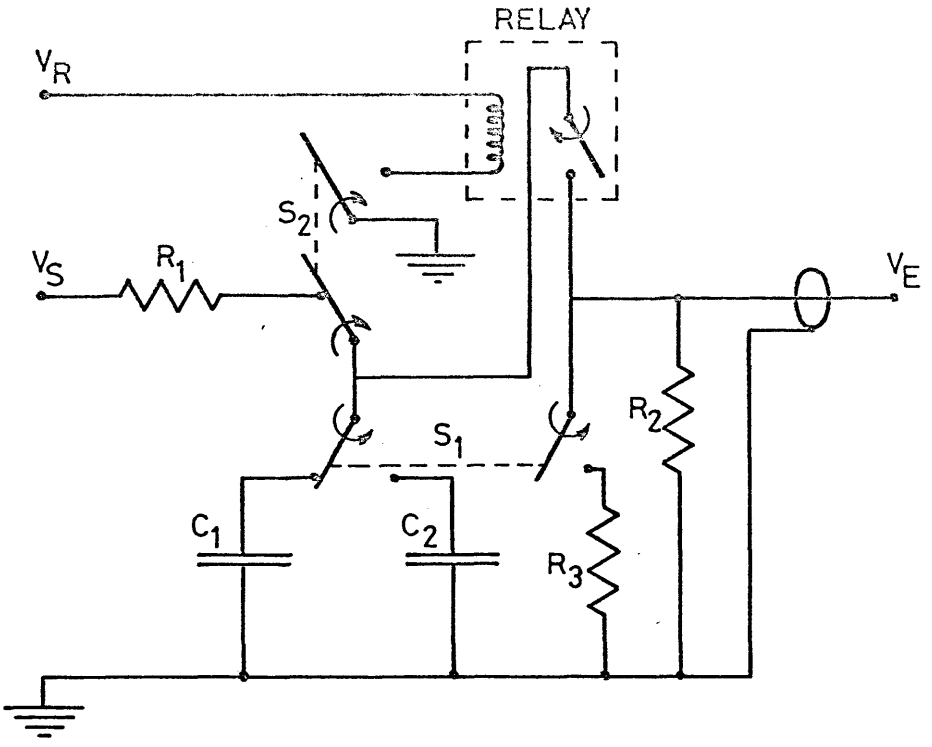

KEY TO SIMBOLS

R_1 = 100 KΩ

R_2 = 1 MΩ

R_3 = 100 Ω

C_1 = 0.1 μF

C_2 = 1000 pF

V_s = DC supply voltage

V_r = Relay supply voltage

V_e = Output signal to the exciter

S_1 = Dual pole toggle switch (sets step or pulse type excitation)

S_2 = Dual pole pushbutton switch (disconnects the input supply and triggers the relay)

Fig 4.3- Pulse generator circuit diagram.

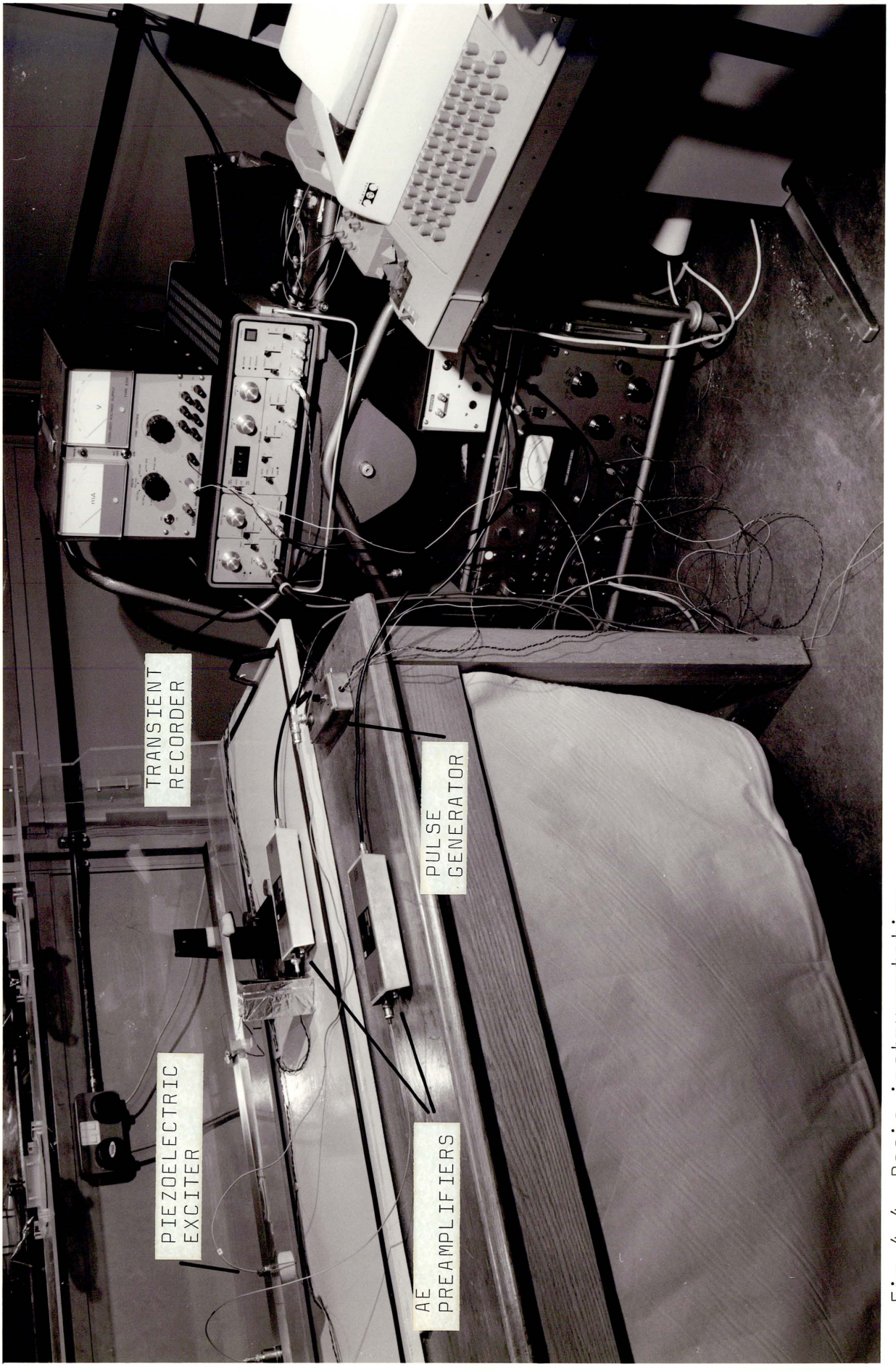

Fig 4.4- Basic instrumentation.

TRANSDUCERS

Systems for the measurement of AE phenomena are based upon one of the following principles:

- Optical interference fringes generated with lasers
- The relationship between Capacitance, Charge and Voltage for capacitives devices or some polymeric films
- The piezoelectric effect present in some natural crystals and man-made synthetic salts

The application of laser based systems is mostly related to transducer calibration work, and has been so far restricted to the laboratory environment due to the amount and cost of the equipment involved.

Capacitive transducers can be of two fundamentally different types: those consisting of thin polymeric films with one or two electrodes plated on them, and transducers made with a massive rigid electrode, usually using air as a dielectric. Polymeric film transducers have had very limited application to AE signature analysis, while transducers with rigid electrodes are mainly used in research or calibration work within laboratory environments. They present an extremely high susceptibility to airborne electromagnetic interference coupled with low sensitivities, besides very stringent requirements regarding the electrodes surface quality and alignment, and the surgical cleanliness of the dielectric gap to prevent sparking due to the necessary DC bias voltage.

Capacitive transducers also suffer from serious geometrical limitations since their sensitivity depends upon the surface area of the sensitive face, while the dimensions of this sensing face limits the frequency response of the transducer. For instance, in the case of

microphone type transducer with a flat circular sensing electrode, the diameter of this electrode limits the frequency response to laterally incident surface waves to such an extent that their application has basically been restricted to epicentral measurements.

A design modification which extends the frequency response of capacitive transducers consists of manufacturing the sensing electrode in a cylindrical shape, and positioning it with its axis parallel to the surface of the specimen and perpendicular to the direction of incidence of the surface waves, effectively producing a "line transducer". However, such a design is extemely directional, and its application is limited to modelling situations where there is previous knowledge of the location of the excitation source.

Because of the above reasons, the transducers most widely applied to AE field work are piezoelectric, manufactured either with natural crystals or synthetic salts. Natural piezoelectric materials have the advantages of being more homogeneous, and their resonances occur at higher frequencies than for their synthetic counterparts of the same dimensions. However, synthetic piezoelectric elements are cheaper to manufacture and shape into almost any imaginable geometry, their polarization being induced during manufacture and thus being independent from crystal structure orientations, and their sensitivity and capacitance coefficients are several orders of magnitude greater than those from natural crystals.

Cost reasons have fundamentally conditioned the wide application of synthetic piezoelectric materials to the manufacture of industrial transducers, and this has in turn influenced the amount of research work into accurate means of calibration.

Accumulated experience with the design of such transducers as piezoelectric accelerometers, has led to the development of transducers capable of producing signals representing accurately the detected vibrations, free from resonance caused distortions, for frequency ranges beyond the typical vibration ranges of interest. However, although the idea of developing AE piezoelectric transducers with flat frequency

responses may be appealing, the author is convinced this is not possible with piezoelectric materials available today, especially if broadband responses over frequency ranges of 2 MHz or more are desired.

A possible way to overcome these limitations involves the construction of piezoelectric transducers, whose frequency response is ensured to be within the dynamic range of the instrumentation conditioning and storing the signals. And once the signals are conveniently stored, the colouring introduced by the corresponding transducer can be removed through de-convolution methods, thus recovering the true waveform.

It was in this direction that the transducer development work was orientated, and besides the report on such development, the present chapter also covers the attempts at building some capacitive transducers intended as standards for calibration purposes, and a piezoelectric exciter actually used during the experimental work for the development of transducers.

5.1 CAPACITIVE TRANSDUCER

Two transducers, similar to those used at the National Bureau of Standards, Washington, USA (22), and at Dunegan/Endevco, San Juan Capistrano, Cal, USA (32), were manufactured, intended as standards in the calibration by comparison of piezoelectric transducers.

They consisted of a solid mild steel cylinder, constituting one plate of a capacitor assembly, while the specimen, acting as the second plate, complements the assembly (see fig. 5.1). Their operation is explained by the physics principles governing charged capacitors in equilibrium: if the dielectric permeability is altered by, for instance, a change of thickness, the capacitance of the system will be changed, which in turn will force changes upon the polarization voltage and the accumulated charge in order to restore electrostatic equilibrium.

If an amplifier with very high input impedance is connected with a capacitive transducer of this kind, the accumulated charge will not be able to vary at a sufficiently fast rate as to counteract the variations in capacitance, thus inducing an electric signal superimposed to the equilibrium DC voltage.

The nature of the surface waves to be detected with these transducers make it necessary for the sensing electrode to have a cylindrical shape, whose maximum allowable diameter is determined by the wavelength of the uppermost frequency to be accurately measured. It is widely accepted that a transducer with the above geometry and using air as dielectric, will present its lowest resonant frequency or frequencies in direct relation to the support geometry, which can be designed to ensure these resonances to be well below 20 KHz. The higher frequency resonances will be mainly due to standing waves in the dielectric gap, which are of the order of 40 MHz for the usual magnitudes of air dielectric gaps.

The calculated response for these transducers is obtained from the physical model of an infinitely long cylindrical conductor, running parallel to an infinite flat conductive surface. Considering small variations of the dielectric gap, the transducers can be considered to have an output proportional to the variation of the dielectric gap:

$$V = - V_o \frac{s}{2S}$$

where $\underline{V}$ is the output AC signal, V_o is the DC bias voltage applied to the transducers, $\underline{S}$ is the nominal dielectric gap, and $\underline{s}$ is the surface displacement.

The above equation was obtained from one of the references (32), however, a complete development for such expression from the basic physical model is included in Appendix A.

Dimensions for the construction of the transducers were obtained from the Rayleigh wave speed for the bar specimen and the frequency range of interest. The Rayleigh wave speed was calculated

from the elastic constants for mild steel to be approximately

$$c = 2983.8 \frac{m}{sec}$$

This value was obtained with the equations given by S.P.Timoshenko and J.N.Goodier (43)

$$c = \alpha \sqrt{\frac{G}{\rho}}$$

where $\underline{G}$ is the elastic shear modulus for the specimen, $\underline{\rho}$ is its density, and $\underline{\alpha}$ is a coefficient equal to the minimum positive real root in the equation

$$\alpha^6 - 8\alpha^4 + 8(3 - \frac{1 - 2\nu}{1 - \nu}) \alpha^2 - 16 \left[1 - \frac{1 - 2\nu}{2(1 - \nu)} \right] = 0$$

where $\underline{\nu}$ is the Poisson's ratio.

Since the frequency range of interest had been decided to be 20 KHz to 2 MHz, the shortest wave length to be accurately measured should be

$$\lambda_{\ell} = 1.492 \text{ mm}$$

A transducer capable of detecting any frequency should have zero width, constituting a true line transducer. However, since this is physically impossible, some degree of averaging over the sensitive width of the transducer will always occur (see fig. 5.1). Additionally, the greater the inertia of the sensing electrode, the lower its fundamental resonance and the more accurate the resulting measurements, thus making it desirable to have the sensing electrode as massive as possible.

A criterion for a compromise was established by considering as active only the section of the cylindrical electrode surface whose distance from the specimen ranges between the minimum value $\underline{S}$ and twice that value (see fig. 5.1) and taking half the shortest wavelength of interest as the longest section of surface wave to be averaged.

Using the same notation as shown in figure 5.1:

$$m = 2a \sin\theta$$
$$S = a(1 - \cos\theta)$$

The problem thus established is dependent upon the minimum distance between electrode and specimen, which in the case of the transducers manufactured for the project, was set by using thin polycarbonate film shims.

The thinnest obtainable polycarbonate film had an average thickness of 2 μm, and was kindly supplied by Bayer UK Ltd., free of charge. However, due to difficulties is obtaining tolerances of less than ± 0.5 μm for the flatness across the width of the bar specimen and for the electrode, the average dielectric gap was taken as 3 μm, a value close to the average obtained later by experimental measurements.

From the maximum wave section to be averaged by the transducer, the following ratio can be established:

$$\frac{S}{m} = \frac{1 - \cos\theta}{2 \sin\theta} \geqslant \frac{3\mu m}{0.75\ mm}$$

$$\Longrightarrow \quad 1 - \cos\theta - 8 \times 10^{-3} \sin\theta \geqslant 0$$

The first quadrant root for the above equation is

$$\theta \geqslant 0.9153^{o}$$

Introducing the limit value of $\underline{\theta}$ into the expression for m:

$$a \leqslant \frac{m}{2 \sin\theta} = 23.48\ mm$$

which gives the maximum radius for the electrode, thus limiting its diameter at $\sim$47 mm.

The transducers were manufactured from a mild steel cylindrical bar having a diameter of 6.35 mm, and a length of 45 mm, illustrated in figure 4.1.

An experimental measurement of the resonant frequency for the electrode, supported at both ends by a single layer of narrow polycarbonate shims, resulted in a value of approximately 7.3 KHz, while the resonant frequency for the same electrode supported by a double layer of shims was approximately 5 KHz, showing a ratio close to $\sqrt{2}$, as would be expected from a single degree of freedom model.

This evidence was considered sufficient to guarantee a flat frequency response over the bandwidth of interest, however the response of the transducers to actual surface wave excitation was found to be most unsatisfactory. The transducers suffered from sparking and short circuit contacts across the dielectric gap.

The electrodes and bar specimen were hand lapped for a second time to improve the surface tolerances, using diamond lapping compound with 1 μm particles, and constantly checking for the amount of surface deviation from a straight line across the width of the bar, but the best tolerance ever achieved was ± 0.5 μm.

A measurement of the surface roughness for the cylindrical electrodes showed an overall roughness of 0.1 μm rms, in compliance with the lapping compound manufacturers specification, and the overall deviation from a straight line along the electrodes was found to be within ± 0.2 μm, better than expected and considerably better than for the bar.

However, in a recent paper by D.G.Eitzen et al (44), some guidance was for the first time obtained with regards to the required tolerances for a successful system. The surface condition for the assembly described in this reference is of optical quality, with a maximum deviation of ± 0.1 μm over any section 50 mm (2 in) long. This data automatically ruled out any hopes for achieving a working capacitive transducer system with the facilities available within the Institute.

The author found most frustrating the fact that precision limitations in the manufacture of the electrodes and bar specimen prevented the application of a system which had been calculated to function properly, was reported a successful device by various

researchers, and consumed a considerable amount of fruitless effort in manufacturing and testing both the electrodes and the impedance matching head amplifiers, whose diagram is shown in figure 5.2, and whose calibration curves are shown in figures 5.3 and 5.4

Nevertheless, it was decided to include the above information as it is firmly believed that once the manufacturing tolerance problems are overcome, for instance, by contracting the manufacture of electrodes and specimen outside the Institute, the prospective user will possess all necessary information to assemble and utilize this type of transducer, gathered within a single source.

5.2 PIEZOELECTRIC EXCITER

The unsatisfactory results obtained with the spark excitation system led to the assembly of an electric pulse generator (described in section 4.3), together with a piezoelectric exciter.

The design of the exciter was reasonably simple, consisting of a narrow strip of piezoelectric ceramic, mounted on a wear plate of the same material but unpolarized, and provided with an overall shielding cover as shown in figure 5.5, also illustrated at its mounted position in figures 4.1 and 4.4.

The active element in the transducer was cut from a PZT-5A ceramic blank having a thickness of o.5 mm, to ensure a resonance in the thickness mode of $\sim$ 3.7 MHz, this figure being obtained from the information supplied by the piezoelectric ceramic manufacturers (VERNITRON Ltd., Thornhill, Southampton). The width of the active strip element was fixed at 2 mm, for this was the smallest dimension that could be reasonably handled with the machining facilities available, since precautions had to be taken to ensure that the long edges for the strip were parallel.

The wear plate was also cut from a blank 0.5 mm thick, and with a surface area large enough to allow a metallic shield cover to be fixed. This wear plate, being unpolarized and without electrodes,

acted as an insulating coupling layer, thus employing the same material as for the active element ensured the optimum acoustical impedance for an exciter which could be used with any specimen material.

The internal surface of the wear plate was coated with vacuum deposited silver, in order to ensure good shielding against electromagnatic interference if the transducer was used as a sensor, and to prevent the radiation of interference when using the transducer as an exciter.

The active element was mounted on the wear plate with its positive face upwards, bonded with silver loaded epoxy resin to ensure a good grounding contact. Great care had to be taken at the bonding stage to prevent any surge of conductive resin short-circuiting the two poles of the active element, as this was only 0.5 mm thick. After soldering the signal lead, the shielding case was fixed in position also using silver loaded epoxy resin.

In order to calculate the requirements for the pulse generator circuit, the capacitance of the exciter was calculated from the manufacturer's data, where the relative dielectric constant in the direction of polarization is given as

$$\varepsilon_{33} = 1700 \qquad (\varepsilon_0 = 8.85 \times 10^{-12} \frac{F}{m})$$

From this value, the capacitance for the active element was calculated to be

$$C = \frac{\varepsilon_0 \, \varepsilon_{33} \, A}{t} = 2.17 \text{ nF}$$

where A is the surface area (72 mm^2) and t is the thickness (0.5 mm).

This estimate was compared with an experimental measurement of the capacitance for a ceramic blank, with the same thickness and total area of 1000 mm^2, which resulted equal to 28.45 nF. This value corresponded to a capacitance of 2.048 nF for a strip with the dimensions of the active element in the exciter, and both values were considered sufficiently close to be accepted.

The above figures meant that the charge accumulated in a 0.1 μF capacitor should be sufficient to drive the exciter to a peak voltage practically equal to the DC supply level for the circuit, even considering the load due to the cabling.

Although the design of the exciter is inherently highly directional, its use was primarily intended for the bar specimen, thus its shape was specially suited to generate excitations with a uniform profile across the width of the bar, expected to travel along the bar as surface waves in liquids travel along a channel. It was also expected that the surface disturbances generated at either side of the exciter would be symetrical to each other.

Monitoring the signal from the pulse generator into the exciter on a fast storage oscilloscope, showed a rise time of less than 0.1 μsec, thus ensuring the contents of frequencies well in excess of 2 MHz, and although a proper calibration for the pulser was never performed, the frequency analysis of the outputs from the majority of the tested transducers showed frequencies components even beyond 2.5 MHz, within the dynamic range of the transient recorder. This fact, in addition to an excellent repeatability rendered the exciter as ideal for the comparative study and development of transducers.

Proof of its suitability and linearity was found from the comparison of various piezoelectric outputs, normalized with respect to the input to the exciter, when using either step function or pulse type signals. Except for the distortion introduced by the periodic fall of amplitude in the step function spectrum, the results were practically identical. Figures 5.6.a and b correspond to the normalized output amplitude spectra for one of the transducers tested, when excited with a step function and with a pulse generated waves.

Having achieved the implementation of a suitable source of excitation, the research could continue with the development of those transducers which would ultimately be used in the practical measurement and analysis of the AE pulses.

5.3 PIEZOELECTRIC TRANSDUCERS

Since it had been decided to attempt the design and construction of a piezoelectric transducer with characteristics better suited to AE signature analysis than those obtained from commercial transducers available at the time, a design strategy and a set of objectives had to be established.

Naturally, information on the detailed design and construction of commercial transducers was not readily available, and most published literature was only related to the active piezoelectric elements, thus basic manufacture techniques also had to be devised.

VERNITRON Ltd., from Thornhill, Southampton, were selected to be the piezoelectric ceramics suppliers, as they had normally provided the Department with such materials. And since no previous experience was possessed to ascertain beforehand the shape and size of the piezoelectric elements to be required, it was decided to purchase the piezoelectric ceramic material in blanks of two different thicknesses, from which the required elements would later be cut with the aid of an ultrasonic drill.

Two X-cut quartz crystal discs, with resonant frequencies of 2 MHz and 5 MHz,were also purchased for comparison purposes.

From the technical information supplied by the piezoelectric ceramic manufacturers (45) and (46), the ceramic designated as PZT-5A was selected as the most appropriate for AE transducers, due to its relatively high sensitivity (the second highest in the range) while having a superior temperature and time stability, good fatigue endurance, a maximum working temperature of 250^{o}C, and a Curie temperature point of 365^{o}C.

The thicknesses selected for the ceramic blanks were 1 mm and 0.5 mm, with associated resonances of 1.9 MHz and 3.8 MHz respectively. The blanks were provided with silver fired electrodes,

polarized in the thickness direction, and their size being the largest that could be supplied (20 x 50 mm^2).

For the possible provision of wear plates for the transducers, a short literature review was conducted regarding the influence that the wear plate material might have upon the response of the finished transducers, and the same material was selected in function of its acoustic impedance effects.

It is a well known principle in acoustics that in order to ensure a minimum of acoustic attenuation across the interface of three layered media, the acoustic impedance of the middle layer should be equal to the geometrical mean of the impedances for the other two layers. In the case of a transducer, this imposes a dependance for the wear plate material (the middle layer) in terms of the specimen material.

Since the transducers were intended for general use, with any specimen material, the solution opted was to manufacture the wear plates with the same acoustic impedance as the sensing element. Therefore, extra ceramic blanks were purchased, with the same dimensions (20 x 50 mm^2), and thicknesses of 0.5 mm and 1 mm, without being polarized or plated with electrodes.

5.3.1 Literature Review

The amount of literature found directly related to the design and construction of AE transducers was far from extensive, and at the early stages of the project it only included the technical information from the piezoelectric ceramic manufacturers (45) and (46), a paper by H.L.Dunegan et al (47), and a paper by C.A.Tatro (48), the latter two published from the Livermore Laboratories, University of California, Livermore, Cal., USA.

In their paper, Dunegan et al (47) present a rather detailed description of conventional single ended and differential transducers, including cut views and a schematic diagram of a simple transducer

section. A basic orientation for the dimensioning of the sensing element is also given, in terms of the resonance coefficients for the piezoelectric material used. However, the resonant frequency value thus obtained is no more than an estimate of the true resonance to be detected experimentally.

Tatro (48), in his paper, presents a comprehensive review of piezoelectric materials which could be used to manufacture AE transducers, comparing their qualities, and including other types of transducers such as an accelerometer, a capacitive microphone, and an inductance flat coil transducer.

From the comparison of sensitivity and inherent capacitance figures, Tatro concluded that the piezoelectric ceramic PZT-5 (a predecessor of PZT-5A) offered the best combination of qualities, making it the best selection.

A cut view diagram of a simple transducer was also included, together with the basic design methodology for sensors, some advice with regards to the signal amplifiers required and a number of ways to overcome the mechanical and acoustic background noise problems.

The design methodology presented for the sensing element in the transducer, is intended for transducers used for event detection, which means that the sensors are used over narrow band-widths containing their resonance frequencies in order to achieve maximum sensitivity. However, for the purpose of signature analysis, a better knowledge of the resonant modes and coupling effects within the sensing element is required at the design stage. In this respect, a paper by G.K.Lucey (49) was found particularly useful, since it contains two equations specially suited for the calculation of the fundamental resonant frequency for piezoelectric discs, whose dimensions make them boundary cases between thick rods and thick discs, as is usually the case with AE transducer sensing elements.

Lucey further verified his results by calculating the fundamental resonant frequency for aluminium cylinders which had been

experimentally tested by G.W.MacMahon (50), and the comparison of results was most satisfactory.

From the study of Lucey's equations, it became clear that the fundamental resonance of piezoelectric elements with usual dimensions would be dominated by the radial mode. In fact, a reduction of thickness from 1 mm to 0.5 mm for discs 4 mm in diameter, increases their fundamental resonance frequency by only 3.3%, implying that the gain of range below resonance is grossly outweighed by the loss in sensitivity.

However, the main excitation to AE transducers is produced by surface displacements normal to the sensing face, especially if the coupling between transducer and specimen is achieved using lubricants or resin. Therefore, unless there is strong cross-coupling between the radial and thickness modes, the fundamental radial resonance should not prevent the detection of higher frequencies within the dynamic range of the signal conditioning and storing instrumentation.

An important study of the effects of the couplant layer upon the frequency response of transducers was published by R.Hill and S.M.A. El-Dardiry (51), in which particular attention was given to the resonance problems originated by the couplant layer. The study consisted in the modelling by digital computer means of the transducer response to simulated AE pulses, introducing the effects of the couplant layer in terms of an acoustic power transmission coefficient, defined as a function of the acoustic impedances for the specimen, couplant and transducer.

The results of this analysis are presented as a family of curves, representing the variation of the acoustic power transmission coefficients as a function of frequency, for various thicknesses of grease couplant. From these curves it is clear that the couplant thickness must be kept at the minimum possible (about 10 μm or less) in order to maintain the amount of high frequency attenuation within acceptable levels.

Finally, a paper which was found to be most interesting from the design point of view, was published by B.K.Christoffersen and T.R.Licht (52), from Brüel & Kjær. In this work, four different transducer configurations are presented with their typical frequency responses, obtained with a reciprocity based method of calibration, formerly described by Hatano and Mori (35).

The combination of schematic diagrams for typical transducer designs and their associated responses, was found most helpful as a guide for the development of special purpose transducers. In particular, a diaphragm type of transducer, designed and developed by Brüel and Kjær and described in the paper, was to become the basis for the most successful transducers developed during the project.

5.3.2 Transducer Design and Development

Before the development of transducers could begin, a set of basic guidelines had to be defined in order to establish some initial restrictions to an otherwise immensely wide scope of problems. These guidelines were established as a number of fundamental aims to be met by the new transducers:

a - The transducers should have a minimum response bandwidth of 2 MHz. If the response of the transducers could not be "flat", it should at least be within the dynamic range of the signal recorder (38 to 40 dB).

b - The piezoelectric sensing elements should be well shielded against extraneous electromagnetic interference, and electrically insulated from the specimen.

c - The transducers should possess as rugged a construction as possible, in order to withstand the severities from industrial environments.

d - Their sensitivity and noise ground level should be, if not better, at least comparable to typical values for commercial transducers.

The problem of ensuring a wide frequency response concerns primarily the geometry of the sensing element, and the way it is coupled to the surface of the specimen. Calculations of the fundamental resonant frequency of small PZT-5A discs showed that the radial mode dominated the fundamental resonance of elements with typical dimensions, thus a small diameter was necessary to attain a good frequency response. However, the low capacitance values resulting from too small dimensions was a constraint to be considered, and as a compromise solution, a diameter of 4 mm was selected for the sensing elements which were cut from blanks 1 mm and 0.5 mm thick, to build several transducers among the first batch to be tested.

An additional disc with diameter of 2 mm and 1 mm thickness was also prepared, with a calculated fundamental frequency of 903 KHz. However, since its small dimensions were expected to cause too low sensitivity and capacitance figures, it was decided to provide it with some kind of mechanical amplification, which took the form of a truncated cone wave guide, made of aluminium.

As a basis for comparison, two X-cut quartz crystal discs, with resonant frequencies at 2 MHz and 5 MHz, were obtained to be used as sensing elements.

Several commercial transducer manufacturers had in the past attempted to overcome the problem of low frequency resonances in typical sensing elements by using an assembly of two or more concentric rings and discs, carefully tuned for particular frequencies, in order to balance their resonances and obtain a flatter frequency response. However, these transducers were reported to produce an almost random phase response, probably due to the interaction of the different resonances from the several elements. Additionally, the assembly of the various concentric elements is a rather complicated process, requiring very high precision if directionality for the finished transducer is to be kept at acceptable levels.

As an alternative to the conception of composite sensing elements, it was decided to test an irregularly shaped element, which

should, at least in theory, overcome the problem of phase response. The element was built by cutting three holes of different size at asymmetrical positions, from a disc of PTZ-5A, 10 mm in diameter and 1 mm thick. The main idea behind such a design was to produce an element with a constantly changing section, aiming at achieving distributed resonances throughout the whole element, and thus avoiding strong amplitude peaks in the frequency response.

Once the geometry of the sensing elements had been decided, the problem of assembling these within the transducer had to be solved. Traditional configurations used by commercial transducer manufacturers incorporate a rigid wear plate onto which the sensing element is attached, to provide coupling to the specimen whilst ensuring electrical insulation.

The alternative configuration presented in the paper by Christoffersen and Licht (52), incorporates a metallic diaphragm made of a special copper-beryllium alloy, to support the sensing element. The coupling to the surface of the specimen is provided by a glass contact shoe, in the shape of a spherical cap, and the contact between the shoe and the specimen surface is ensured by the tension in the diaphragm.

The use of such a metallic diaphragm was considered impractical from the manufacturing point of view, and objections were raised from the mechanical impedance effects of a metallic diaphragm upon the response of the transducer. Nevertheless, the idea of suspending the sensing element free from rigid components in the transducer was found most attractive, and the decision was made to build several transducers of a similar design, incorporating a polymeric film diaphragm.

A first batch of eight transducers was manufactured and tested to compare their performance, and those producing the best responses were later to be modified in an attempt to improve them, and reach the final versions which would be calibrated. All tests were performed on the steel bar specimen, and employing the piezo-

electric pulser as the source of excitation. The transducer output signals were normalized in terms of the input signal to the exciter, and since the tests were performed for a constant distance of 60 mm between exciter and sensors, the method provided a good basis of comparison for the performance of the different transducers, regardless of not having evidence of the true frequency contents in the surface waves generated.

Figure 5.7 displays the components of a typical diaphragm transducer, including a casing, terminal connector, diaphragm clamping ring, piezoelectric ceramic blanks mounted on glass plates, from which the disc elements were cut, sensing elements and contact shoes ready to be mounted, and a piece of mylar film with the sensing element already mounted and provided with the signal wire.

The ceramic blanks had to be mounted upon a rigid base before the disc sections could be properly cut with the aid of an ultrasonic drill. Several substances were tested for this purpose, including shellac, various plastic cements, glues and paints. However, the substance which produced the best results in terms of ease of handling and time, was sealing wax. The method of application consisted of heating the glass plates with a hot air gun, until the melting wax would adhere and remain fluid. A thin layer of wax was then spread over the glass while maintaining its temperature to continue fluid. The ceramic blanks were then pressed against the soft wax, keeping the temperature high enough to allow the wax to flow outwards, leaving a thin film between the ceramic blank and the glass plate.

Precautions had to be maintained not to burn the wax or to overheat the polarized ceramic blanks, with the risk of reaching the Curie point for localized sections.

In order to protect the silver plated electrodes on the active ceramic blanks from abrasion during the cutting process, the exposed electrode was coated with protective paint (appearing white in fig. 5.7). Once cut, the elements were removed by using the hot air gun, heating slowly the assembly until the wax melted and the

discs could be lifted with tweezers. When cool, the elements were immersed in a bath of acetone, which softened the remains of sealing wax and protective paint, allowing these to be removed.

After cleaning, the sensing elements were bonded to either a piece of mylar film or a ceramic wear plate, using silver loaded epoxy resin. This prevented the insulation of the negative pole and facilitated the gounding connection.

Since the silver opoxy resin requires a moderately high temperature to cure properly, the transducer components being bonded were kept under proper conditions by using a 60 Watt light bulb, which ensured a good setting of the resin whilst preventing the damage of the diaphragm films.

To provide good shielding against electromagnetic interference and the grounding connection for the sensing element, the inner side of the diaphragms and wear plates was coated with silver loaded conductive paint.

A thin flexible wire was attached to the positive pole of the sensing element either by soldering, or bonding it with silver loaded epoxy resin.

Once the sensing elements were propertly mounted, their signal wire attached, and the supporting base (either diaphragm or wear plate) had been coated with silver paint, the assemblies were tested for short circuits created by surges of silver epoxy or conductive paint, and those assemblies passing the test were mounted on a metal casing and finished with a connector.

Rigid wear plates carrying the sensing elements were attached to the transducer casings by bonding them with silver loaded epoxy, whilst mylar diaphragms were attached to the casings with clamping rings, which ensured a certain amount of tension in the diaphragms, and they were secured from slipping with fast setting epoxy resin.

Transducers with a rigid ceramic wear plate were provided with a protective silicone rubber ring to prevent the edges from being knocked against hard objects.

Figure 5.8 shows six representative types of transducers from those developed during this stage of the project, while figure 5.9 shows a close-up view of two diaphragm transducers, one with contact shoe and one without.

The first diaphragm transducer to be built and tested was provided with a glass contact shoe in the shape of a spherical cap, similar to the configuration described by Christoffersen and Licht (52), illustrated in figure 5.8, and whose section is presented in figure 5.10.

When subjected to test, it was found that the tension in the mylar film was not sufficient to ensure constant contact between the glass shoe and the specimen, thus the response for high frequencies was very poor. The application of couplant to the contact area did not improve the siutation due to the shape of the contact shoe, and consequently this design was abandoned at a very early stage.

Several transducers were then built using the diaphragm configuration, but with no contact shoe, as illustrated in figure 5.11. The test results obtained with these transducers were considerably better, since the application of couplant would ensure better acoustic transmission from the specimen to the sensing face of the transducer. However, the design presented two serious handicaps: the diaphragms were not protected and proved too vulnerable to rupture problems, unless extreme care was taken not to apply excessive pressure over the transducer against the specimen, and the tension in the diaphragms was not sufficient to control the thickness of the couplant layer, causing noticeable variations in the response of the transducers every time they were removed and re-installed, in addition to rather low sensitivities.

In order to improve the coupling between the sensing element and the specimen, a contact shoe in the shape of a ceramic disc with the same dimensions as the sensing element, was added to the diaphragm transducer design, as shown in figure 5.12. Unlike the case of a spherical cap contact shoe, the coupling between the shoe and specimen is ensured by the couplant resin, while the mylar diaphragm tension is sufficient to press the smaller area of the contact shoe against the specimen, thus providing a better control of the couplant layer thickness.

Figures 5.13 and 5.14 show the remarkable difference in sensitivity achieved with the addition of a flat contact shoe, for otherwise identical transducers.

Two more transducers were built with a diaphragm construction, using X-cut quartz crystal discs, with resonant frequencies at 2 MHz and 5 MHz, as sensing elements. These transducers were similar in construction to the design of figure 5.11, and were not provided with contact shoes because the diameter of the quartz discs was considered to be too large (10 mm). Their responses can be observed in figures 5.15 and 5.16, and their comparison with previously obtained characteristics (see fig. 5.14) shows a lower overall sensitivity and a similar decay for high frequencies.

The transducer incorporating a conical wave guide made of aluminium (see fig. 5.8) was designed as an experiment to test the feasibility of using such wave guides as mechanical amplifiers in conjunction with smaller piezoelectric elements, for the construction of AE transducers. A diagram detailing this transducer is included as figure 5.17, and the results from its test are shown in figure 5.18. The response obtained was flatter, if less sensitive, than the response from a commercial "flat frequency response" transducer, whose response is included for reference purposes in figure 5.19. However, the response from the wave guide transducer was found to decay too sharply for frequencies above 1 MHz to be acceptable, thus the search for a better transducer was continued.

Finally, two transducers incorporating rigid ceramic wear plates were built, the wear plates being cut from ceramic blanks 0.5 mm thick, in order to maintain the acoustic attenuation to a minimum. One of these transducers, represented in figure 5.20, contained a single PZT-5A disc, 4 mm in diameter and 1 mm thick, and its response is shown in figure 5.21.

Comparing this response with those from other transducers, it can be noticed that the spectrum was smoother, containing less marked resonance peaks. This was attributed to the wear plate introducing some damping in the radial direction, thus reducing the coupling of this vibration mode from the thickness mode.

The second transducer built with a rigid wear plate contained an asymmetrical sensing element, consisting of a PZT-5A disc with a diameter of 10 mm and thickness of 1 mm, in which three holes had been cut at random positions, to upset the distribution of the typical resonances. Figure 5.22 shows a schematic view of this transducer and sensing element, and figure 5.23 represents the response obtained with this design, showing a much wider frequency range than would be expected from a simple disc with the original dimensions of the element.

At this stage, considerations were for the first time made with regards to the effects upon the transducer response from the lack of symmetry. When a transducer is located at an epicentral position, that is, it is mounted on the surface of the specimen directly above the source of excitation, the elastic waves will reach the sensing face of the transducer from a perpendicular direction, thus the orientation of the transducer should have no effect whatsoever upon the generated response. However, for the majority of detected AE phenomena the transducer will not be located at the epicentral position, and therefore, the excitation arriving at the transducer will, in general, reach the sensing element from a radial direction, and consequently, the orientation of an asymmetrical sensing element must be expected to have some influence upon its response. If there is no major difference in terms of overall sensitivity, there will certainly be a difference in terms of phase.

This transducer was tested for the effects of orientation, and figures 5.24a, b, c and d show the results obtained after rotating the transducer about its axis, at constant intervals of 90^{o}. From these results it was concluded that a transducer used for omni-directional signature analysis must be manufactured with a symmetrical sensing element, since it is not possible to establish the direction of incidence of a particular excitation, in order to apply the appropriate correction to the signal. Therefore, the frequency characteristics for the transducer should be independent from its orientation.

Other transducers whose construction maintained axial symmetry were also tested for directionality effects, and although the detected differences in the response were not as marked as in the above case, they were nevertheless present. This was attributed to the level of precision achievable with manual construction methods, consequence of the transducers being prototypes and the fact that the assembly methods and materials were experimental. However, it is believed that proper assembly jigs should allow the construction of the transducers with sufficient precision as to minimise the directionality effects, specially in the case of diaphragm transducers, in which the sensing element and contact shoe assembly remain practically isolated from the casing, and therefore free from its interaction, being held in position by a highly flexible and resilient support.

The most important conclusions from the initial phase of transducer design and development were:

- The diaphragm configuration provided with a contact shoe seemed to be the most promising design.
- The dimensions of the sensing element and contact area between transducer and specimen had a direct influence upon the frequency range of the transducer. This observation had already been reported (52), and is caused by the geometrical coupling of the different frequency components

being dictated by the ratio of their wave length to the diameter of the sensing element.

- Great care must be dedicated to the precise assembly of the transducers if axial symmetry is to be ensured, in order to produce omni-directional transducers.

Before an attempt at improving a particular transducer design could be made, attention had to be given to additional aspects like the influence that different coupling substances might have upon the response of transducers, and the effects that damping or loading of the sensing element would produce.

In order to study the influence of coupling agents, sets of three tests were performed with various transducers, using three different couplant agents. One of these sets of tests is represented by figures 5.25a, b and c, where the same transducer was tested using light viscosity oil, silicone rubber and water based resin, respectively, as couplants for both exciter and sensing transducers.

From the comparison of the latter three graphs it is clear that the light viscosity oil produces inferior results to the other two couplants, whilst between silicone rubber and resin there seems to be only minor differences. However, repeating the tests after removing the transducer, cleaning the contact areas, and replacing it with the same couplant, indicated a much better repeatability for the water based resin, and a certain tendency by the silicone rubber to corrode the surface of the specimen, probably due to the acetic acid released during its curing process. Therefore, the resin was selected as the couplant to be used for all experiments.

Although a permanent couplant, like epoxy resin, would probably provide a more stable performance of the transducer, the use of such a couplant would prevent the removal of the transducer without destroying it, and consequently it was not considered.

Additional tests were performed after adding silicone rubber or epoxy resin to a number of already tested transducers, in order to ascertain any advantageous effects from introducing a certain degree of damping.

Figure 5.26 shows the response of the rigid wear plate transducer described in figure 5.20, after the application of epoxy resin completely coating the sensing element. The comparison of the newly obtained response with the response previous to introducing damping (fig. 5.21), indicates an overall reduction in sensitivity of approximately 5 dB, and although the characteristic response was slightly modified, there is no evidence of a reduction of the resonance peaks due to damping effects.

Figure 5.27 shows the response from the rigid wear plate with asymmetrical sensing element, illustrated in figure 5.22, after the application of epoxy resin. Comparing the new response with the results prior to the application of damping (fig. 5.23) there is indication, as in the above case, of an overall reduction in sensitivity without any specific advantage with regards to the frequency response. Indeed, the response after applying the resin shows a reduced sensitivity for frequencies above 1 MHz, and there were no improvements with regards to the high directionality of this transducer.

In order to test the effects of silicone rubber as a damping agent, a diaphragm type transducer, similar in design to figure 5.12, was tested before and after applying the rubber compound, and figures 5.28a and b show the corresponding obtained responses. As in the case of epoxy resin, the silicone rubber produced an overall reduction of the transducer sensitivity by approximately 6 dB, with little or no effects to the actual shape of the spectrum.

Since those transducers which had epoxy resin or silicone rubber applied to them could not be recovered later to their original condition, the number of transducers thus modified was small. However, it was considered at the time that the above evidence was

sufficient to support the use of transducers without the types of damping tested so far.

One final modification was left, and this gave quite successful results. It consisted of the application of a certain amount of impedance loading to the sensing element, in the form of a small dome of silver loaded epoxy resin, as illustrated in figure 5.29. Since the application of this loading had to be effected prior to the assembly of the transducers, it was not possible to establish a direct comparison of responses before and after its introduction. However, the designs to which this modification was introduced were similar to transducers already tested, as can be appreciated from figure 5.29.

Transducer No.9 was built with both sensing element and contact shoe having a thickness of 0.5 mm, whilst transducer No.10 was built with these components having a thickness of 1 mm, and although their responses were not identical, both of them had a maximum range of variation of 30 dB for their amplitude spectra, as shown in figure 5.30, well within the dynamic range of the transient recorder.

The improved response from these transducers was attributed to further damping of the radial mode of vibration produced by the silver loaded epoxy dome.

Even though the latter transducers cannot be accepted as the optimum possible designs, and there certainly is room for improvement, either by introducing electronic components into the designs to reduce resonant peaks or by redesigning the sensing element, it was considered that a practical limit to this section of the work had to be established in order to proceed with the remaining objectives of the project.

The comparison of the test results from the latter transducers with those obtained from the best commercial transducer available (see fig. 5.19), further encouraged the opinion to conclude the development of transducers and concentrate on the research work for a calibration method.

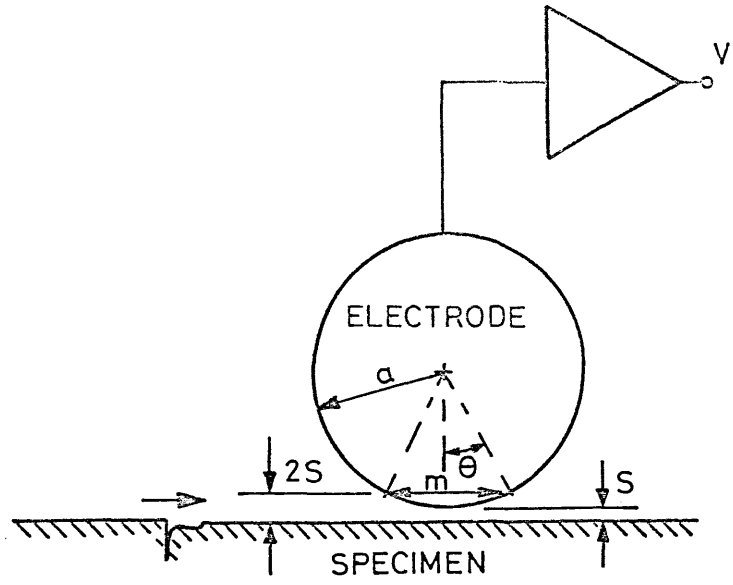

Fig 5.1- Capacitive transducer diagram.

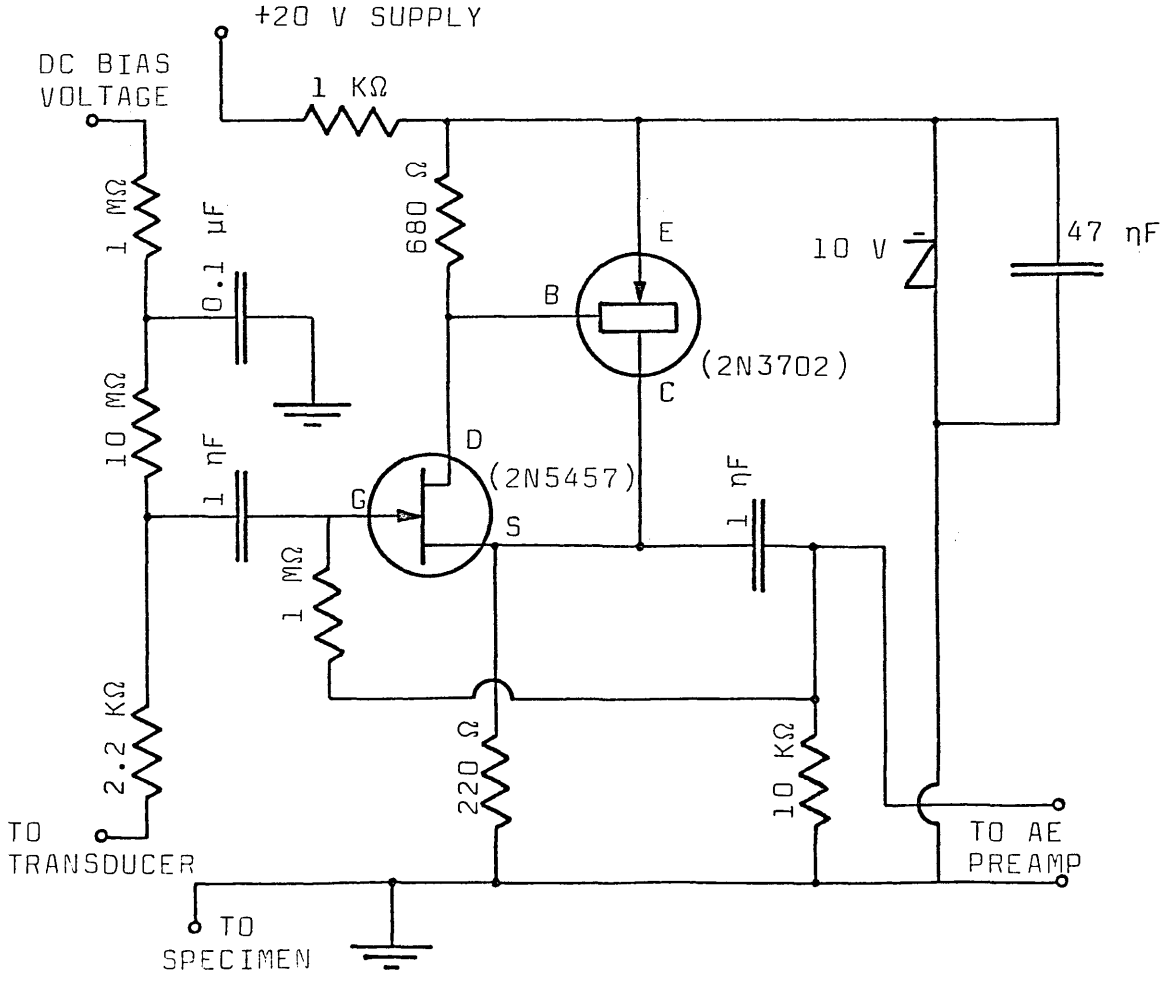

Fig 5.2- Capacitive transducer driver circuit.

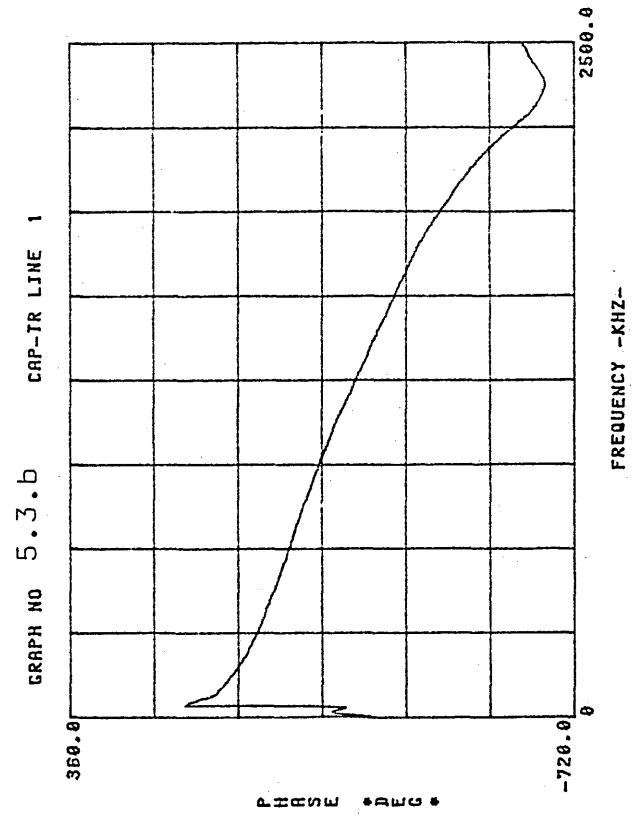

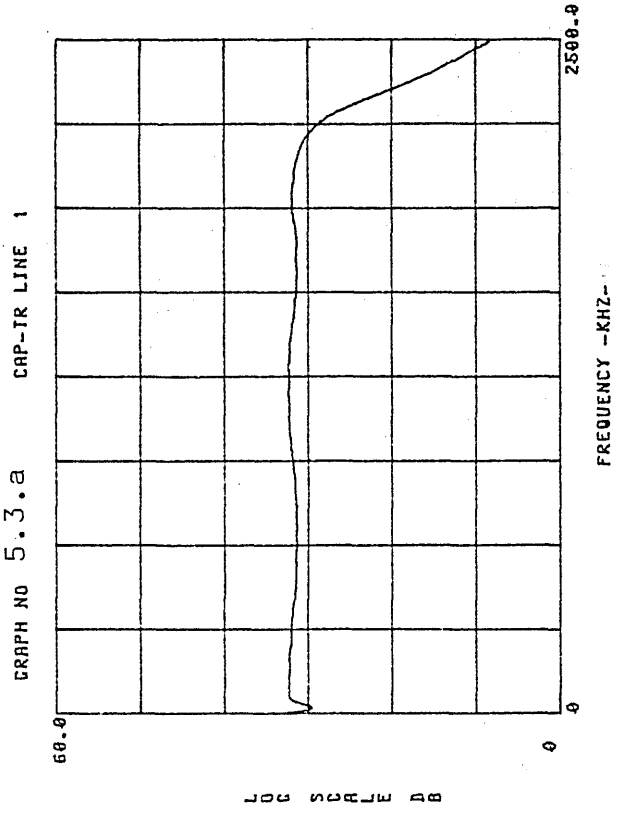

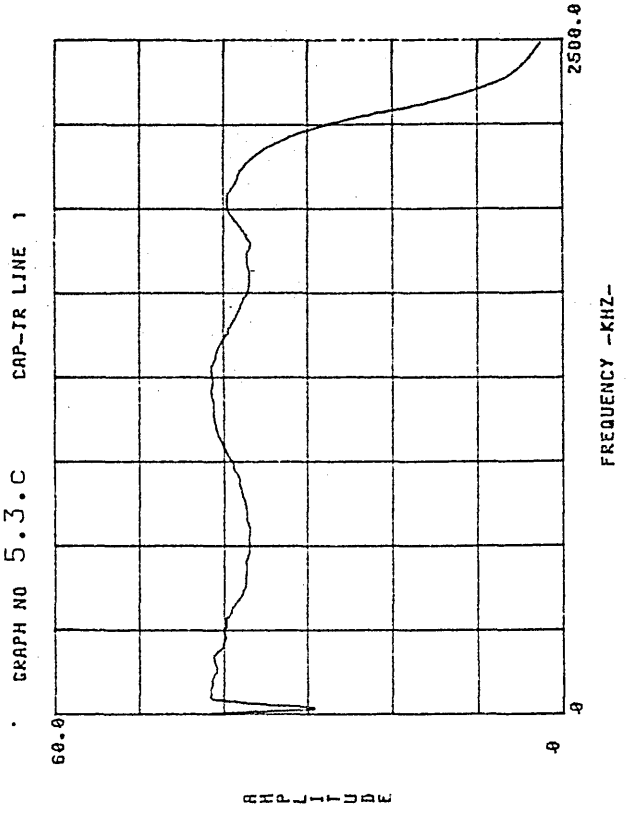

Fig 5.3- Calibration curves for capacitive transducer amplifier line 1.

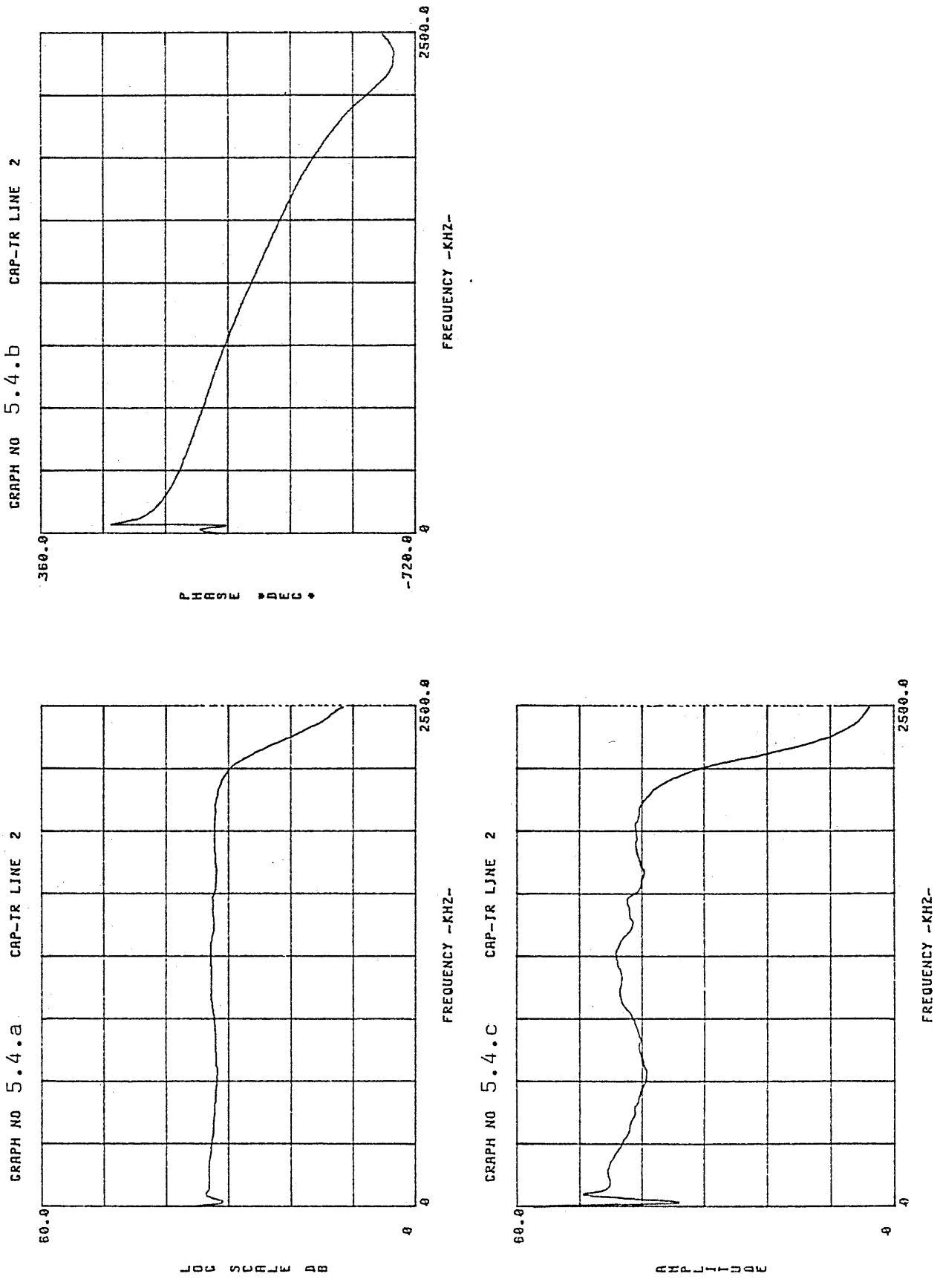

Fig 5.4- Calibration curves for capacitive transducer amplifier line 2.

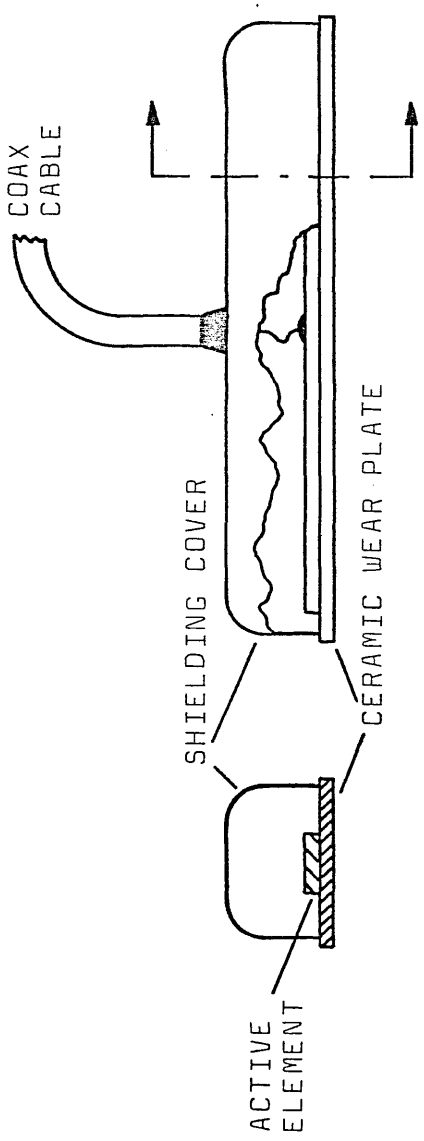

Fig 5.5- Descriptive diagram of the piezoelectric exciter.

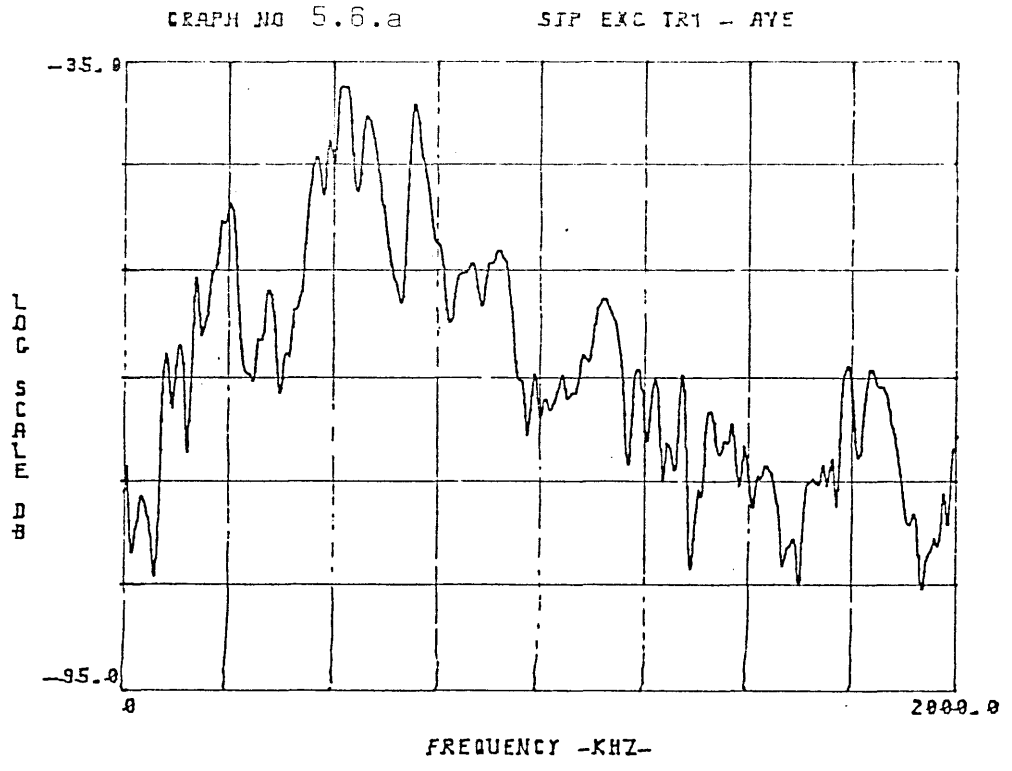

Fig 5.6.a- Normalized response of transducer 1 to a step function signal generated excitation.

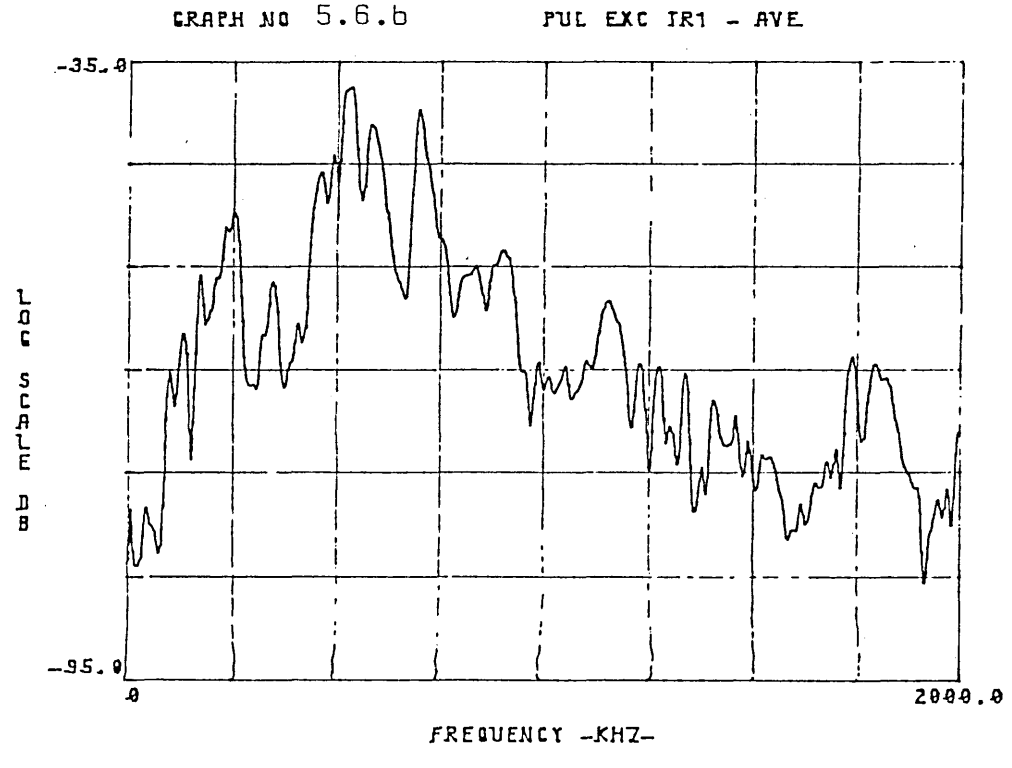

Fig 5.6.b- Normalized response of transducer 1 to a fast pulse signal generated excitation.

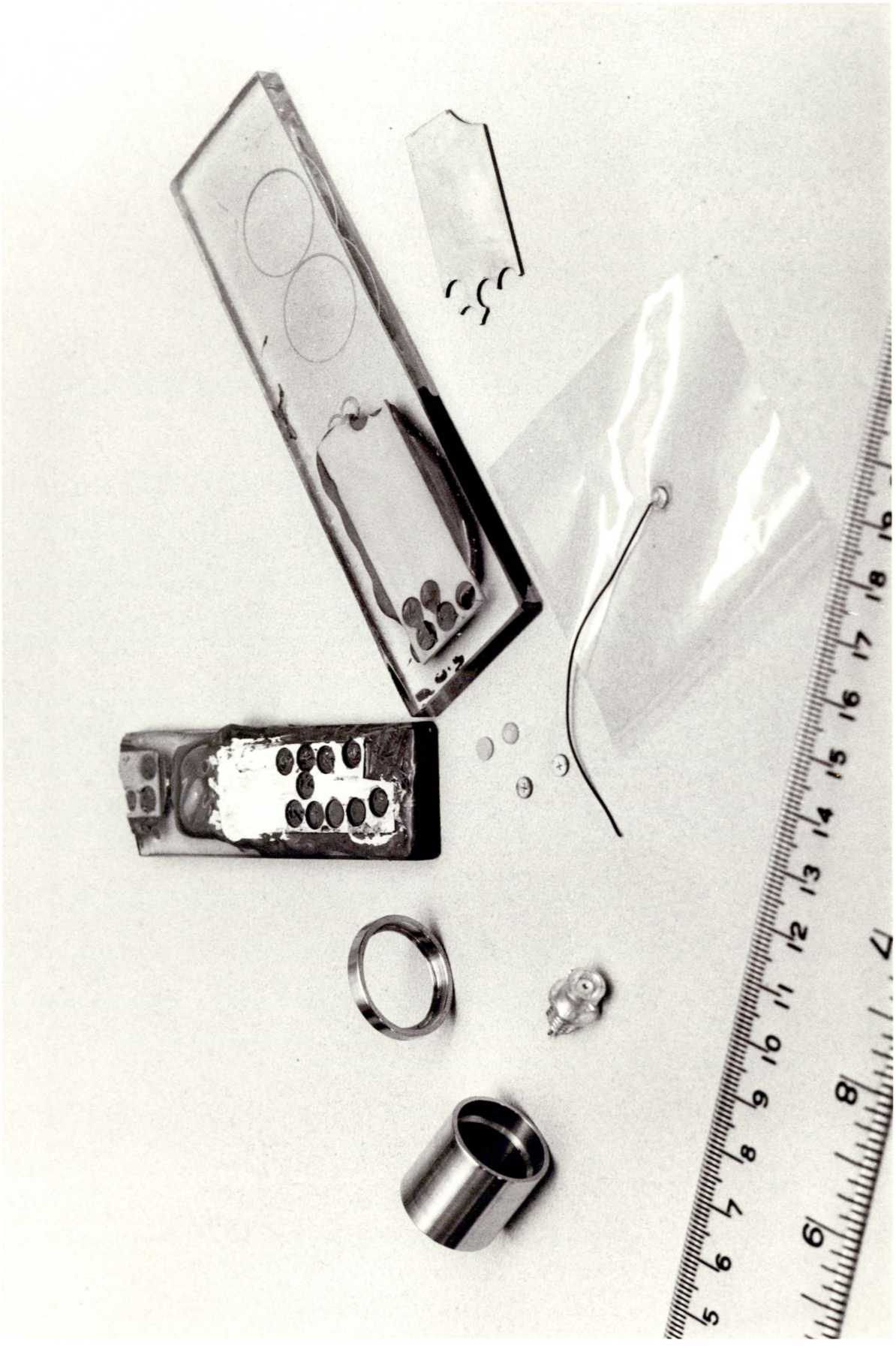

Fig 5.7- Components of a typical piezoelectric transducer with diaphragm configuration.

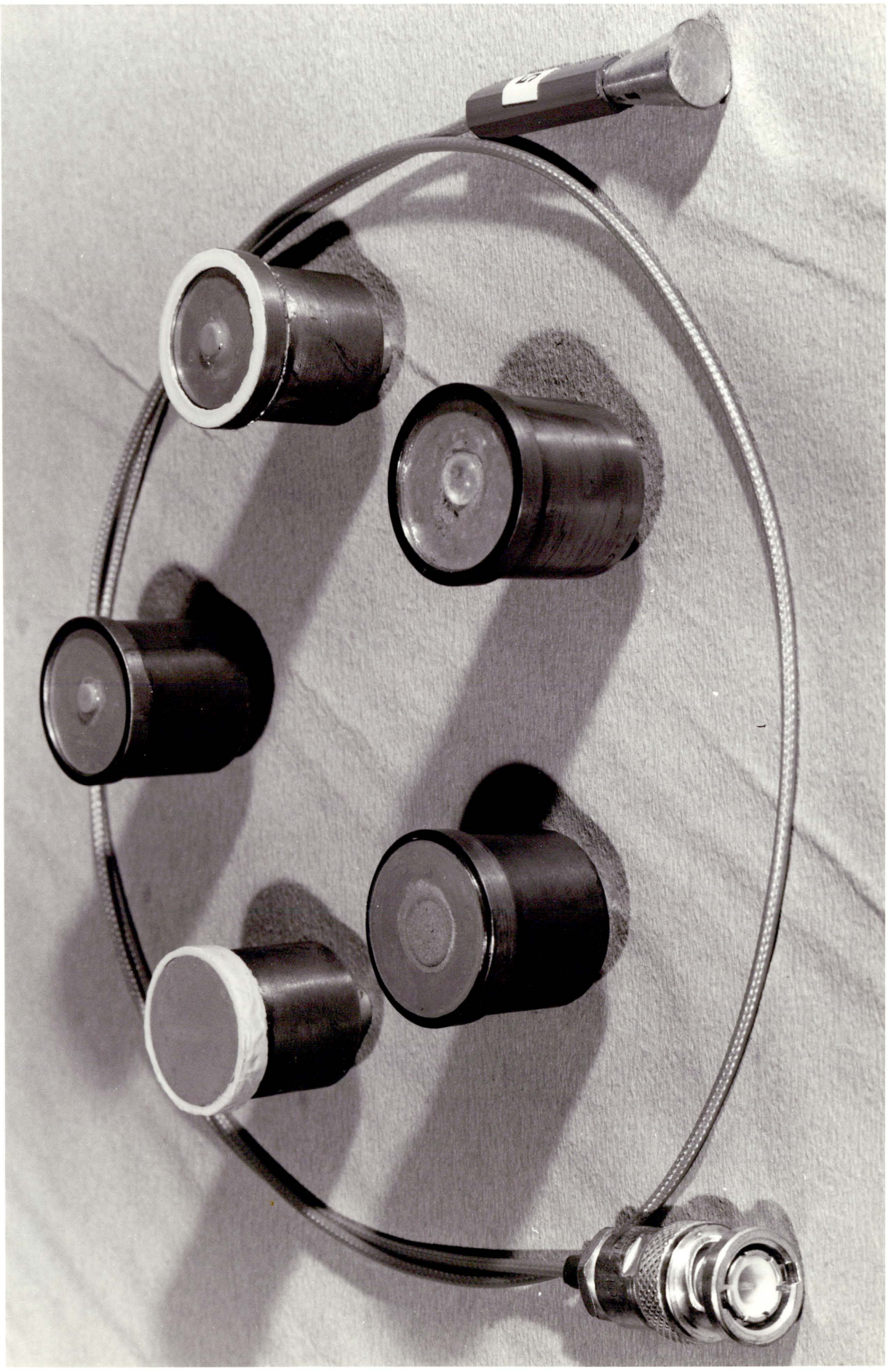

Fig 5.8- Six representative types of piezoelectric transducers.

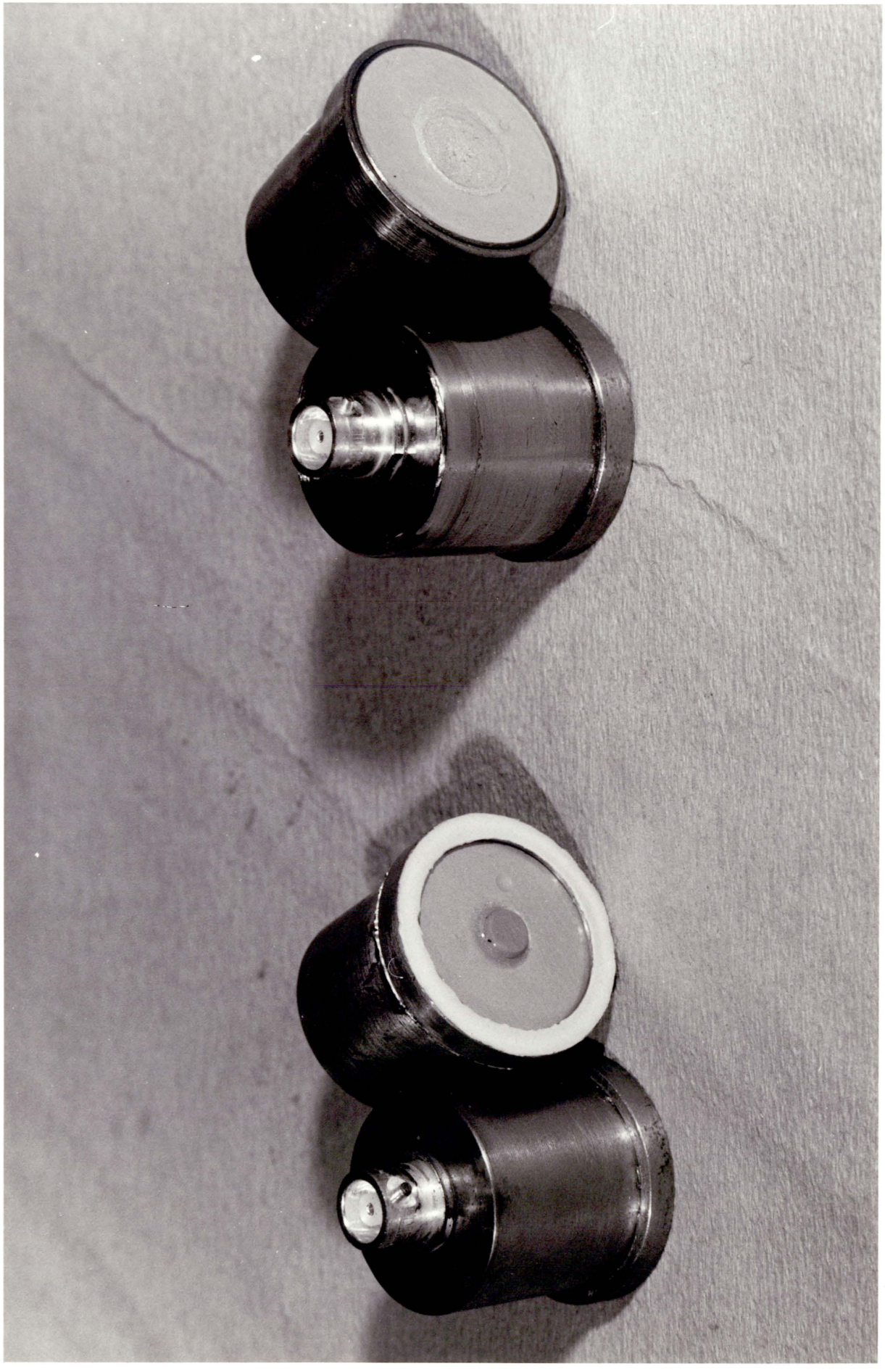

Fig 5.9- Close-up view of diaphragm transducers.

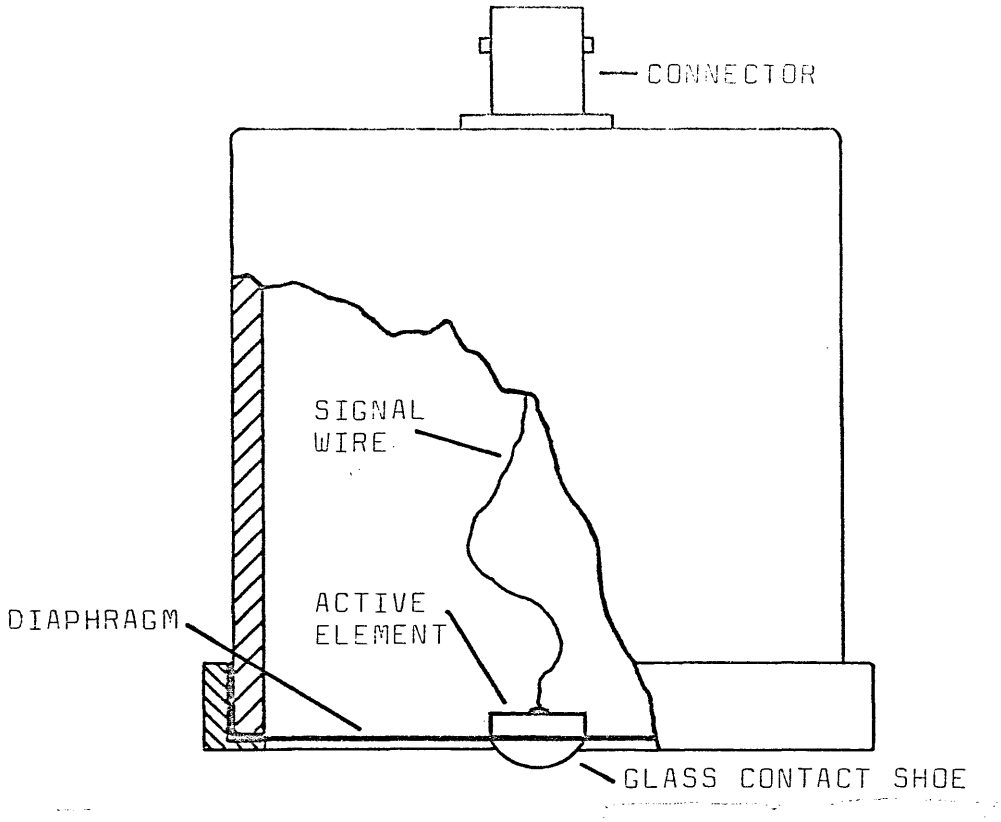

Fig 5.10- Diaphragm transducer with spherical glass contact shoe.

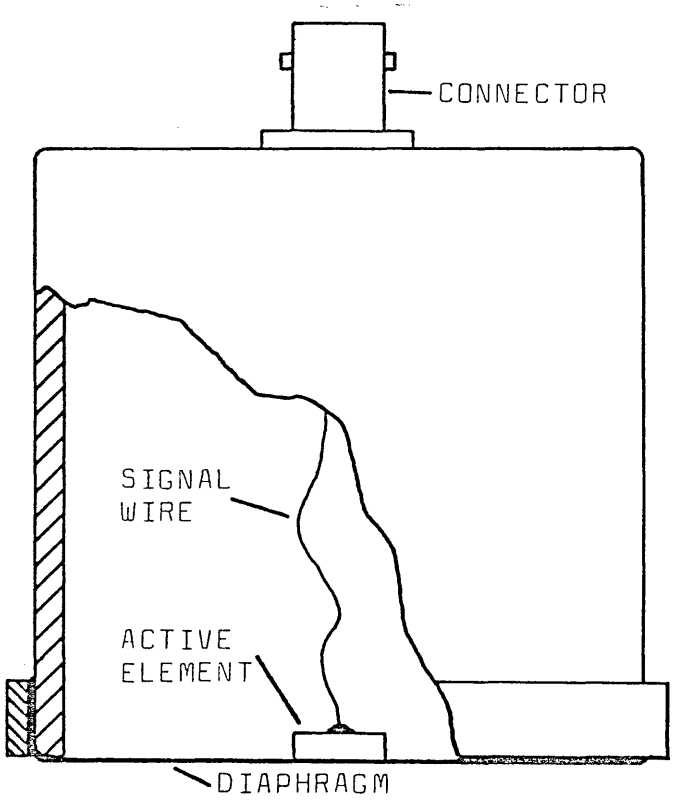

Fig 5.11- Diaphragm transducer without contact shoe.

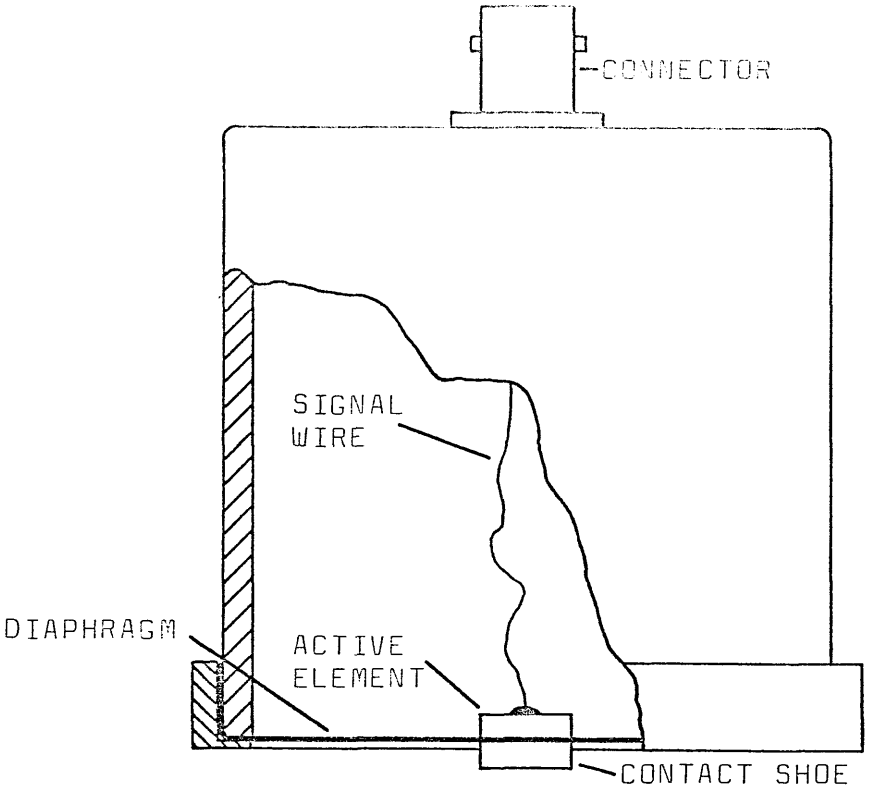

Fig 5.12- Diaphragm transducer with ceramic contact shoe.

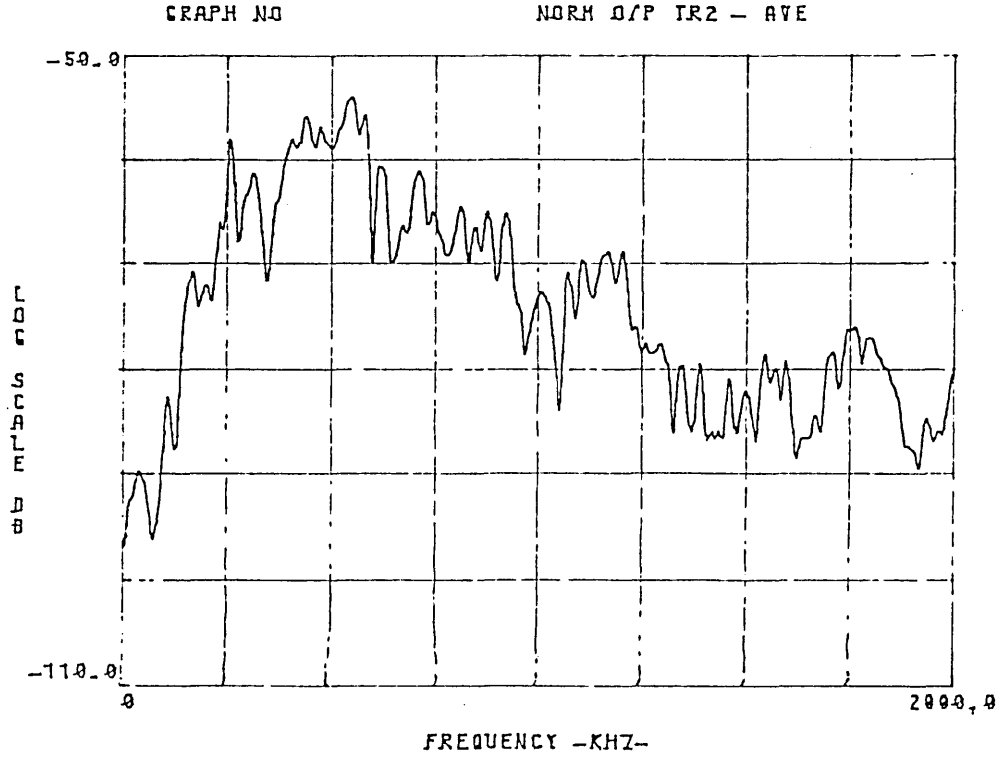

Fig 5.13- Frequency response from a diaphragm transducer without contact shoe.

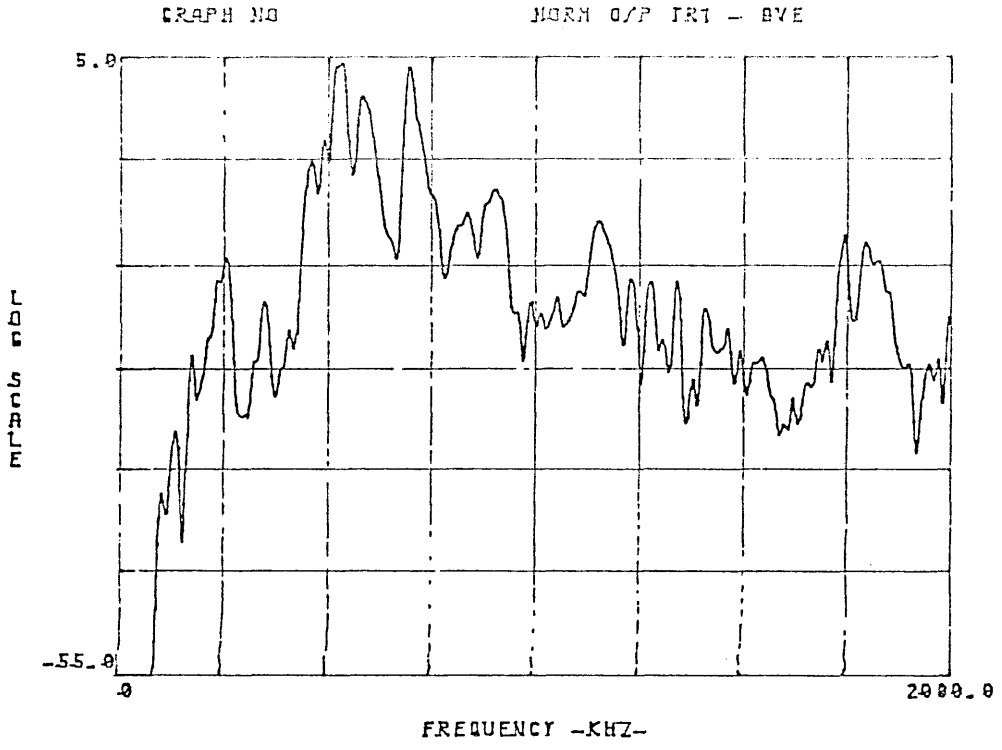

Fig 5.14- Frequency response from a diaphragm transducer with ceramic contact shoe.

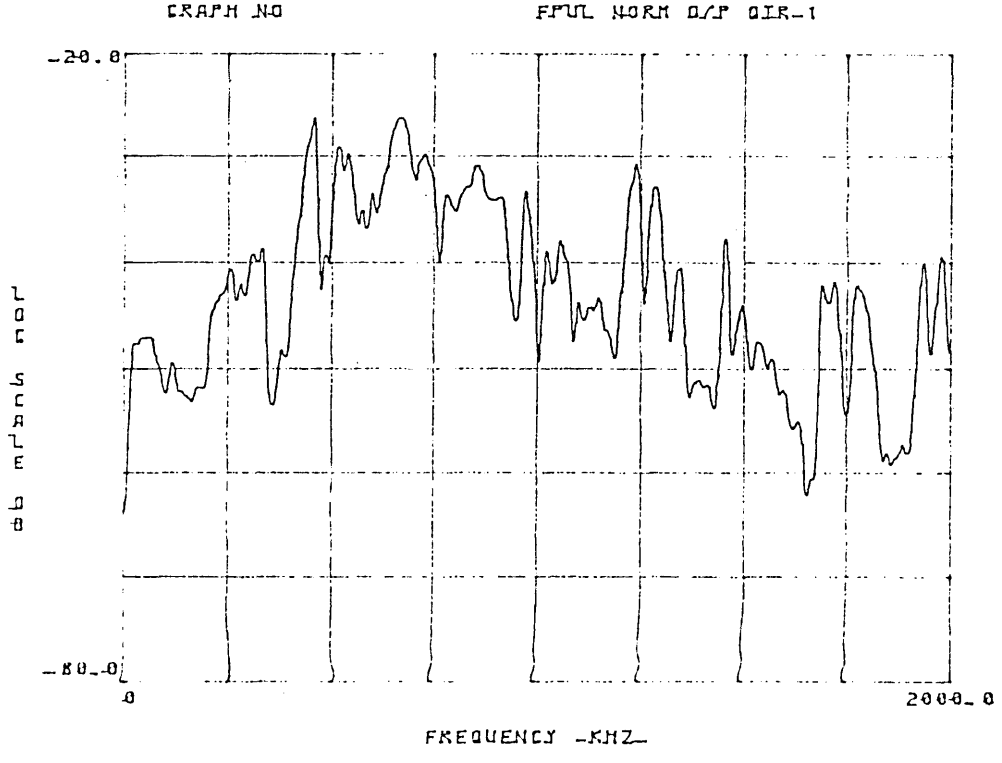

Fig 5.15- Frequency response from a quartz transducer (5 MHz nominal freq).

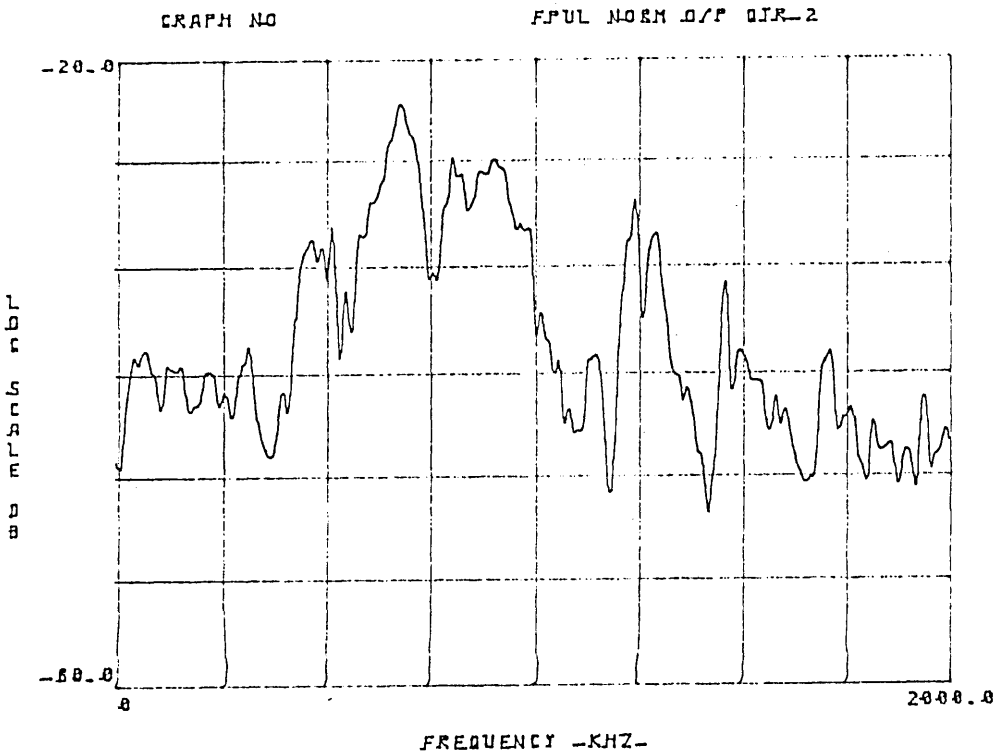

Fig 5.16- Frequency response from a quartz transducer (2 MHz nominal freq).

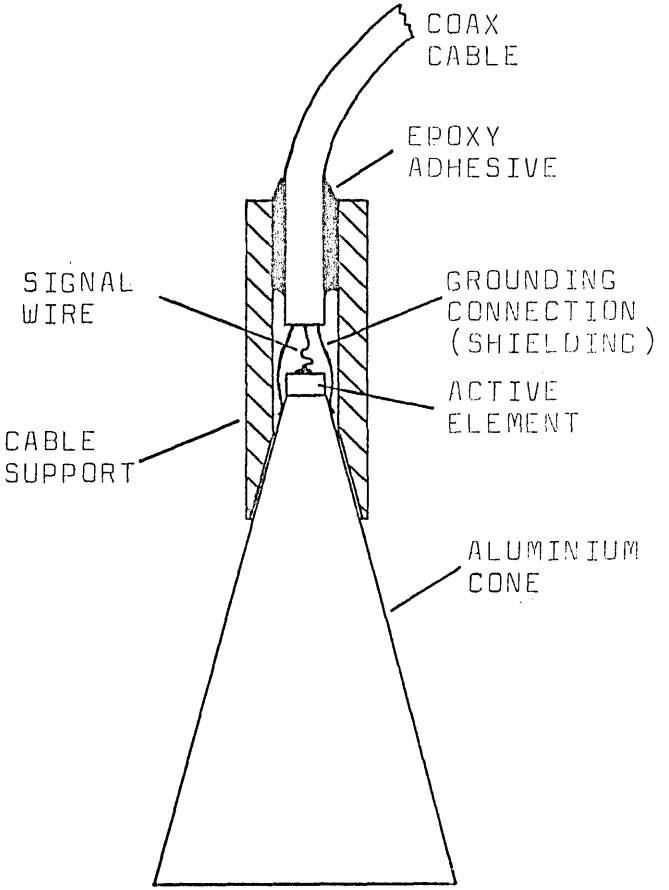

Fig 5.17- Wave guide transducer diagram.

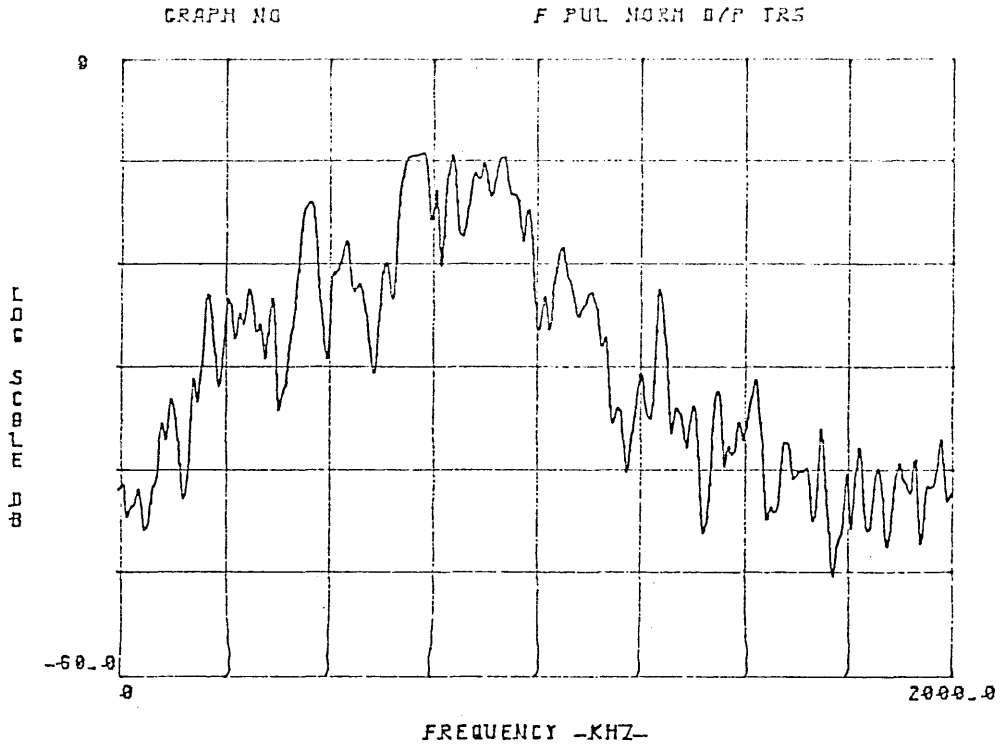

Fig 5.18- Frequency response from wave guide transducer.

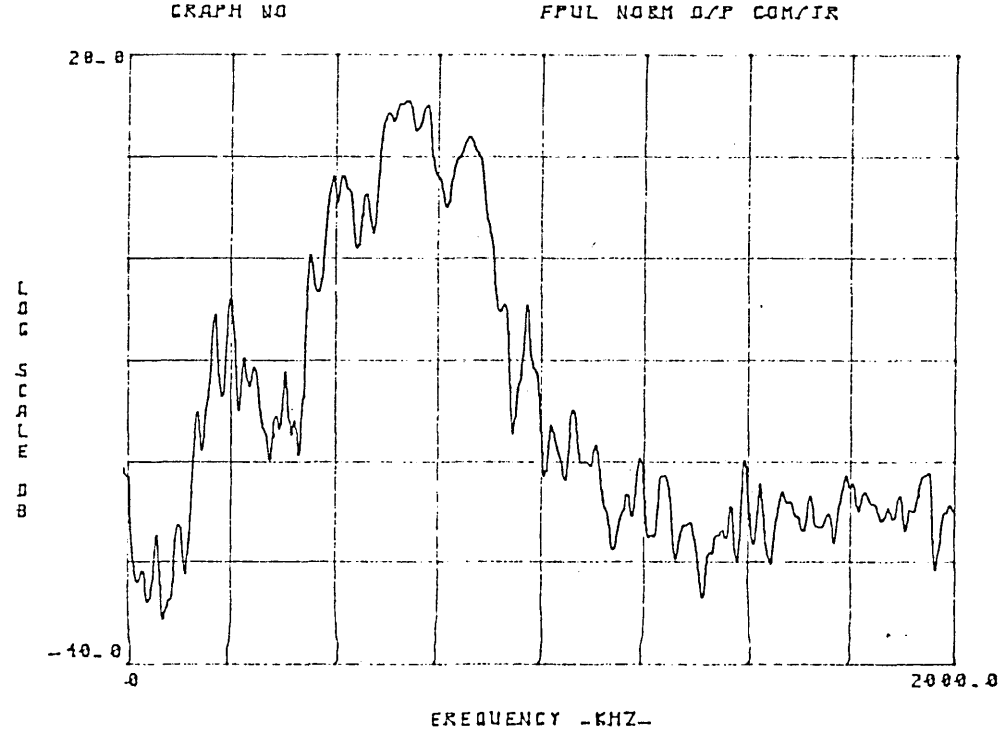

Fig 5.19- Frequency response from commercial "flat frequency response" transducer.

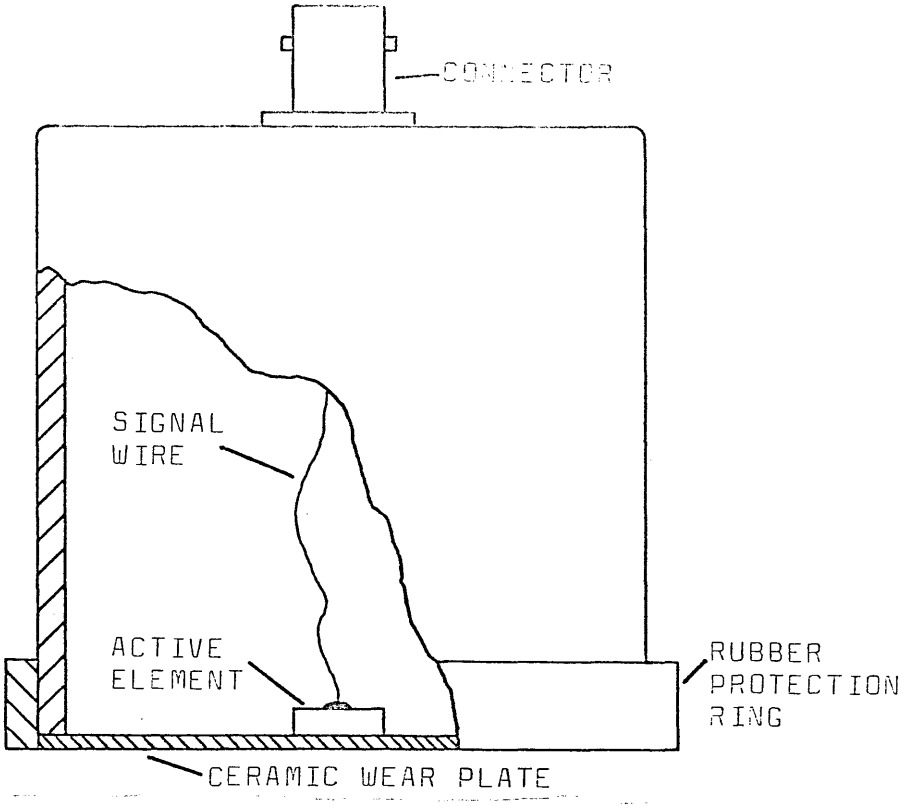

Fig 5.20- Ceramic wear plate transducer diagram.

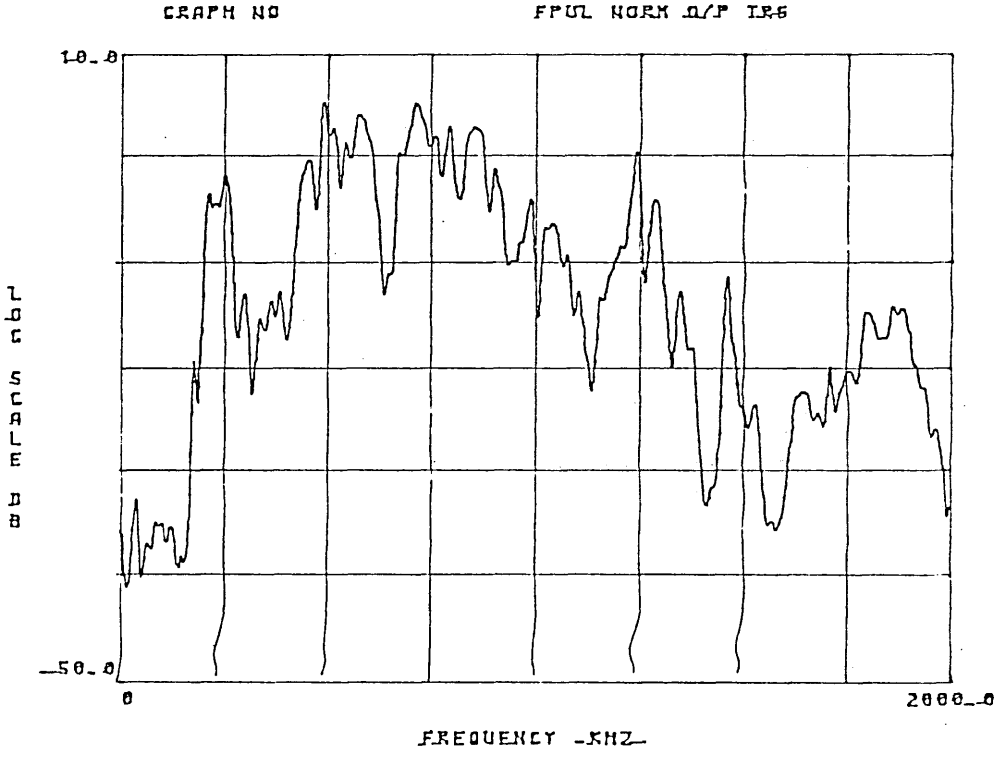

Fig 5.21- Frequency response from ceramic wear plate transducer.

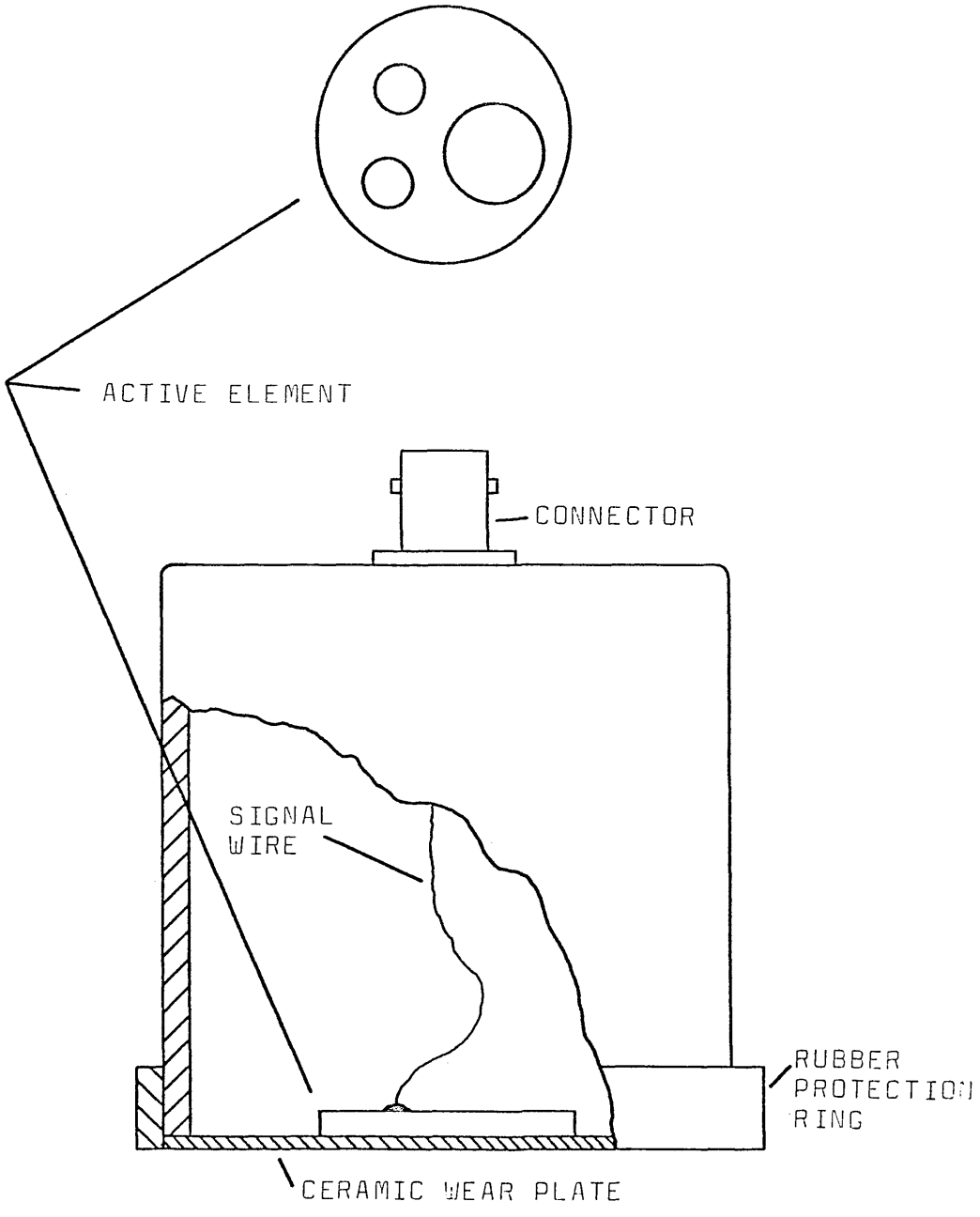

Fig 5.22- Asymmetric element transducer diagram.

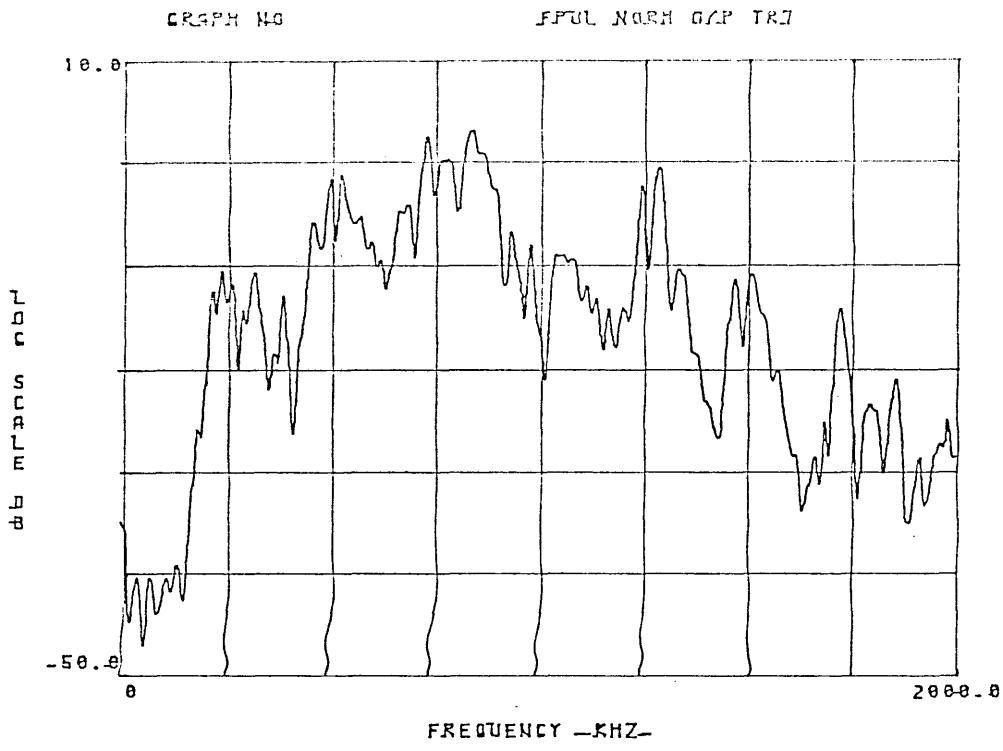

Fig 5.23- Frequency response from asymmetric transducer (No 7).

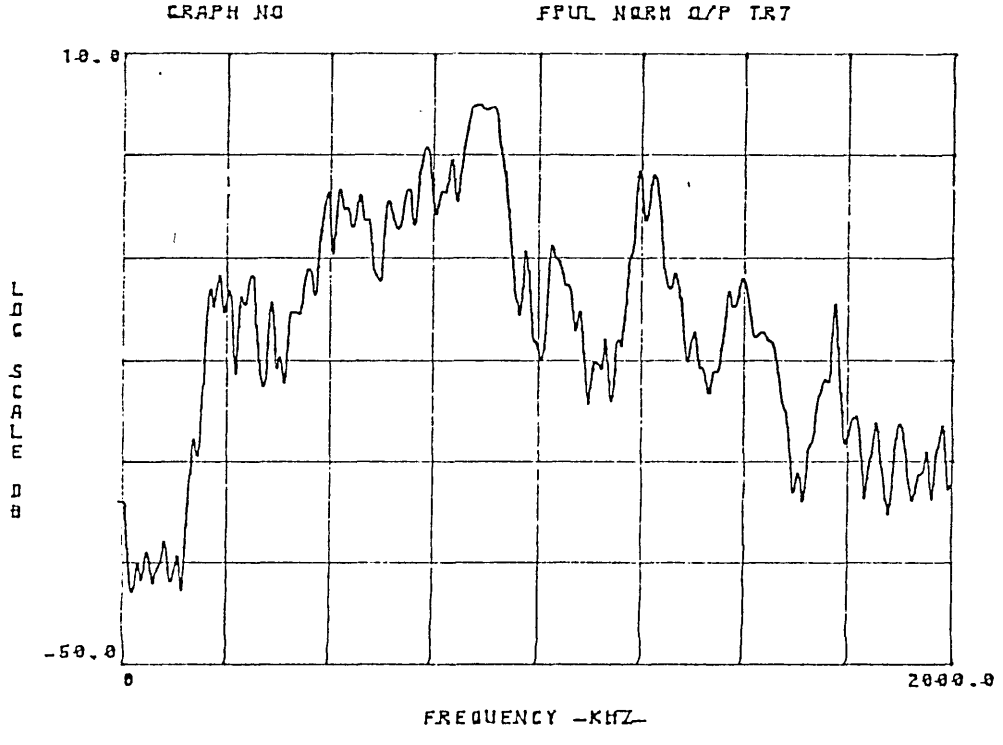

Fig 5.24.a- Frequency response from transducer No 7, with the orientation mark set for 0^{o}.

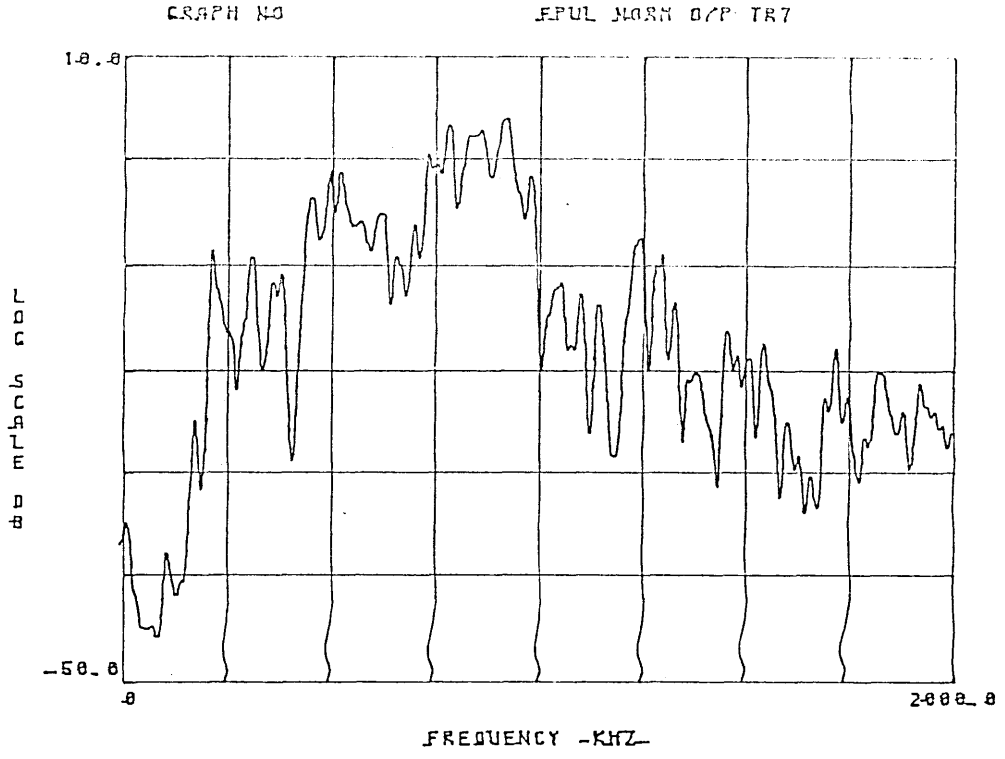

Fig 5.24.b- Frequency response from transducer No 7, after a clockwise rotation of 90^{o}.

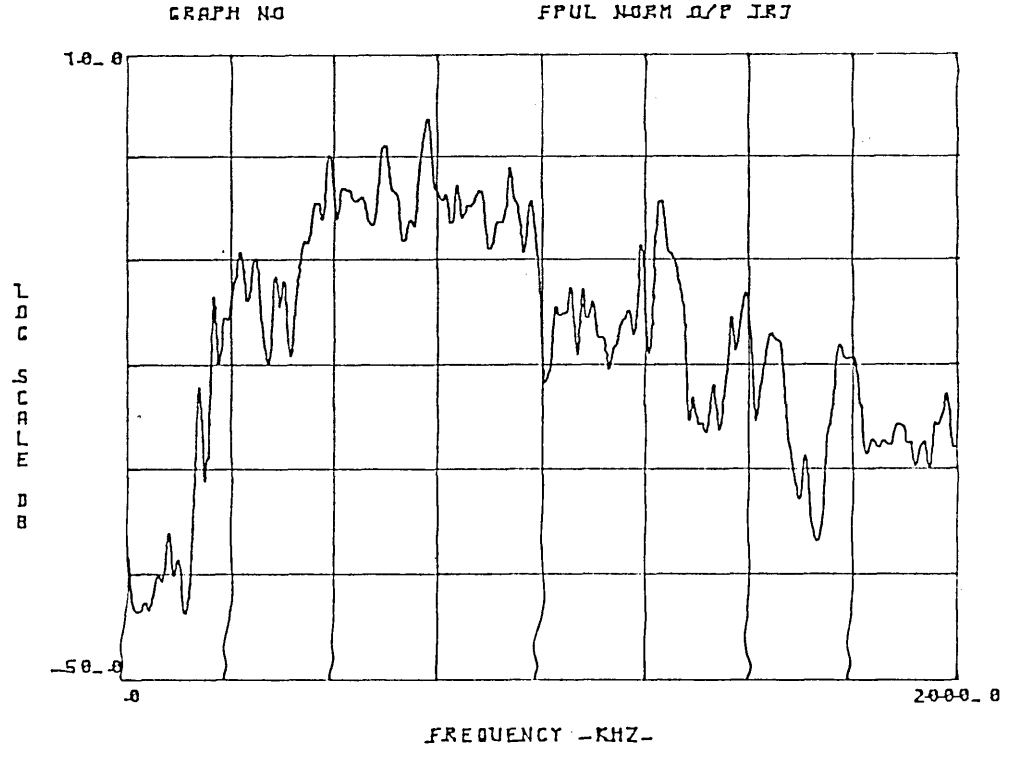

Fig 5.24.c- Frequency response from transducer No 7, after a clockwise rotation of 180^{o}.

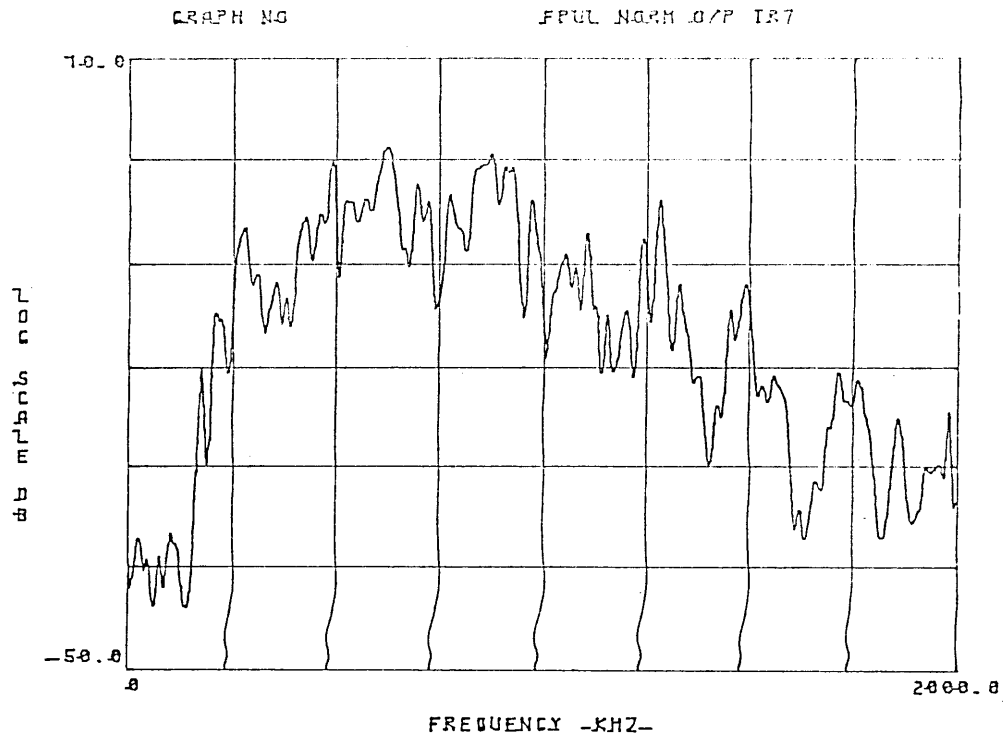

Fig 5.24.d- Frequency response from transducer No 7, after a clockwise rotation of 270^{o}.

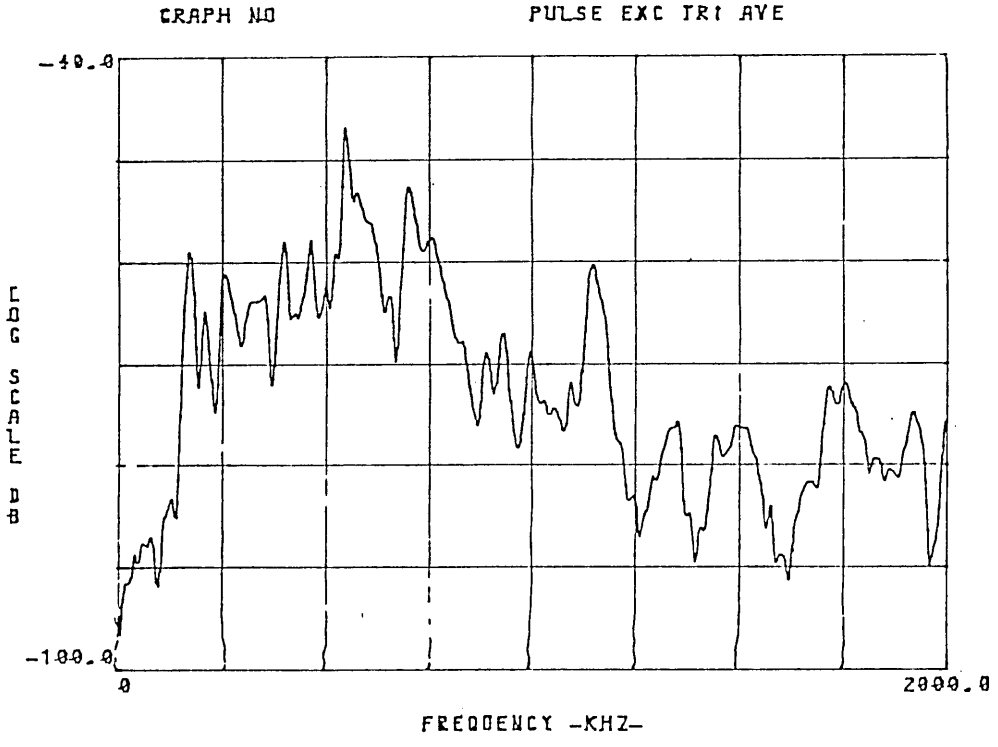

Fig 5.25.a- Frequency response of transducer No 1, using light viscosity oil as couplant.

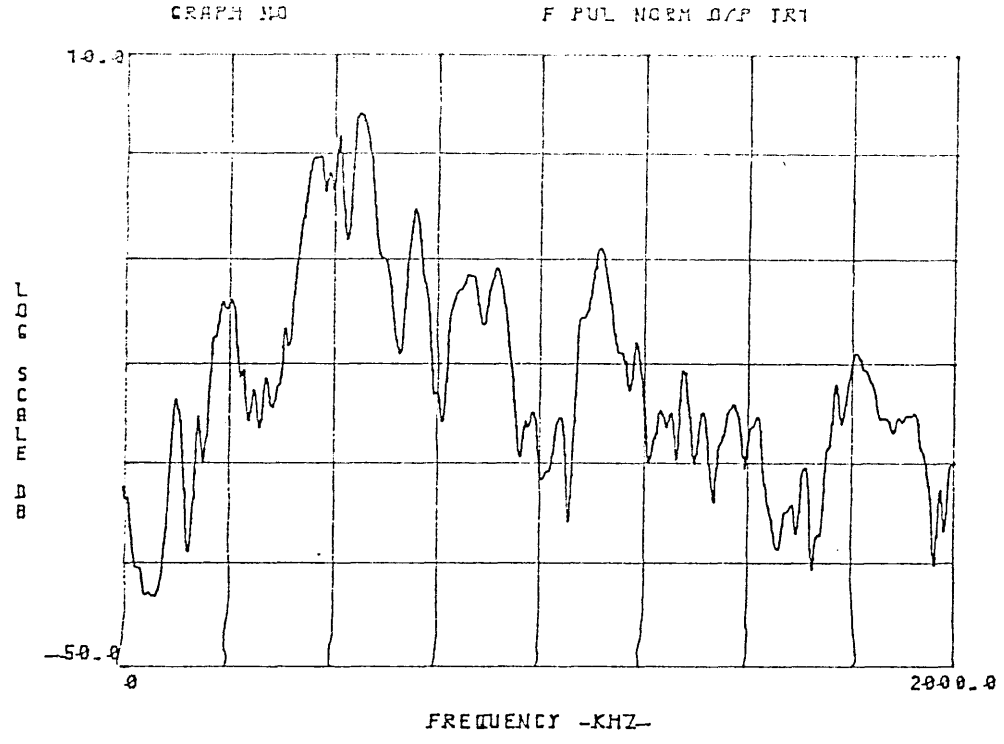

Fig 5.25.b- Frequency response of transducer No 1, using silicone rubber as couplant.

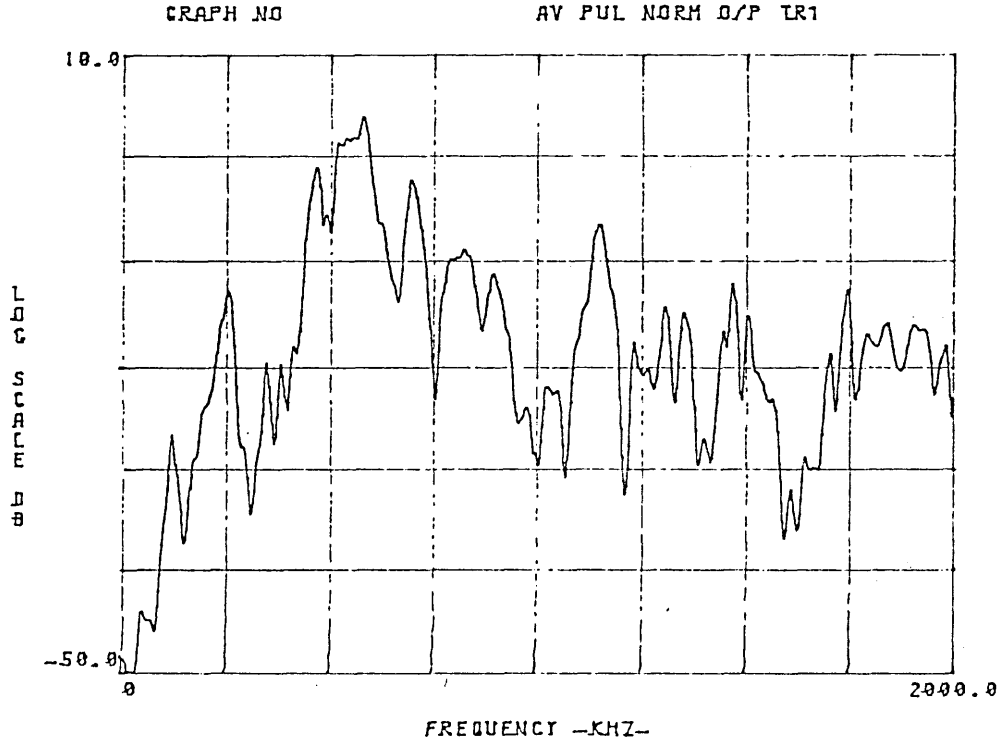

Fig 5.25.c- Frequency response of transducer No 1, using water based resin as couplant.

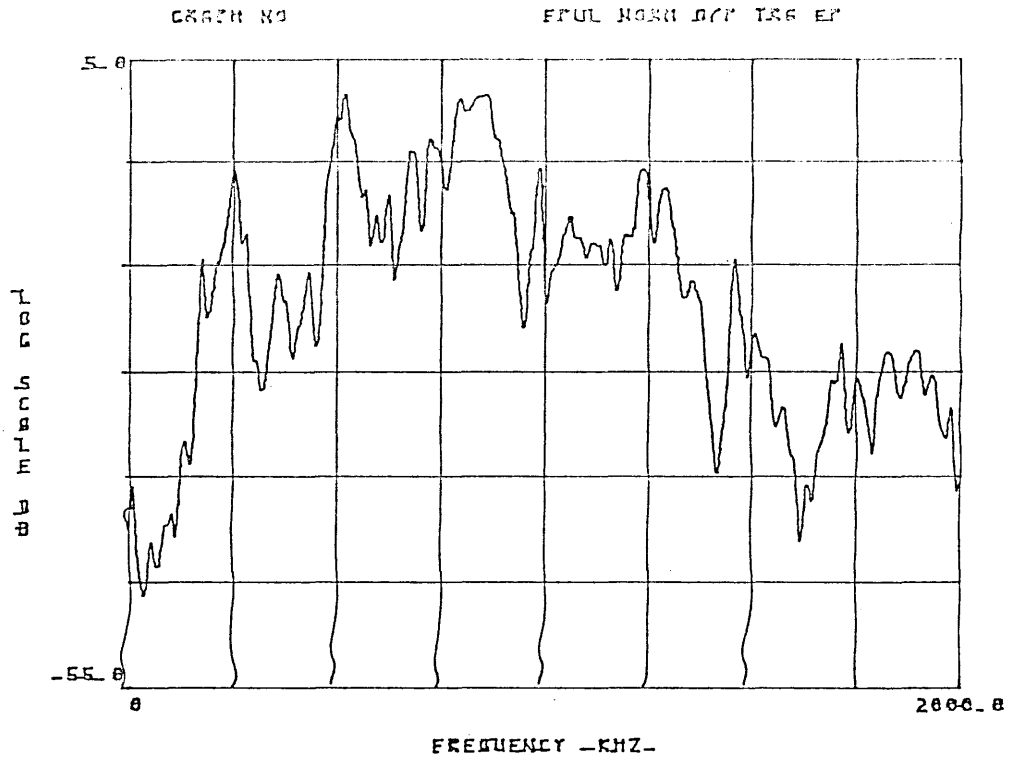

Fig 5.26- Frequency response from transducer No 6, after introducing damping. (Epoxy Resin)

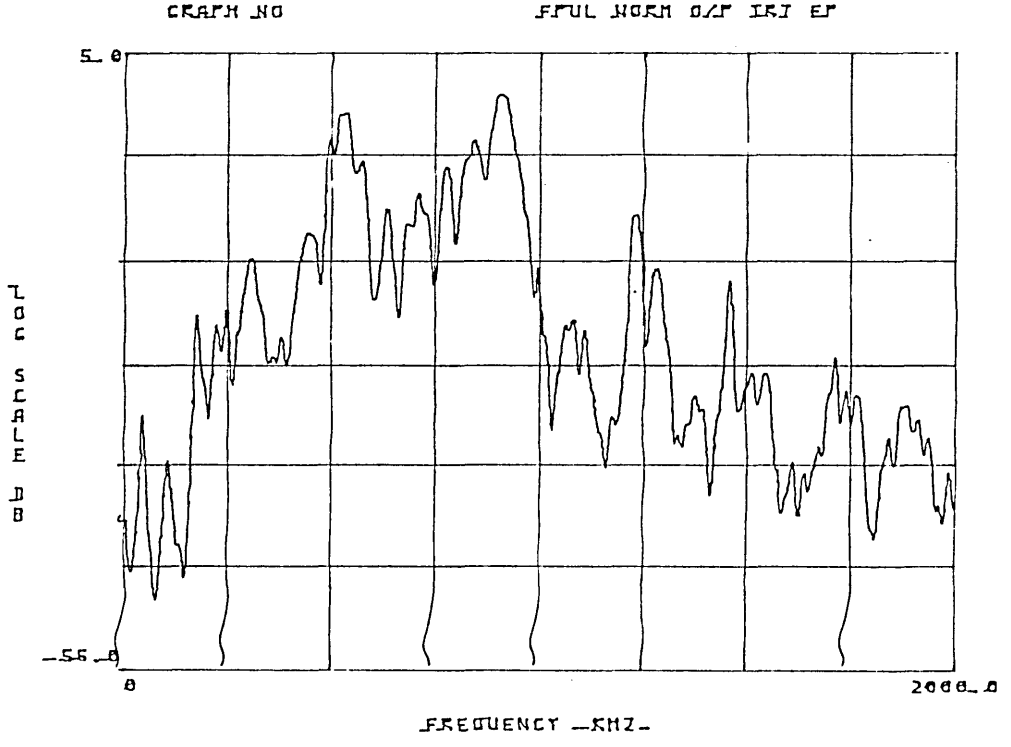

Fig 5.27- Frequency response from transducer No 7, after introducing damping. (Epoxy Resin)

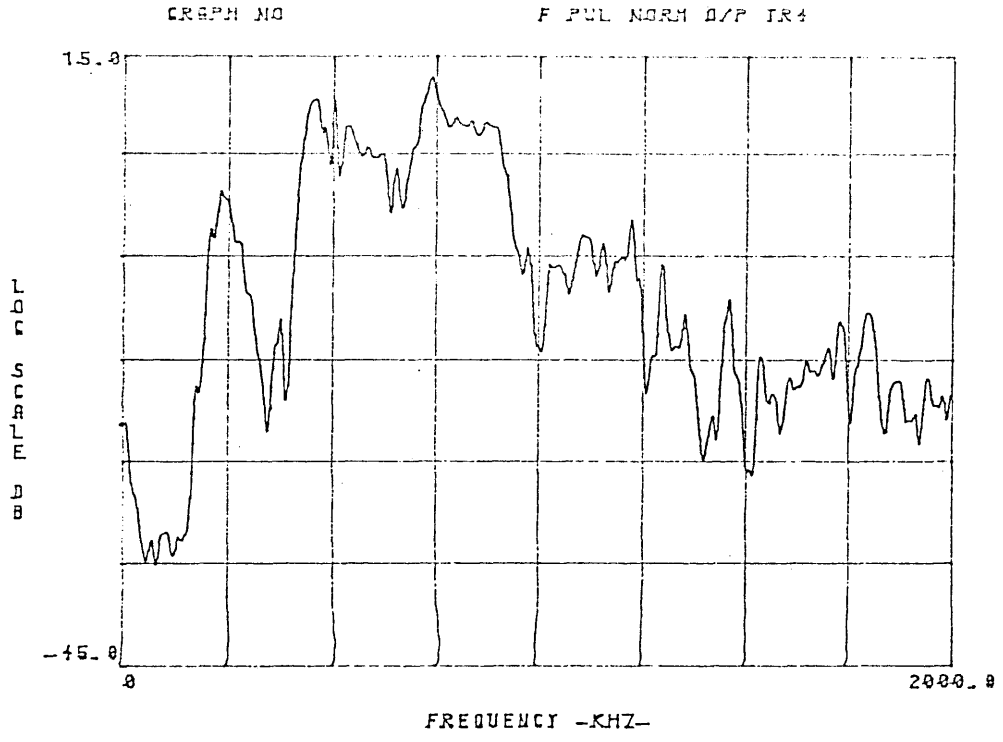

Fig 5.28.a- Frequency response from transducer No 4, without damping.

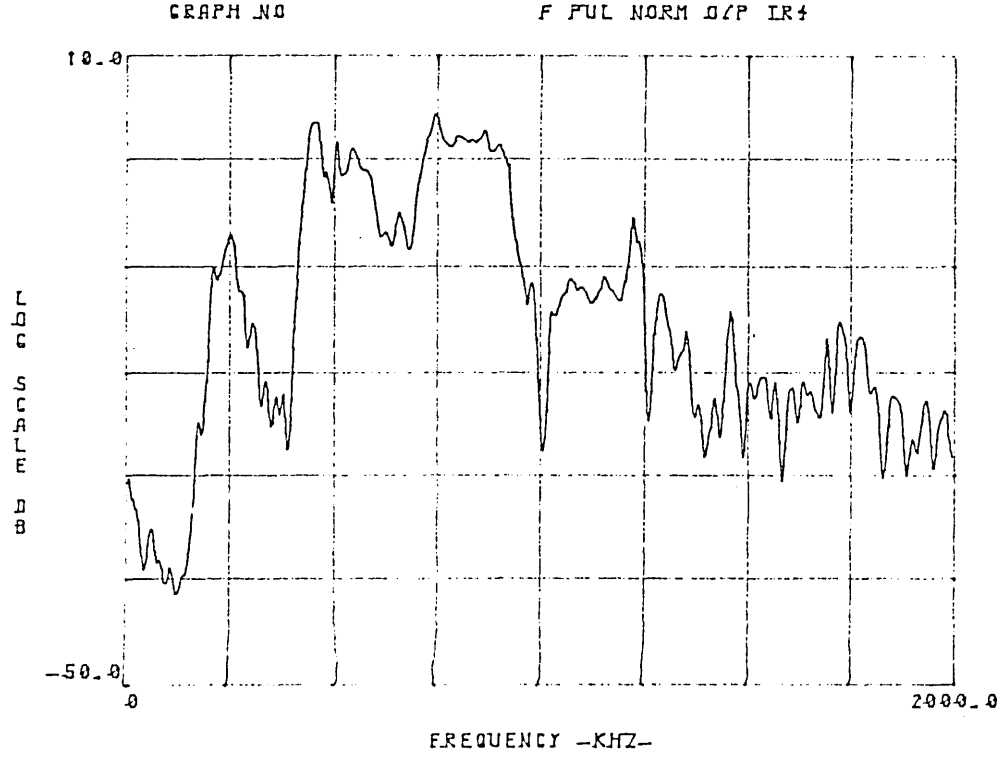

Fig 5.28.b- Frequency response from transducer No 4, after applying silicone rubber damping.

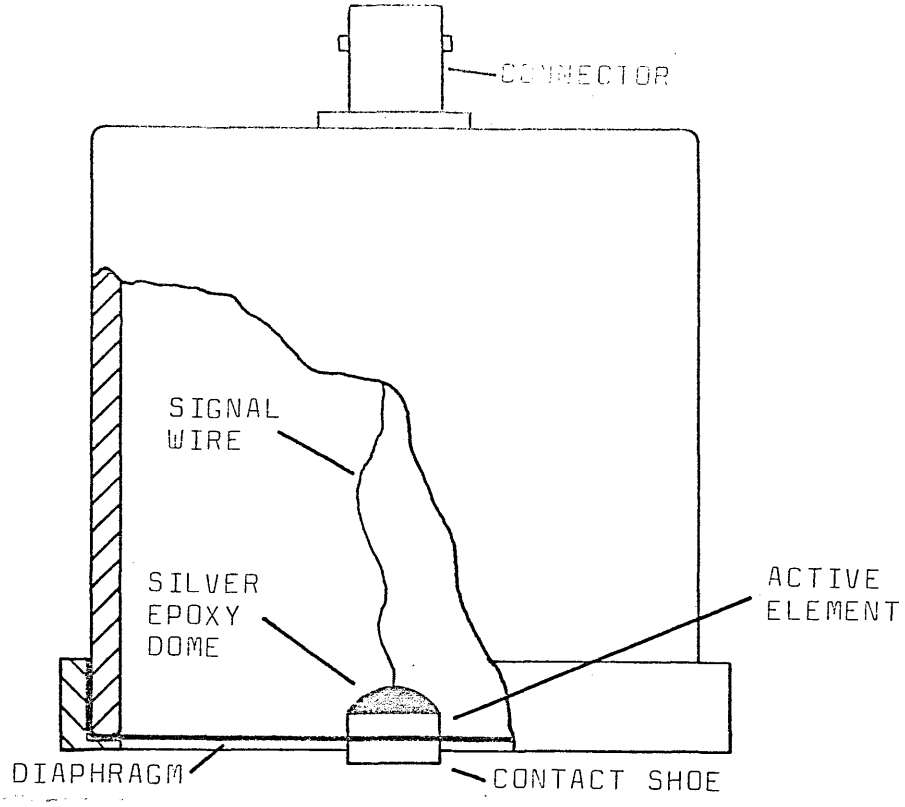

Fig 5.29- Piezoelectric diaphragm transducer with inertial loading.

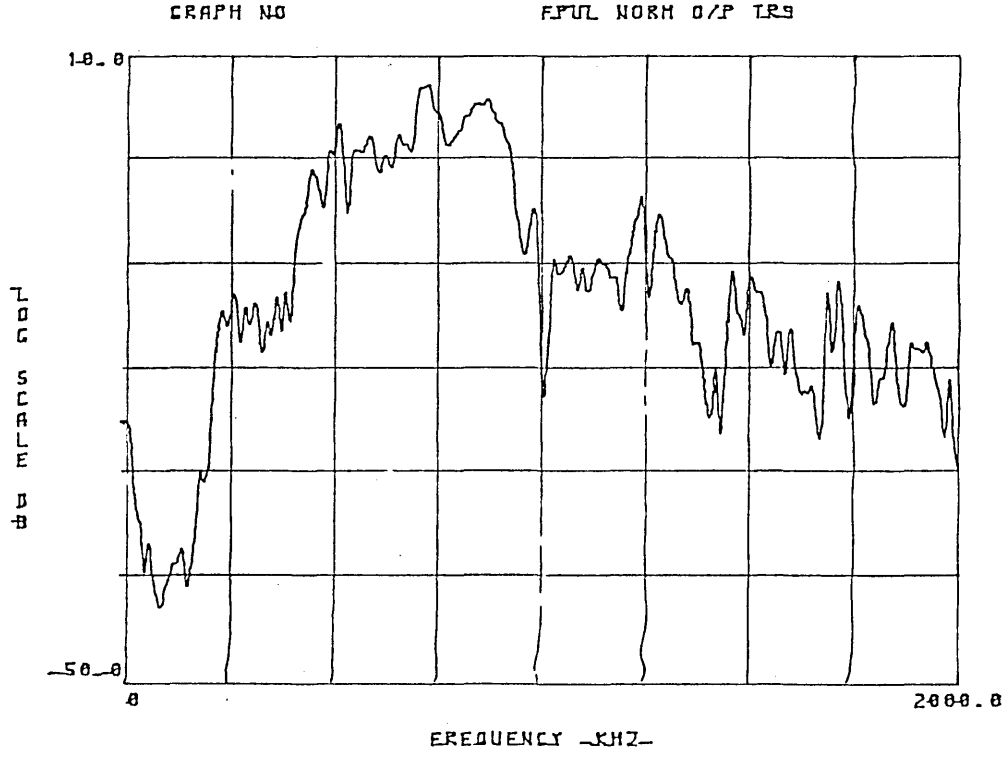

Fig 5.30- Frequency response from transducer with inertial loading.

CALIBRATION METHOD

Acoustic Emission as a technique, like so many scientific disciplines, has had to evolve from its initial primitive stage of pure and simple detection, to the later stage of measurement. Such a natural process of evolution is motivated by the necessity of correlating experimental observations with the phenomena which caused them, and by the interest felt by the individuals working within the discipline to establish a common basis for comparing their results.

The achievement of a standard baseline for comparison, automatically transforms what would otherwise be mere observations into measurements, and the process of attaining such a standard is precisely the subject of the present chapter.

As explained in chapters 1 and 2, the progress of AE methods has been dictated by the advances made in the necessary instrumentation, and the development of new and better equipment for specific applications has, in turn, increased the demand for more precise methods of calibration and specification.

These facts are especially illustrated when examining the progress made in the design of new transducers and methods for their calibration, from the published literature.

6.1 LITERATURE REVIEW AND DISCUSSION

Numerous methods have been devised and developed to achieve the calibration of transducers in terms of overall sensitivity and frequency response, employing diverse configurations and excitation mechanisms, although the fundamental basis behind these methods is either the reciprocity principle, or the reference to theoretical models.

One of the pioneering methods of calibration to become widespread among transducer manufacturers during the sixties and early

seventies, consisted in mounting the transducer directly on top of the active surface of a standard exciter, which had previously been calibrated underwater, as a receiver, with the well established far field method for hydrophones.

The calibration of the AE sensor was achieved by feeding a continuous sinusoidal signal into the exciter, sweeping the frequency over the desired range of interest, while the resulting output amplitude was registered as a spectrum in terms of frequency.

Although this method was still being used in research work published as late as 1968 (47), concern was already growing with regards to the nature of the excitation not being representative of true AE mechanisms.

As a result of the search for alternative methods of excitation, a new technique was presented by L.J.Graham in 1971 (53), which used the impingement of small particles as the basic source of excitation. The particles were driven by a continous stream of air (like a sand-blaster), and were directed against a metal block, upon which the transducer was mounted.

The method was expected to represent the transient character of AE events, since each one of the particle impacts is a transient itself; while the superposition of the multiple impacts was considered to produce a white noise spectrum. However, growing scepticism over the flatness of the excitation spectrum motivated the development of a "white noise generator", by L.J.Graham and G.A.Alers (20). In the new system, the excitation was generated by grinding small silicon carbide particles with a rotating glass rod against a metal plate, upon which the transducer was mounted. The flatness of the excitation spectrum was established by means of a capacitive microphone, which also indicated the overall level of excitation, thus allowing the calculation of the transducer sensitivity.

An equivalent method developed independently in Canada by S.L.McBride and T.S.Hutchison (30), utilizes a gas jet blown through

a narrow capillary against a cylindrical block, onto which the transducer is mounted. The parameters of capillary length and bore diameter, separation from the block, and gas pressure, were developed from multiple tests, until a suitable frequency distribution for the produced excitation was achieved. The amplitude spectrum for the excitation was determined by using an X-cut quartz crystal disc, with its calculated fundamental resonance at 5 MHz, which was assumed to have a flat frequency response for frequencies up to 1 MHz (the calibration bandwidth).

The method for obtaining the calibration curves was similar in all three techniques described above, and consisted in producing a direct amplitude spectrum with a sweep frequency analyser.

Although the random character of these sources of excitation was considered to represent better true AE phenomena, criticisms were still raised concerning the duration of the process, since any continuous type excitation, whether random or not, disregarded the transient nature of AE events, and might induce an emphasis of transducer resonances and standing waves fixture.

The search for transient methods of excitation produced two very important techniques, which are still under current use. One of these techniques, developed by R.L.Bell (31), from Dunegan/Endevco, utilizes an electric spark of short duration as the prime source of excitation. The system was originally designed with the spark generated at constant intervals, while a sweep frequency analyser was used to produce a narrow band spectrum of the transducer output.

The short duration of the spark was considered to generate an excitation with a flat frequency distribution, although no provision was made to monitor this. A later modification of the method included the use of a capacitive transducer, as a reference standard, for the correction of the obtained calibration in terms of deviations in the excitation spectrum.

A second technique was developed at the National Bureau of Standards, Washington, USA, by F.R.Breckenridge et al (22), and

consisted in using a step forcing function generated by the brittle fracture of small glass capillary sections, employing a massive block as the transmission media, and including a capacitive transducer as reference standard. However, the actual calibration of transducers was achieved by injecting short bursts of sinusoidal signals into a DC biased electrostatic transducer, and directly monitoring the output level of the sensor under test for the different carrier frequencies. The flat frequency response of the capacitive devices was established by comparing the resulting output signal from the fracture of glass capillary sections, with the calculated surface displacement predicted by the theoretical results of C.L.Pekeris (37), published in 1955.

Additional proposed methods of calibration include those proposed by W.C.Leschek (34), and H.Hatano and E.Mori (35), based upon the reciprocity principle. In the method presented by Leschek, a standard transducer is calibrated in a difused acoustic far field, using a steel block, and water as the transmitting media. Once the sensitivity of the standard transducer is determined, the calibration of other sensors is achieved by comparison, using random noise signals to generate a continous excitation via a piezoelectric exciter. The method has strong resembalances to the traditional hydrophone based calibration methods, with the use of random noise as the major difference.

The technique developed by Hatano and Mori relies upon the calculation of a reciprocity constant for the transducers, derived from a first order approximation of the equations governing the Rayleigh wave acoustic field for an elastic media. The surface wave excitations are generated with a warbling tone signal, and the actual calibrations are achieved by measuring the current consumed by the exciter, and the voltage output from the sensor.

Both these methods were found to disregard the transient character of the AE phenomena, although the calculation procedure for the reciprocity constant suggested by Hatano and Mori was found attractive.

The literature reviewed up to this point refers only to amplitude frequency response characteristics for the transducers, and no mention is made in any of the above papers, of phase characteristics. This conception for the calibration of transducers had been inherited from the analysis of continous vibrations, where the phase information, if at all required, corresponds to frequencies too low for the instrumentation to have any significant effect. Extending this traditional conception into AE work led Graham and Alers to the mistaken conclusion that "AE in many materials tends to be nearly 'white noise', at least up to 2 MHz" (20).

The cause for their confusion can easily be understood from the fact that a very short duration transient will produce a flat amplitude spectrum (impulse spectrum), similar to that of white noise. However, the phase spectrum for the transient signal will contain a very definite structure, whereas that from white noise will be random.

Therefore, the calibration of a transducer in terms of amplitude only, will allow the de-colouring of the signal amplitude spectra. However, the information contained in the transducer amplitude spectrum will not be sufficient to recover the true surface wave, since the de-convoluted phase information will be missing.

Some methods of signal processing reviewed later, avoid the problem of calibrating the transducer in terms of phase by obtaining the transfer function of the transducer in the time domain, and performing all convolution and de-convolution processes also in the time domain.

The above literature was the only information available at the time when work commenced on the calibration procedure. However, The aim to recover the true surface wave from the transducer output had been established from the beginning of the project, thus the need for taking phase into account was kept present whenever the feasibility of a particular calibration method was considered.

Towards the end of the work, additional literature was obtained in relation to AE transducer calibration, which was employed

as a basis for comparison of the method developed through this project. However, this additional material did not contribute to the background for this section of the research work. A short review of these papers is nevertheless included since they represent the up-to-date state of the art, and the contained results provide a good source of reference.

6.1.1 Literature Update

A comprehensive literature review was published by A.E.Lord (54) in 1981, making special emphasis upon the calibration and source recognition aspects of AE experimental research, as developed by Breckenridge et al (22), and later applied by Sachse and Ceranoglu (38)(55), and Feng and Whittier (32). The review also includes more theoretical aspects related to the transfer function for the transmitting media (Green's function), and the papers representing major contributions to the development of Green's functions for elastic plates, allowing the displacement to forcing function relationship to be established, and later applied to the calibration of transducers.

Results found included, illustrated the main ideas behind this line of work. For example, the epicentral response of a plate to a step force on the opposite side, off epicenter displacement responses on both sides of the plate to the same forcing function, and the Green's functions associated.

The remainder of the review covers the research work at Harwell, on the study of AE mechanisms in materials, and performed with true AE phenomena rather than modelled excitations. Also included are short reviews on AE optical detection, signal analysis, the influence of material phase changes upon AE, the effects of dislocations, magnetomechanical effects, fatigue monitoring, and some practical applications. These topics will not be discussed here because they bear no relevance to the work presented in this thesis.

The first set of results published concerning the measurement of step force induced responses in elastic plates, was presented

by W.Sachse and A.Ceranoglu at two conferences during 1979 (38)(55). Their work is founded upon the theoretical calculations of Green's functions for epicentral responses in elastic plates, and the calibration of the transducers is achieved by the time domain deconvolution of the transducer response with the theoretical Green's function. As a means of ascertaining the accuracy of the process, the signals from a capacitive transducer are also displayed. However, no frequency response curve is shown for the calibrated transducer, which prevents the assessment of the frequency range of the measurements.

The first paper to contain a transducer calibration composed of an amplitude and a phase spectra was published in 1981 by N.N.Hsu and F.R.Breckenridge (56), which is basically an update of the work formerly published by Breckenridge et al (22) back in 1975.

In their paper, Hsu and Breckenridge reviewed alternative calibration methods based upon the use of a helium gas jet as the source of excitation, reciprocity techniques, and the step force method (22). From this review, the step force method is favoured because of being backed by an explicit theory relating input force to displacement, employing a well characterised surface wave pulse, relying upon a true displacement sensor (capacitive transducer) as standard, and preserving the signals in their time history form.

The hypotheses necessary to support such calibration method, also valid for the method developed during the present work, can be outlined as follows:

- The transducers under test are sensitive only in the direction normal to their active face.
- The contact area of the sensor is considered to be sufficiently small for it to behave as a point transducer.
- There is good linearity between input excitation and output signal.
- The output signal will have decayed to zero before any reflection from the specimen edges reaches

the transducer, since the use of any gating process to prevent recording reflections which in any way truncates the main transient, will introduce errors.

The calibration of a transducer included in the paper is reproduced in figures 6.1.a and b. Although the method seems well designed and implemented, several observations should be made regarding these results.

The use of a step forcing function produces a surface displacement with characteristics similar to a step function itself. This can be appreciated from figure 6.2, which represents the recorded trace of the surface pulse as detected by a capacitive transducer, where the signal can be seen to consist of a pulse type function superimposed to a step. A surface pulse with such a shape will produce an amplitude spectrum whose magnitude will fall periodically, as shown in figure 6.3, which is the spectrum of a simple step function.

In general, piezoelectric transducers cannot produce a similar type of spectrum because the inherent noise ground level will prevent the output signal spectrum from falling below a limit. Therefore, when performing a frequency domain de-convolution between the transducer output and the signal from the capacitive sensor, the result will be vulnerable to distortion, as shown by figure 6.1.a.

In the case of the presented phase response, it is most doubtful that a piezoelectric transducer, with an amplitude response as indicated in figure 6.1.a, will have a phase characteristic like the one plotted in figure 6.1.b. The reasons that can be speculated to justify such a result are:

- The result was achieved after averaging several experimental runs without taking into account errors introduced by the recording method.
- The dynamic range of the signal recorder used to store the signals was not sufficient to register accurately those frequency components above 400 KHz.

If the result was achieved after averaging several experimental runs, and no provision was made to correct the phase errors introduced at the multiplexing stage of the digital sampling process, this may have caused the phase values randomly distributed from record to record, to average to zero. This problem also occurs when smoothing a phase spectrum contained within a single cycle, for example 0^{o} to 360^{o}, and whose angle values should vary over several cycles in order to produce a single continuous curve.

The effect of those frequency components having a magnitude comparable to the noise ground floor level of the signal storing instrument, is to produce random phase values; and trying to average or smooth these will bring them close to the centre value in the phase cycle, for example 180^{o} for the range 0^{o}-360^{o}, or 0^{o} for the range $\pm 180^{o}$.

A paper bearing special relevance to this work was published in 1979 by Y-H.Pao et al (40), on the calculation of transient waves in elastic plates. The paper contains the derivation of a method for calculating the surface displacements on a plate due to various idealized excitations, based upon the generalized ray theory for the propagation of waves, and modelled responses are calculated by numerically integrating the derivated equations, with the aid of rather involved mathematical procedures to define the contours of integration.

As an illustration of the potential for the model, typical responses to modelled forcing functions are calculated and displayed, which constitute the first set of such type of results ever published. A later paper by A.Ceranoglu and Y-H.Pao (41), which corresponds to the short version of the PhD thesis by Ceranoglu, was published in 1981, covering the same subject of propagation of elastic pulses in a plate, from a more general level and achieving greater detail.

The only sources of reference for the type of experimental measurements performed in this section of the project, were the latter two papers (40)(41), and the calculated responses of the plate to modelled excitations included in these papers, were therefore used to

compare the level of accuracy achieved with the method developed in the present section of this work.

A paper by J.E.Michaels et al (39) was published in the last quarter of 1981, which contained the experimental measurements achieved by applying the Green's function expressions developed by Pao and Ceranoglu. The results contained in this paper are important since they illustrate the differences produced by the physical size of the plate specimen. Similar sets of experiments are performed with a large steel plate, with dimensions 450 x 450 mm^2 and 30.175 mm thickness, and a smaller plate of the same material, with dimensions 103 x 110 mm^2 and thickness of 12.37 mm.

The experimental lay-out employed for this paper is different from the arrays used for the present research project, and the late date of publication in relation to the stage of progress of the project prevented the necessary modifications to perform similar tests. However, the results were found nevertheless useful to assess the suitability of thin plates (like the one employed as specimen for this work) for calibration work purposes.

The paper also illustrates the different type of responses obtained when using the pencil lead fracture method of excitation instead of the fracture of glass capillary sections. These differences are mainly due to the pencil fracture not producing a proper step forcing function.

Finally, a progress report was presented at the Electric Power Research Institute, Palo Alto, Cal, U.S.A., by D.G.Eitzen et al (44), in which further details were published on the method of calibration developed by F.R.Breckenridge and his co-workers (Refs. 22 and 56), with an updating on all the modifications introducted. The report emphasizes the substitution of the glass capillary fracture source by a pencil lead fracture method of excitation, and the authors claim to be the first team to implement a digital method of deconvolution in the time domain.

A new piezoelectric transducer design is announced in the paper, whose response to a pencil lead fracture excitation resembles remarkably well the response from the capacitive displacement transducer. However, no frequency response calibration is given for this transducer.

6.2 CALIBRATION METHOD DEVELOPMENT

The main objective behind the present research programme was to recover the true surface waveform from the output signal produced by the transducer, and in order to achieve this, a suitable method for calibrating the transducer had to be implemented.

The method for recovering the surface waveform which seemed most practical, consisted in the de-convolution of the transducer output signal by its transfer function, performed in the frequency domain. This idea can be clearly illustrated by considering a surface disturbance $f(t)$ arriving at the transducer, whose transfer function is represented by $r(t)$, and generating an output signal $s(t)$. Since no conventional notation could be found to cover all variables considered in the present chapter whilst in accordance with the notation employed so far, a notation list for this chapter is included in Appendix B, as a reference for the reader.

Considering the transducer as a linear system, the transformation of the surface wave into output signal can be expressed by the equation:

$$f(t) * r(t) = s(t)$$

where '*' indicates the convolution of the functions in the time domain. In terms of the Fourier transforms from the three functions, the same equation can be written:

$$F(\omega) \cdot R(\omega) = S(\omega)$$

Since the records stored in the transient recorder correspond to the electric output from the transducer, the recovery of the original surface wave will involve a process of de-convolution by the transducer transfer function:

$$f(t) = [f(t) * r(t)] * [r(t)]^{-1} = s(t) * [r(t)]^{-1}$$

and in the frequency domain

$$F(\omega) = F(\omega) \cdot R(\omega) \cdot \frac{1}{R(\omega)} = \frac{S(\omega)}{R(\omega)}$$

The implementation of such a process of de-convolution, or convolution by the inverse transfer function, implies the necessity for determining the transfer function of the transducer.

An important observation which should be made at the present stage, refers to the fact that the Fourier transform of a real function in the time domain is a complex function, which can be considered in terms of its real and imaginary components, or as a vector function in terms of an amplitude and a phase spectra. In order to simplify the calculations, it was decided to work in the frequency domain, defining the transforms in terms of amplitude and phase.

The method of calibration initially considered, was based upon the comparison of the output from the transducer under calibration with that from a capacitive displacement sensor, as described in reference (22) and (32), using a steel bar as the transmitting media, and electric sparks as the source of excitation.

Figure 6.4 shows the schematic array of transducers to achieve the necessary measurements, and considering the output of the capacitive reference transducer (designated by $\underline{C(\omega)}$) as an accurate representation of the surface wave form, the absolute calibration of the piezoelectric sensor can be achieved by the de-convolution process:

$$R(\omega) = \frac{S(\omega)}{C(\omega)}$$

Such calibration method relies upon the physical model of the capacitive transducer truly representing its response, and the hypothesis that the surface waves arriving at both transducers are symmetrical to each other, with respect to the source.

For the reasons explained in section 4.3, the spark excitation system was found unsatisfactory, and it was consequently replaced by a pulse generator-piezoelectric exciter system. Additionally, the impossibility of achieving a surface finish within the required

tolerances for the specimen, prevented the proper performance of the capacitive reference transducers, as indicated in section 5.1.

A seach for alternative methods of calibration from the available literature, suggested the possibility of implementing a method based upon the reciprocity principle, similar to the methods described in references (34) and (35). Since the method of calibration to be adopted was intended for industrial application, it was considered that a system based around a massive steel block, as described in references (22) and (32), would prove impractical, besides its dependency from capacitive type transducers.

Closer examination of the reciprocity based methods published, inspired some doubts with respect to the suggested expressions for the calculation of the reciprocity factor. However, an idea of defining the problem from a different point of view resulted from this study, the idea consisting in the consideration of the exciter effects not in terms of force, but in terms of the surface disturbance generated. This can be illustrated by representing the electric pulse going into the exciter by $\underline{x(t)}$, or $\underline{X(\omega)}$ in the frequency domain, and the exciter transfer function in terms of the surface disturbance as $\underline{e(t)}$, and $\underline{E(\omega)}$. The process of generating a surface disturbance can be described by the equations:

$$x(t) * e(t) = f(t)$$

$$X(\omega) \cdot E(\omega) = F(\omega)$$

The main thought behind this approach was that a given combination of transducer and specimen should present similar resonance characteristics regardless of whether the transducer acts as an exciter or as a sensor, and the difference between the two functions will be reflected in the corresponding sensitivity level or mechanical coupling factor, both constant for a particular transducer and independent from frequency. This means that the transfer function associated with a given transducer, should have the same shape, varying only in magnitude. In terms of the above equations:

$$R(\omega) = \text{Constant} \cdot E(\omega)$$

Although these ideas may seem rather adventurous, a set of experiments was devised to test their feasibility, and the results obtained were satisfactory.

6.2.1 Preliminary Experiments

Figure 6.5 shows the schematic array of transducers 9 and 10, both built with a diaphragm configuration and including ceramic wear plates as shown in figure 5.29, and a capacitive transducer used as an exciter. The piezoelectric transducers were mounted on the bar specimen, separated by a distance of 60 mm between centres, and the capacitive exciter was mounted at mid distance from the two (see Fig. 6.5).

For the first experimental run, an electric pulse was fed into transducer 9 which acted as exciter, while transducer 10 worked as sensor. Both input and output signals were stored simultaneously with the transient recorder, and later transferred to the computer for processing and analysis. The procedure was repeated ten times, to perform an ensemble-average in the frequency domain of the amplitude spectra.

Monitoring the input to the exciter made it possible to normalize the output from the sensor, in order to obtain the frequency response for the chain of exciter - specimen - sensor, as produced by a flat frequency input signal.

The experimental run described above can be expressed mathematically in terms of the Fourier Transforms of the signals, transfer functions and surface disturbances as follows:

$$X_9 \cdot E_9 = F_9$$

$$F_9 \cdot G_{9,10} = F_{10}$$

$$F_{10} \cdot R_{10} = S_{10}$$

where the frequency argument of the functions is omitted to simplify the notation, the subindices refer to each transducer, and $G_{9,10}$

represents the specimen transfer function between the two sensors, in terms of surface disturbances only (not force).

Grouping the above expressions into a single equation:

$$X_9 \cdot E_9 \cdot G_{9,10} \cdot R_{10} = S_{10}$$

and normalizing the sensor output in terms of the exciter input signal:

$$E_9 \cdot G_{9,10} \cdot R_{10} = \frac{S_{10}}{X_9}$$

The normalized spectra from the ten measurements were ensemble-averaged, and the result is displayed in figure 6.6.

The role of the two transducers was reversed, and a new set of ten recording was performed. After transforming the records to the frequency domain and normalizing the output spectra, a similar set of results was obtained:

$$E_{10} \cdot G_{10,9} \cdot R_9 = \frac{S_9}{X_{10}}$$

The new set of spectra was ensemble-averaged, and the result is displayed in figure 6.7. From the comparison of figures 6.6 and 6.7, it is apparent that the spectra are very similar in shape, although they differ in magnitude. This can be expressed as follows:

$$\frac{S_{10}}{X_9} = \text{Constant} \cdot \frac{S_9}{X_{10}}$$

$$\Longrightarrow E_9 \cdot G_{9,10} \cdot R_{10} = \text{Constant} \cdot E_{10} \cdot G_{10,9} \cdot R_9$$

However, since the bar specimen is homogeneous and has a uniform section, and the position of the transducers is symmetrical:

$$G_{9,10} = G_{10,9}$$

$$\Longrightarrow E_9 \cdot R_{10} = \text{Constant} \cdot E_{10} \cdot R_9$$

This finding bears great significance since it implies that at least one of the following conditions must hold true:

a) $E_9 = \text{Constant} \cdot E_{10}$

and

$R_9 = \text{Constant} \cdot R_{10}$

which is most unlikely from the fact that each transducer is built with ceramic elements of different thickness.

b) $E_9 = \text{Constant} \cdot E_{10} = \text{Constant} \cdot R_9 = \text{Constant} \cdot R_{10}$

which is even less likely than condition (a)

c) $\frac{E_9}{R_9} = \text{Constant} \quad \frac{E_{10}}{R_{10}} = k$

where $\underline{k}$ is not a function of frequency.

A third experimental run was performed, this time using the capacitive transducer as exciter, and capturing the output signals from both sensors 9 and 10. The experimental procedure can be expressed in terms of the following equations:

$$X_c \cdot E_c \cdot G_{c,9} \cdot R_9 = S_9$$

$$X_c \cdot E_c \cdot G_{c,10} \cdot R_{10} = S_{10}$$

Although it was not possible to normalize the responses from the sensors in this case, this difficulty posed no problem since all records showed good repeatibility, and the simultaneous recording of both output signals ensured their correspondence to the same input.

Figures 6.8.a and 6.8.b show the above results after averaging and smoothing, and although both spectra display a similar trend inversely proportional to frequency, the two spectra are clearly different in shape, specially for the lower end of the frequency range. Therefore, from the above evidence:

$$S_9 \neq \text{Constant} \; S_{10}$$

$$\Longrightarrow \; X_c \cdot E_c \cdot G_{c,9} \cdot R_9 \neq \text{Constant} \cdot X_c \cdot E_c \cdot G_{c,10} \cdot R_{10}$$

Since the excitation signal and exciter were the same for both measurements:

$$\Longrightarrow \quad G_{c,9} \cdot R_9 \neq \text{Constant} \cdot G_{c,10} \cdot R_{10}$$

The conditions of homogeneity and section uniformity for the bar specimen, imply that the transfer functions of the specimen from the centrally located exciter to either sensor must be equal (see Fig. 6.5). Thus:

$$G_{c,9} = G_{c.10}$$

$$\Longrightarrow \quad R_9 \neq \text{Constant} \cdot R_{10}$$

The above result means that the transfer functions for the two sensors are different in shape, and therefore their ratio is not constant with respect to frequency, which automatically discards conditions (a) and (b), and consequently condition (c) must be true:

$$\Longrightarrow \quad \frac{E_9}{R_9} = \text{Constant} \cdot \frac{E_{10}}{R_{10}} = \text{Constant} \cdot \frac{E_i}{R_i} = k$$

and this condition, in turn, supports the hypothesis that both transfer functions for a reciprocal transducer working as a sensor and as an exciter, have spectra with the same shape, varying in terms of magnitude. Thus:

$$\Longrightarrow \quad E_9 = k_9 \cdot R_9$$

and in general terms

$$E_i = k_i \cdot R_i$$

Before continuing with the development of the calibration method, it was decided to test the same sort of relationships in terms of phase, since the amplitude spectra studied up to this point did not fully represent the Fourier transforms of the transfer functions.

However, it was impossible to obtain coherent phase results from experiments performed on the bar specimen, regardless of the correction of those errors introduced by the analogue to digital

conversion process of the signals (Ref.23). The only explanation found for this lack of phase coherence in the measurements made on the bar, was surface wave interference resulting from reflections, generated at the side edges of the bar as the main waveform front travels along the specimen.

In order to overcome these difficulties, a new experimental rig was designed, using a steel plate as specimen, as described in section 4.2 of this work. Figure 6.9 shows a typical transducer array to perform the calibration measurements on the new specimen.

A further set of experiments was performed, to examine whether the conclusions drawn from the results achieved with the bar specimen would also hold true for the elastic plate, and to integrate phase into the calculations. Four experimental runs were implemented using two transducers only for each test, as illustrated in figure 6.9, and storing simultaneously the input signal to the transducer acting as exciter, and the output from the one working as sensor.

All transducers employed were marked to allow their positioning in terms of the contact shoe, and their accurate orientation to obviate errors introduced by directionality effects (refer to section 6.3.2 and figures 5.24.a - d).

For the first experimental run, a pulse signal was fed into transducer 9 and the generated surface disturbance was detected by transducer 10. After normalizing, ensemble-averaging and smoothing, the resulting spectra are illustrated in figure 6.10. Figure 6.11 illustrates the results obtained after reversing the role of both transducers. Comparing these two sets of results, some minor differences were detected for the lower frequency end of the amplitude spectra, although the phase spectra were practically identical. Tests of this type were repeated several times, producing equivalent results which demonstrated the repeatibility of the method.

For the next experimental runs, transducer 9 was substituted by another piezoelectric transducer (designated as No.1), and a fresh

set of records was stored and similarly processed, the results of which are illustrated in figure 6.12. Figure 6.13 shows similarly obtained results, with transducer 10 working as the sensor and transducer 1 as the exciter. The comparison of these two sets of results definitely show marked differences between the obtained amplitude and phase spectra.

From the analysis of the above experimental results, it was considered that the conclusions drawn from the tests performed on the bar specimen had been corroborated with the steel plate experiments; that is, a particular combination of transducers should produce normalized responses whose spectral shape is independent from which transducer has been used as exciter or sensor, both in terms of amplitude and phase, and the differences between the two transducers will be reflected in the sensitivity levels obtained in either direction.

6.2.2 Calibration Procedure

Before continuing with the actual calibration of the transducers, it was decided to establish the methodology to be followed in terms of a simple idealized model, by disregarding the effects introduced to the signals by the instrumentation (amplifiers, filters, recorder), and the transformation of the surface waveform as it travels over the elastic plate.

In order to achieve the calibration of one transducer, for example transducer 9, in relative terms and using a reciprocity technique, a minimum of two experimental measurements will be necessary.

The first experimental run will consist in monitoring the output from transducer 10, and the input to transducer 9 generating the corresponding excitation. Maintaining the same notation as listed in Appendix B, this first measurement can be expressed as follows:

$$X_9 \cdot E_9 \cdot R_{10} = S_{10}\Big|^{I}$$

and normalizing the output signal from transducer 10

$$E_9 \cdot R_{10} = \left.\frac{S_{10}}{X_9}\right|^{I} \qquad (1)$$

Using a common source of excitation, for example a surface disturbance $f_1(t)$, arriving simultaneously at both transducers 9 and 10, the resulting outputs will correspond to the same excitation:

$$F_1 \cdot R_9 = S_9\Big|^{II}$$

$$F_1 \cdot R_{10} = S_{10}\Big|^{II}$$

and calculating the de-convolution between the two stored signals:

$$\frac{F_1 \cdot R_9}{F_1 \cdot R_{10}} = \left.\frac{S_9}{S_{10}}\right|^{II}$$

$$\Longrightarrow \quad \frac{R_9}{R_{10}} = \left.\frac{S_9}{S_{10}}\right|^{II} \qquad (2)$$

Calculating the convolution of equations (1) and (2):

$$E_9 \cdot R_{10} \cdot \frac{R_9}{R_{10}} = \left.\frac{S_{10}}{X_9}\right|^{I} \cdot \left.\frac{S_9}{S_{10}}\right|^{II}$$

$$\Longrightarrow \quad E_9 \cdot R_9 = \left.\frac{S_{10}}{X_9}\right|^{I} \cdot \left.\frac{S_9}{S_{10}}\right|^{II} \qquad (3)$$

However, from the preliminary experimental work (section 6.2.1), it had been concluded that the ratio between the transfer functions of a transducer, working as an exciter and as a sensor, is independent from frequency. Thus:

$$E_9 = k_9 \cdot R_9$$

Substituting E_9 in equation (3):

$$k_9 \cdot (R_9)^2 = \left.\frac{S_{10}}{X_9}\right|^{I} \cdot \left.\frac{S_9}{S_{10}}\right|^{II}$$

Transposing k_9, and extracting the square root from the above expression:

$$R_9 = \sqrt{\frac{1}{k_9}} \cdot \sqrt{\frac{S_{10}}{X_9}\Big|^{I} \cdot \frac{S_9}{S_{10}}\Big|^{II}} \qquad (4)$$

If the reciprocity factor k_9 can be calculated, the resulting transfer function will represent the absolute calibration of transducer 9. However, if the reciprocity factor cannot be defined or calculated, the result from expression (4) will constitute a relative calibration; that is, it will contain all the information necessary to recover the input waveform shape, although the scaling factor defining the absolute magnitude will still be missing.

It was considered, however, that the fundamental objective in the development of an AE signature analysis method was to recover the true surface waveform shape, as this arrives at the sensing transducer, in order to apply whatever method of analysis is considered best, without interference from the sensor used. Within this frame of thought, the scaling aspect of the calibration process could be left as a secondary problem, to be overcome later, for example, by a process of comparison with a standard transducer.

The main feature of such a procedure is the characterisation in shape of the transducer frequency response, being achieved "in situ", with the corresponding results remaining in the computing equipment used later to process the signals from the calibrated transducer. And the actual sensitivity level for the sensors can easily be introduced as a scaling factor.

6.2.3 Implementation of the Method

The practical implementation of the apparently simple method described, presented numerous difficulties originating from the necessity of introducing a transmission media for the surfave waves, if meaningful results were to be obtained. The difficulties encountered can be illustrated by the following considerations:

- Some means had to be provided to study the effects of the transmission media upon the surface waves, as these propagate.
- Due to directionality effects detected in the transducers, it was not possible to guarantee that the surface waves generated by a piezoelectric exciter, would propagate and reach simultaneously two different locations with exactly the same shape, thus making the measurements indicated as step II impossible.
- Great care must be taken to ensure that all measurements performed correspond to the same type of surface wave. This means that in general, a calibration valid for Rayleigh type of surface waves will produce faulty results for epicentral type excitations.

In view of these observations, the basic procedure described was modified accordingly. The first experimental measurement, involving transducer 9 as exciter and transducer 10 as sensor, can be represented by the expression:

$$X_9 \cdot E_9 \cdot G_{9,10} \cdot R_{10} = S_{10}\Big|^{I}$$

and in normalized form

$$E_9 \cdot G_{9,10} \cdot R_{10} = \frac{S_{10}}{X_9}\Big|^{I} \qquad (5)$$

The results after averaging and smoothing are represented by figure 6.10.

Since it is not possible to ensure the simultaneous arrival of a particular excitation to both transducers 9 and 10, an alternative procedure was used to achieve equivalent results to those of expression (2). Using transducer 1 as exciter and monitoring the generated pulse with transducer 9:

$$X_i \cdot E_1 \cdot G_{1,9} \cdot R_9 = S_9\Big|^{II}$$

$$\Longrightarrow E_1 \cdot G_{1,9} \cdot R_9 = \frac{S_9}{X_1}\Big|^{II} \qquad (6)$$

The corresponding results are represented by figure 6.13. Substituting transducer 9 with transducer 10, and repeating the procedure:

$$X_1 \cdot E_1 \cdot G_{1,10} \cdot R_{10} = S_{10}\Big|^{III}$$

$$\Longrightarrow \quad E_1 \cdot G_{1,10} \cdot R_{10} = \frac{S_{10}}{X_1}\Big|^{III} \tag{7}$$

The results obtained after averaging and smoothing are represented by figure 6.12. Calculating the de-convolution between expressions (6) and (7):

$$\frac{E_1 \cdot G_{1,9} \cdot R_9}{E_1 \cdot G_{1,10} \cdot R_{10}} = \frac{\frac{S_9}{X_1}\Big|^{II}}{\frac{S_{10}}{X_1}\Big|^{III}}$$

Since both sensors 9 and 10 were located at the same position when making the above measurements, the transfer functions corresponding to the exciter and steel plate remained constant, thus:

$$G_{1,9}\Big|^{II} = G_{1,10}\Big|^{III}$$

$$E_1\Big|^{II} = E_1\Big|^{III}$$

$$\Longrightarrow \quad \frac{R_9}{R_{10}} = \frac{\frac{S_9}{X_1}\Big|^{II}}{\frac{S_{10}}{X_1}\Big|^{III}} \tag{8}$$

Calculating the convolution of expressions (5) and (8):

$$E_9 \cdot G_{9,10} \cdot R_{10} \cdot \frac{R_9}{R_{10}} = \frac{S_{10}}{X_9}\Big|^{I} \cdot \frac{\frac{S_9}{X_1}\Big|^{II}}{\frac{S_{10}}{X_1}\Big|^{III}}$$

$$\Longrightarrow E_9 \cdot G_{9,10} \cdot R_9 = \frac{S_{10}}{X_9}\Big|^{I} \cdot \frac{\frac{S_9}{X_1}\Big|^{II}}{\frac{S_{10}}{X_1}\Big|^{III}} \qquad (9)$$

In order to reach the relative calibration of transducer 9 as indicated in equation (4), the transfer function for the plate $G_{9,10}$ should be calculated beforehand. Such an obstacle could be overcome if the results of equation (5) were obtained with an experimental array independent from the steel plate, and therefore independent from its transfer function. However, the only alternative way to achieve the results of equation (5) is through a back-to-back assembly of the two transducers, and such an array produces the propagation of elastic waves in a direction perpendicular to the sensitive faces of the transducers, as for epicentral measurements. This type of wave propagation disregards the typical transmission and capture of AE generated waves, which will be mainly composed of Raleigh waves whenever the transducer is located at a distance from the epicenter. Indeed, tests performed with back-to-back measurements produced results which could not be related to those measurements performed on the steel plate.

Finally, it was decided to introduce an approximation of the plate transfer function into the calibration process, by modelling the transformations undergone by the surface waves as they propagate from the exciter to the sensor transducer.

A series of experiments was performed on the steel plate by generating surface waves with transducer 9 working as an exciter, and measuring them with transducer 10, positioned at different distances from the exciter. From the comparison of the amplitude spectra, a gradual emphasis of the lower frequencies was noticed as the distance

between the transducers was increased, although this effect was not very pronounced for short distances. From the comparison of the phase spectra, a gradual increase in the slope of the phase curves was detected as the distance between the transducers was incremented.

The measured slope from the phase spectra was plotted in terms of the distance between the two transducers, and the resulting points seemed to lay very close to a straight line. As a refinement of these experiments, a new set of tests was performed using both transducers 9 and 10 working as sensors, and generating the excitations with a pencil lead source.

Figure 6.14 illustrates the arrangement of transducers and source for these experiments. A first measurement was made with the transducers positioned at the same distance from the source, and subsequent records were made as one of the transducers was moved to positions further away from the source. By refering all measurements to the one made from equidistant transducer positions, the resulting phase spectra were almost straight lines, with slopes proportional to the difference in distance from the source of the transducers. These results are displayed in figure 6.15.

The above findings can be interpreted as an indication that Rayleigh waves travel as a pack, with all frequencies propagating at the same speed. Since phase was always measured with reference to the transducer closest to the excitation source, or to the exciter input signal, and establishing a phase shift of 0^{o} for zero frequency, a relative phase lag for the different frequency components was introduced.

The phenomenon can be illustrated by considering a surface wave pulse travelling from transducer 9 to transducer 10. The pulse will take a finite time interval to cover the distance between the two transducers, and if upon arrival at transducer 10 it is refered to the pulse as seen by transducer 9, the comparison will show that very low frequency components, having wavelengths approaching infinity, will have arrived within practically the same wavelength arc section;

while high frequencies will have arrived after a number of wavelengths, hence the relative phase lag.

If the above interpretation of the phase spectra slope increment with distance was correct, it should be possible to obtain an accurate measurement of the Rayleigh wave speed from figure 6.15. The slope of the graph was measured to be approximately 0.125 Deg/KHz mm, and the inverse of this figure gives:

$$c = \frac{1}{0.125} \cdot 360 \cdot 10^3 \frac{mm}{sec} = 2.88 \cdot 10^3 \frac{m}{sec}$$

This value compared favourably with that calculated from the elastic constants of mild steel: $2.98 \cdot 10^3$ m/sec, presenting a difference of just 3.4%, and with the value: $2.91 \cdot 10^3$ m/sec, obtained from the rise-time difference of pulses propagating along the bar specimen.

The study of the amplitude spectra did not produce any definite conclusion which would contribute to establishing a relationship for the emphasis of certain frequency components in terms of the distance between transducers, and consequently, the emphasized frequency components were believed to be directly related to resonances within the plate specimen.

In view of these results, the transfer function of the plate was modelled only in terms of the phase shift introduced to the signals, disregarding the amplitude effects. It is important to underline at this stage that the transfer function for the plate, as used in the convolution equations of the calibration method, represents the changes introduced to the shape of the waveform as it travels along the surface of the plate, and not the transformation of the forcing function into surface wave response, which is the conventional meaning attached to the Green's function.

Introducing the inverse phase effects of the plate into equation (9):

$$E_9 \cdot R_9 = [G_{9,10}]^{-1} \cdot \frac{S_{10}}{X_9}\Big|^{I} \cdot \frac{\frac{S_9}{X_1}\Big|^{II}}{\frac{S_{10}}{X_1}\Big|^{III}}$$

Substituting E_9 in terms of the reciprocity factor:

$$k_9 \cdot (R_9)^2 = [G_{9,10}]^{-1} \quad \frac{S_{10}}{X_9}\Big|^{I} \cdot \frac{\frac{S_9}{X_1}\Big|^{II}}{\frac{S_{10}}{X_1}\Big|^{III}}$$

and extracting the square root of last expression:

$$R_9 = \sqrt{\frac{1}{k_9}} \cdot \sqrt{[G_{9,10}]^{-1} \cdot \frac{S_{10}}{X_9}\Big|^{I} \cdot \frac{\frac{S_9}{X_1}\Big|^{II}}{\frac{S_{10}}{X_1}\Big|^{III}}} \qquad (10)$$

The calculation of such expressions involved a rather long process of data handling, which comprised the storage of ten records for each of the experimental measurements designated as I, II , and III, and the transformation of all data to the frequency domain, normalizing the measurements through the de-convolution of signals, ensemble-averaging and smoothing the results from each experimental run (I, II, III), further de-convolution of result II by result III, and convolution of the product with measurement I. The resulting phase spectrum was then corrected for the relative lag introduced by the plate transfer function.

Further corrections had to be introduced in order to remove the distortions produced by the signal conditioning equipment (amplifiers and filters), and to this effect the piezoelectric transducer amplification lines 1 and 2, corresponding to each channel of the transient recorder, were calibrated, and their frequency response characteristics are displayed in figures 6.16 and 6.17. In the case of input signals to the exciters, these were not amplified prior to filtering and storing, and therefore only the effects from the anti-aliasing filters had to be considered (whose calibration curves are included as figures 2.4 and 2.5).

The calibration of the signal conditioning lines was performed taking into consideration the length of the cables involved, in order to obviate relative phase shifts introduced by different lengths of cable.

Finally, considerable thought had to be given to the physical meaning of extracting the square root of equation (10). Taking each of the frequency components of the argument inside the radical as a vector, represented by its amplitude $\underline{A}$, and phase angle $\underline{\theta}$ over the range $\pm 180^{o}$ (one cycle), the square root vector can be defined in terms of an amplitude equal to $\sqrt{A}$, and a phase angle equal to $\theta/2$. However, the new range for the phase angle will be reduced to $\pm 90^{o}$, which will introduce phase errors. Since the generic expression for the phase angle of the argument has the form $\theta \pm n \cdot 360^{o}$, and $\underline{n}$ integer, the phase for the square root vector contains an uncertainty of $\pm n \cdot 180^{o}$. That means, the square root of a vector can be represented by either of two vectors, symmetrical with respect to the origin of coordinates, as illustrated in figure 6.18. This uncertainty becomes evident from the mathematical analysis of the square root of a vector, calculated in terms of the coordinate components.

The only way found to overcome this obstacle was to assume that the phase angle characteristic of a physical system, such as an AE transducer, must be a continuous curve, and therefore its phase spectrum cannot present sudden jolts of $\pm 180^{o}$. Based upon this assumption, the phase angle of the square root argument was trend shifted to produce a continuous curve, prior to its halving.

The end result of the above long-winded process consists of an amplitude and phase spectra, illustrated in figure 6.19, which represents the frequency response characteristic in relative terms for transducer 9.

Although it is possible to repeat the whole process described in order to calibrate other transducers, it is more practical to employ transducer 9 (once calibrated) as standard, and obtain further calibrations by comparison.

6.3 DISCUSSION OF RESULTS

As a means of assessing the quality of the obtained calibration, it was decided to process a surface wave pulse, generated with a known forcing function, and compare the results with those published in references (40) and (41).

Since it had been impossible to implement the glass capillary fracture method of excitation, the surface waves were generated by fracturing pencil leads, a method already discussed as capable of producing satisfactory results.

Figure 6.20 shows a record of the raw signal produced by transducer 9 from a pencil fracture generated pulse. Figure 6.21 shows the same pulse after de-convolution by the transducer characteristics, and after removal of the effects introduced by the signal conditioning instrumentation (amplifiers and filters). Finally, the corrected record was integrated with respect to time, and the result is displayed in figure 6.22.

The reason for integrating the signal with respect to time is that piezoelectric transducers with small inertia loading, or with damping loading, are basically sensitive to velocity (Ref.20).

To facilitate the comparison of the de-convoluted pulse, a new plot was produced with the time axis expanded, shown in figure 6.23, while figure 6.24 illustrates the calculated surface displacement generated by a pure step forcing function, copied from reference (41). The similarity of these two totally independent results was found most satisfactory, since one of them is the produce of a 100% experimental method, while the other is 100% the produce of a theoretical model. However, the two signatures also present differences which must be analysed in the light of the following observations:

a - The de-convoluted transducer signal shows the absence of low frequency components, mainly due to the transducer having a very low sensitivity for frequencies below 150 KHz. The sensitivity level shown in the calibration curve of transducer 9 (Fig. 6.19) for

frequencies below 30 KHz is an error, introduced by the 20 KHz high-pass filters in the pre-amplifiers.

b - The leading edge of the de-convoluted pulse shows oscillations which are not present in the calculated waveform. This difference is believed to be the produce of the transducer being unable to reproduce the low frequency components of the signature with fidelity, and the effect of ringing from the sensor which is not totally removed by the de-convolution process.

c - The measured pulse of figures 6.20 to 6.23 was generated with the fracture of a lead pencil, whose forcing function is not a pure step function, and the corresponding surface waves have been shown to present some differences with respect to those generated by the fracture of glass capillaries (Ref.39). These differences are mainly represented by the absence of high frequency components, due to a longer rise time for the forcing function, and a certain increase of oscillations in the pulse.

d - The calculated response shown in figure 6.24 corresponds to the waveform at a distance of four plate thicknesses from the source, while the de-convoluted pulse of figure 6.23 was measured at a distance of approximately 2.6 times the thickness of the plate, taken from the centre of the transducer contact shoe to the point of excitation.

In order to investigate the effects of detecting the surface waves from different distances to the source of excitation, a series of pulses were generated at regular intervals of 5 mm, at distances from 20 mm to 50 mm. The raw signals stored are shown in figures 6.25.a to g, while figures 6.26.a.a to 6.26.g.b illustrate the corresponding raw amplitude and phase spectra. From these spectra it can be noticed that the amplitude distribution maintains a close resemblance for distances of 20, 25 and 30 mm, while greater modifications are obvious as the distance from the source was increased to 35 mm and beyond. This observation seems to indicate that the model for the plate transfer function, as introduced in the calibration

process, is not accurate, and can only be considered adequate as a first approximation for small distances, which should not be greater than three times the thickness of the plate.

The comparison of the raw phase spectra indicates a progressive loss of phase coherence for high frequencies, as the distance from the source is increased. For distances of 20, 25 and 30 mm the phase measurements were accurate over a frequency range up to 1.5 MHz. The impossibility of measuring phase beyond 1.5 MHz is seen as a consequence of the longer rise time of the excitation.

As the distance of the transducer from the source was increased beyond 35 mm, the frequency range for the accurage measurement of phase dropped to less than 1.25 MHz. This is believed to be the effect of interference generated by the reflection and mode conversion of elastic waves within the plate, whose speed of propagation is different to that of Rayleigh waves. This observation had already been reported by J.E.Michaels et al (39).

Figures 6.27.a to g show the pulses after de-convolution and integration. From this series of results, the pulse of figure 6.27.c is practically identical to the pulse shown in figure 6.22, both corresponding to the same distance of 30 mm.

Figure 6.27.f, corresponding to the pulse measured from a distance of 45 mm, shows good resemblance to figure 6.28, which illustrates the calculated step force function for a distance of six times the thickness of the elastic plate. Once again, the difference in corresponding distance between the calculated and measured results is approximately two plate thicknesses. This discrepancy can be caused by the thickness of the plate being too small compared with the size of the transducer sensing face, resulting in the loading of the plate specimen by the transducer, and the influence of non-linear responses due to the magnitude of the excitation when compared with the dimensions of the specimen.

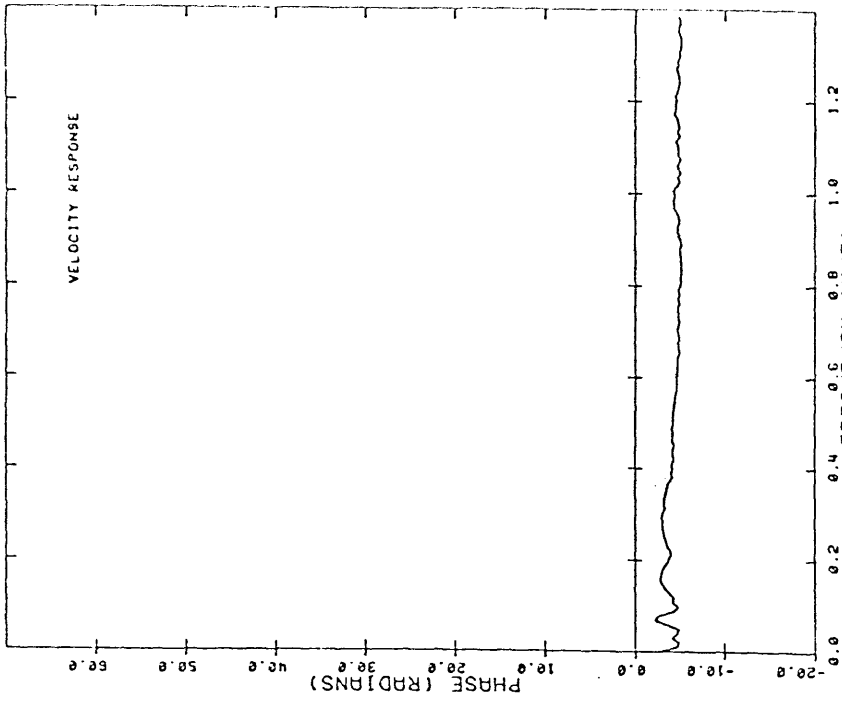

Fig 6.1.b- Transducer calibration copied from Ref (56). Phase characteristic.

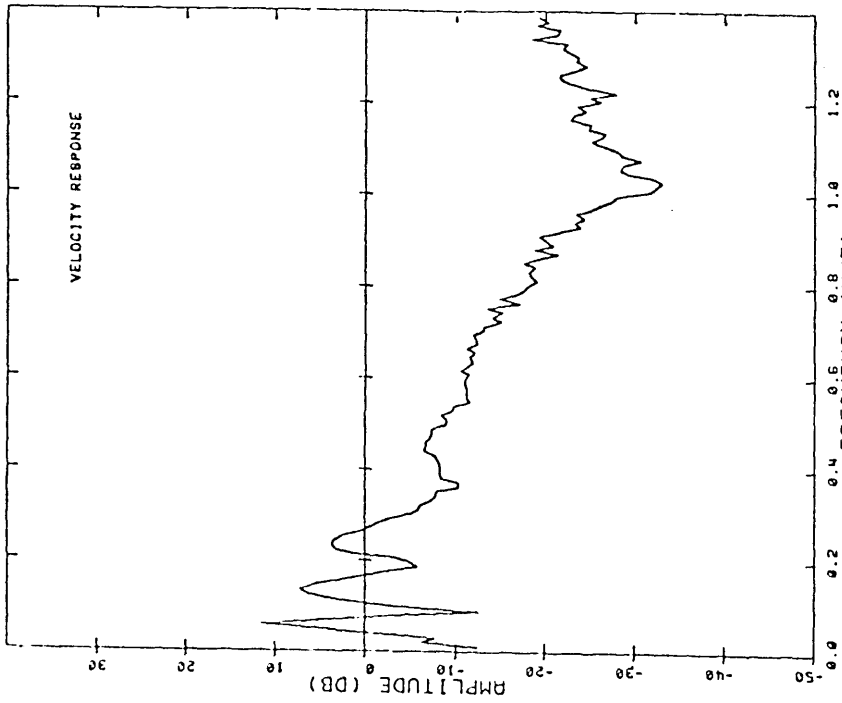

Fig 6.1.a- Transducer calibration copied from Ref (56). Amplitude response.

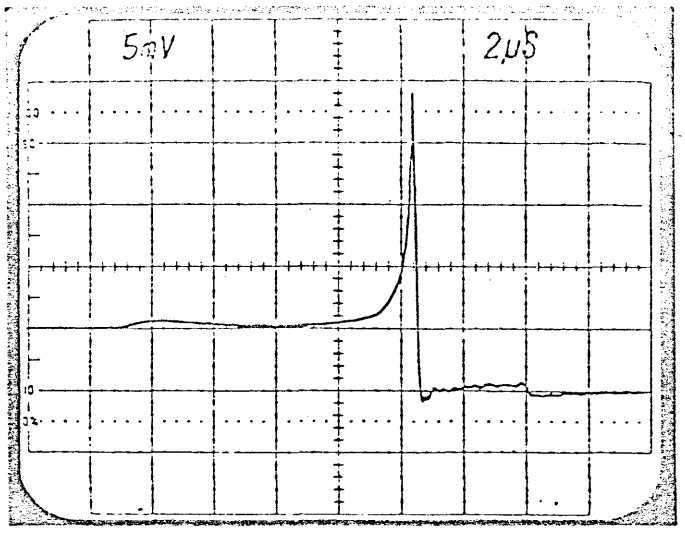

Fig 6.2- Semi-infinite body surface response to a step forcing function as measured by a capacitive displacement transducer. Copied from Ref (56).

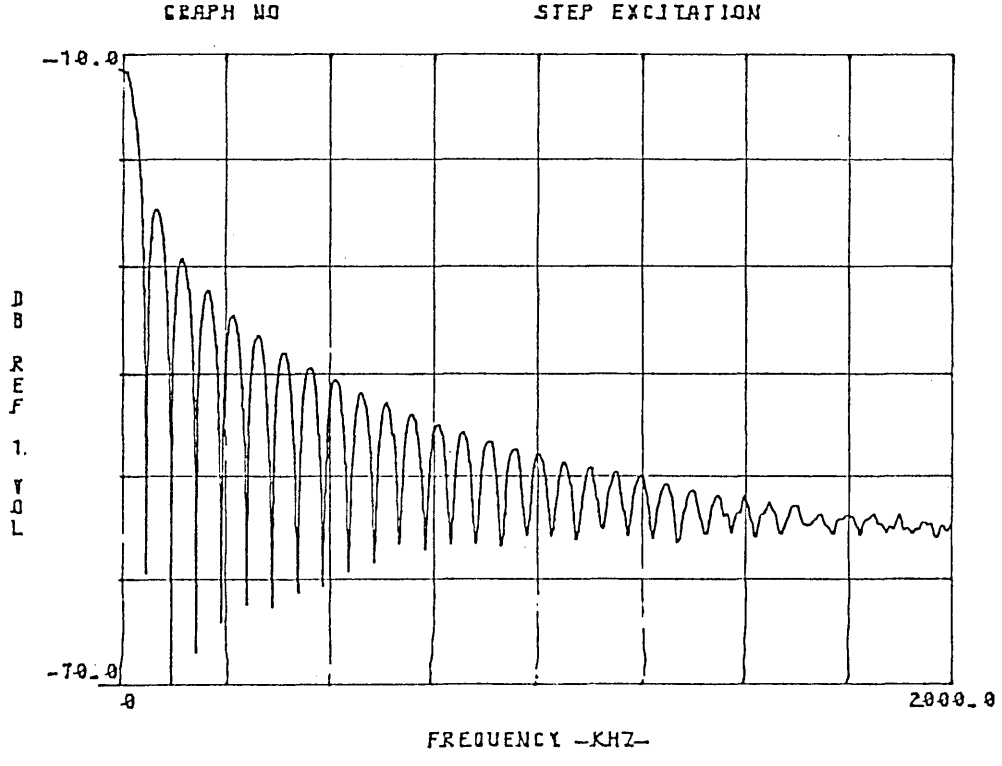

Fig 6.3- Amplitude spectrum of a step function in log scale. Note the periodic fall in amplitude shown.

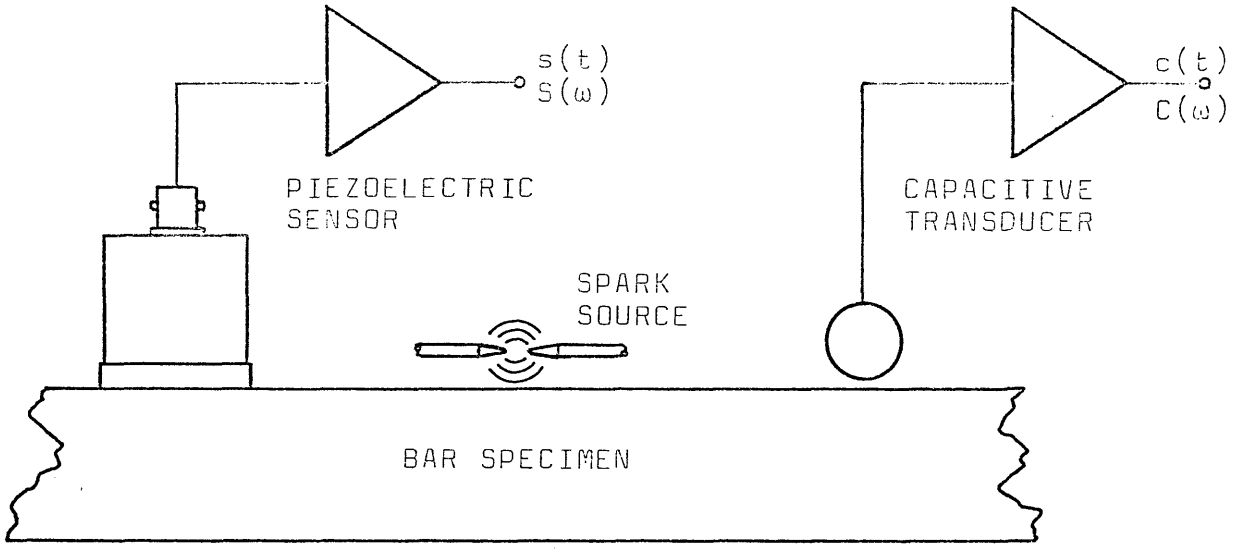

Fig 6.4- Schematic array for the calibration of transducers by comparison.

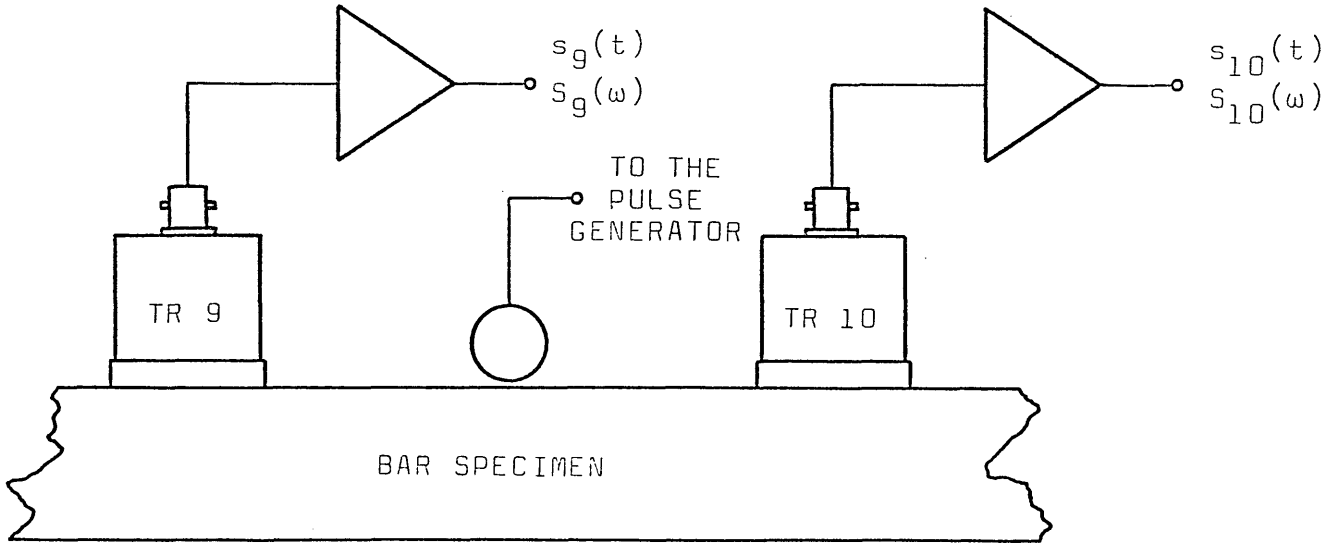

Fig 6.5- Schematic array used for the preliminary experiments.

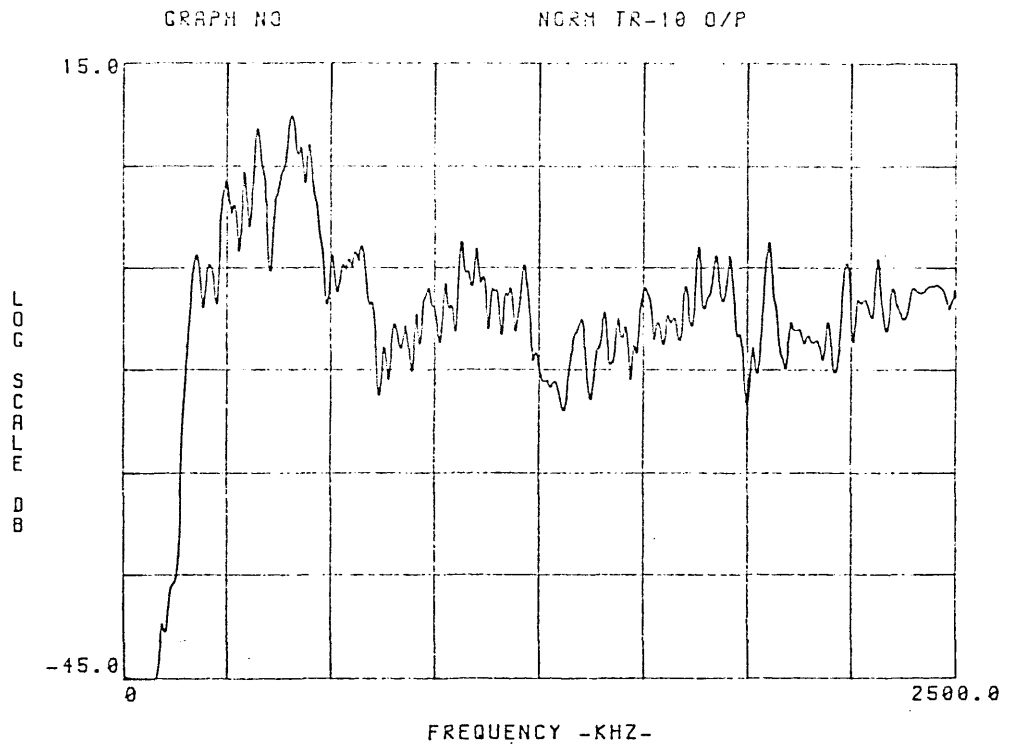

Fig 6.6- Normalized output from transducer No 10, using transducer No 9 as exciter.

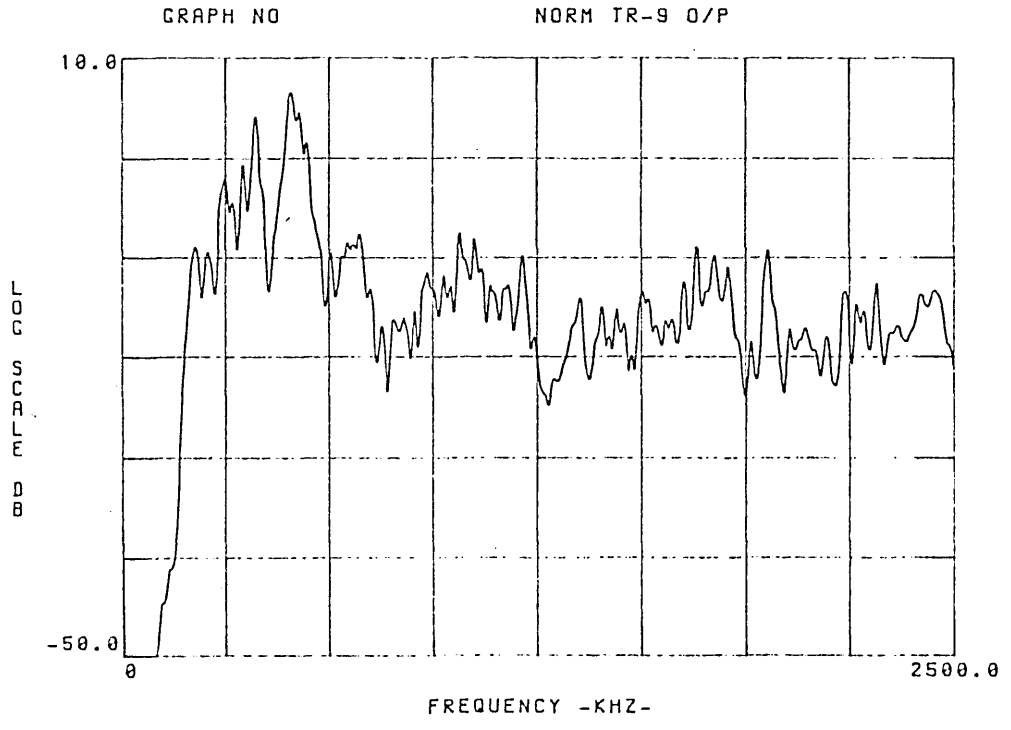

Fig 6.7- Normalized output from transducer No 9, using transducer No 10 as exciter.

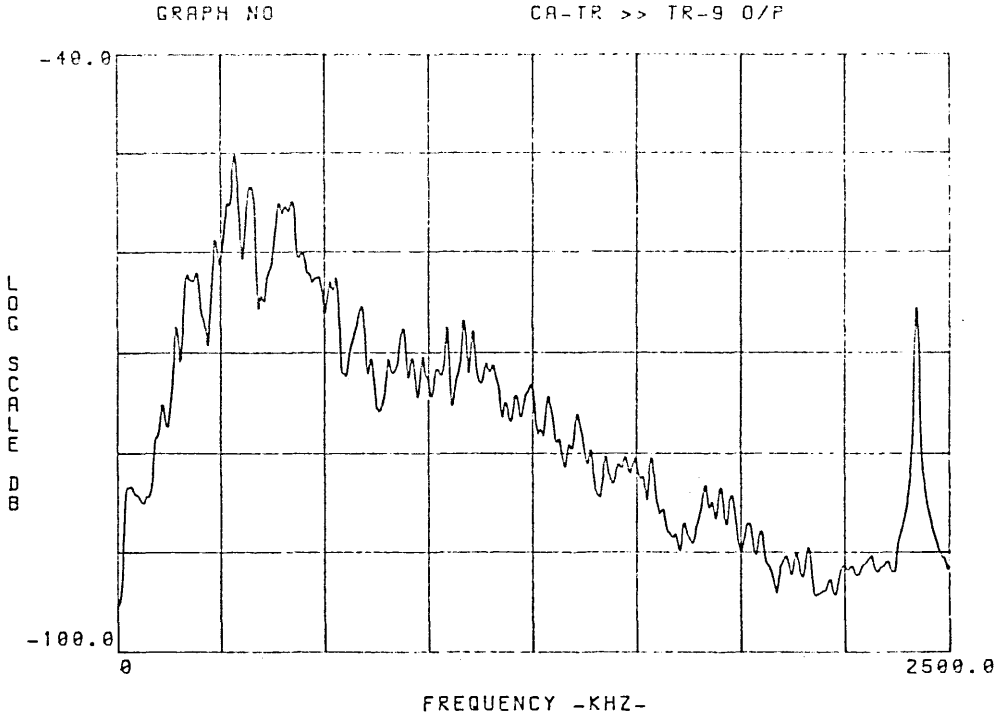

Fig 6.8.a- Normalized output from transducer No 9, using a capacitive transducer as exciter.

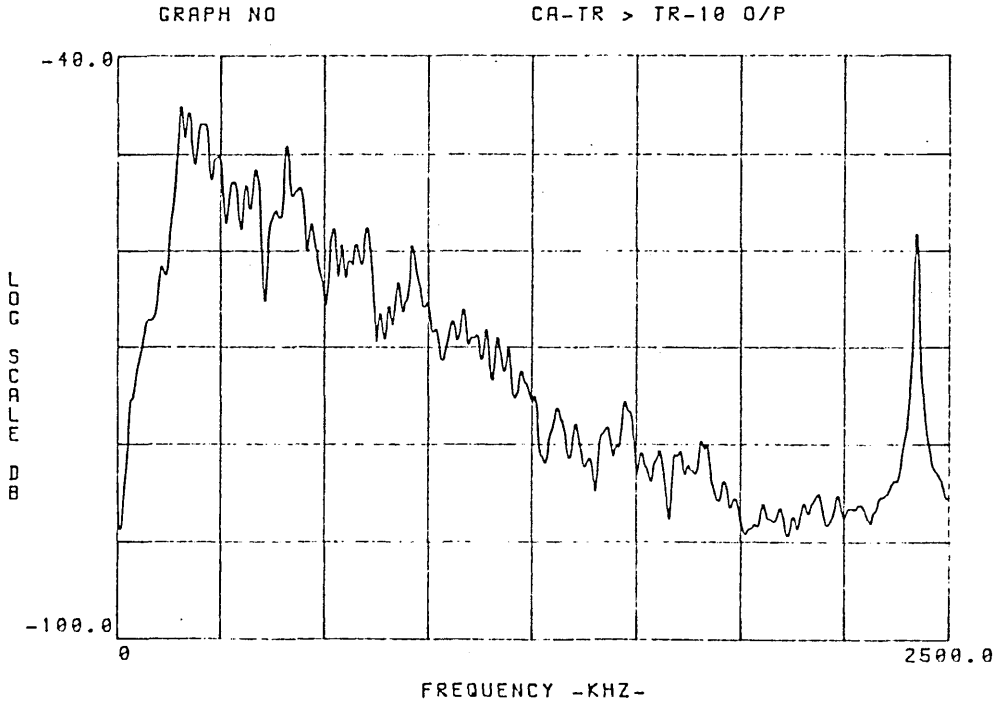

Fig 6.8.b- Normalized output from transducer No 10, using a capacitive transducer as exciter.

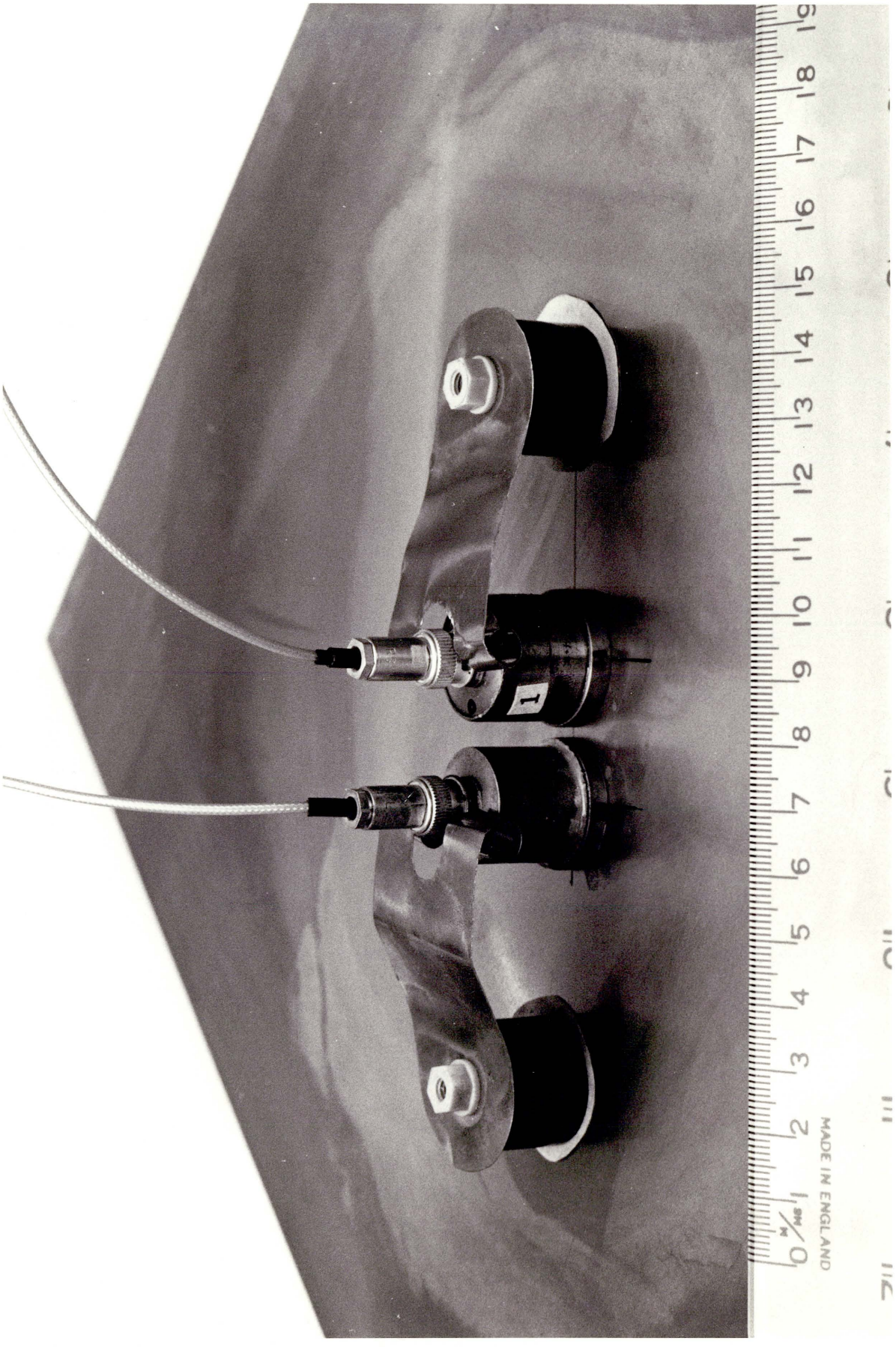

Fig 6.9- Typical transducer array for measurements on the plate specimen.

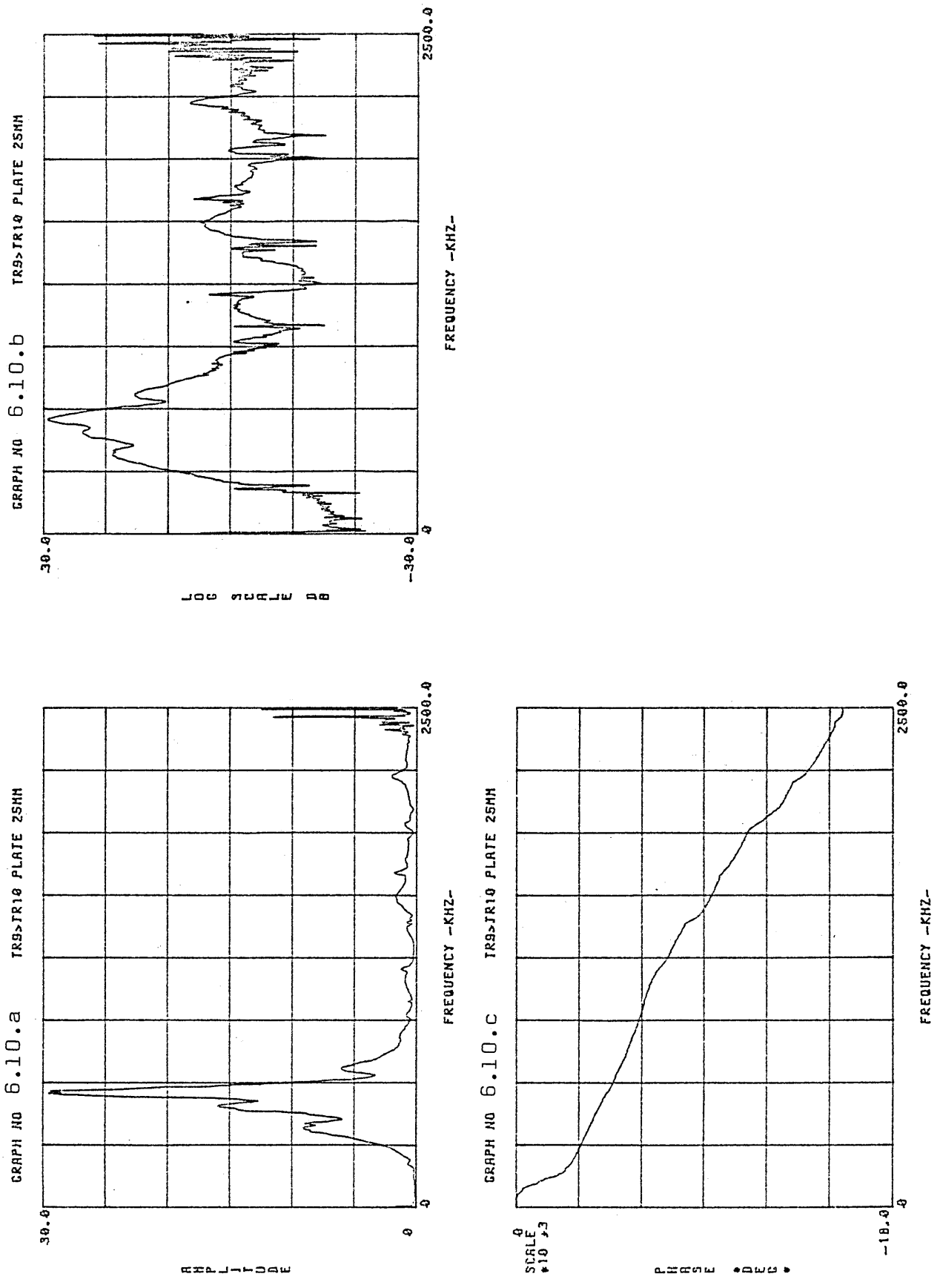

Fig 6.10- Normalized response from TR 10, on the plate, using TR 9 as exciter.

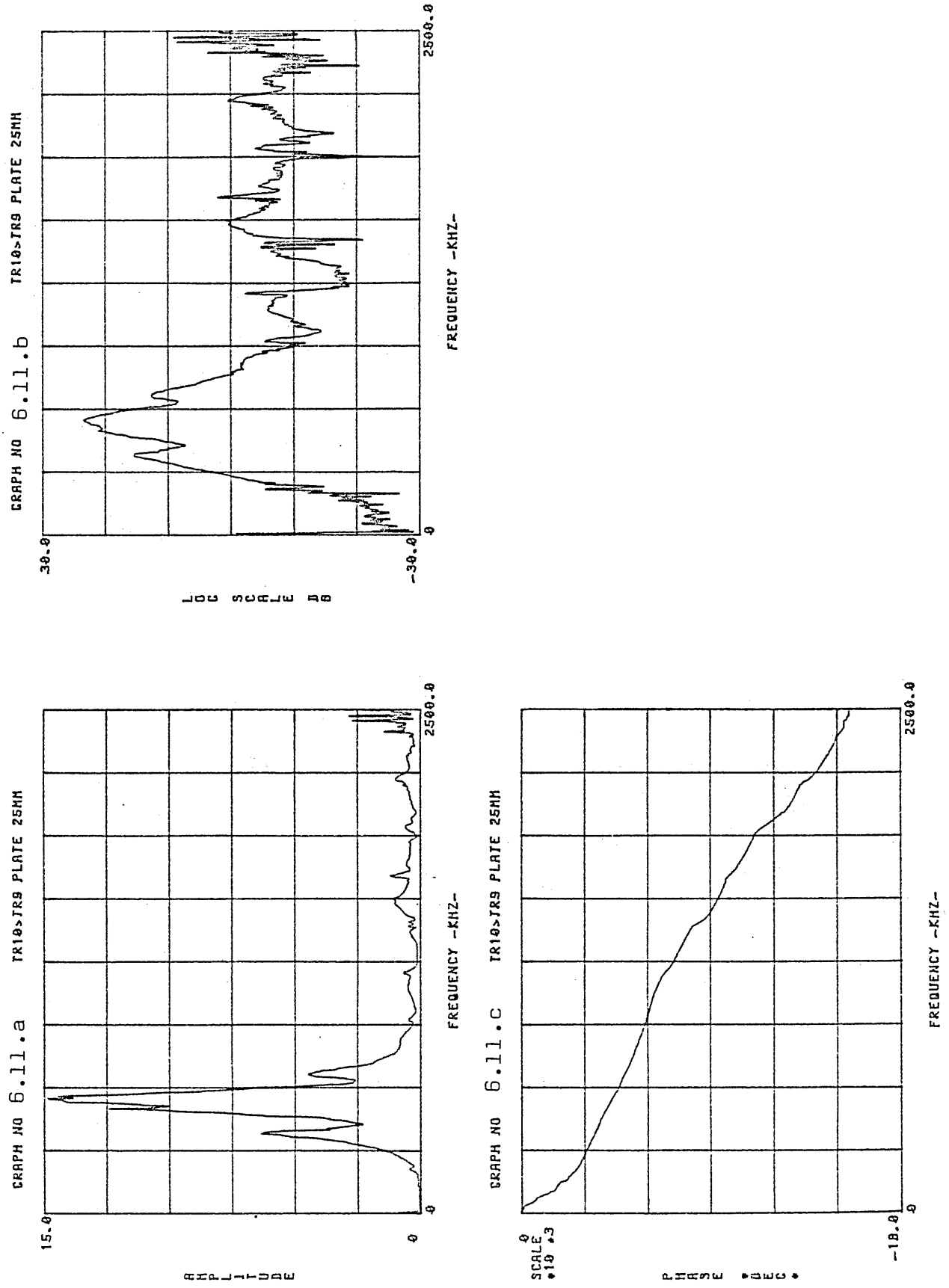

Fig 6.11- Normalized response from TR 9, on the plate, using TR 10 as exciter.

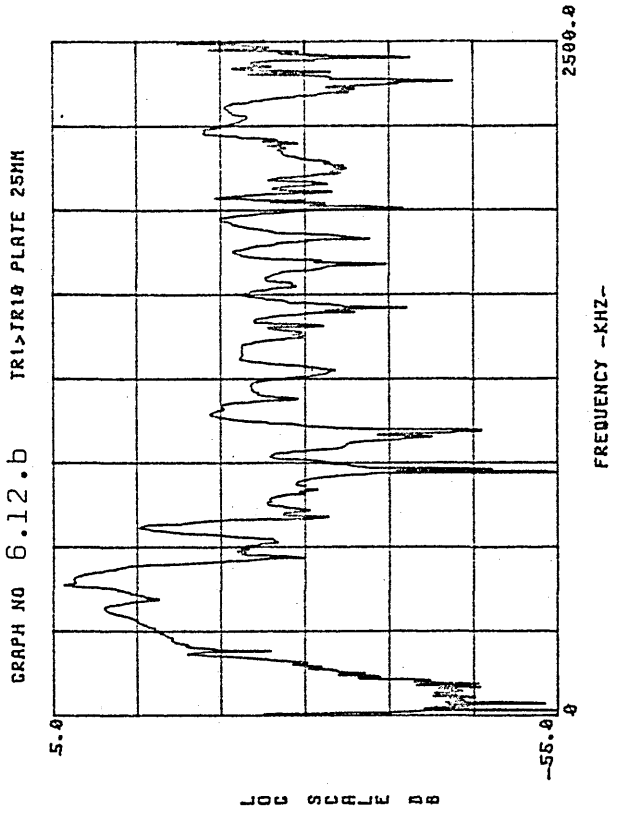

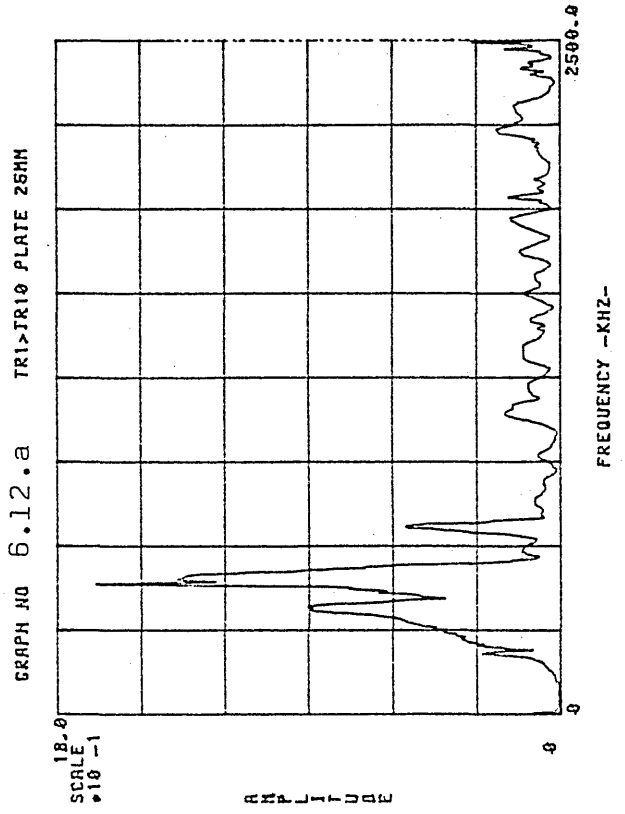

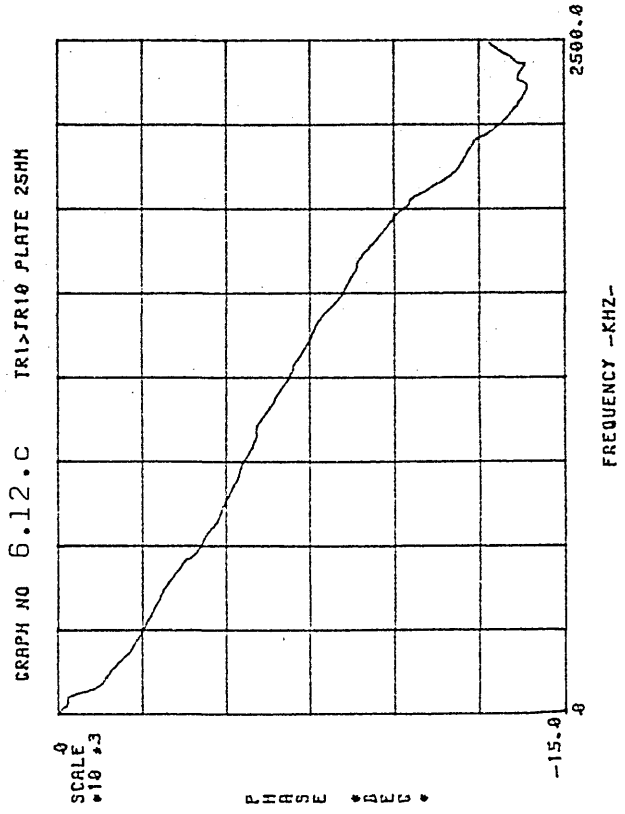

Fig 6.12- Normalized response from TR 10, on the plate, using TR 1 as exciter.

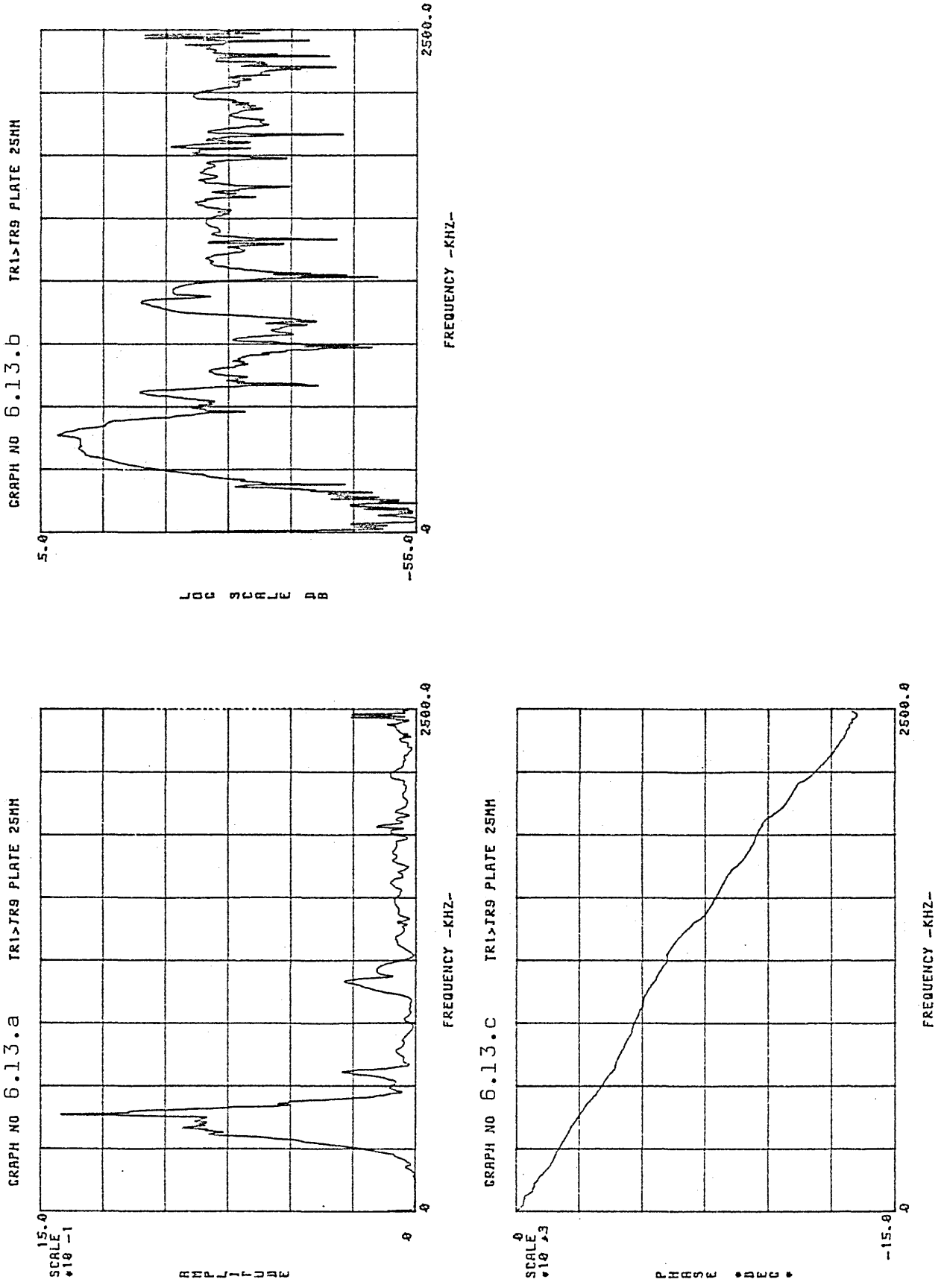

Fig 6.13- Normalized response from TR 9, on the plate, using TR 1 as exciter.

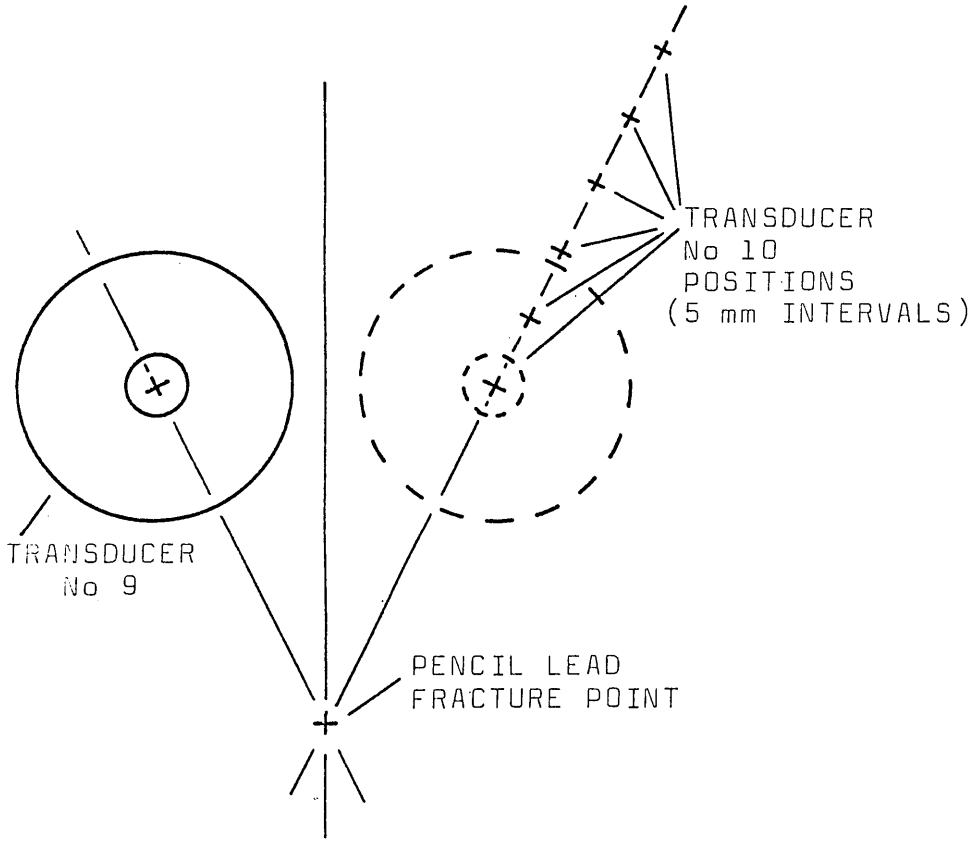

Fig 6.14- Transducers and excitation point arrangement, to measure the phase spectra slope in function of distance.

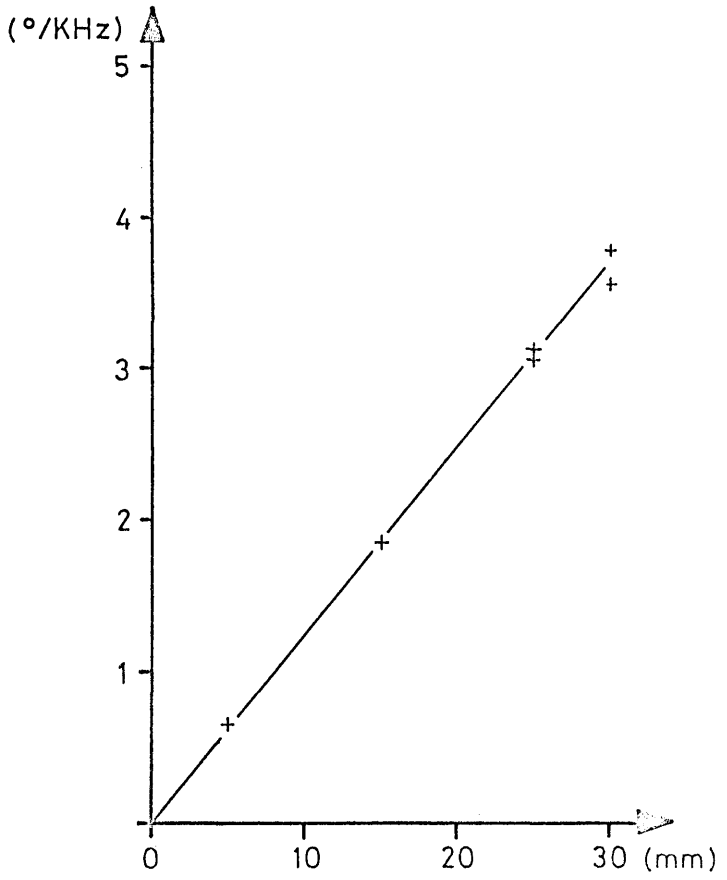

Fig 6.15- Phase spectra slope in function of transmission path length (in degrees).

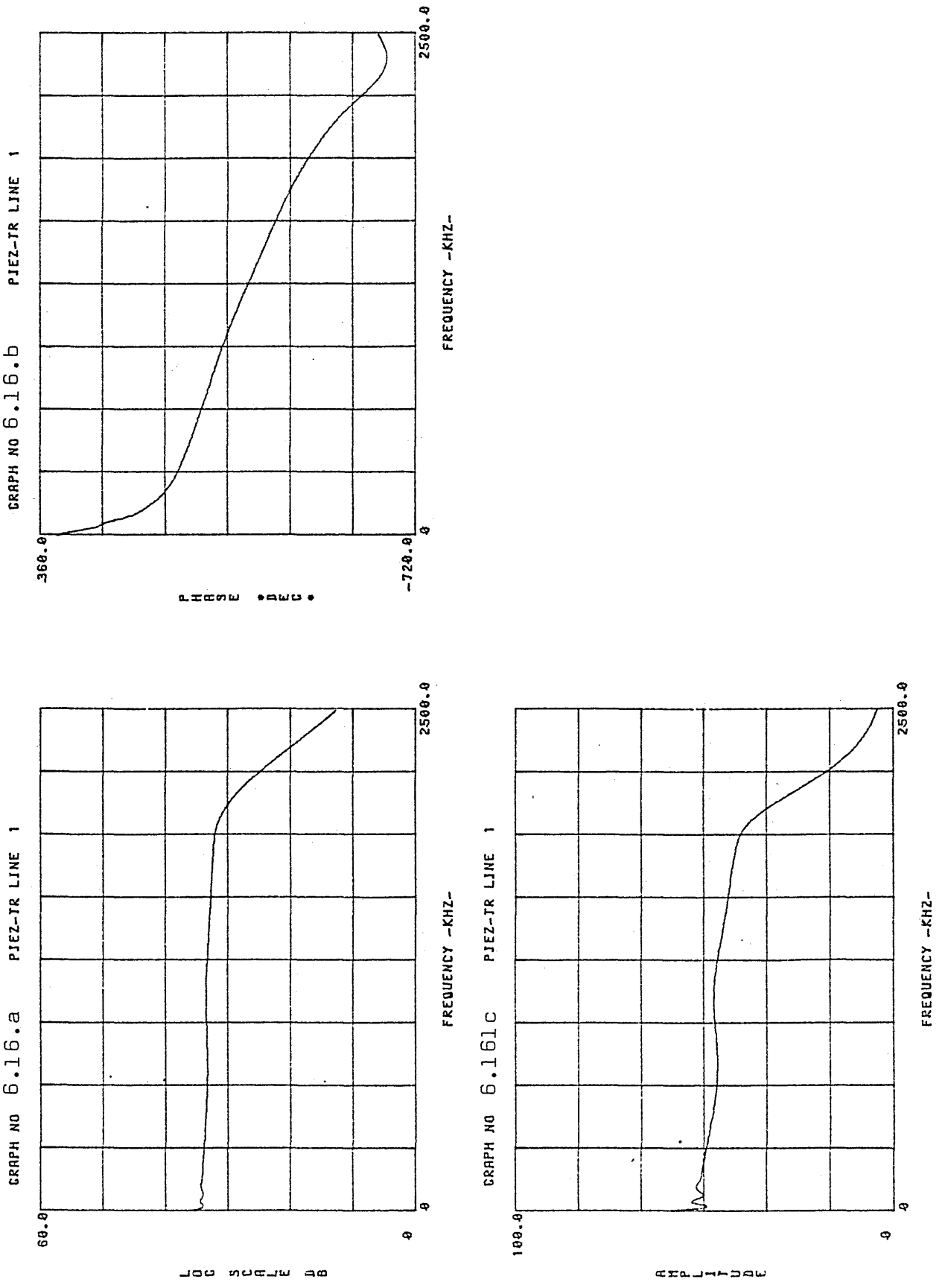

Fig 6.16- Signal conditioning line 1 calibration.

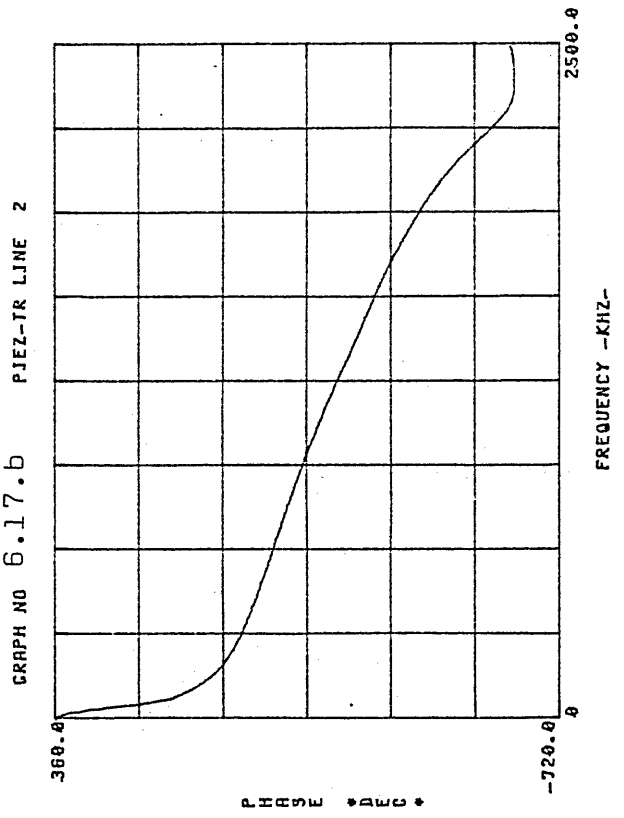

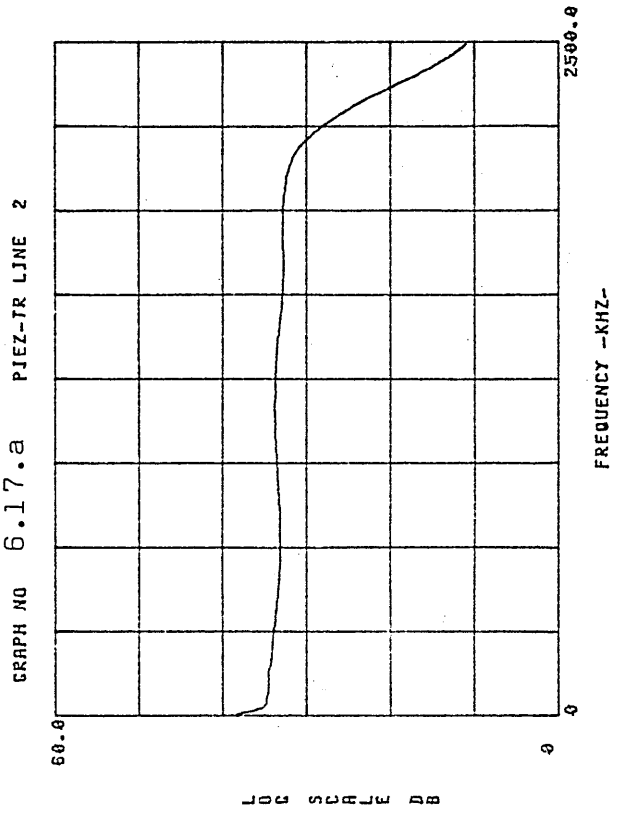

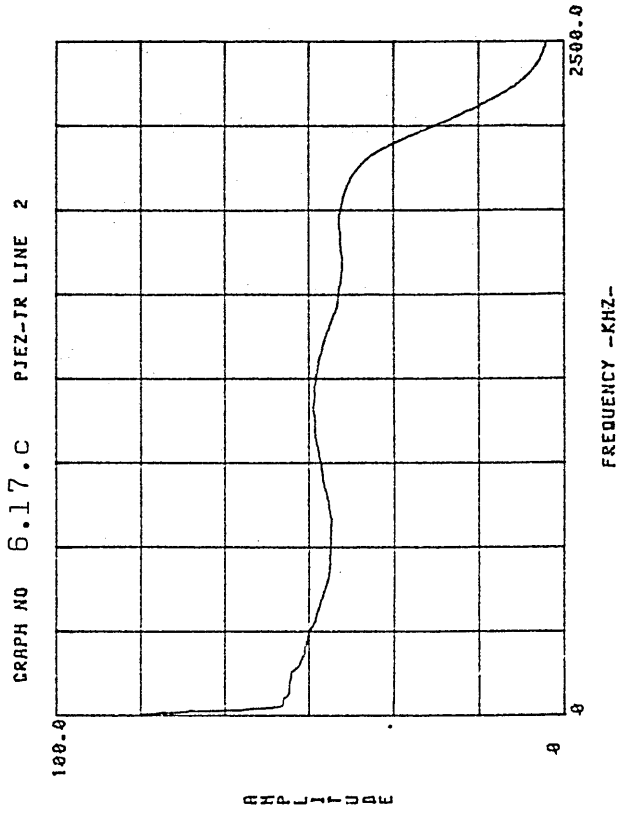

Fig 6.17- Signal conditioning line 2 calibration.

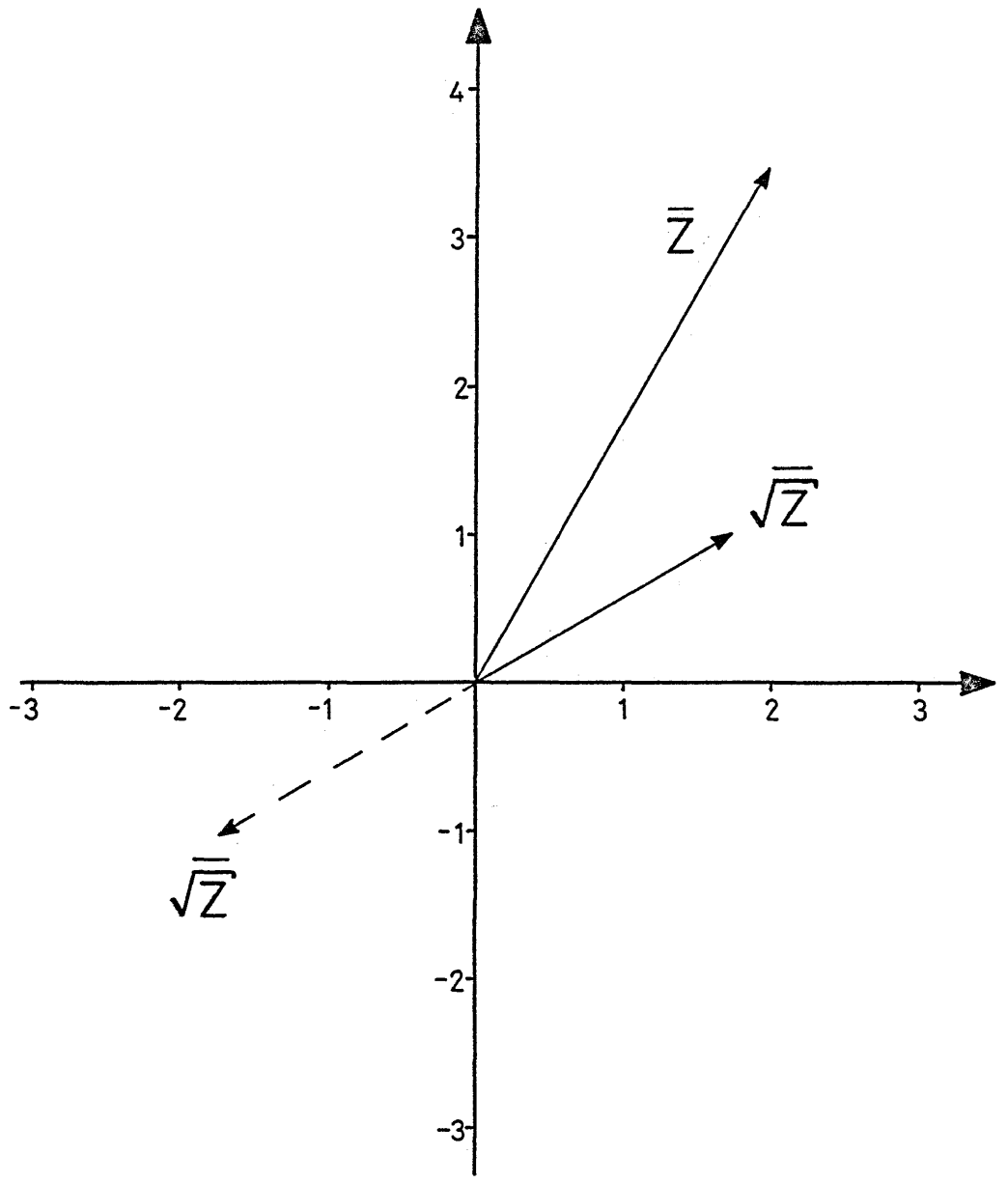

Fig 6.18- Illustration of the uncertainty in calculating the square root of a vector.

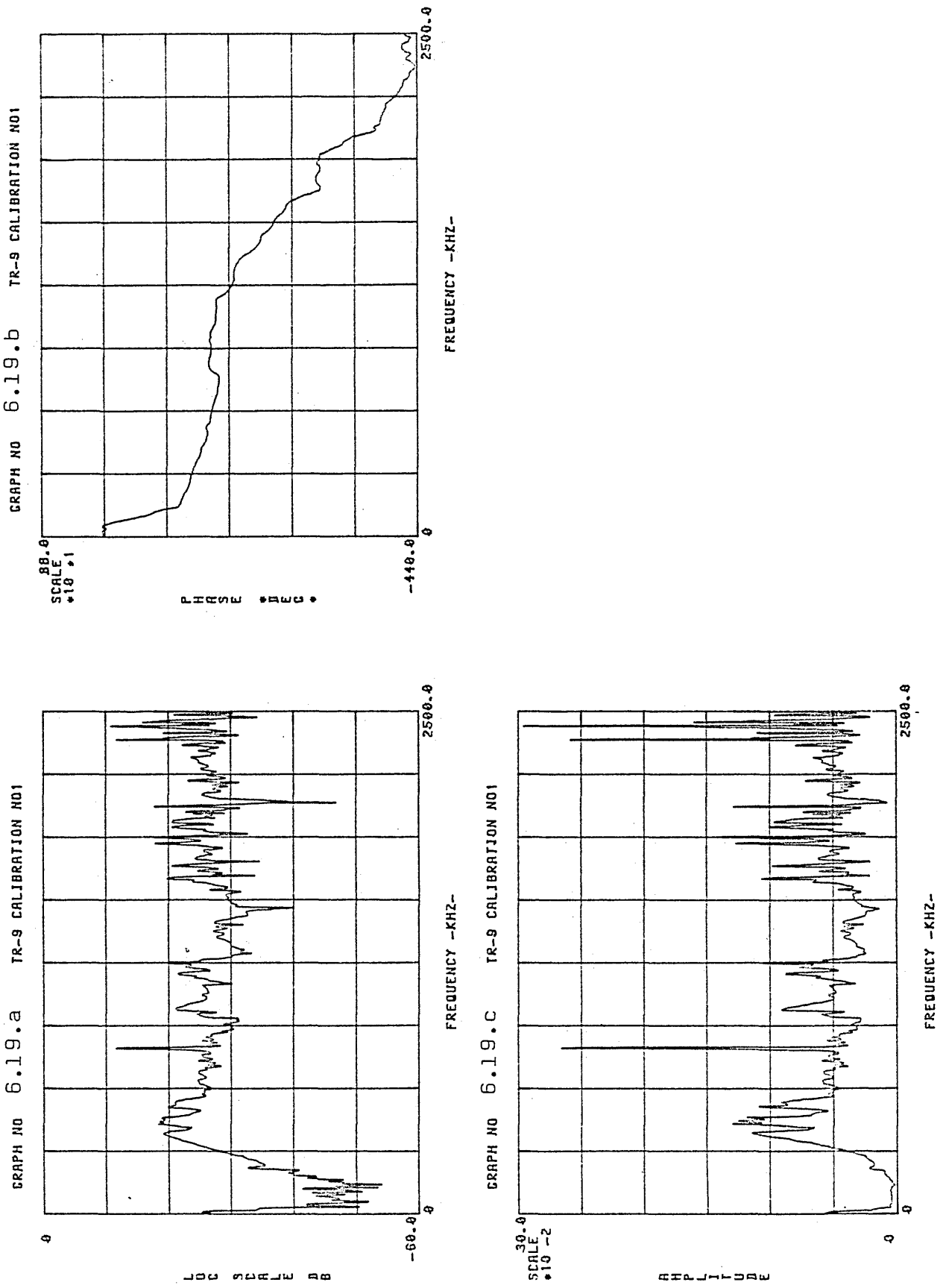

Fig 6.19- Relative calibration of transducer No 9.

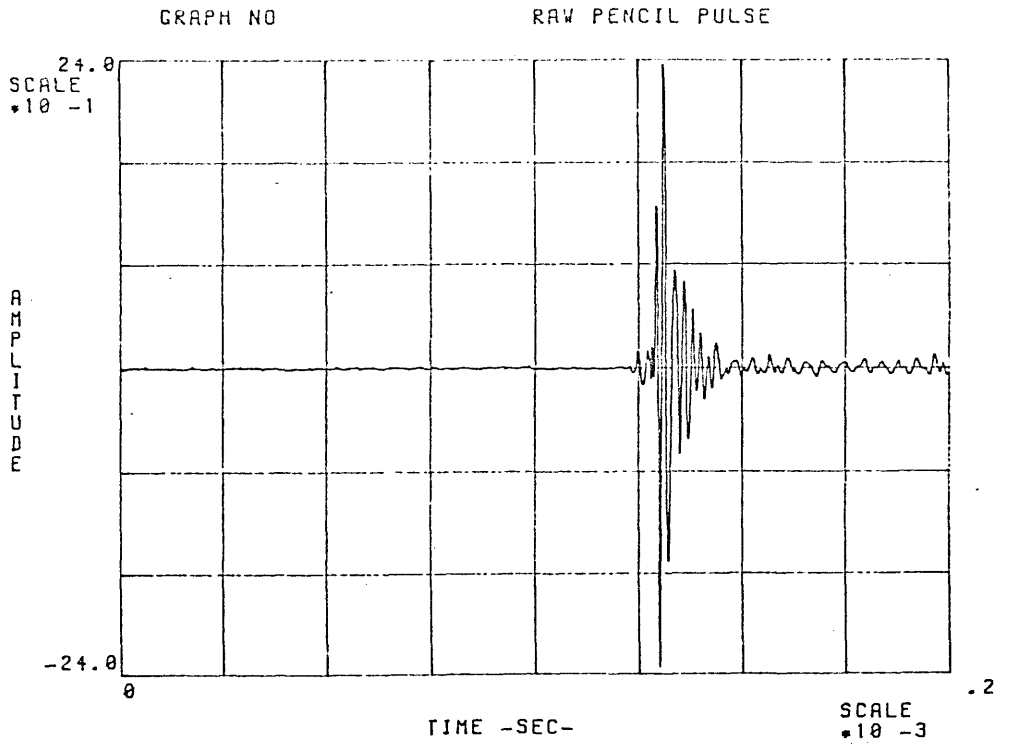

Fig 6.20- Raw signal from a pencil fracture generated pulse.

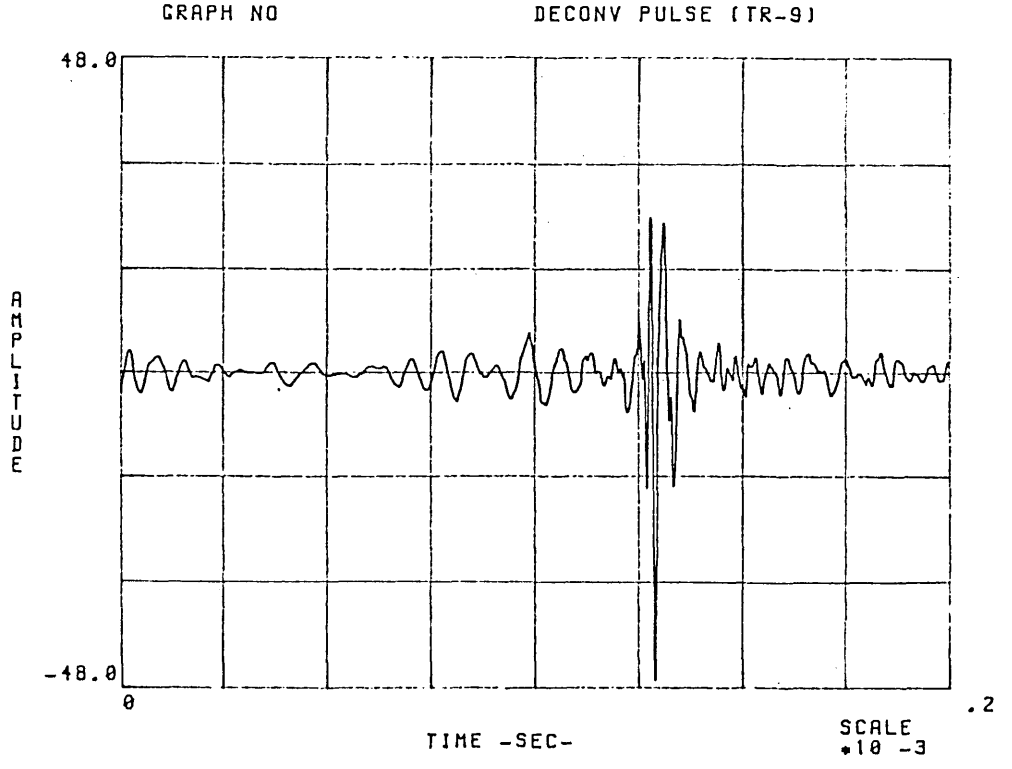

Fig 6.21- Same pulse as above after de-convolution by the transducer and instrumentation calibrations.

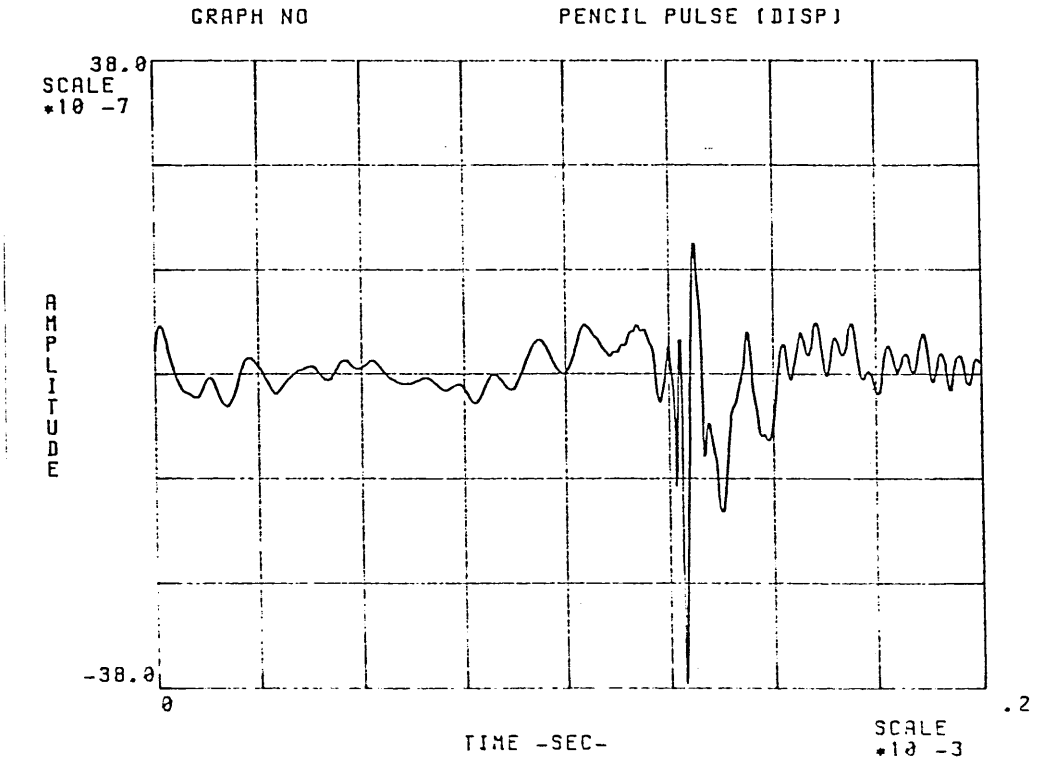

Fig 6.22- Pulse from Fig 6.21, after integration with respect to time (to obtain displacement).

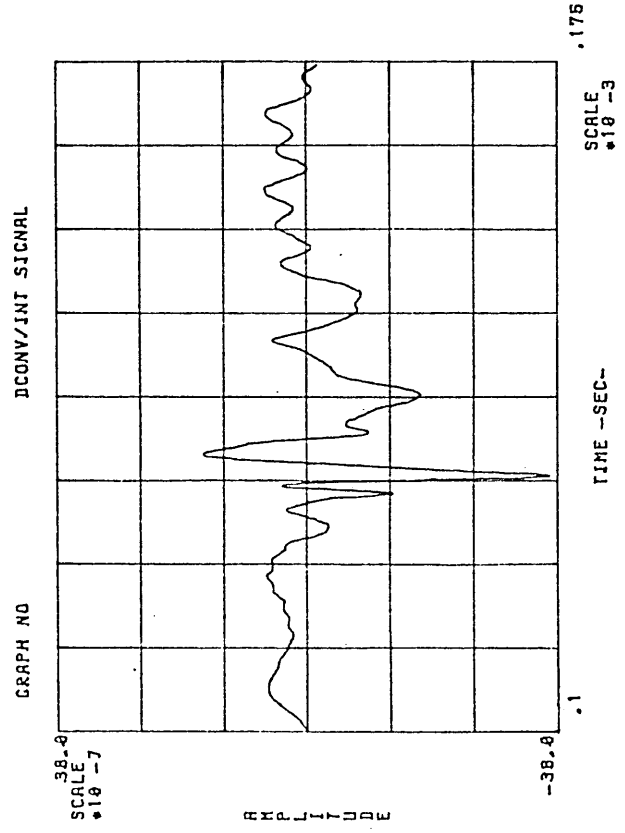

Fig 6.23- Time expanded version of Fig 6.22.

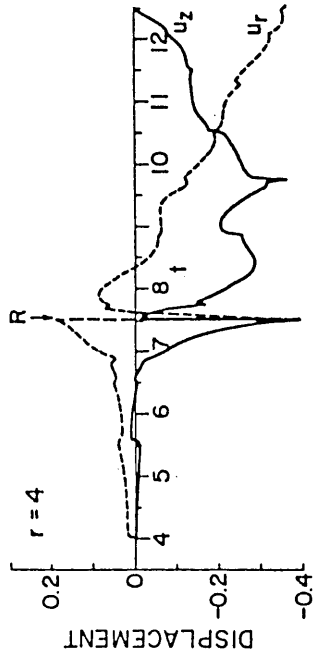

Fig 6.24- Theoretically calculated displacement (u_z), copied from Ref (41).

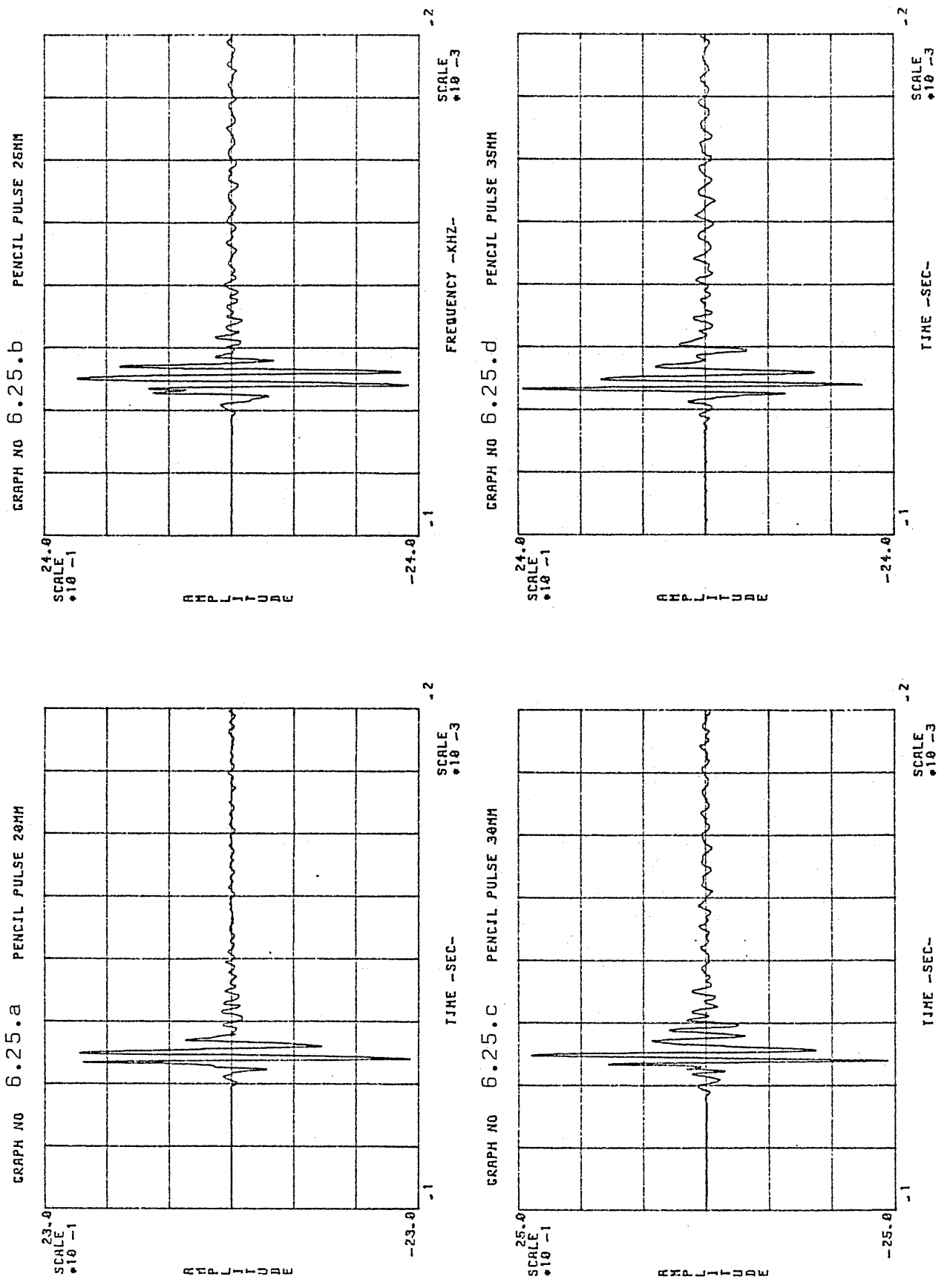

Fig 6.25.a to g- Pencil lead generated pulses, detected at different distances from the source.

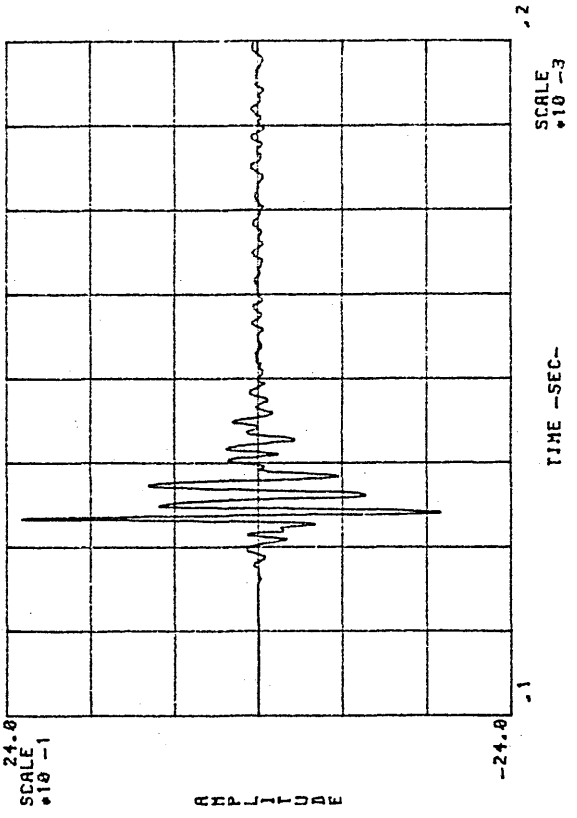
GRAPH NO 6.25.f PENCIL PULSE 45MM
24.0
SCALE
*10 -1
-24.0
-1
.2
SCALE
*10 -3
TIME -SEC-
AMPLITUDE

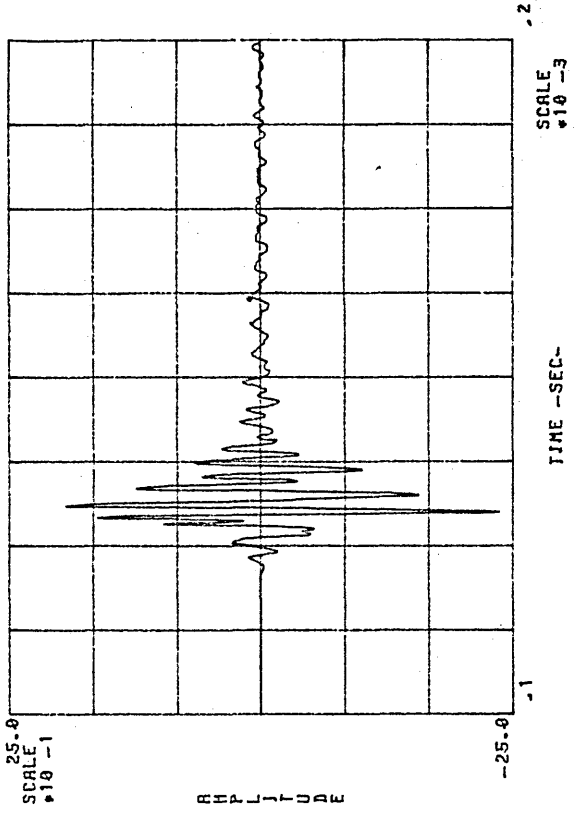
GRAPH NO 6.25.e PENCIL PULSE 40MM
25.0
SCALE
*10 -1
-25.0
-1
.2
SCALE
*10 -3
TIME -SEC-
AMPLITUDE

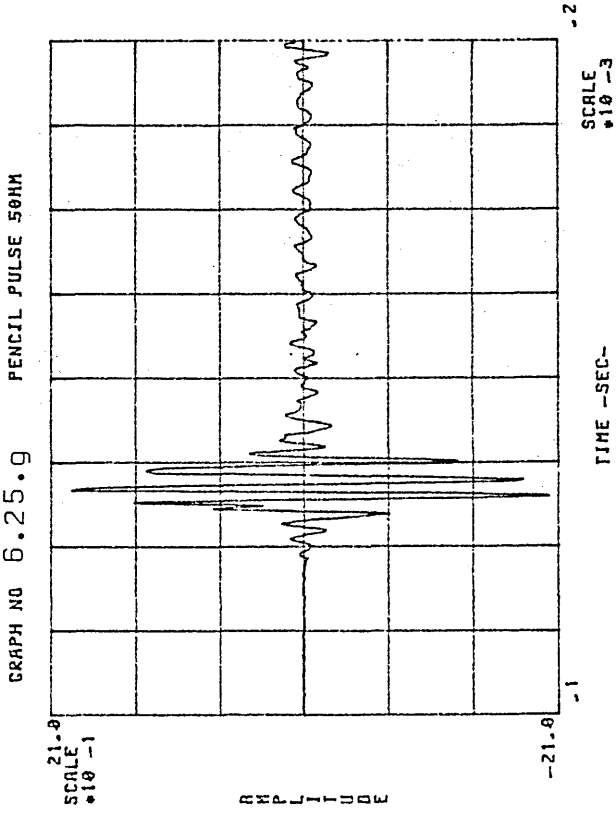
GRAPH NO 6.25.g PENCIL PULSE 50MM
21.0
SCALE
*10 -1
-21.0
-1
.2
SCALE
*10 -3
TIME -SEC-
AMPLITUDE

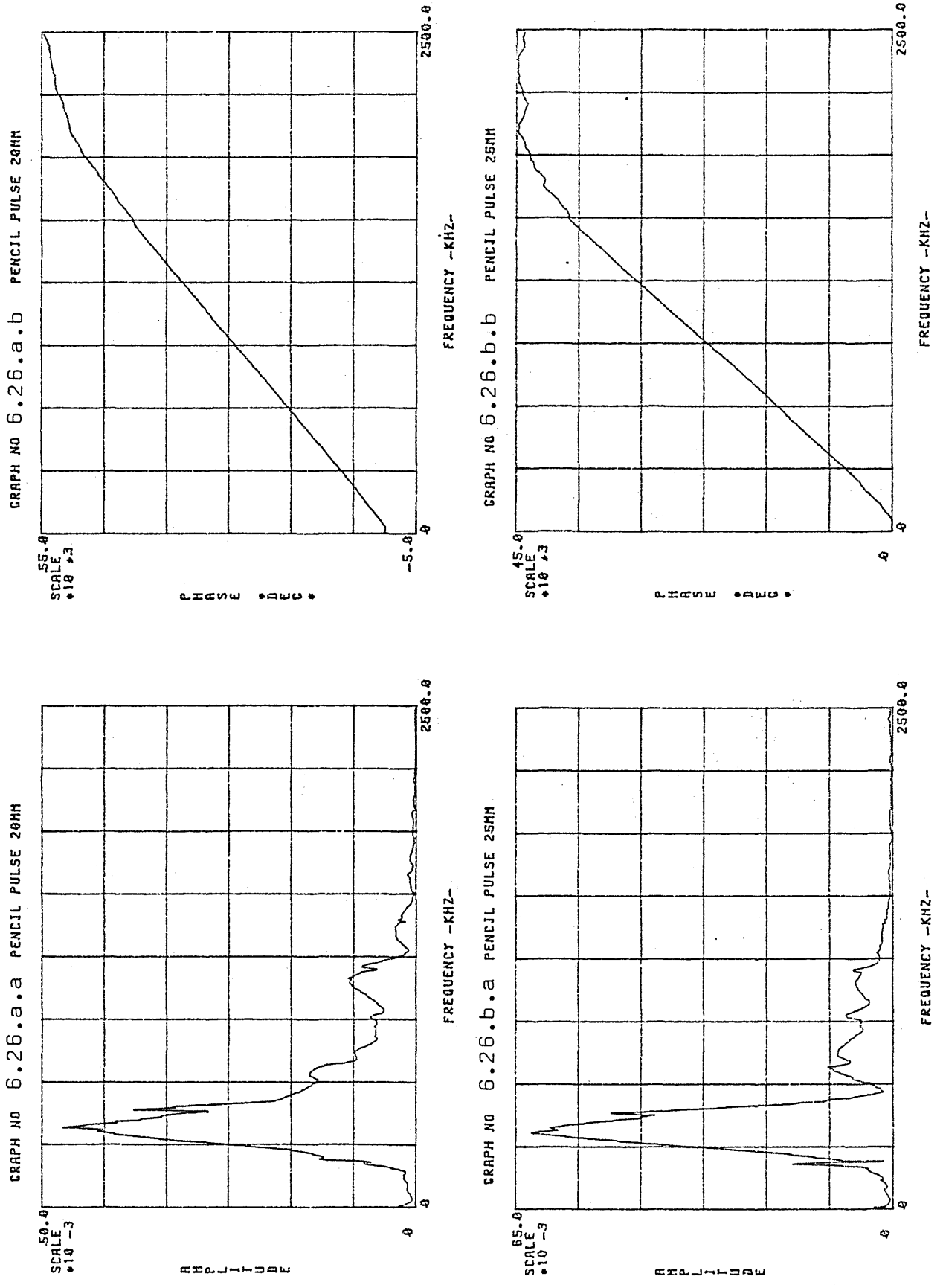

Fig 6.26.a.a to 6.26.g.b- Raw amplitude (a) and phase (b) spectra from the corresponding pulses in Fig 6.26.a to g.

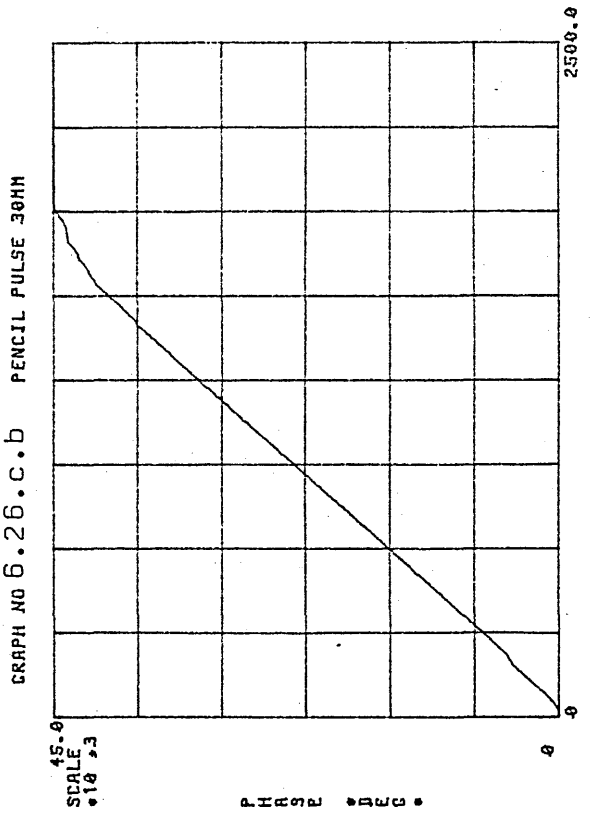
GRAPH NO 6.26.c.b PENCIL PULSE 30MM
45.0
SCALE
*10 *3
0
0
2500.0
PHASE *DEG*
FREQUENCY -KHZ-

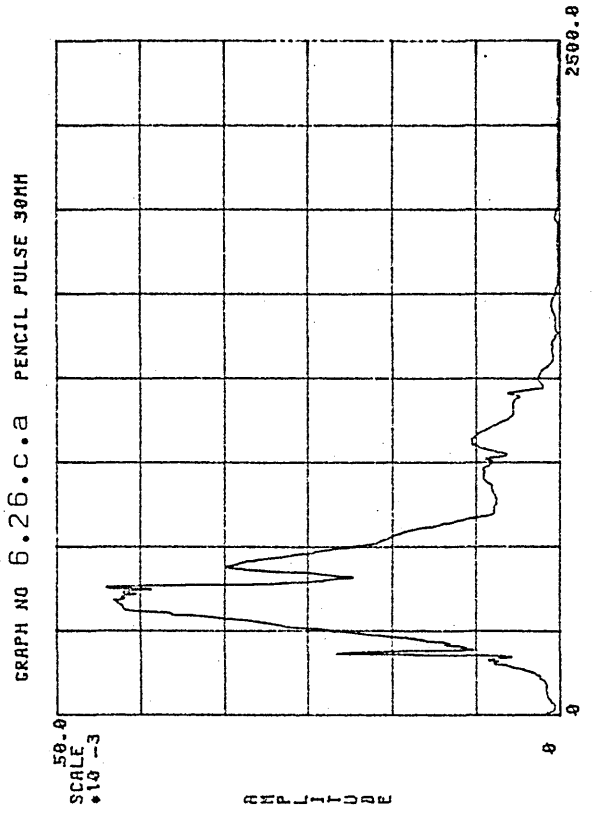
GRAPH NO 6.26.c.a PENCIL PULSE 30MM
50.0
SCALE
*10 -3
0
0
2500.0
AMPLITUDE
FREQUENCY -KHZ-

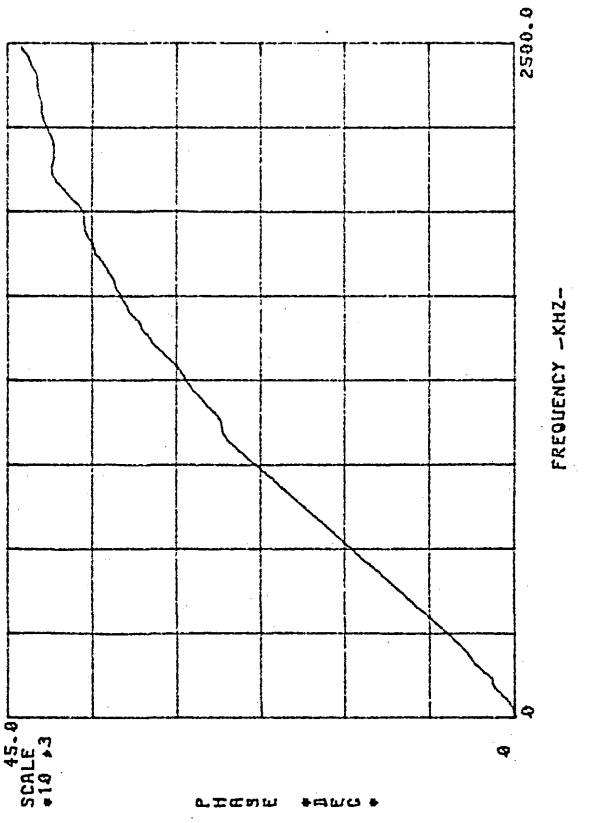
GRAPH NO 6.26.d.b PENCIL PULSE 35MM
45.0
SCALE
*10 *3
0
0
2500.0
PHASE *DEG*
FREQUENCY -KHZ-

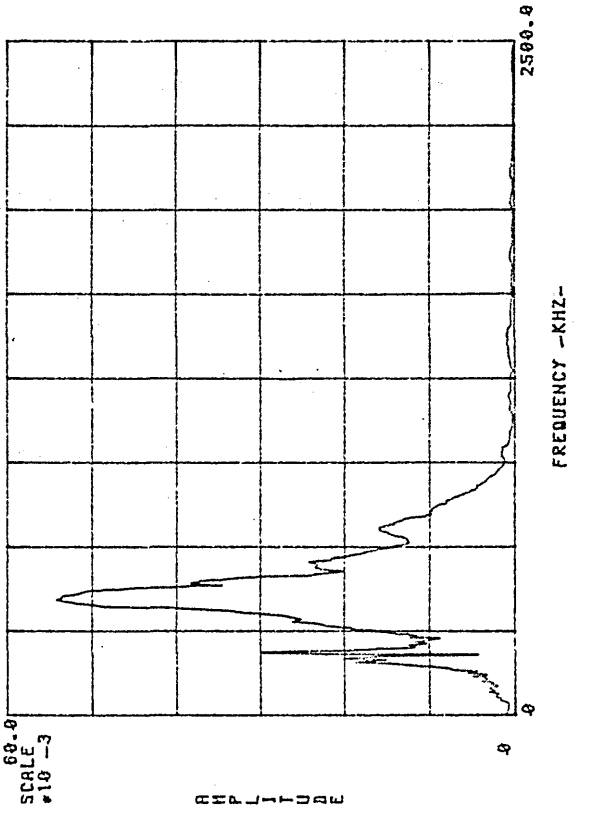
GRAPH NO 6.26.d.a PENCIL PULSE 35MM
60.0
SCALE
*10 -3
0
0
2500.0
AMPLITUDE
FREQUENCY -KHZ-

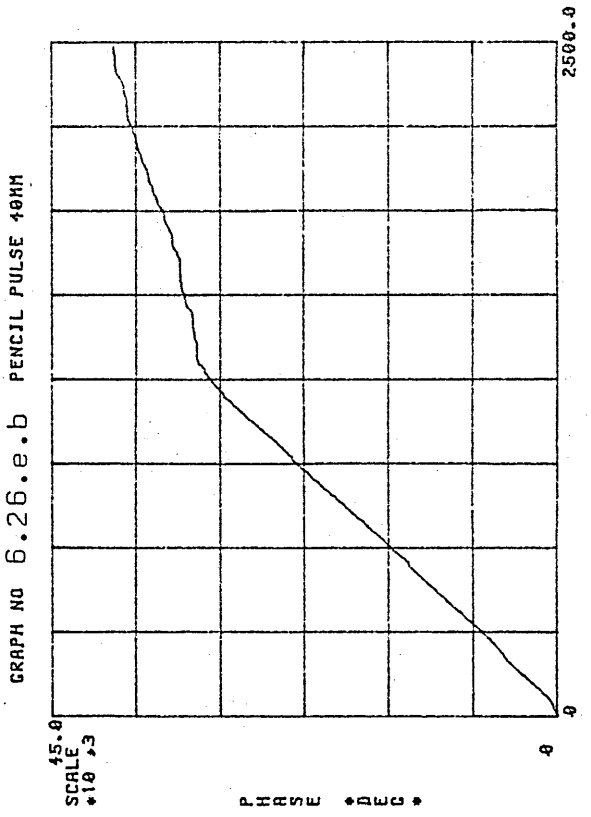
GRAPH NO 6.26.e.b PENCIL PULSE 40MM
45.0
SCALE
*10 **3
0
0
2500.0
FREQUENCY -KHZ-
PHASE *DEG*

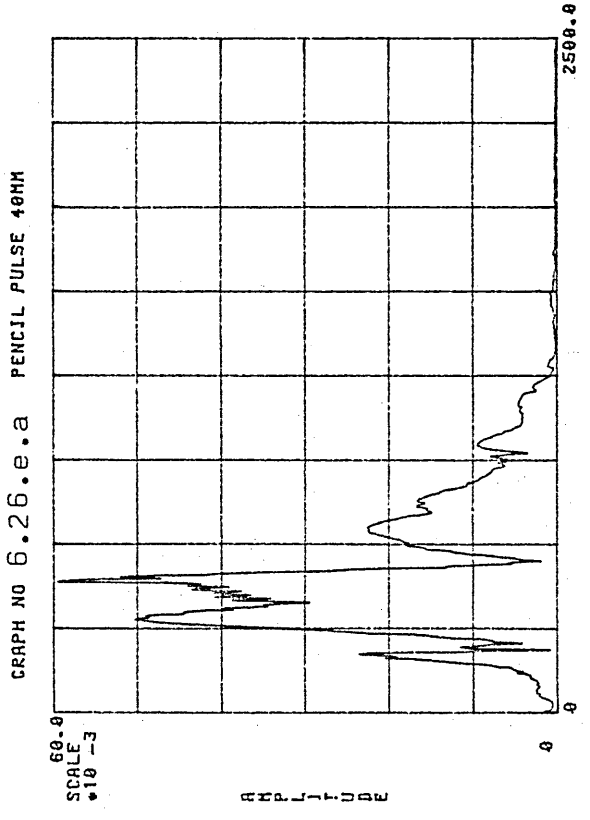
GRAPH NO 6.26.e.a PENCIL PULSE 40MM
60.0
SCALE
*10 -3
0
0
2500.0
FREQUENCY -KHZ-
AMPLITUDE

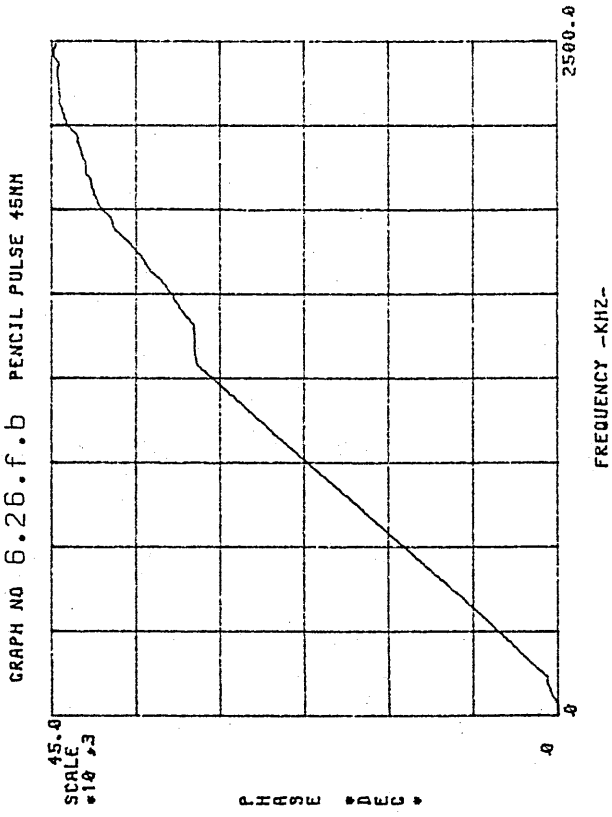
GRAPH NO 6.26.f.b PENCIL PULSE 45MM
45.0
SCALE
*10 **3
0
0
2500.0
FREQUENCY -KHZ-
PHASE *DEG*

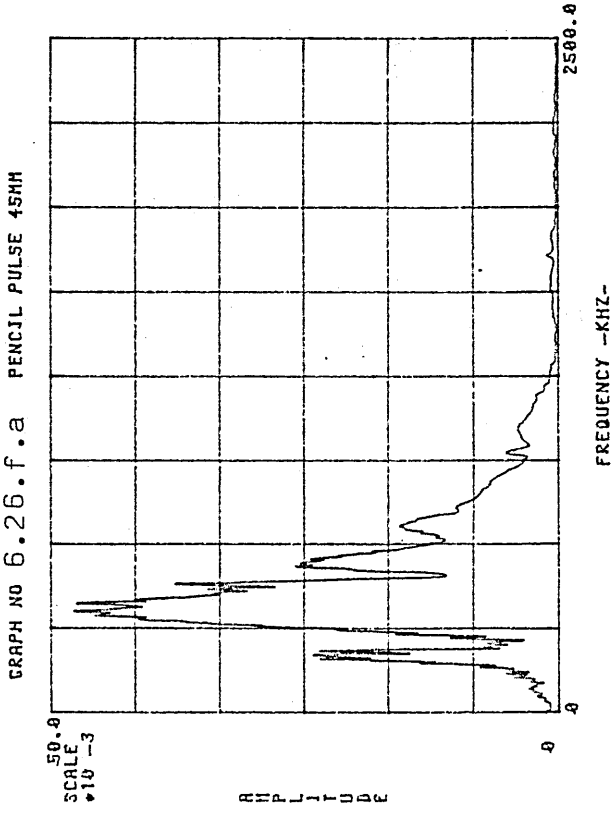
GRAPH NO 6.26.f.a PENCIL PULSE 45MM
50.0
SCALE
*10 -3
0
0
2500.0
FREQUENCY -KHZ-
AMPLITUDE

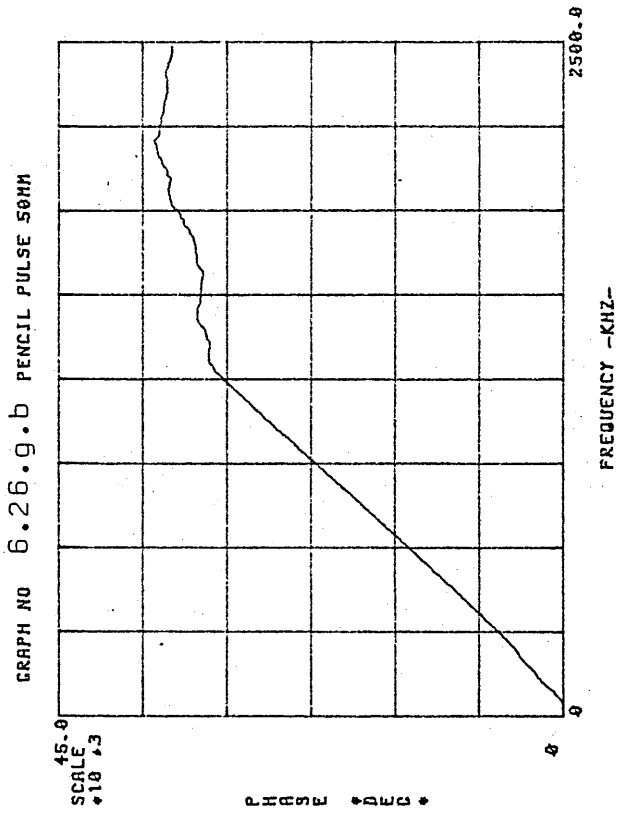
GRAPH NO 6.26.g.b PENCIL PULSE 50MM
45.0
SCALE
*10 *3
0
0
2500.0
PHASE *DEG*
FREQUENCY -KHZ-

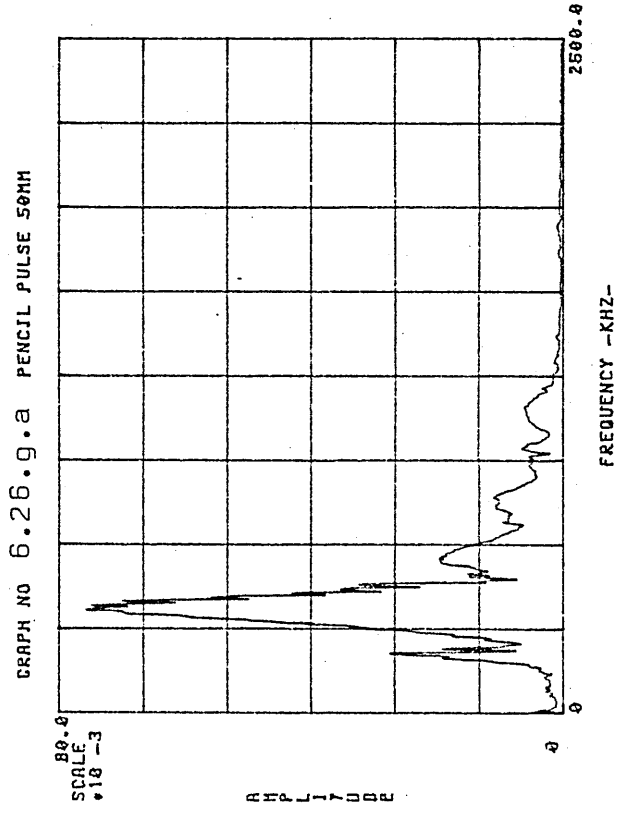
GRAPH NO 6.26.g.a PENCIL PULSE 50MM
80.0
SCALE
*10 -3
0
0
2500.0
AMPLITUDE
FREQUENCY -KHZ-

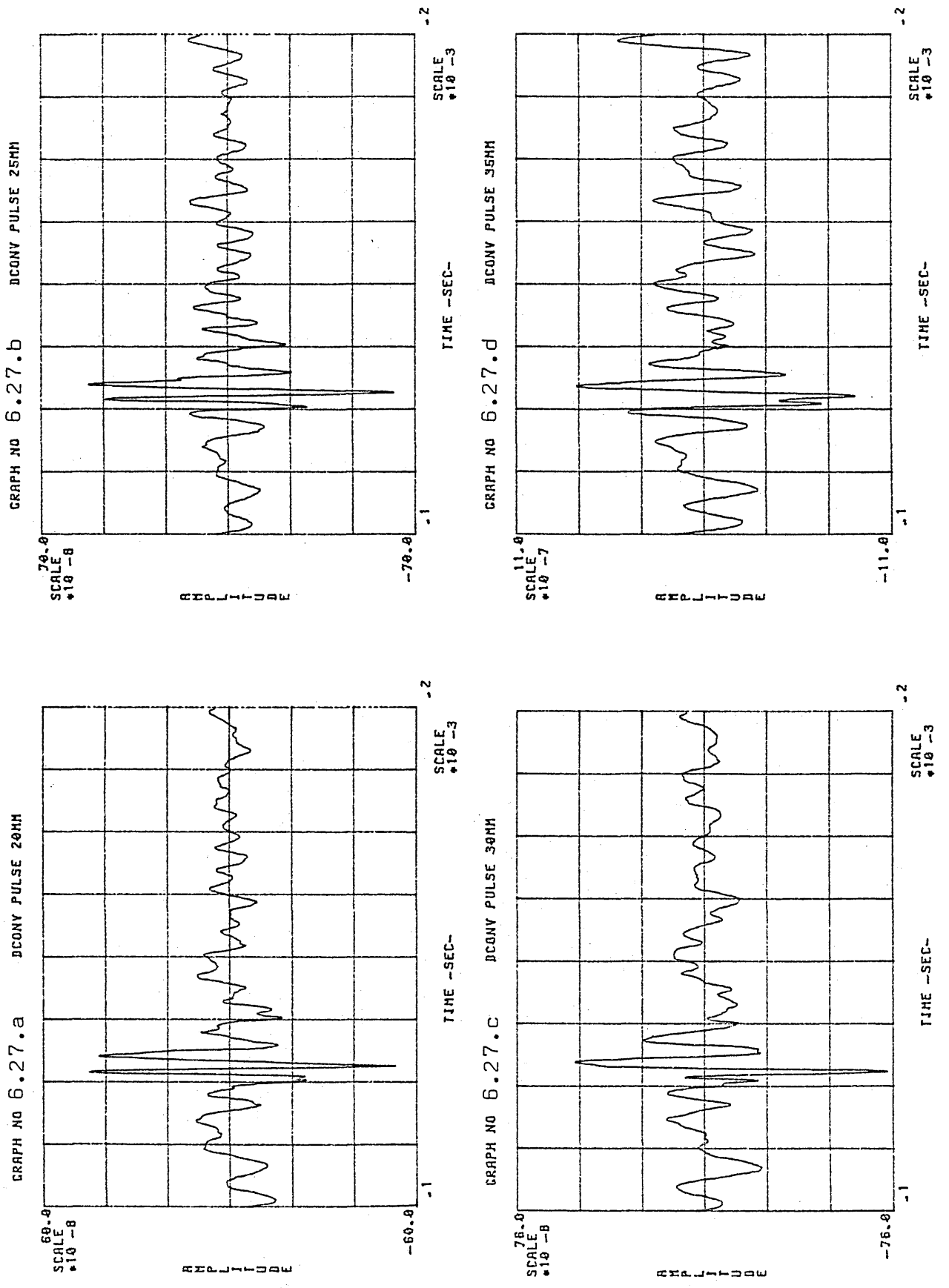

Fig 6.27.a to g- De-convoluted and integrated records from the corresponding pulses in Fig 6.25.a.to g.

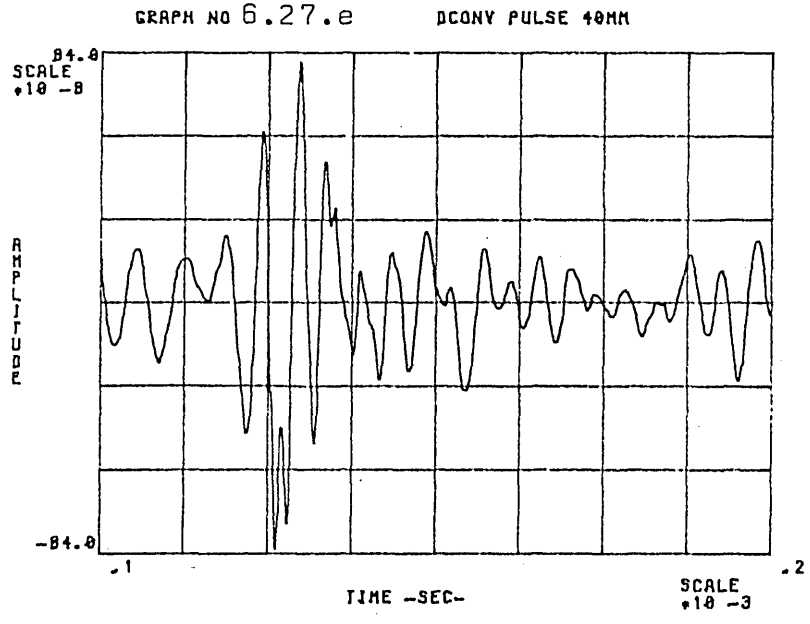

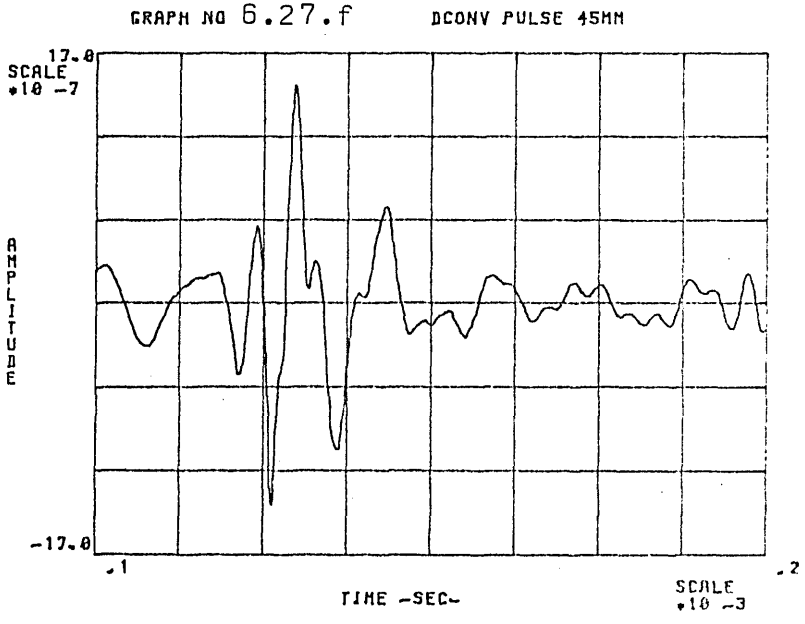

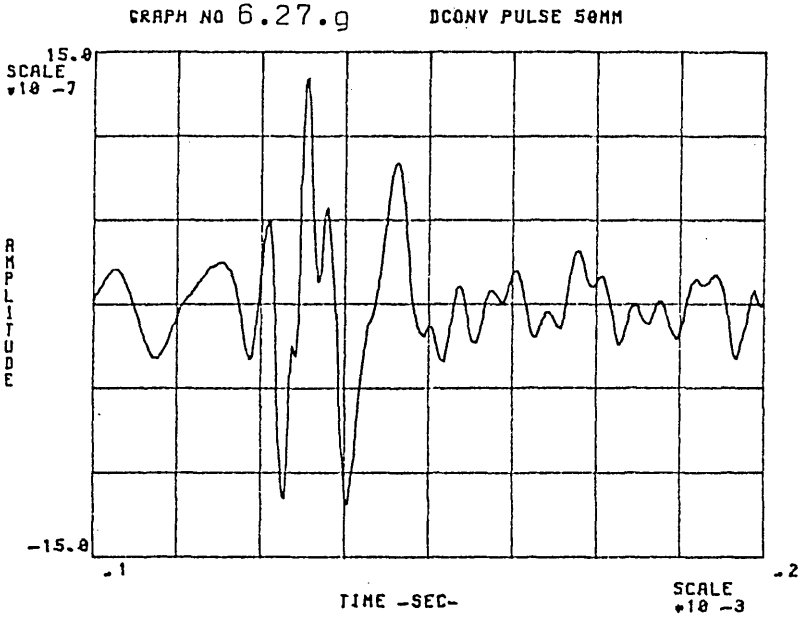

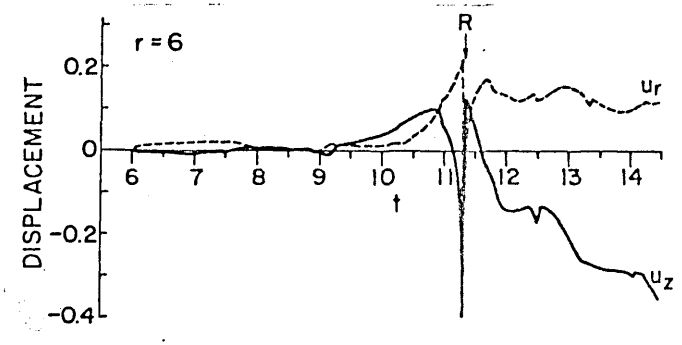

Fig 6.28- Theoretically calculated displacement (u_z), copied from Ref (41).

CONCLUSION

In the broadest possible terms, the present work basically consists in the implementation of a series of experimental techniques, derived from basic linear systems theory concepts.

Although the background theory necessary for the development of the project was not excessively involved, the implementation of those methods devised was fraught with technical difficulties related to the instrumentation, which consumed the greater portion of the time span dedicated to the research work.

Besides the fulfilment of initial objectives, the research programme has produced a number of findings, which make a contribution to the understanding of the problems related to the analysis of AE signatures. For example, the detection of directionality effects in the transducers; the presence of phase errors in the signal records, introduced by the signal storing device; and the effects of loading and coupling to the high frequency response from the transducers.

Additionally, the project has produced a series of definite achievements which are considered of relevance to the "state of the art". Among these, the development of a transducer with characteristic bandwidth of 300 KHz - 2 MHz was seen as a major breakthrough, specially in view of the frequency response from the best commercial alternative available at the beginning of the project.

Another very satisfying achievement was the provision of a method to overcome the phase errors introduced to the data records by the sampling/multiplexing process of the signals. Indeed, no reference was found to provide support in the solving of this particular problem, which is of capital importance for the successful implementation of a reciprocity method of calibration using transient type excitations. The technique developed for the correction of these phase errors was also considered of important value in the implementation of digital systems for the processing of signals in general,

with particular application potential in the calibration of electronic instrumentation using transient signals.

On the data processing aspects of the project, the successful implementation of the frequency domain convolution and deconvolution of data was also seen as an important achievement, since most of the literature reviewed reported difficulties encountered with the phase of the signals, and consequently all meaningful results published to the present were achieved through convolution and deconvolution processes in the time domain.

The author considers that as long as adequate precautions are taken regarding the processing of phase information, the implementation of the convolution processes in the frequency domain offer the advantage of reducing the computing time and memory capacity necessary, and therefore it constitutes a preferable option to the time domain methods.

Most of the conclusions drawn from the interpretation of the results achieved are included within the discussion and development of the research work. However, in order to underline the most relevant findings, these will be listed in sections corresponding to the related chapters of this thesis.

Finally, a series of guidelines are given for future work, which can be developed from the results achieved so far.

7.1 CONCLUSIONS

7.1.1 Signal Processing Hardware

- The instrumentation system implemented for the capture and processing of the signals proved both practical and efficient in overall terms, being capable of processing transients with a bandwidth of 2 MHz.

- A more flexible control of the record length than allowed by the transient recorder would have been desirable, although such control can be effected later, from the data handling software.

- From conventional standards on the digital conversion of signals, the sampling frequency is commonly fixed at approximately 2.5 times the highest frequency in the bandwidth of interest. However, although a factor of 2.5 is adequate for the digitization of continuous signals, a higher factor is required when sampling short duration transients covering less than 30 to 50% of the record length, as was the case for most AE experimental measurements. For example, for a signal bandwidth of 2 MHz, the minimum sampling rate should have been 5 MHz, however, the results obtained after repeated tests showed rather poor accuracy. Consequently, the sampling rate of the recorder was increased to the maximum possible of 10 MHz.

- The use of anti-aliasing filters proved crucial for the measurement of phase. Although the natural roll-off in sensitivity and gain from the transducers and amplifiers for frequencies above 2 MHz, was sufficient to prevent alisasing effects in the amplitude spectra, filters had to be introduced into the signal conditioning lines, in order to achieve the measurement of phase spectra.

- The overall performance of the signal processing equipment was basically restricted by the dynamic range of the transient recorder, which is an 8-bit device. The whole system performance could be improved considerably with a 12-bit recording instrument.

7.1.2 Data Processing Software

- Before ensemble-averaging data in the frequency domain, it was essential to correct the phase information contained in the records with respect to the same reference; and the results obtained from the averaging and smoothing process were of far superior quality, when the calculations were performed with the real and imaginary components of the Fourier transforms, rather than the amplitude and phase spectra.

This implied the conversion of the amplitude and phase spectra of each record into the real and imaginary component spectra prior to their averaging, and the conversion of the averaged and smoothed results back to the amplitude and phase form. This sequence of conversions of the data slowed down the averaging process quite considerably, but the quality of the final results overweighed this penalty.

- It was possible to implement the convolution and de-convolution of data in the frequency domain, which allowed achieving the results with simpler calculation algorithms, and offered the additional bonus of reducing the necessary computing time and memory capacity.

- The program for calculating the inverse Fourier transform from data in the frequency domain was improved by the provision of high-pass and low-pass filtering windows, which allowed the control of interference of noise outside the frequency band of interest.

- Although taper windowing functions are widely used in the digital processing of signals, it was found that their application to transient signals tended to impair the phase information contained in the data records, and therefore they were never used for calibration purposes.

The author does not recommend the use of such shaping windows when intending the convolution of data in the frequency domain.

7.1.3 Experimental Model

- The best method of excitation among the different techniques tested, was achieved with the pulse generator - piezoelectric exciter combination, since this system was capable of generating surface waves with the flattest raw amplitude spectra, besides allowing the easy monitoring of the input signal to the exciter.

- From the experimental results obtained, it is clear that a bar shaped specimen suffers from excessive interference caused by wave reflections from the side edges, which renders it useless for reciprocity calibration methods. In this respect, the elastic plate specimen represents a far better alternative, with the added advantage of having been modelled mathematically.

7.1.4 Transducers

- The diaphragm configuration for the design of AE transducers has shown specific advantages of sensitivity and frequency response, when compared with more traditional configurations.

- The experimental results obtained indicate that loading the active element of the transducers with damping, produced no improvement in terms of the flatness of the frequency response, whereas it reduced the overall sensitivity level.

- A small amount of inertial loading increased the sensitivity of the transducers for both ends of the frequency range, producing effectively flatter responses without impairing the overall sensitivity level. It is believed that the form in which this loading was applied (see Fig. 5.29), also produced the beneficial effect of damping the radial mode of vibration in the active elements of the transducers.

- From the study of directionality effects present in the tested transducers, the evidence suggests that those having rigid wear plates offer a limited potential for signature analysis, with the diaphragm configuration constituting a far better option.

- The use of contact shoes constitutes a fundamental requirement for the proper function of the diaphragm type transducers, and great care must be taken during the cutting and assembly processes to avoid mis-alignment, and to ensure the maximum possible of axial symmetry in order to maintain directionality effects to a minimum.

- The commercial couplant resin used (from Dunegan/Endevco), was found to produce the most satisfactory results. However, the successful performance of such a couplant was partially due to the relatively large contact area between specimen and contact shoe (4 mm in diameter). It is feared that a reduction in size of this contact area would facilitiate the intrusion of air to the interface between transducer and specimen, thus impairing the performance of the couplant.

Nevertheless, the relatively low cost of production of the diaphragm transducers, could make it an economically viable solution to install the transducers on a permanent basis, employing epoxy resin as couplant.

7.1.5 Calibration Method

- It is obvious from the discussion of results in section 6.3, that the calibration method presented consitutes just a first approximation towards the achievement of an accurate 100% experimental method for the calibration of AE transducers.

Criticisms to the implemented technique are the achievement of the calibration only in relative terms, although the discussion of the method justifies the approach taken; the crude model employed to represent the specimen transfer function; and the discrepancy in distance from the source of excitation emerging between the calculated and measured surface pulses.

There is considerable room for improvements in all of these aspects, however, as already explained, most of the time available for the project was spent in implementing the necessary hardware and software facilities to perform this study.

- The analysis of the results obtained indicates that a reciprocity calibration technique based upon 100% experimental measurements is a viable proposition, simple enough to be implemented within an industrial environment, thus facilitating the processing "in situ" of AE signatures by computer means.

- From the results obtained and the study of related literature, it was concluded that the thickness of the plate employed as specimen was too small, in comparison with the size of the contact shoe in the transducers. This may account for most of the discrepancies between calculated and experimental results.

- The analysis of results, supports the theory that detected AE surface waves are mainly constituted by Rayleigh waves, whenever the

transducer is not located at the epicenter, or further than six times the plate thickness from the source.

7.2 FUTURE WORK PERSPECTIVES

The results obtained from the present research project indicate than an infrastructure has been layed down for conducting research work on AE signature analysis. However, as happens with all scientific or technological research, there will always be room for improvements in each of the areas covered by the project.

A set of suggestions are therefore listed as guidelines, for the reader interested in persuring further research into the subjects treated here, with the aim of heightening those aspects which need most urgent attention. These recommendations are organized under the heading of the aspect to which they refer.

7.2.1 Signal Processing Hardware

The accuracy of the results could be considerably improved by increasing the dynamic range of the sampling and storing device used. The transient recorder employed for this project had an effective dynamic range of 38 to 40 dB, which makes difficult the accurate measurement of the higher frequency components in the bandwidth of interest, due to the tendency by the lower frequency components to overshadow the higher frequencies in the surface waves. Indeed, the signal recorder greatly limited the dynamic range of the transducer preamplifiers, which have a typical range value of 74 dB.

Another limiting aspect from the transient recorder was the maximum sampling rate which, although adequate for continous signals with a bandwidth of 2 MHz, should be increased to maintain the response bandwidth for fast transients.

Digital storing devices are being improved on an almost daily basis, and there are already better instruments on the market capable of faster sampling rates, while instruments based upon 12-bit digitiz-

ing systems are being developed to reach bandwidths into the megahertz region. Therefore, if a new system is to be acquired to perform research work similar to the present project, it is specially advisable to perform a thorough market research in relation to the sampling and storing device.

The remaining instrumentation, with the exception of transducers, is considered to be adequate for most AE signature analysis over the frequency range of 20 KHz to 2 MHz.

7.2.2 Data Processing Software

A definite advantage of maintaining the data processing software structured in separate program units, has been the easy modification of extension of a particular program without affecting the rest of the package. This allowed maintaining the software in a dynamic state, subject to being modified in accordance to the progress made in any other aspect of the work.

The description of programs and subroutines in this thesis, corresponds to the final form of the software at the conclusion of the experimental work. It is therefore expected that some further modifications will be necessary as the research work is continued into improving the remaining aspects of the project.

However, a relatively simple modification which would facilitate greatly the handling of the signal time histories, consists in the provision of editing facilities for the records as they are transmitted from the transient recorder to the computer, prior to their processing.

7.2.3 Experimental Model

One aspect which requires modification before continuing any research work on the calibration method, is the geometry of the steel plate specimen. The experimental evidence suggests that the surface area of the tested plate specimen (305 x 305 mm^2) should be sufficient

for the accurate measurement of short duration transients, without interference from side reflections, as long as the distance between source and transducer is maintained small (about 10% of the specimen width). A larger surface area would allow the experimental study of the specimen transfer function for distances greater than 30 mm.

However, it is firmly believed that the ratio of the specimen thickness to the transducer sensing element diameter should be increased, in order to achieve better accuracy in the calibration of transducers, and a minimum thickness of 25 mm is suggested.

Typical precautions to be taken when preparing a plate specimen for tests, are the removal of surface irregularities such as cracks, inclusions and machining trails, leaving the surface to be used for measurements with a finish of 0.5 μm rms, if only piezoelectric transducers are to be used; and a surface finish of optical quality, flat within 0.1 μm for any circular section 50 mm in diameter, if capacitive displacement transducers are intended to be used.

7.2.4 Transducers

As indicated in the corresponding chapter, the transducers used for the development of the calibration method were not selected as an ultimate design, but as a suitable option, with characteristics superior to the commercial alternatives available at the commencement of the project.

Although the diaphragm configuration is considered to be the best design so far for the analysis of AE signatures, improvements in the frequency response of the sensors can be achieved through the modification of several aspects in the design.

For example, the lower frequency end of the response could be improved by increasing the inertia loading of the sensing elements. In a report by Eitzen et al (44), a claim is made of having constructed a peizoelectric transducer, capable of producing a response proportional to displacement very similar to that of a capacitive transducer. This is said to have been achieved by loading the sensing element with a

brass cylinder, thus lowering the fundamental resonance frequency of the thickness mode.

Another area in which research can be conducted is the introduction of electronic passive elements to the design of transducers, in order to shape the frequency response by reducing the most significant peaks in the characteristic amplitude spectrum. Additional work is also necessary on the study of directionality effects and their control, in order to achieve truly omnidirectional transducers.

Finally, the feasibility of producing transducers with smaller sensing elements and contact shoes should be investigated, in order to develop physical sensors with performance closer to true point transducers; that is, transducers with the same characteristics for epicentral and Rayleigh waves measurements.

7.2.5 Calibration Method

The technique developed constitutes only the basis from which a full calibration method can be developed, and the results obtained so far are evidence of the feasibility of the technique.

The aspect requring the most urgent attention is the development of a proper model for the transfer function of the plate. This can be based upon the models of the Green's function developed by Pao and Ceranoglu (40)(41), modifying it accordingly to suit the reciprocity method in terms of surface disturbance only, and testing the model developed with experimental measurements.

The tests for the model of the plate transfer function would not require the transducers to be calibrated, as long as the measurements are made consistently, and with the same transducers.

Once a proper model for the transfer function of the specimen is obtained, this should be introduced into the calibration process in order to refine the technique.

Finally, some method to assess the absolute sensitivity of the transducers must be developed. The alternative techniques possible are the comparison with a standard, or the application of a theoretical model (like the one developed by Pao and Ceranoglu), to calculate the expected magnitude for the signals.

7.2.6 Signature Analysis

The present research project only covered those aspects leading to the recovery of the shape of the surface wave arriving at the transducer, and therefore all the questions related to the actual analysis of the recovered waveform have remained unanswered.

Research work could develop following the techniques for analysis in current use by the two main groups of researchers in this area, consisting in the identification of the source forcing function, or the application of shock spectral analysis to the recovered surface wave. Altneratively, new parameters have been proposed for the analysis of AE signatures, by W.J.Pardee (57), from the Rockwell International Science Center.

In his interesting paper, Pardee proposes the characterization of AE waves in terms of invariant parameters. A demonstration is provided to argue that AE phenomena propagating within an isotropic, homogeneous plate present four invariant parameters: energy, two momentum components parallel to the specimen surface, and angular momentum; and experimental techniques for measuring these parameters are suggested.

This newly proposed method of analysis opens completely new horizons for the research of new techniques on the diagnosing of AE sources.

REFERENCES

1. Portevin, A. Le Chatelier, F. — "Comptes Rendus" No.176, pp.507-510, France, 1923

2. Joffe, A. — "The Physics of Crystals" New York, 1928, p.50

3. Klassen - Nekludowa — "Physik" No.55, p.555, 1929

4. Kaiser, J. — "Untersuchungen Uber Das Auftreten Geräuschen Beim Zugversuch" PhD Thesis, Technische Hochscule, Munich, 1950

5. Bentley, M.N. — MSc Thesis, 1976, Cranfield Institute of Technology, Cranfield, Bedford

6. Board, D.B. — "Incipient Failure Detection in CH-47 Helicopter Transmissions" ASME paper No. 75-WA/DE-16, Dec. 1975

7. Bloch, H.P. — "Development and Experience with Computerized Acoustic Incipient Failure Detection (IFD) Systems" ASME paper No. 77-PET-2, 1977

8. Hartmen, W.F. — "Towards Standards for Acoustic Emission Technology" Non Destructive Testing Standards - a review, Procs. of a Symp. ASTM, 19-21 May, 1976, USA ASTM STP 625

9. Liptai, R.G., Harris, D.O., Engle, R.B., Tatro, C.A. — "Acoustic Emission Techniques in Materials Research" Int.J. of NDT, 1971, Vol.3, pp.215 - 275

10. Dunegan, H.L., Green, A.T. "Factors Affecting Acoustic Emission Response from Materials" Materials Research and Standards, MTRSA, Vol.11, No.3, 1971

11. James, D.R., Carpenter, S.H. "Acoustic Emission Test Facility" The Review of Scientific Instruments, Vol.42, No.8, pp.1131-1136, Aug.1971

12. Carlyle, J.M., Scott, W.R. "Acoustic-Emission Fatigue Analyzer" Exp.Mech. Vol.16, No.10, pp.369-372, Oct.1976

13. Bathias, C., Brintet, B., Sertour, G. "Can the Initiation of Fatigue Cracks be Detected by Acoustic Emission? - Application to High Strength Alloys for Aeronautics" L'Aeronautique & L'Astronautique, Vol.66, pp.41-45, 1977

14. Lindley, T.C., Palmer, I.G., Richards, C.E. "Acoustic Emission Monitoring of Fatigue Crack Growth" Matls.Sci.and Eng. Vol.32, pp.1-15, 1978

15. Graham, L.J., Alers, G.A. "Frequency Spectra of Acoustic Emissions Generated by Deforming Metals and Ceramics" IEEE Ultrasonic Symposium, Boston, USA, 1972

16. Buck, O., Pardee, W.J. "Acoustic Emission Signature Analysis (Technical Progress Report 2 for Period 1/3/79 - 20/2/80)" Rockwell International Science Center, Thousand Oaks, Cal., USA, 1980 DOE/ER/02029

17. Houghton, J.R., Packman, P.F. — "Pulse Analysis of Acoustic Emission Signals" NASA Contractor Report 2927, Contract NSG-8012, Dec.1977

18. Ono, K. — "Acoustic Emission and Microscopic Deformation and Fracture Processes" Proceedings of the Second Acoustic Symposium, Tokyo, Japan, 2 - 4 September 1974. Also UCLA-ENG-7465, School of Eng.& App.Sci., UCLA, Los Angeles, Cal, USA

19. Graham, L.J., Alers, G.A. — "Investigation of Acoustic Emission from Ceramic Materials" AD 745000, Final Report, Naval Air Systems Command, Contract No. N00019-17-C-0344, May 1972

20. Graham, L.J, Alers, G.A. — "Acoustic Emission in the Frequency Domain" Monitoring Structural Integrity by Acoustic Emission, ASTM STP 571, 1975, pp.11-39

21. Curtis, G. — "ACOUSTIC EMISSION - 4 Spectral Analysis of Acoustic Emission" Non-Destructive Testing, April 1974, pp.82-91

22. Breckenridge, F.R., Tschiegg, C.E., Greenspan, M. — "Acoustic Emission: some applications of Lamb's problem" J.Acoust.Soc.Am., Vol.57, No.3, pp.626-631, March 1975

23. Bannister, R.H., Oliveras, J. — "Phase Correlation in High Frequency Digital Recordings: a method for multiplexed signals phase correction" Submitted for publication to the Institute of Physics, Scientific Instruments (Journal of Physics E), 1982

24. Delagrange, A.D. "Design Active Elliptic Filters with a 4-function Calculator" EDN, March 3, 1982

25. Beauchamp, K.G. "Signal Processing Using Analogue and Digital Techniques" George Allen & Unwin Ltd., 1973

26. Beauchamp, K.G. "Walsh Functions and their Applications" Academic Press, London, 1975

27. Rabiner, L.R., Rader, C.M. "Digital Signal Processing" IEEE Press, New York, 1972

28. Oliveras, J. "Analysis Software for Acoustic Emission" Internal Progress Report, School of Mech.Eng., CIT, Cranfield, Bedford, June 1980 Submitted to the SRC as part of Report No. SME/AM/1821

29. Graham, L.J., Alers, G.A. "Spectrum Analysis of Acoustic Emission in A533-B Steel" Materials Evaluation, Feb.1974, pp.31-37

30. McBridge, S.L., Hutchison, T.S. "Helium Gas Jet Spectral Calibration of Acoustic Emission Transducers and Systems" Canadian Journal of Physics, Vol.54, No.17, 1976, pp.1824-1830

31. Bell, R.L. "Acoustic Emission Transducer Calibration - Transient Pulse Method" Technical Report DE-73-3, Dunegan/Endevco, San Juan, Capistrano, Cal, USA

32. Feng, C., Whittier, R.M. "Acoustic Emission Transducer Calibration Using Transient Surface Waves and Signal Analysis" Technical Report DE-79-1, Dunegan/Endevco, San Juan, Capistrano, Cal., USA

33. Curtis, G. "A Broadband Polymeric Foil Trandsducer" Ultrasonics, July 1974, pp.148-154

34. Leschek, W.C. "Acoustic Emission Transducer Calibrator" Materials Evaluation, Feb.1975, pp.41-48

35. Hatano, H., Mori, E. "Acoustic-Emission Transducer and its Absolute Calibration" J.Acoust.Soc.Am., Vol.59, No.2, Feb.1976, pp.344-349

36. Lamb, H. "On the Propagation of Tremors over the Surface of an Elastic Solid" Philosophical Transactions, Royal Soc., London, Ser.A, 203, pp.1-42, 1904

37. Pekeris, C.L. "The Seismic Surface Pulse" Nat.Acad.Sci., Vol.41, 1955, pp.469-480

38. Sachse, W., Ceranoglu, A.N. "Experiments with a Well Characterised Acoustic Emission System" Procs. Ultrasonic Int.Conf., Graz, Austria, 1979, pp.138-145

39. Michaels, J.E., Michaels, T.E., Sachse, W. "Applications of Deconvolution to Acoustic Emission Signal Analysis" Materials Evaluation, Vol.39, Oct.1981, pp.1032-1036

40. Pao, Y-H., Gajewski, R.R., Ceranoglu, A.N. "Acoustic Emission and Transient Waves in an Elastic Plate" J.Acoust.Soc.Am., Vol.65, No.1, Jan.1979, pp.96-105

41. Ceranoglu, A.N., Pao, Y-H. "Propagation of Elastic Pulses and Acoustic Emission in a Plate" Part 1, 2 and 3, J.of App.Mech, Vol.48, March 1981, pp.125-147

42. Egle, D.M., Brown, A.E. "A Note on Pseudo-Acoustic Emission Sources" J.of Test and Eval., JTEVA, Vol.4, No.3, May 1976, pp.196-199

43. Timoshenko, S.P., Goodier, J.N. "Theory of Elasticity" Third Edition. McGraw-Hill Kogakusha Student Edition

44. Eitzen, D.G., Breckenridge, F.R., Clough, R., et al "Summary of Fundamental Developments for Quantitative Acoustic Emission Measurements" Electrical Power Research Institute, Palo Alto, Cal., USA. Report No. EPRI NP 1877, June 1981

45. ----- "Five Modern Piezoelectric Ceramics" Bulletin No. 66011/F, Rev.Jan. 1976, VERNITRON Ltd., Thornhill, Southampton

46. ----- "Specific Purpose Transducers in PZT Ceramics" Bulletin No. 66047/A, Rev.Jan. 1975, VERNITRON Ltd., Thornhill, Southampton

47. Dunegan, H.L., Brown, A.E., Knauss, P.L. "Piezoelectric Transducers for Acoustic Emission Measurements" TID-4500, UC-34, Physics, Report No. UCRL-50553, Dec.1968, UC, Liv., Cal., USA

48. Tatro, C.A.
"Acoustic Emission Sensors and Instrumentation"
TID-4500, UC-38, Engineering and Equipment, Report No. UCRL-51320, Jan.1973, UC, Liv., Cal., USA

49. Lucey, G.K.
"Resonant and Antiresonant Frequencies of Thick Discs and Thick Rods"
J.Acoust.Soc.Am., Vol.46, No.6, 1968, pp.1324-1328

50. McMahon, G.W.
"Experimental Study of the Vibrations of Solid, Isotropic, Elastic Cylinders"
J.Acoust.Soc.Am., Vol.36, No.1, 1964, pp.85-92

51. Hill, R., El-Dardiry, S.M.A.
"The Effect of Geometry on Acoustic Emission"
Procs. of the Inst.of Acoust. Symposium on Acoustic Emission, London, 20-21 Dec. 1976

52. Christoffersen, B.K., Licht, T.R.
"ACOUSTIC EMISSION TRANSDUCERS - New Calibration and Construction Methods"
Technical Report, Brüel & Kjær, DK-2850, Nærum, Denmark

53. Graham, L.J.
"Acoustic Emission Transducer Characterisation"
North American Rockwell Report No. SCTR-71-19

54. Lord, A.E.
"Acoustic Emission - An Update"
Physical Acoustics, Vol.XV, pp.295-360, 1981.
Academic Press Inc., New York, USA

55. Sachse, W., Ceranoglu, A. "Absolute Measurements with Piezoelectric Transducers" Ultrasonics Symposium Procs., IEEE, Cat.No. 79CH1482 9SU, 1979

56. Hsu, N.N., Breckenridge, F.R. "Characterization and Calibration of Acoustic Emission Sensors" Materials Evaluation, Vol.39, No.1, pp.60-68, 1981

57. Pardee, W.J. "Elastic Wave Invariants for Acoustic Emission" J.Acoust.Soc.Am., Vol.70, No.1, July 1981, pp.110-115

BIBLIOGRAPHY

Bleaney, B.I., Bleaney, B. "Electricity & Magnetism" Third Edition, Oxford University Press, 1976. ISBN 019 85 1141 8

APPENDIX A

CAPACITIVE TRANSDUCERS

The theoretical model of these transducers is based upon the hypothetical case of an infinitely long cylindrical conductor parallel to an infinite flat conducting surface (see Fig. 1).

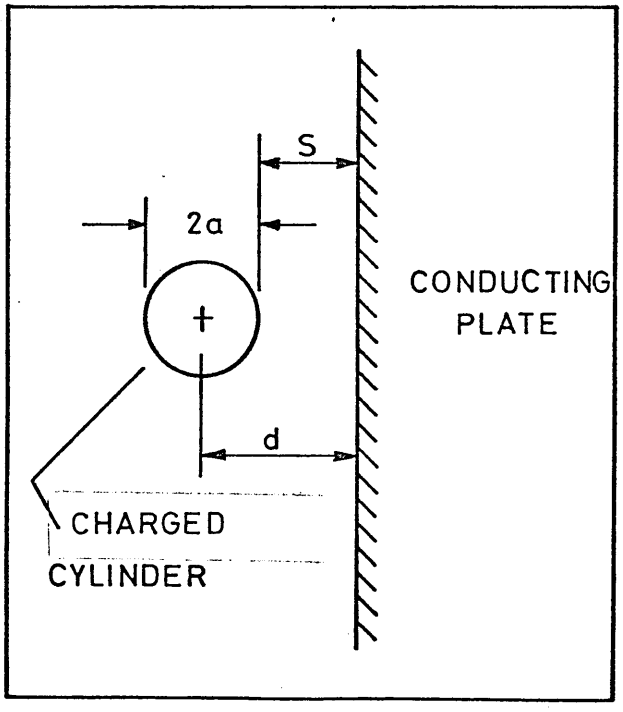

Fig 1- Capacitive Transducer Model.

The capacitance per unit length for such a system is:

$$C_L = \frac{2\pi\varepsilon}{L_n\left[\frac{d+\sqrt{d^2-a^2}}{a}\right]} \qquad (1)$$

where:

C_L = Capacitance per unit length

ε = Dielectric permitivity

d = Distance from axis of cylinder to surface

a = Cylinder radius

Considering the dimensions of the transducer used by Dunegan/· Endevco (Ref.32), the theoretical model (Eq.(1)) gives a value of 8.47 pF, while the experimentally measured capacitance was 8.5 pF, showing a remarkable agreement.

To obtain the equation describing the transducer output in terms of surface displacement, it is necessary to start from the theoretical model (Eq. (1)).

The logarithmic term can be expanded into a Taylor series:

$$L_n\left[\frac{d+\sqrt{d^2-a^2}}{a}\right] = L_n\left[\frac{d+\sqrt{d^2-a^2}}{a}\right]\Bigg|_{d_o} + \left.\frac{1+\dfrac{d}{\sqrt{d^2-a^2}}}{d+\sqrt{d^2-a^2}}\right|_{d_o} (\Delta d) +$$

$$+\frac{1}{2}\left[\frac{d}{(d^2-a^2)^{3/2}}\right]\Bigg|_{d_o} (\Delta d)^2 + \ldots\ldots \qquad (2)$$

Here, the distance $\underline{d}$ can be substituted by the sum of the radius $\underline{a}$ plus the gap $\underline{\delta}$ (see Fig. 1),

$$d = a + \delta \quad \text{and} \quad \Delta d \equiv \Delta\delta$$

and the transducer gap can be, in turn, substituted in terms of the static or equilibrium value $\underline{S}$ and the surface displacement $\underline{s}$:

$$\delta = S - s \Longrightarrow \Delta d \equiv \Delta\delta = -s$$

where $\underline{s}$ is taken normal to the flat surface and towards the cylindrical electrode.

Using these substitutions, expression (2) can be transformed into a McLaurin series:

$$L_n\left[\frac{d+\sqrt{d^2-a^2}}{a}\right] = L_n\left[\frac{a+S+\sqrt{2aS+S^2}}{a}\right] +$$

$$+ \frac{1}{a+S+\sqrt{S+2aS}}\left[1+\frac{a+S}{\sqrt{S^2+2aS}}\right](-s) +$$

$$+ \frac{1}{2}\frac{a+S}{(S^2+2aS)^{3/2}} s^2 + \ldots\ldots$$

$$L_n \left[\frac{d + \sqrt{d^2 - a^2}}{a} \right] = L_n \left[1 + \frac{S + \sqrt{2aS + S^2}}{a} \right] +$$

$$- \frac{s}{\sqrt{S^2 + 2aS}} + \frac{1}{2} \cdot \frac{(a + S)\, s^2}{(2aS + S^2)^{3/2}} + \ldots . \qquad (3)$$

Since the term $\frac{S + \sqrt{2aS + S^2}}{a} \ll 1$, in the first member of the series Eq.(3), the natural logarithm may be approximated by the term itself. In doing so, and neglecting all infinitessimal terms of order greater than one:

$$L_n \left[\frac{d + \sqrt{d^2 - a^2}}{a} \right] \simeq \frac{S + \sqrt{2aS + S^2}}{a} - \frac{s}{\sqrt{2aS + S^2}} \qquad (4)$$

At this stage, it can be noticed that $a \gg S$ for the case of the transducer, therefore S^2 can be neglected in front of $2aS$ inside the radicals, thus:

$$L_n \left[\frac{d + \sqrt{d - a^2}}{a} \right] \simeq \frac{S}{a} + \frac{2S - s}{\sqrt{2aS}} \qquad (5)$$

Returning now to the theoretical model (Eq. (1)), and substituting the logarithmic term by expression (5) :

$$C_L \simeq \frac{2\pi\varepsilon}{\frac{S}{a} + \frac{2S - s}{\sqrt{2aS}}} \qquad (6)$$

The transducer must be charged initially be means of a DC bias voltage V_o, and it is assumed that during sudden changes of the gap, the electric charge will remain constant. Therefore, the voltage at a particular instance will be:

$$V = \frac{Q}{C} = \frac{Q_L}{C_L} = \frac{Q_L}{2\pi\varepsilon} \left[\frac{S}{a} + \frac{2S - s}{\sqrt{2aS}} \right] \qquad (7)$$

with the bias voltage V_o corresponding to zero surface displacement ($-s = 0$), thus:

$$V_o = \frac{Q_L}{2\pi\varepsilon}\left[\frac{S}{a} + \frac{2S}{\sqrt{2aS}}\right] \tag{8}$$

Taking the ratio between the two voltages:

$$\frac{V}{V_o} \cong \frac{\frac{S}{a} + \frac{2S}{\sqrt{2aS}} - \frac{s}{\sqrt{2aS}}}{\frac{S}{a} + \frac{2S}{\sqrt{2aS}}} = 1 - \frac{\frac{s}{\sqrt{2aS}}}{\frac{S}{a} + \frac{2S}{\sqrt{2aS}}} \tag{9}$$

From this last expression, the produced signal can be deduced, since it will appear as a voltage change superimposed on top of the bias voltage:

$$\Delta V = -V_o \frac{\frac{s}{\sqrt{2aS}}}{\frac{S}{a} + \frac{2S}{\sqrt{2aS}}} = -V_o \frac{a\,s}{S\sqrt{2aS} + 2aS} \tag{10}$$

And once again, since $S \ll a$, the term $\sqrt{2aS}$ can be neglected in comparison with $2a$, thus:

$$V \cong -V_o \frac{s}{2S} \tag{11}$$

The geometric parameters for the built transducers were substituted into Eqs. (10) and (11), and their ratio was calculated to be 0.981, which corresponds to an approximation of around 2%.

This level of accuracy is adequate for engineering measurements, therefore Eq. (11) is to be considered as the transducer characteristic.

APPENDIX B

Due to the impossibility of adopting a conventional system of notation from the diversity of topics covered in the present work, the following notation list is included as a reference for chapter 6.

$x(t)$, $s(t)$, $e(t)$, ...	- Non capitals represent functions in the time domain.
$X(\omega)$, $S(\omega)$, $E(\omega)$, ... X, S, E, ...	- Capitals (whether including the argument or not) represent the functions in the frequency domain.
$x_i(t)$, $X_i(\omega)$, X_i, ...	- Numerical subindices refer to the corresponding transducer or location.
$x(t)\|^{I}$, $X(\omega)\|^{I}$, $X\|^{I}$, ...	- Roman numerals indicate a particular experimental set-up or measurement.
$x(t)$, $X(\omega)$, X	- Electrical input to the exciters.
$s(t)$, $S(\omega)$, S	- Output signal from the sensors.
$e(t)$, $E(\omega)$, E	- Transfer function for the exciters.
$f(t)$, $F(\omega)$, F	- Surface disturbance on the specimen.
$r(t)$, $R(\omega)$, R	- Transfer function for the sensors.
k	- Reciprocity constant, independent of frequency.
$G_{i,j}(\omega)$, $G_{i,j}$	- Transfer function of the plate between locations $\underline{i}$ and $\underline{j}$, in terms of surface waves only (not force).
c	- Speed of Rayleigh waves on the transmitting specimen.
$*$	- Symbol for convolution in the time domain